

University of Montana

ScholarWorks at University of Montana

Graduate Student Theses, Dissertations, &
Professional Papers

Graduate School

2008

GEOMORPHOLOGICAL MAPPING OF THE K2 AREA, PAKISTAN USING GIS AND REMOTE SENSING

Deborah Jeanne Belden
The University of Montana

Follow this and additional works at: <https://scholarworks.umt.edu/etd>

Let us know how access to this document benefits you.

Recommended Citation

Belden, Deborah Jeanne, "GEOMORPHOLOGICAL MAPPING OF THE K2 AREA, PAKISTAN USING GIS AND REMOTE SENSING" (2008). *Graduate Student Theses, Dissertations, & Professional Papers*. 489.
<https://scholarworks.umt.edu/etd/489>

This Thesis is brought to you for free and open access by the Graduate School at ScholarWorks at University of Montana. It has been accepted for inclusion in Graduate Student Theses, Dissertations, & Professional Papers by an authorized administrator of ScholarWorks at University of Montana. For more information, please contact scholarworks@mso.umt.edu.

**GEOMORPHOLOGICAL MAPPING
OF THE K2 AREA, PAKISTAN
USING GIS AND REMOTE SENSING**

By

Deborah Jeanne Belden

B.A., The University of Montana, Missoula, Montana, 2003

Thesis

presented in partial fulfillment of the requirements
for the degree of

Master of Arts
in Geography

The University of Montana
Missoula, MT

Spring 2008

Approved by:

Dr. David A. Strobel, Dean
Graduate School

Dr. Ulrich Kamp, Chairman
Department of Geography

Dr. Anna Klene
Department of Geography

Dr. Scott Woods
Department of Ecosystem and Conservation Sciences

Geomorphological Mapping of the K2 Area, Pakistan, Using GIS and Remote Sensing

Chairperson: Dr. Ulrich Kamp

Geomorphological mapping assists in evaluating the polygenetic role of glaciation, mass movement denudation, and fluvial erosion in landscape development. A series of thirteen 1:100,000 geomorphological maps covering the area between Skardu and K2 were produced using field mapping and photography, GPS measurements, ASTER satellite imagery, and digital elevation model (DEM) analyses. Satellite and morphometric analyses were performed using GIS software. The landforms are described in relation to geology, geomorphological processes, and altitudinal zones. Case studies include flash flood deposits, active landslide areas, sackungen, and rock avalanches. The Skardu Basin has tills preserved on many higher slopes, and sand dunes cover wide areas of fluvial sediments from a braided river system. Extensive alluvial and debris fans make up the Shigar Valley, and a *sackung* follows an anticline on its western ridge. In the narrow Braldu Valley between Dassu and Askole, many fans are deeply dissected, and extensive landsliding is common on the steep slopes. Strath terraces reveal former higher riverbeds and high fluvial erosion rates. Outburst flood deposits from temporary lakes that formed behind former landslides or moraines are located in several locations. Between Skardu and K2, tributary glaciers deposited lateral and terminal moraines. Thick debris covers most of the glaciers; Baltoro Glacier shows a rough topography with countless supra-glacial and para-glacial lakes. Analysis of landform types helps to understand the dominance of individual geomorphological processes. Glacial, fluvial, and tectonic processes each play an important role in the relief production of the study area. This is the first complete geomorphological map series of the area and it provides important insight into the nature of topographic evolution in this region.

Keywords: geomorphology, Karakoram, K2, GIS, glaciation, mapping, Pakistan, remote sensing

DEDICATION

I dedicate this paper to my family. It has been a long time getting here! You have been patient, helpful and encouraging. Mom and Dad, thanks for teaching me the meaning of “Watch me can’t!” Martin and Jessica, you are great cheerleaders. I hope your thesis goes a little bit easier after the experience you gained with mine! Keith, you should get an honorary degree for all the work you have put into my degree! I could not have done it without all of you. You rock!

ACKNOWLEDGEMENTS

This thesis relied on the fieldwork of Dr. Ulrich Kamp and the other participants of the 2005 NSF K2 field trip. Thank you, Ulli, for your time and knowledge to guide me on this project. Thank you to my committee members, Anna Klene and Scott Woods, for your knowledge in the classroom and the time you spent with me through the years to get to this point. This project owes a lot to your expertise. Thank you, Jack Donahue, for introducing me to the field of Geomorphology!

If I have seen farther, it is by standing on the shoulders of giants. -- Isaac Newton

Table of Contents

DEDICATION	iii
ACKNOWLEDGEMENTS	iv
List of Figures	viii
List of Tables	xiii
List of Geology Maps	xiv
List of Cross-Sections	xv
List of Maps	xvi
I. INTRODUCTION	1
1. Background	3
2. Statement of Objectives	9
II. STUDY AREA	10
1. Topography	11
2. Geology	12
3. Climate.....	14
4. Glacial System	15
5. Hydrological System.....	16
6. Vegetation	17
III. METHODS	21
1. Introduction.....	21
2. Field Data.....	21
3. Satellite Imagery and Digital Elevation Model.....	24
4. Google Earth Satellite Imagery.....	25

5. Geological Base Map Preparation.....	26
6. Morphometric Analysis	28
7. Geomorphological Mapping	31
8. Geomorphological Map Preparation.....	34
IV. RESULTS	36
1. Geomorphological Summary	36
2. Past Glaciations.....	37
2.1. Moraines and Till Deposits.....	37
2.2. Trimlines	43
2.3. Roche Moutonnée and Transfluence Pass	46
3. Mass Movements	48
3.1. Rock Avalanches	52
4. Fans	54
5. Terraces	58
5.1. Erosional Terraces.....	58
5.2. Depositional Terraces	59
6. Flood Deposits	61
7. Sackungen	63
8. Geologic Fault Lines	65
V. DISCUSSION	69
1. Skardu Basin	69
1.1. Satpura Lake	69
1.2. Faults.....	71

1.3. Bunthang deposit	73
2. Shigar Valley	76
3. Braldu Valley	80
4. Rivers and Erosion	84
VI. CONCLUSION	85
REFERENCES	88
APPENDIX A	94
Identification Methods	94
Appendix B	98
Coordinate Systems	98
Appendix C	99
Geology	99
Appendix D	105
Cross-sections	105
Appendix E	119
GPS data, coordinates, elevations, reference to photos.	119
APPENDIX F	142
Maps	142

List of Figures

Figure 1. Topographical map after Norin (1925). Scale text is inaccurate. Scale bar represents 60 km. Map is shown to indicate Norin’s study area and generality of features. K2 is in the upper right hand corner.....	2
Figure 2. Location map showing areas mentioned in text. Background is a mosaic of ASTER bands 3, 2, 1 overlain on the ASTER 15×15 m DEM.....	3
Figure 3. Geomorphologic-sedimentological map of the Skardu Basin, mapped by Owen, (Derbyshire and Owen, 1997).....	5
Figure 4. Catastrophic rock avalanche deposits in the Karakoram after Hewitt (1998). Hewitt interprets the deposit in the mouth of the Satpura Valley (“S” in the map) southwest of Skardu as a rock avalanche deposit.	7
Figure 5. K2-Karakoram study area in northern Pakistan. Nanga Parbat and Mt. Everest are shown for geographic reference (satellite image from Google Earth).....	10
Figure 6. Geology of the Karakoram ,Searle et al. (1991). See appendix C for legend and reproduced digital map by D. Belden.	13
Figure 7. (A) Flood plain and alluvial fan in the Shigar Valley. (B) Apricot trees and row crops in Mungo. (C) Poplar trees on the flood plain in the Skardu Basin.....	18
Figure 8. Vegetation on river terrace and on till.....	19
Figure 9. Wheat fields on a river terrace in Askole.	19
Figure 10. Vegetated debris fan at Baltoro Glacier.	20
Figure 11. Grasses on hillside in Urdukas above Baltoro Glacier. Bedrock is polished by glacier.....	20
Figure 12. Strath terrace and roche moutonnées in the Dassu area, and the corresponding geomorphological map of the Dassu area.	22
Figure 13. Shaded relief map of the study area in the K2-Karakoram with GPS locations and data.	23
Figure 14. ASTER 3-2-1 satellite imagery of the study area (left) and generated digital elevation model (DEM; right). Five ASTER scenes were merged to cover the study area.....	24

Figure 15. Potential misinterpretation of landforms due to seasonal snow cover: while the ASTER image (left) leads to the interpretation of a seasonal snowfield covering a moraine, the Google image (right) reveals that it is a rock glacier.	25
Figure 16. Geology map of the study area in the Central Karakoram. The map was digitized using the geological map after Searle (1991). Each color represents a rock type and black lines represent faults. See appendix C for full size map and legend.	27
Figure 17. Digitized geology map overlain on ASTER satellite imagery of the Skardu and Shigar areas showing discrepancies.	28
Figure 18. Maps for glacier interpretation: contours superimposed on; ASTER (left), slope angle (middle), and shaded relief (right).	30
Figure 19. Analysis of geomorphology of the Shigar Valley: field photograph (left), contour and slope angle map (right). The rock avalanche deposit (red box) is visible in the photograph and slope map, but not in the 100 m contour map.	31
Figure 20. Google Earth image (left) and ASTER/GIS data (right) showing a lakebed bench (LB) and the Bunthang sequence (B) in the Skardu Basin.	32
Figure 21. Work map of the Dassu area including GPS locations, view direction of photographs, and notes from field book or GPS entry.	33
Figure 22. ASTER satellite imagery, 3-2-1 composite, overlain on the ASTER DEM. .	35
Figure 23. Lateral moraine, alluvial fan and glacial bench in the Shigar Valley.	38
Figure 24. Skardu Basin. (B) Bunthang deposit; (L) lake sediments; (M) three moraine ridges on Karpochi Rock. (R) Shigar River joining the Indus River at Skardu.	39
Figure 25. Remnant of lateral moraine.	40
Figure 26. In the Askole area, lateral moraines of a former tributary glacier that reached down into the Braldu Valley are surrounded by younger alluvial fans.	40
Figure 27. The terminal moraine of Biafo Glacier and remnants of former lateral moraine. Biafo Glacier is to the left of photo.	41
Figure 28. Glacial till and polish on the Braldu Valley slope south of the Biafo Glacier snout.	42
Figure 29. A lateral moraine along Biafo Glacier is evidence for former higher glacier surface.	42

Figure 30. Trimlines on the northern slope of the Braldu Valley in the fore field of Baltoro Glacier. The convex shape sections in the slope indicate former glacial valley walls. Till also indicates former height of glacier.....	44
Figure 31. Slope profiles identifying three sets of trimlines (see grade breaks) in the Shigar Valley. Cross-section maps for all valleys are reproduced in appendix D....	45
Figure 32. Stronodoka Pass is a U-shaped transfluence pass. It is the result of a former Shigar Valley Glacier. While the main glacier turned west into the Skardu Basin, parts of the ice flowed across the ridge directly south into the Indus Valley.	47
Figure 33. Roche Moutonnée in the Stronodoka Pass east of the Skardu Basin. The flow direction was north (left) to south (right).....	47
Figure 34. Landsliding in the Chakpo area in Braldu Valley. The red box outlines the landslide area in the three figures. Profiles show the narrow gorge of the here antecedent Braldu River. Cross-sections C and D are through landslide and epigenetic gorge. See appendix D for cross-section maps and appendix F for detail maps.	48
Figure 35. Epigenetic gorge associated with an historic landslide near Chakpo in the Braldu Valley.	49
Figure 36. A landslide blocked the road between Askole and Chakpo in the Braldu Valley after heavy rainfall in July 2005.....	50
Figure 37. Older lichen-covered (A) and younger lichen-free (B) boulders in the Dassu gorge testifying the ongoing mass movement activity.	51
Figure 38. Rock avalanche deposit damming the Satpura River and forming the Satpura Lake south of Skardu. Images A and B are looking south. Red dashed lines on Map C are approximate locations of faults. See appendix F for map legend and large scale map.....	52
Figure 39. (A), Rock avalanche deposit and source scarp of the avalanche (red box). (B), Rock avalanche deposit in the Shigar Valley near the confluence with the Basha River.....	53
Figure 40. Debris cone in the Braldu Valley.	54
Figure 41. Vegetated alluvial fan, low, broad deposit in the Shigar Valley.	55

Figure 42. Alluvial fan in the Braldu River valley, with multiple deposition events and fluvial erosion.	56
Figure 43. Geographic location of fans.....	58
Figure 44. Three generations of depositional terraces and one erosional bedrock terrace between Chakpo and Askole in the lower Braldu Valley.	59
Figure 45. Glacial and alluvial river terrace in the upper Braldu Valley. Note people next to boulders for scale.	60
Figure 46. Flood deposits in Chakpo area in the lower Braldu Valley. Note person in photo for scale.....	62
Figure 47. Sackung above Mungo on the ridge separating the Shigar and Braldu valleys. (A) Photo looking down into sackung basin. (B) GoogleEarth image. (C) Geomorphologic map.....	63
Figure 48. Lacustrine sediments, soil and organics within the Mungo sackung depression.	64
Figure 49. Sackung near Bhundo, GoogleEarth image and detail of Skoro map (appendix F).	65
Figure 50. Fault lines (red) in the geological map.....	66
Figure 51. Slope map of the Masherbrum Range in the K2-Karakoram. Light yellow color represents low slope angle. Arrows point to features that are fault related. The red lines are the fault lines after Searle (1991).	67
Figure 52. Bedrock bedding planes (yellow lines) between 45 and 90 degree, and debris fans in the Baltoro Valley.	68
Figure 53. Skardu Basin, showing relative elevations of major features. The Deosai Plateau is south, at the headwaters of the Satpura River.	70
Figure 54. Geology map, each color represents a different rock type. See appendix C for legend. Solid red lines are faults mapped by Searle. Dashed red lines are faults inferred by this study.	72
Figure 55. The former glacial valley floor is evidenced by the curve of the bedrock on the right side of the photo. View is from the Shigar Valley, south into the Skardu Basin.	73
Figure 56. Profile of the glacial valley floor seen in Figure 55.	74

Figure 57. Profile across Skardu Basin, lakebeds, and Bunthang sediments.	74
Figure 58. Skardu Basin with trim lines indicated by arrows.....	75
Figure 59. Shigar Valley. (R) Shigar River, (AF) alluvial fan, (DF) debris fan, and (T) trimline.....	77
Figure 60. Shigar Valley, Upper trim line or planation surface.....	78
Figure 61. Profiles of west side of Shigar Valley, showing trimlines and upper planar surface.....	79
Figure 62. Contours of Planation surfaces at elevations 4200 m and 5200 m. Proposed Basin floor at elevation 3000 m.	80
Figure 63. Braldu Valley seen from the ridge of the Mungo sackung. Here, the valley is a gorge with mass movement deposits and debris fans.	81
Figure 64. Baltoro Glacier and Baltoro Valley with glacial outwash plain.....	82

List of Tables

Table 1. Glacial history, after Seong et al. (2007).	37
Table 2. Distribution of fans throughout the study area.	57

List of Geology Maps

Geology 1. Geology legend after Searle 1991.	100
Geology 2. Geology map based on Searle.	101
Geology 3. Geology and Geomorphology.	102
Geology 4. Faults Geomorphology and ASTER.	103
Geology 5. Glaciers, moraines and fans.	104

List of Cross-Sections

Cross-section 1. Project area.....	106
Cross-section 2. Skardu Basin.	107
Cross-section 3. Skardu Basin trim lines.	108
Cross-section 4. Satpura Lake.....	109
Cross-section 5. Satpura Lake impoundment.	110
Cross-section 6. Shigar valley trim lines.	111
Cross-section 7. Skoro area trim lines.	112
Cross-section 8. Mungo area trim lines.	113
Cross-section 9. Chakpo area.....	114
Cross-section 10. Biafo Glacier trim lines.....	115
Cross-section 11. Paiju area.	116
Cross-section 12. Baltoro Glacier.....	117
Cross-section 13. Concordia trim lines.....	118

List of Maps

Map 1. Legend.....	143
Map 2. Tsordas: ASTER imagery.....	144
Map 3. Tsordas: geomorphological map.....	145
Map 4. Tsordas: slope map.....	146
Map 5. Skardu: ASTER imagery.....	147
Map 6. Skardu: geomorphological map.....	148
Map 7. Skardu: slope map.....	149
Map 8. Shigar: ASTER imagery.....	150
Map 9. Shigar: geomorphological map.....	151
Map 10. Shigar: slope map.....	152
Map 11. Skoro: ASTER imagery.....	153
Map 12. Skoro: geomorphological map.....	154
Map 13. Skoro: slope map.....	155
Map 14. Mungo: ASTER imagery.....	156
Map 15. Mungo: geomorphological map.....	157
Map 16. Mungo: slope map.....	158
Map 17. Dassu: ASTER imagery.....	159
Map 18. Dassu geomorphological map.....	160
Map 19. Dassu slope map.....	161
Map 20. Chakpo: ASTER imagery.....	162
Map 21. Chakpo: geomorphological map.....	163
Map 22. Chakpo: slope map.....	164
Map 23. Askole: ASTER imagery.....	165
Map 24. Askole: geomorphological map.....	166
Map 25. Askole: slope map.....	167
Map 26. Korophon: ASTER imagery.....	168
Map 27. Korophon: geomorphological map.....	169
Map 28. Korophon: slope map.....	170
Map 29. Paiju: ASTER imagery.....	171
Map 30. Paiju: geomorphological map.....	172

Map 31. Paiju: slope map.....	173
Map 32. Liligo Glacier: ASTER imagery.....	174
Map 33. Liligo Glacier: geomorphological map.....	175
Map 34. Liligo Glacier: slope map.	176
Map 35. Biange: ASTER imagery.....	177
Map 36. Biange: geomorphological map.....	178
Map 37. Biange: slope map.	179
Map 38. Concordia: ASTER imagery.....	180
Map 39. Concordia: geomorphological map.	181
Map 40. Concordia: slope map.	182
Map 41. Satpura rock avalanche: ASTER imagery.	183
Map 42. Satpura rock avalanche: geomorphological map.....	184
Map 43. Satpura rock avalanche: slope map.	185
Map 44. Tsago rock avalanche: ASTER imagery.	186
Map 45. Tsago rock avalanche: geomorphological map.	187
Map 46. Tsago rock avalanche: slope map.....	188
Map 47. Mungo sackung: ASTER imagery.....	189
Map 48. Mungo sackung: geomorphological map.	190
Map 49. Mungo sackung: slope map.	191
Map 50. Bhundo sackung: ASTER imagery.....	192
Map 51. Bhundo sackung: geomorphological map.	193
Map 52. Bhundo sackung: slope map.....	194
Map 53. Tostun flood deposits: ASTER imagery.....	195
Map 54. Tostun flood deposits: geomorphological map.	196
Map 55. Tostun flood deposits: slope map.....	197
Map 56. Chakpo flood deposits: ASTER imagery.	198
Map 57. Chakpo flood deposits: geomorphological map.....	199
Map 58. Chakpo flood deposits: slope map.....	200
Map 59. Landsliding and epigenetic gorge: ASTER imagery.....	201
Map 60. Landsliding and epigenetic gorge: geomorphological map.....	202
Map 61. Landsliding and epigenetic gorge: slope map.	203

Map 62. Transfluence pass: ASTER imagery.....	204
Map 63. Transfluence pass: geomorphological map.	205
Map 64. Transfluence pass: slope map.....	206

I. INTRODUCTION

K2, or Chogori as it is known locally, was first identified by T. G. Montgomerie of the British Royal Engineers in 1856. In 1860 and 1861, H. H. Godwin-Austen surveyed the Shigar and Braldu Valleys and Baltoro Glacier. In 1892, W. M. Conway explored the glaciers and valleys of Balistan. The K2 area has been the subject of many geoscientific studies, but a complete geomorphological map of the area had never been produced. The first descriptions of glacial geomorphology in the area were by Drew (1873) and Dainelli (1922). Drew (1873) concentrated on the alluvial and lacustrine deposits. Dainelli (1922) described four glacial advances based on valley floor deposits and perceived terminal moraines. Norin (1925) produced a map to accompany his “Preliminary Notes on the Late Quaternary Glaciation of the North-Western Himalaya” (Figure 1). His base map was the Survey of India map, scale 1:1,000,000, on which he indicated lacustrine and glacial deposits. These include conglomerates, gravels, and terminal moraines. In his opening statement, Norin (1925: p.165) wrote:

“During my work in the Kashmir and Balistan I encountered several interesting phenomena, which seemed to me to be of importance as to their bearing on the question of a former extensive glaciation within these regions. The short time at my disposal has not permitted such a thorough survey of certain points as may be necessary for a definite solution of the problems. If notwithstanding I publish these notes, it is for the purpose of drawing the attention of later visitors to these still debatable problems.”

This thesis will address these debatable problems. Geomorphological mapping between Skardu and K2, including the Skardu Basin, Shigar and Braldu valleys, will identify erosional and depositional landforms (Figure 2). The ultimate outcome is an

understanding of the influence of glaciation, mass movement, and fluvial erosion on shaping the landscape of the K2-Karakoram.



Figure 1. Topographical map after Norin (1925). Scale text is inaccurate. Scale bar represents 60 km. Map is shown to indicate Norin’s study area and generality of features. K2 is in the upper right hand corner.

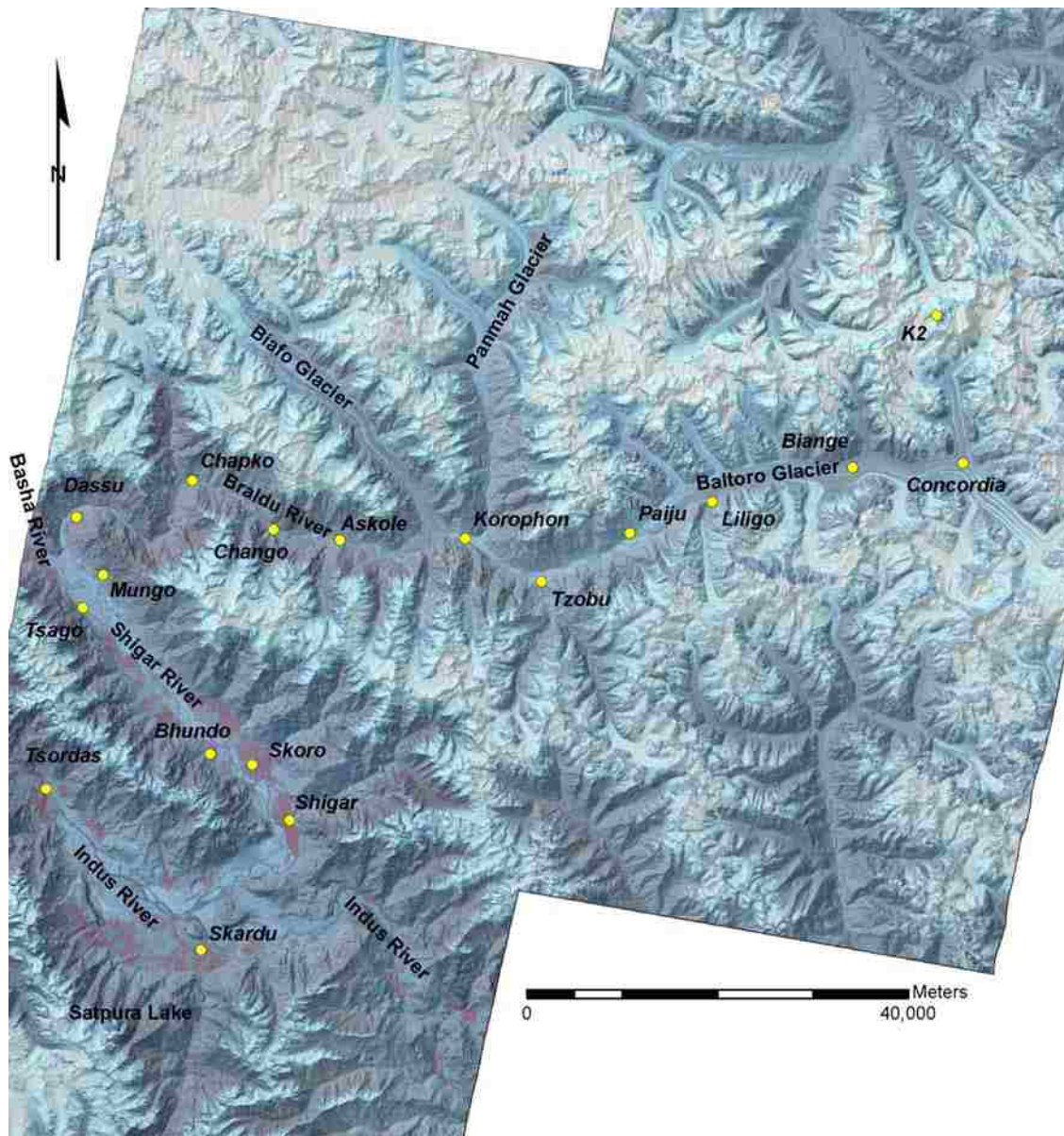


Figure 2. Location map showing areas mentioned in text. Background is a mosaic of ASTER bands 3, 2, 1 overlain on the ASTER 15×15 m DEM.

1. Background

The studies of Dainelli (1922) and Norin (1925) formed the basis for interpreting the general geomorphology and glacial history of the Central Karakoram. Norin (1925) described Balistan as a region of rift valleys and found large terminal moraines at

elevations of ~2400 m above sea level (asl). He reconstructed four glaciations whose glaciers dammed the valleys with large moraines, creating lakes in many places. His map indicates lacustrine sediments along the valley walls from Katarah to the confluence of the Basha and Braldu rivers. Within the Braldu Valley, Norin (1925) identified two terminal moraines with the upstream moraine impounding glacial gravels and varves. Subsequent studies confirmed or rejected such early hypothesis of four former glaciations and the designation of moraines.

The geomorphology and sediments of the Skardu Basin were intensively mapped by Owen (1988, in Derbyshire and Owen, 1997), who identified, terraces of floodplains, and fluvial, glaciofluvial and till sediments (Figure 3). Hewitt (1995, 1998, 2002) focused on the rock avalanches found through out the Karakoram, some of which were misidentified as moraines in earlier studies, and the altitudinal zoning of geomorphic processes. The Bunthang sediments on the northern side of the Skardu Basin were first mapped by Dainelli (1922) as morainal and lacustrine material from his second and third glacial stages, respectively. Norin (1925) interpreted the sequence as Indus conglomerates. Cronin (1989, 1993) described them as a 1.24 km thick sequence of glacial, fluvial, lacustrine and alluvial strata. The upper part of this sequence dates to >0.73 Ma based on reversed magnetized mudstone dating. The till at the sequence's bottom has not been dated, but a correlation with the Jalipur till suggests that the Bunthang till is less than 2 Ma old, and represents the oldest sediment exposed in the basin. It is described as being a coarse boulder conglomerate that is also exposed on the Rock of Skardu (Karpochi).

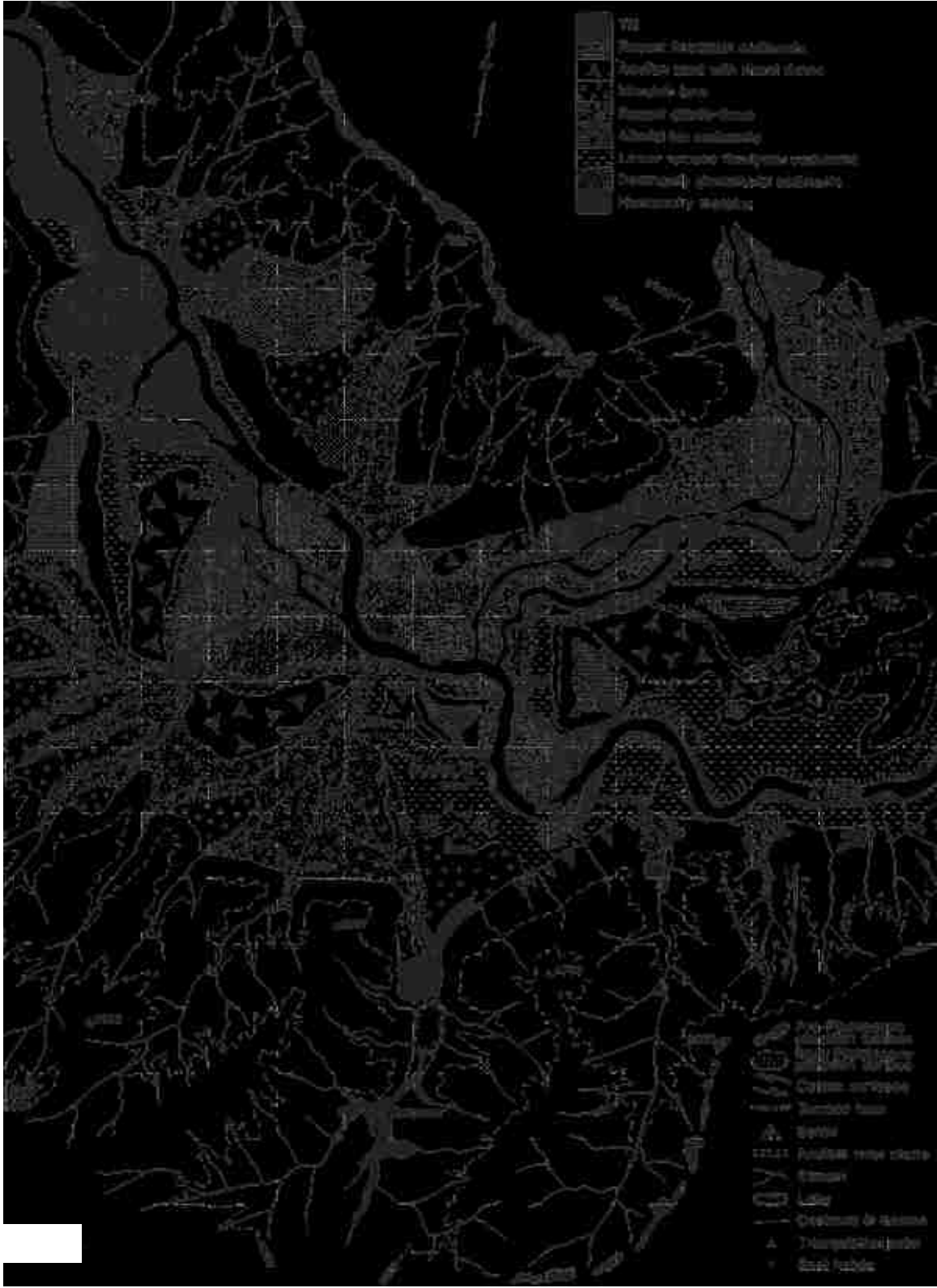


Figure 3. Geomorphologic-sedimentological map of the Skardu Basin, mapped by Owen, (Derbyshire and Owen, 1997).

A landform that is still under debate is the dam of Satpura Lake: is it a terminal moraine or a rock avalanche? Both Cronin (1989) and Owen (1988) agreed with Norin's (1925) original interpretation that Satpura Lake formed behind a terminal moraine. One of Owen's (1988) arguments was that terrace sediments in the mouth of Satpura Valley were deformed by a former Satpura Glacier. In contrast, Hewitt (1995, 1998, and 2002) concluded that Satpura Lake was impounded by a rock avalanche (Figure 4). Seong et al. (2007) mapped portions of the Shigar and Braldu valleys and carried out extensive terrestrial cosmogenic nuclide (TCN) surface exposure dating. Seong et al. (2007) concluded that because of the deformation structures in the Satpura fluvial-lacustrine terraces and their similarity to other terrace structures in the Skardu Basin, the impoundment is a moraine with glaciotectonized sediments. However, they refrained from using this feature to reconstruct the glacial history because of the low equilibrium-line that would be required.

This is an example of how geomorphological mapping will benefit science. It will elucidate the mechanism that created the dam, and therefore the glacial history.

The Karakoram Mountains have been rising since the Indian Plate collided with the Asian Plate about 50 million years ago. Foster et al. (1994) concluded that significant uplift and denudation have occurred over the past 20 million years. The authors used fission-track thermochronology and calculated that 3-4 km of rock has been removed from above the peak of K2, which translates into an exhumation rate of 3-6 mm/yr beginning ~ 5-3 Ma, followed by a rate of 0.5-1 mm/yr after ~2 Ma. The rates may have varied between glacial and interglacial periods.

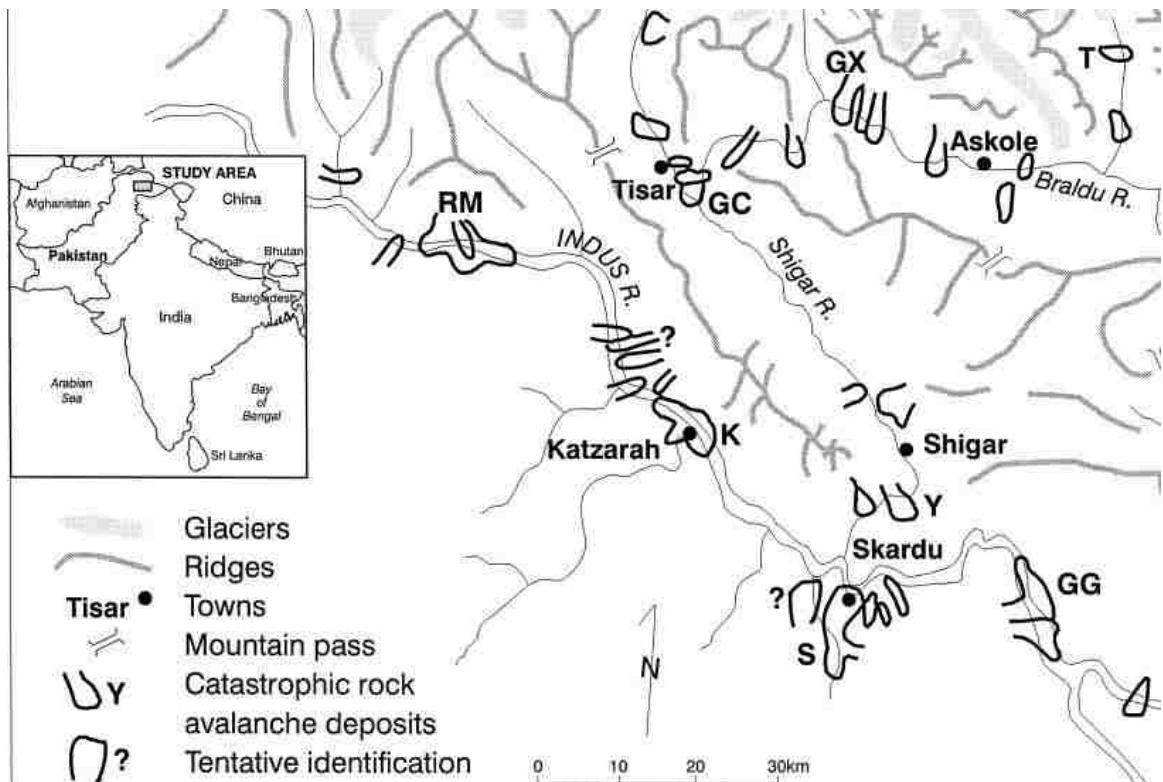


Figure 4. Catastrophic rock avalanche deposits in the Karakoram after Hewitt (1998). Hewitt interprets the deposit in the mouth of the Satpura Valley (“S” in the map) southwest of Skardu as a rock avalanche deposit.

Currently, K2 is rising 2-6 mm/yr (Seong et al., 2008a), and the scientific question is what causes this fast uplift? Is tectonics or denudation responsible for the high uplift rates?

In the French western Alps, van der Beek and Bourbon (2008) studied the morphology to quantify the glacial impact on relief. Their measurements of isostatic relief were insufficient to offset topographic lowering due to denudation. They concluded that isostatic response to glacial erosion has not increased peak elevations significantly.

At Nanga Parbat, the ninth-highest mountain in the world in the nearby western Himalaya, unroofing seems to have been initiated with the capture and diversion of the

Indus River across the massif (Shroder and Bishop, 2000). The river cut down rapidly to become a deep superposed-antecedent trench. Local erosion forced uplift because of rapid surficial unloading, and was reinforced by a positive feedback. As the valleys grew deeper the mountains rose higher. Bishop et al. (2002) conducted spatial analysis of the Nanga Parbat topography using digital elevation models (DEMs). Their results showed that the greatest mesoscale relief was from glaciation. Glaciers had a significant impact on the landscape in terms of erosion and therefore uplift. However, glaciers flowed down the same valleys as now occupied by the Indus and Astor rivers, and it is uncertain how much of the macroscale relief is actually attributable to present day river incision. Therefore, it is important to differentiate between the effects of fluvial erosion and those of glacial erosion.

No high-discharge river exists in proximity of K2 in the Central Karakoram. Therefore, it is the ideal location to study the role of glaciers in denudation processes and shaping the landscape. Seong et al. (2007) defined four glacial stages for the Central Karakoram: Bunthang glacial stage (>0.7 Ma); Skardu glacial stage (marine oxygen isotope stage [MIS] 6 or older); Mungo glacial stage (MIS 2); and Askole glacial stage (Holocene). The authors described that Baltoro Glacier advanced 80 km during the Mungo glacial stage, and a few kilometers from its present ice margin during the Askole glacial stage.

This recent deglaciation is also ideal to study the effects of deglaciation on the landscape. In western Norway, Ballantyne and Benn (1994) studied slope adjustment and resedimentation after deglaciation and found that there was a minimum erosion rate of 50-100 mm/yr. The gradient of the upper rectilinear hill slope was lowered by an average

of 5 degrees, and the lower concave slope had partial infilling, resulting in a gentler overall slope. Debris flows were the main cause of sediment transfer from gullies to fans.

Following deglaciation there is enhanced rock-slope failure due to a combination of stress release and debuttressing (Ballantyne, 2003). Rates of rockwall retreat due to stress-release are roughly an order of magnitude higher than those rates due to freeze-thaw. There is also a temporal pattern of paraglacial rock-slope adjustment. At a study site in the Scottish Highlands, 80% of the talus accumulation occurred within 6,000 years of deglaciation, and only about 20% in the following 11,000 years (Ballantyne, 2003). A model was proposed that the probability of slope failure decreases exponentially with time elapsed since deglaciation.

2. Statement of Objectives

This thesis will use GIS and remote sensing to inventory and map the geomorphological features of the Skardu Basin, Shigar and Braldu Valleys, and Baltoro Glacier. The maps will be used to analyze and identify the agents of landscape evolution in this region of the Karakoram. The analysis will be valuable to resolve past differences in descriptions and aid in future scientific work in the area.

II. STUDY AREA

The study area (35-36° N; 75-77° E) is situated in northeastern Pakistan in the Central Karakoram (Figure 5). It includes the Skardu Basin, and the Indus, Shigar, and Braldu valleys (Figure 2). The Braldu Valley leads to K2, at 8611 m asl the second tallest mountain in the world, at the border with China. The Central Karakoram lies within the India-Asian convergent plate boundary north of the Nanga Parbat-Haramosh syntaxis and includes more than sixty peaks rising above 7000 m asl; besides K2, three other peaks rise above 8000 m asl.

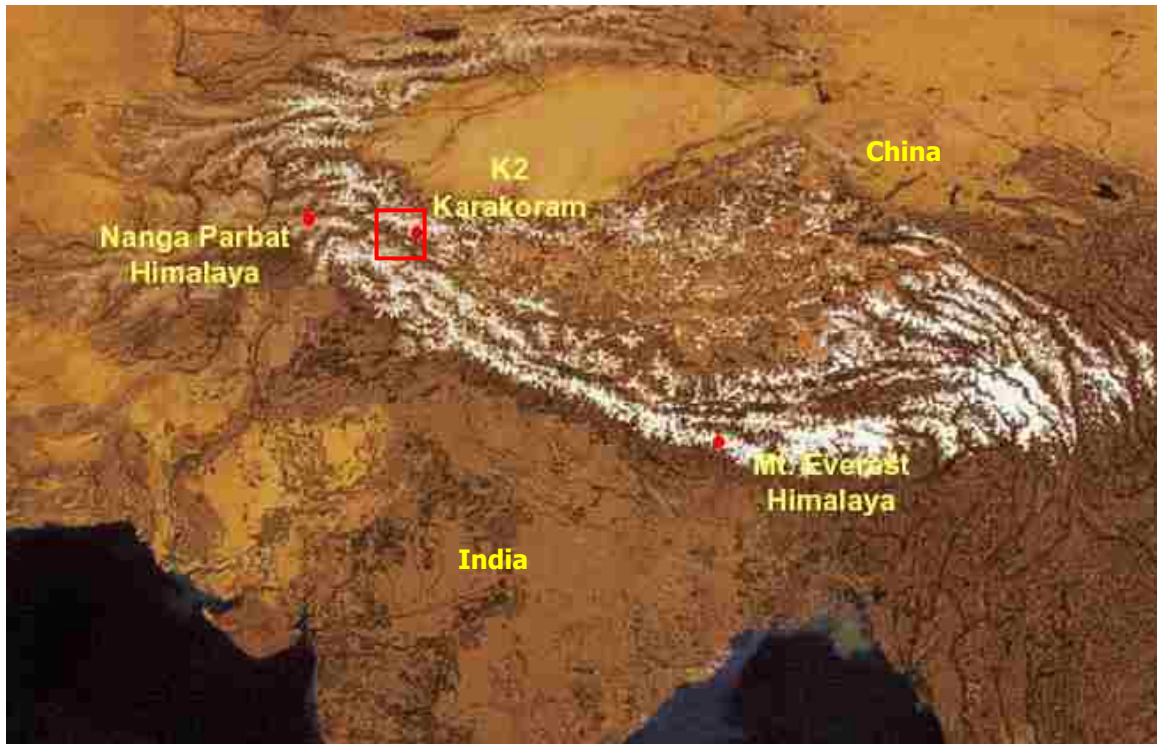


Figure 5. K2-Karakoram study area in northern Pakistan. Nanga Parbat and Mt. Everest are shown for geographic reference (satellite image from Google Earth).

1. Topography

The project area has a relief of ~ 6411 m, from the basin at Skardu to the peak of K2. The description of the project area starts downstream and progresses up river. The confluence of the Indus and Shigar Rivers is the Skardu Basin, an 8000 m wide basin filled with mainly lacustrine and glacial/glaciofluvial sediments. The Shigar Valley is 4000-5000 m wide between the Haramosh and Masherbrum Ranges. The Basha and Braldu Rivers join to form the Shigar River. Valley slopes have a mean angle of 33° and a maximum of 55°. However, nearly vertical slopes exist in each of the bordering mountain ranges. The Shigar Valley is filled with extensive debris and alluvial fans. At the junction of the Braldu and Shigar rivers, a 300 m wide gorge section starts and reaches in an eastward direction upstream to the village of Chakpo. The gorge section of the here antecedent Braldu Valley is the result of intensive uplift of the surrounding mountain ridges. Tectonically, this section is part of a plunging anticline along the Main Karakoram Thrust (MKT) through the Masherbrum Range. The valley sides have a mean angle of 33° and are locally as steep as 60°. Although this section is steep and narrow, many terraces of valley fills exist. Beyond Chakpo, the Braldu Valley begins to widen and is filled with sediment fans. It is 900 m wide east of Askole in the area of Korophon, where the Biafo and Panmah glaciers terminate into the Braldu Valley. Beyond Korophon, the valley narrows again until it reaches the terminus area of the Baltoro Glacier, an area dominated by glacial, glaciofluvial, and fluvial sediments. Here, the Baltoro Valley starts and reaches upstream to Concordia at K2. The Baltoro Valley is up to 2000 m wide with generally steep slopes of often 35-47°, and locally the steepness of the slopes precludes much snow accumulation. Baltoro Glacier is debris-covered and has

an average gradient of 5° , with a gradient of approximately 11° near the terminus. While it is longitudinal to the Braldu River, the other active glaciers of the study area are transverse to the river valleys.

2. Geology

The geology of the area is comprised of three main units (Figure 6): (1) the northern Karakoram terrane with sandstone, limestone and shale, (2) the Karakoram batholith comprised of gneiss, granodiorites, and leucogranite, and (3) the Karakoram metamorphic complex including meta-sediments and orthogneiss (Searle et al., 1986, 1987, 1989). The Haramosh Range is comprised of the Kohistan-Ladakh batholith; the Masherbrum Range and Biafo Glacier region are Karakoram metamorphic series; the Baltoro Glacier region includes Karakoram granitoids. K2, Broad Peak and Muztagh Tower are gneiss. The K2 orthogneiss and Muztagh Tower units predate the India-Eurasia collision and represent Cretaceous subduction along the Shyok Suture. The youngest unit, the Baltoro Plutonic Unit (BPU), is a magmatic phase of the Karakoram batholith with an age of ~ 21 Ma. The BPU makes up the majority of the volume in the Central Karakoram.

The Karakoram Fault (KF) is a right-lateral strike-slip fault aligned NW-SE on the northeastern side of K2. Between 37° and 34° N the fault is transpression, while between 34° and 32° N it is transtension with a 27-km-wide bend in the fault (Rateman et al., 2007). Consequently, there is 150 km of displacement in the Baltoro granite (Searle et al., 1989; Rateman, 2007).

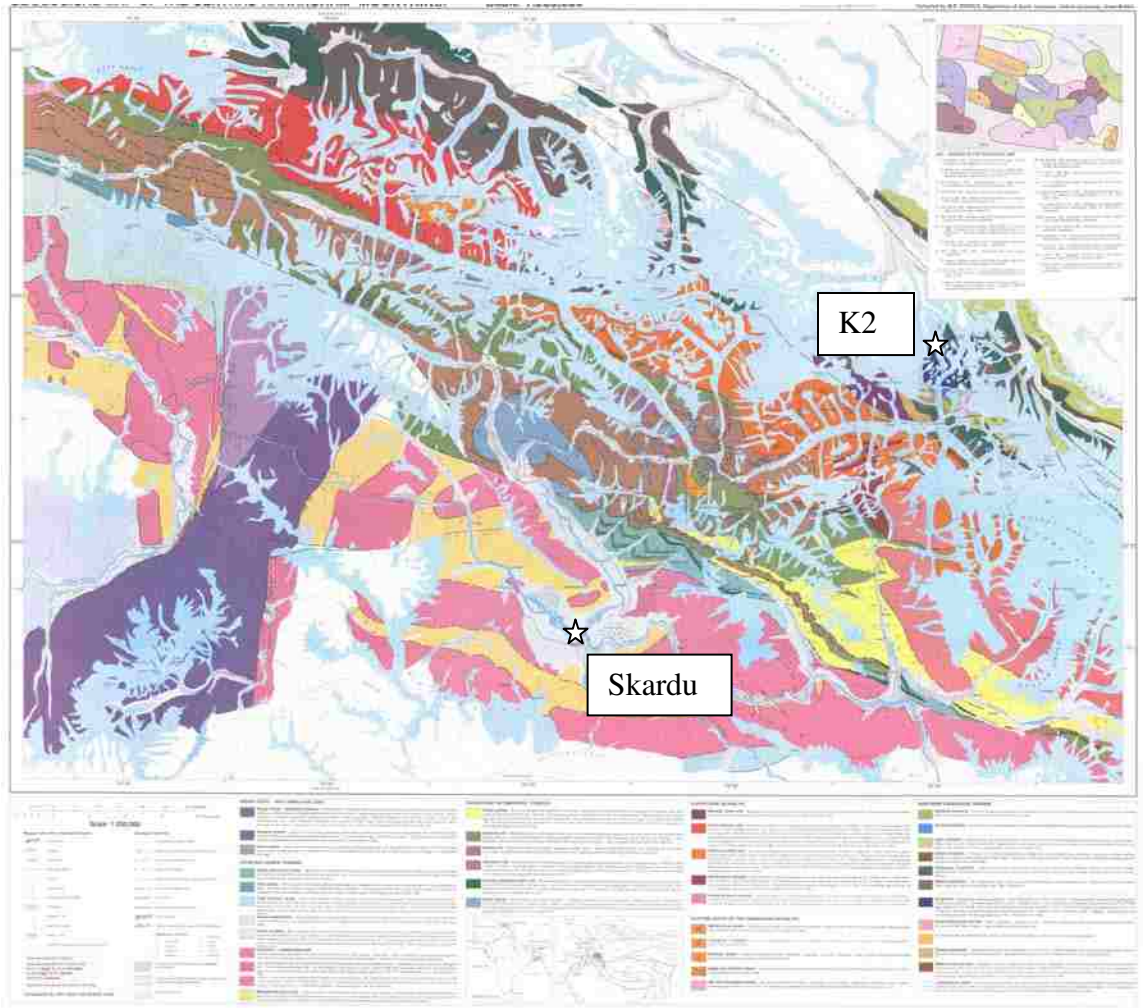


Figure 6. Geology of the Karakoram ,Searle et al. (1991). See appendix C for legend and reproduced digital map by D. Belden.

The Karakoram plate is bounded on the south by the Shyok Suture Zone (SSZ). In the late Tertiary, the SSZ was reactivated by a breakback thrust, the Main Karakoram Thrust (MKT). The MKT travels through the Masherbrum Range. Where it passes through the Braldu Gorge at Dassu, high-grade metamorphic rocks occur on the hanging wall. The northeast side of the MKT is gneiss and schist, while the southwest side, which includes the Shigar Valley, is phyllite, limestone, marl, serpentinite and volcanoclastic conglomerate (Searle et al., 1989).

South of Skardu, two faults curve and meet in the mountains to the east of Satpura Lake. It is a junction of metasedimentary rocks and batholith. There are many more faults, thrust, normal, and strike-slip, within the Central Karakoram (appendix C). The evidence for the faults is the incongruent rock types that adjoin one another.

3. Climate

Hewitt (1989) describes four different altitudinal climate zones in the Karakoram. The arid lands of Zone IV (below 3000 m asl) are subject to drought and desiccating winds. Zone III (~3000-4000 m asl) is a cool sub-humid belt with warm summers, with snow cover for 3-8 months. Zone II (~4000-5500 m asl) is a cold humid belt, with snow cover for 8-11 months. Zones II and III are the areas most subject to freeze-thaw cycles, which can last from 2-12 weeks. Zone I (>5500 m asl) is the perennial ice belt, where glaciers exist and snow avalanches occur.

The climate of the Central Karakoram is humid continental to semi-arid cold desert and characterized by variable weather patterns and large seasonal temperature differences. Temperatures are extreme, with summer highs of 32°C and winter lows of -10°C measured at Skardu (Rao, 2003). Precipitation patterns vary greatly with elevation, aspect, and local relief. The December to May, mean precipitation at Skardu is 166.7 mm, with a maximum of 45 mm falling in March; for June to November it is 72.6 mm, with the minimum of 10.6 mm falling in November (Rao, 2003). Below 3000 m asl, precipitation is less than 200 mm annually. There is an orographic gradient

of precipitation, and above 6000 m asl, the equivalent of 2000 mm falls as snow each year (Khan et al., 2003). Snow accumulation on the Central Karakoram measured at the weather station in Skardu, averaged from 1981-1997, shows that two-thirds occur in winter and spring, supplied by mid-latitude westerlies, while the other one-third are supplied by the Indian summer monsoon (Hewitt, 1989).

4. Glacial System

The Central Karakoram is one of the most heavily glaciated areas outside the Polar Regions. Biafo Glacier is 63 km long and Baltoro Glacier is >30 km long. During past glacial periods, many glaciers were considerably longer, with glaciers reaching into the Skardu Basin (Seong et al., 2007). The glaciers are of winter accumulation type and fed by snowfall and snow avalanching in higher elevations. The avalanches consist of rock as well as snow, and therefore many glaciers are covered by thick debris. If the rock component is higher than the snow and ice component, such as in a decaying glacier or an ice-cored moraine, a rock glacier may form.

Glacier flow rates, as measured by glacial melt, ranges between 100 and 1000 m/year. There is evidence for flow rates of 30 m/day for a glacier in the 1800's (Ahmed, 2003). This high rate of flow results in active glacier erosion and transportation of erosion materials.

The thick debris cover affects the annual ablation rate and the meltwater production. The debris shields and insulates the ice and in some cases, a glacier's terminus exists at lower elevations because of this protection (Shroder et al., 2000). The

heavy debris cover of the ablation zones buffers the glaciers from climate change and may explain the poor correlation of the nineteenth century “Little Ice Age” with the Alps (Hewitt, 1998b).

Globally most glaciers have been receding in past years. However, there are glaciers in the Karakoram that are of surge type and have advanced in recent years, such as Liligo Glacier that joins the Baltoro Glacier (Hewitt, 1998b). All the surging Karakoram glaciers are avalanche-fed and debris-covered.

5. Hydrological System

A major source of water for this area is snowmelt and glacial melt water. Mihalcea et al., (2007) measured the ablation rate on Baltoro Glacier and calculated the meltwater production above 3900 m asl to be about $1.3 \text{ km}^3 \text{ a}^{-1}$. This is comparable to the estimated $1.8 \text{ km}^3 \text{ a}^{-1}$ cumulative precipitation for the Baltoro catchment area. The glaciers of Pakistan’s Northern Areas have been described as having very high “activity indices” (Ahmed, 2003), a measure of the total amount of water that passes through a glacier system each year. The melting of ice has a significant impact on stream flows. The streams of the upper Indus River begin to rise in March with an increase in May. Between July and August, 40-70% of the total runoff occurs, with the discharge being 15-40 times the amount of March runoff (Ahmed, 2003). The Indus River, below the confluence of the Shyok and Braldu rivers has an annual runoff of 240 mm of water, considerably more than the annual precipitation. The discrepancy is due to snowmelt.

6. Vegetation

Because of diverse precipitation patterns and the extreme relief of ~6411 m between Skardu and K2, the vegetation ranges from desert to alpine. There are no natural forests in the study area. In general, vegetation is limited to the depositional environments: flood plains, alluvial fans, former river terraces and moraines (Figure 7 - 9). At higher elevations, vegetation can be found on debris fans and till covers located between the glaciers and the snowline (Figure 10 and Figure 11). The characteristic vegetation is northern dry scrub and includes *Artemisia*, *Berberis*, *Ribes*, *Rosa*, Juniper, Poplar, *Viburnum*, and Willow (Rao et al., 2003). Only 2% of the Northern Areas is cultivable, and presently, only half of the cultivable land is being used to grow grain crops, fruits and vegetables (Khan, 2003). Produce includes wheat, buckwheat, barley, apricot, cherry, apple, mulberry, almond, walnut, potatoes, cabbage, tomatoes, turnips, and onions.

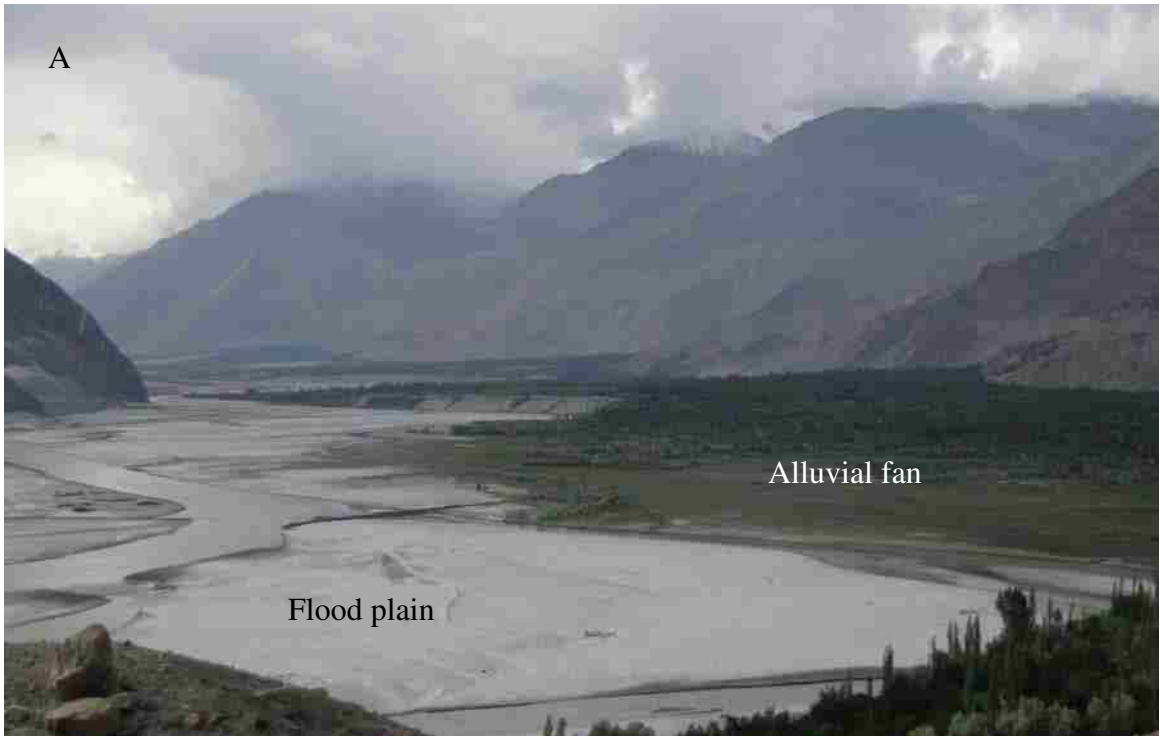


Figure 7. (A) Flood plain and alluvial fan in the Shigar Valley. (B) Apricot trees and row crops in Mungo. (C) Poplar trees on the flood plain in the Skardu Basin.



Figure 8. Vegetation on river terrace and on till.



Figure 9. Wheat fields on a river terrace in Askole.



Figure 10. Vegetated debris fan at Baltoro Glacier.



Figure 11. Grasses on hillside in Urdukas above Baltoro Glacier. Bedrock is polished by glacier.

III. METHODS

1. Introduction

In summer 2005, a National Science Foundation-funded team of geologists, geomorphologists, glaciologists, and climatologists traveled from the city of Skardu to Concordia and further to the K2 base camp to collect geoscientific data meant to improve the understanding of landscape evolution and develop a chronology of former glaciations in the Central Karakoram. The author was not a part of the expedition, however, she had access to all the notes, mapping, global positioning system (GPS) measurements, and hundreds of photographs from the field study to use as the basis for the geomorphological analysis. This thesis is her individual analysis of the geomorphology.

2. Field Data

Photographs from the field, taken by several team members, were organized as a photo inventory covering the complete scientific expedition from Skardu to K2 and back to Skardu. In addition, more than 500 GPS measurements using standard handheld GPS receivers (Garmin) had been taken at each photo point and other points of interest. A Microsoft Excel file was created that listed each GPS point, the photographer, date, photo numbers, site description, coordinates, elevation, and other comments (appendix E). The inventory includes general landscape panoramas and photos of sites of specific interest. The photos are essential for the analysis and understanding of landforms and geomorphic processes. For example, photos help in the interpretation of the stratigraphy of valley

fills such as terraces, fans, fluvial deposits, and till (Figure 8). In addition, the pattern of vegetation and land use cover is identifiable (Figure 9).

The photo inventory includes field notes and field sketch maps taken by team members. For example, the local geomorphology had been hand drawn in the field onto a satellite image at an approximate scale of 1:28,000 for a portion of the area. This information had to be generalized for the 1:100,000 scale of the final geomorphological maps. The mapping and photos were critical for the identification of features such as terrace generations and roche moutonnées (Figure 12).

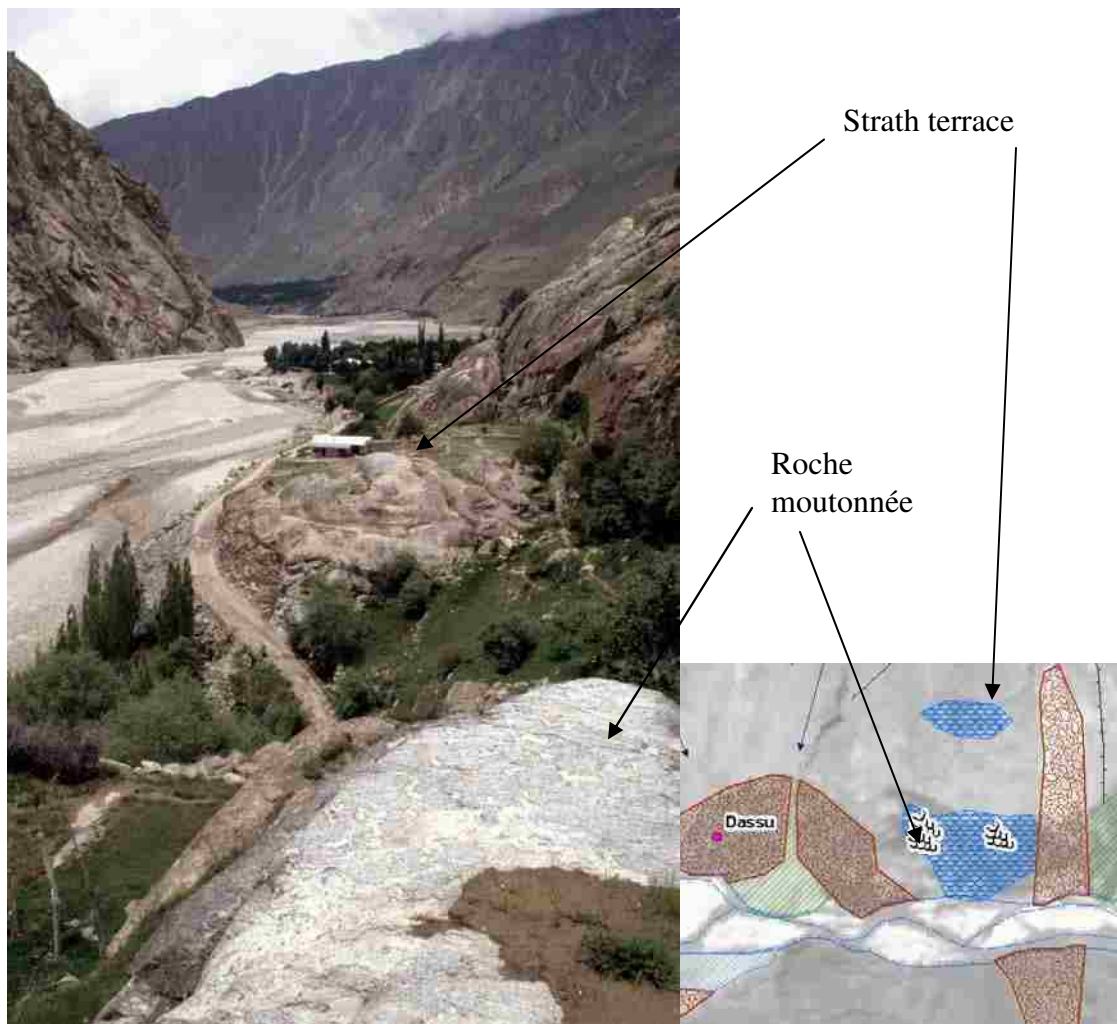


Figure 12. Strath terrace and roche moutonnées in the Dassu area, and the corresponding geomorphological map of the Dassu area.

Photographs, field notes and field maps were matched with the GPS points (Figure 13), which were then transferred to an Excel spreadsheet and finally saved as an ArcGIS-readable file format (dbf).

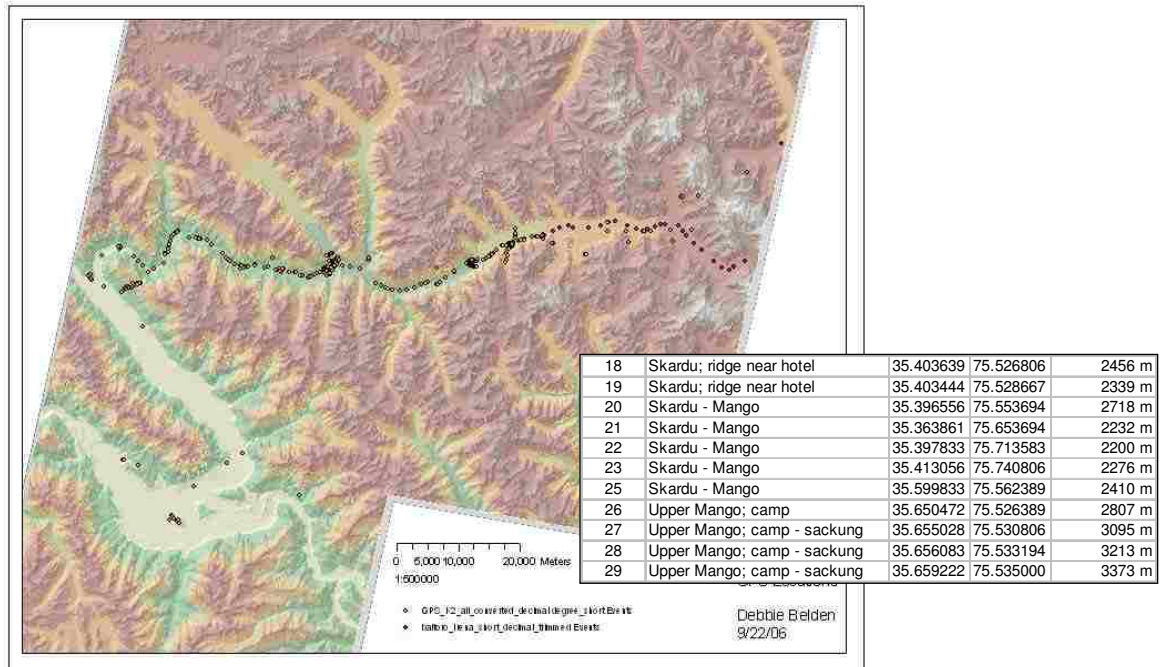


Figure 13. Shaded relief map of the study area in the K2-Karakoram with GPS locations and data.

These photographs, GPS points, and field notes support the lab-based interpretation of the geomorphology. Topological maps, geological maps, and satellite imagery are the basis for geomorphological mapping using legends after Kneisel et al., (1998) and Kamp (1999).

3. Satellite Imagery and Digital Elevation Model

ASTER (Advanced Spaceborne Thermal Emission and Reflection Radiometer) satellite data were used for visual interpretation of geomorphology and basic geomorphometric analysis. ASTER imagery is stereographic and allows the generation of digital elevation models (DEMs) using the visible and near infra-red (VNIR) nadir and backward images (3N and 3B; Kamp et al., 2003). For the study area, a DEM with a horizontal resolution of 15 m was generated using the software SILCAST 1.05 by Jeffrey Olsenholler, Department of Geography and Geology, University of Nebraska – Omaha (Figure 14). To cover the entire study area, five ASTER scenes were merged into a mosaic using the software PCI Geomatica 10.02 (09-11-2000, 05-18-2001, 05-18-2001, 10-03-2002, and 08-28-2004). The mosaic was orthorectified using the DEM, then trimmed to the size of the final study area. The author clipped the mosaic and DEM into four smaller sub-scenes for easier data handling.

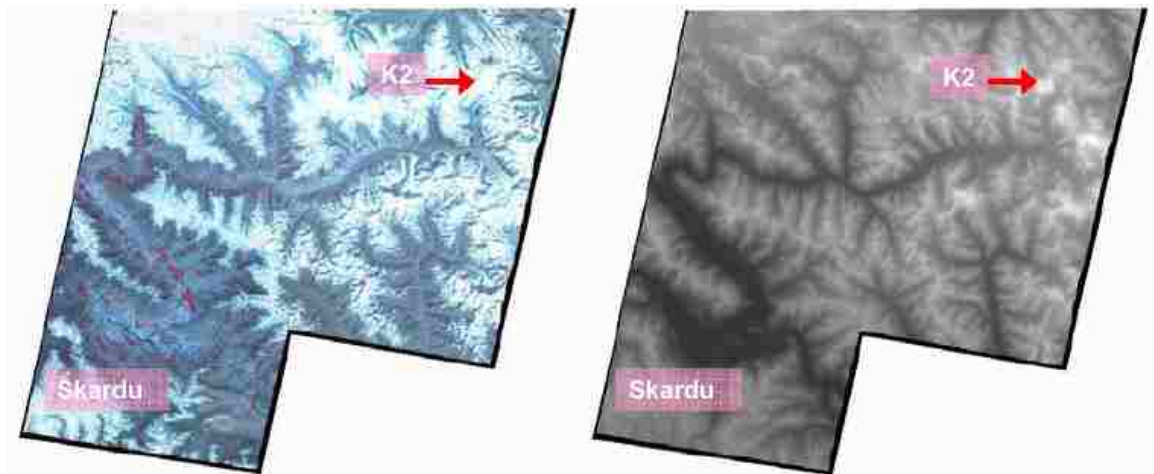


Figure 14. ASTER 3-2-1 satellite imagery of the study area (left) and generated digital elevation model (DEM; right). Five ASTER scenes were merged to cover the study area.

4. Google Earth Satellite Imagery

To aid in the analysis, Google Earth imagery (Image © 2007 TerraMetrics, ©2007 Europa Technologies) was used to supplement the ASTER data and increase the accuracy of the interpretations. Google Earth allows zooming into a feature and viewing in 3D from different angles. Viewing a feature from a landscape perspective rather than a map perspective often made feature identification easier. Several features, such as a sackung and lakebed, will be discussed that were analyzed with GoogleEarth. Care had to be taken when dealing with snow cover in the imagery, because of varying acquisition dates. Google Earth Digital Global Coverage is a mosaic of data from 2002 to 2007; the ASTER scenes used in this thesis date from 2000 to 2004. An example of potential misinterpretation is shown in Figure 15: while the ASTER image leads to the interpretation of a white snowfield, the Google image presents a dry landscape. The analysis revealed that the lobate feature visible in the Google image is a rock glacier and not, as suggested by the ASTER image, a moraine with seasonal snow cover.

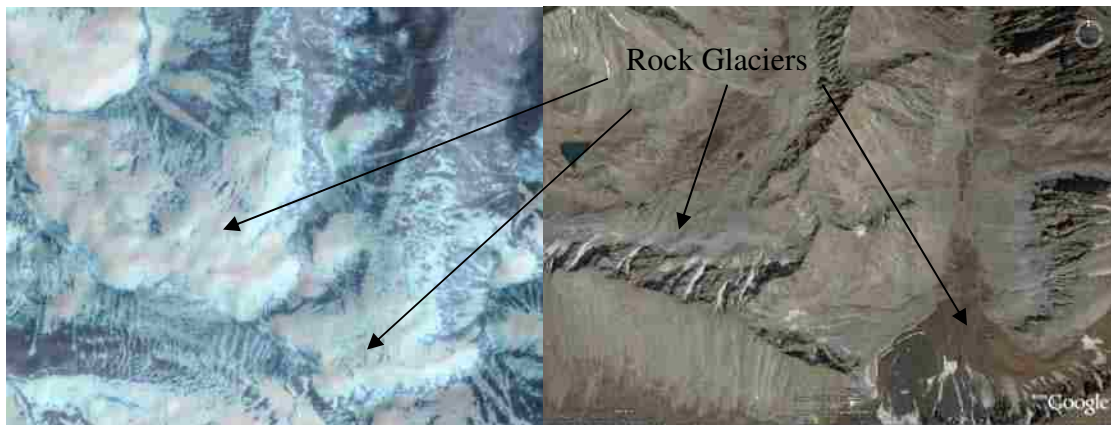


Figure 15. Potential misinterpretation of landforms due to seasonal snow cover: while the ASTER image (left) leads to the interpretation of a seasonal snowfield covering a moraine, the Google image (right) reveals that it is a rock glacier.

5. Geological Base Map Preparation

Using ESRI's ArcGIS 9.1 software, a geodatabase with feature sets for the study area was created to include digitized points, lines and polygons and additional metadata such as lithology and settlements. Using Editor, new features were digitized in feature classes that had been created.

First, the geological map by Searle (1991) (Figure 6) was scanned to a digital image and then cropped to the size of the study area. The scanned image was orthorectified using four reference points employing the GeoRef_affine feature in ArcGIS (for details about the spatial reference see appendix B). In the digitizing process, the geology features of Searle's map were traced by rock type using the sketch tool. Each fault line was also digitized. After the feature was created, the feature was identified in the attribute table using a geologic abbreviation. In this manner, the original paper map was transferred into a digital map (Figure 16). While Searle's original map is of a small scale of 1:250,000 and therefore highly generalizes the geology, the digital map is at a scale of 1:100,000 or larger depending on the complexity of the underlying geology. As a result, the digital geological map does not overlay exactly with the ASTER imagery (Figure 17). Consequently, for the geomorphological analysis, conclusions from geological and tectonic features could only be made in general terms.

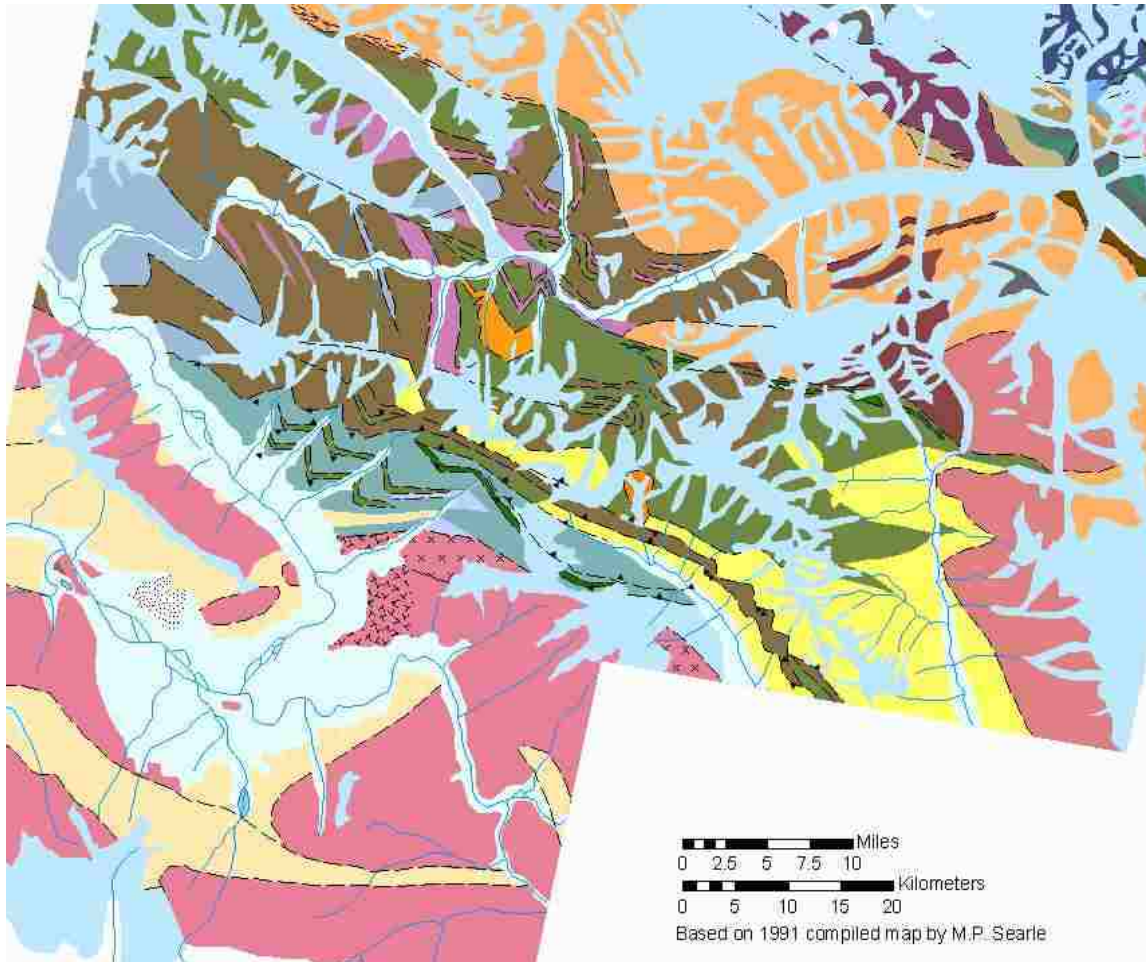


Figure 16. Geology map of the study area in the Central Karakoram. The map was digitized using the geological map after Searle (1991). Each color represents a rock type and black lines represent faults. See appendix C for full size map and legend.

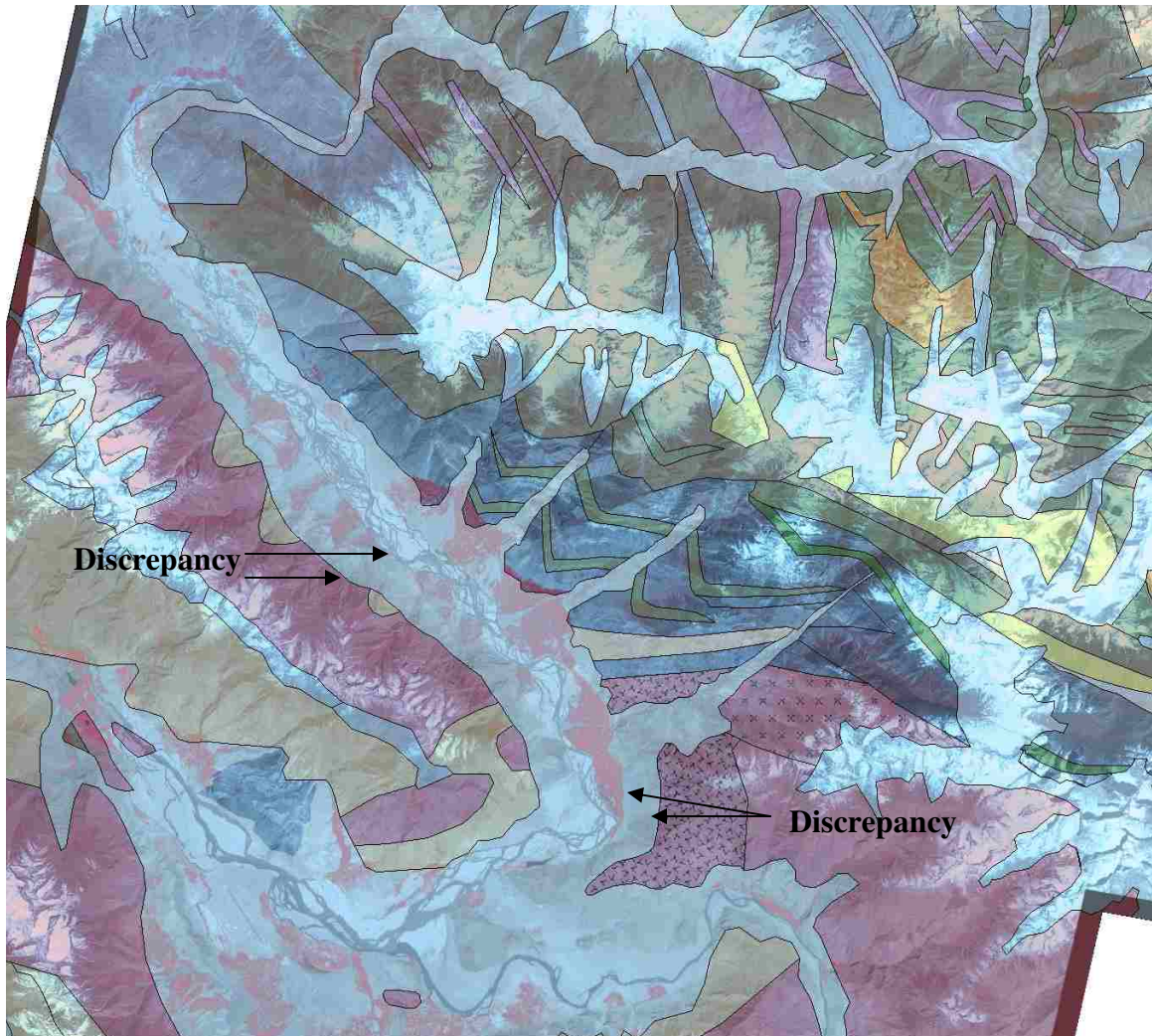


Figure 17. Digitized geology map overlain on ASTER satellite imagery of the Skardu and Shigar areas showing discrepancies.

6. Morphometric Analysis

Maps of contours, slope, and hillshade were extracted, by the author, from the ASTER DEM using ArcGIS 3D Analyst. These maps are in appendix F. The contour intervals were set to 100 m for the general maps and 25 m for the detail maps. The slope map comprises six classes of slope gradient (in degrees): 0-3, 3-12, 12-24, 24-36, 36-45, and 45-90. The color becomes darker as the slope becomes steeper. The slope classes

were assigned based on natural breaks in the data and calculated standard deviations. The intent was to have each landform fall into a unique slope category and to utilize the difference in the angle of repose for various materials. Manual classification, rather than automatic classification, was necessary so that each map would have the same categories. The hillshade is based on the 15m × 15 m cell size of the raster data, with the image drawn along a stretched value color ramp. The slope map and the hillshade map are each built from the 15 m pixel and have a higher degree of detail than the contour map, with a 100 m horizontal resolution.

Each map best represented a different facet of the terrain (appendix F). The three-dimensional view of hillshade was used to define topography of hills and valleys. The slope map detected areas of low slope angle and grade breaks. The contour map helped differentiate between V-shaped and U-shaped valleys. Cross-sections of the contour maps were used to verify locations of terraces and trimlines (appendix D).

In many cases, a combination of two or all three of these maps was necessary for an unambiguous interpretation of landforms. For example, in Figure 18, the ASTER image shows “white” (i.e., flat area) at the head of the valley, but not in the course of the valley. Only the combined slope and contour map shows characteristic patterns of low slope angle and squared contours typical for glaciers. Eventually, the spectral information from the satellite image identifies this glacier as debris-covered (dark “bands” on glacier surface).

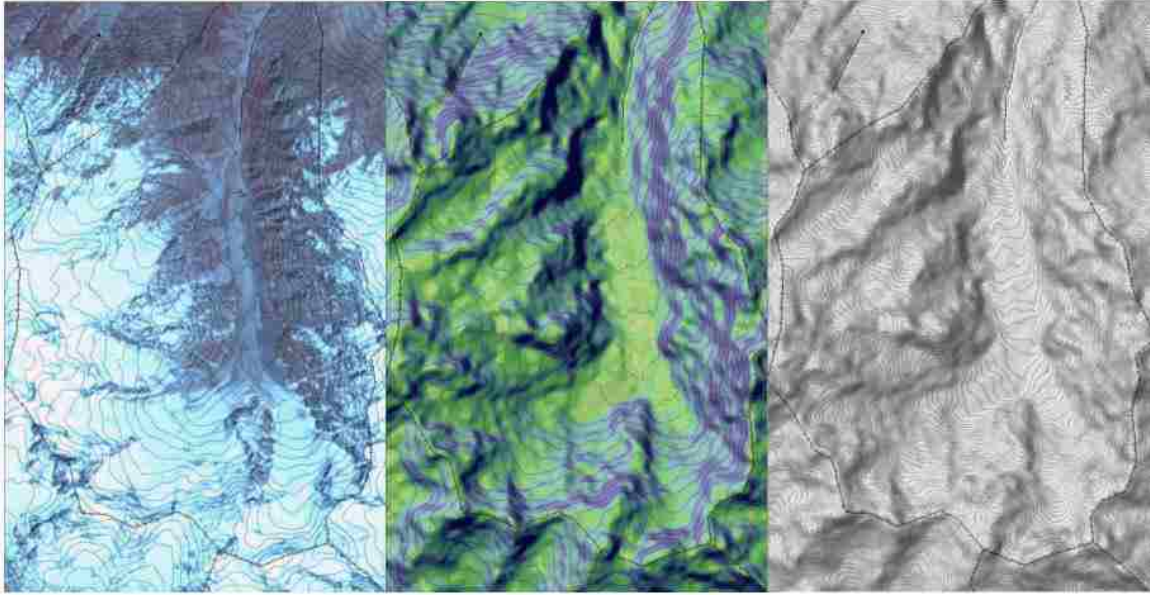


Figure 18. Maps for glacier interpretation: contours superimposed on; ASTER (left), slope angle (middle), and shaded relief (right).

As another example, a combination of slope and hillshade maps was used to identify “grade breaks” or hummocky terrain that was not observable within the contour map. The rock-avalanche deposits in the Shigar River at the confluence of the Braldu and Basha rivers were identified in this manner. Field data were compared to the results from ASTER satellite and DEM analyses. On the slope map in Figure 19, the difference in colors on the river bottom (see red box) indicates an uneven terrain that is consistent with the photograph, but is not captured on the contour map, owing to contour intervals. Often it was necessary to use multiple images to identify and delineate features. The sand dunes in the Skardu Basin, the medial moraines of the Baltoro Glacier, and the edge of fans are other examples of slope and hillshade identifying features that are smaller than the contour interval.

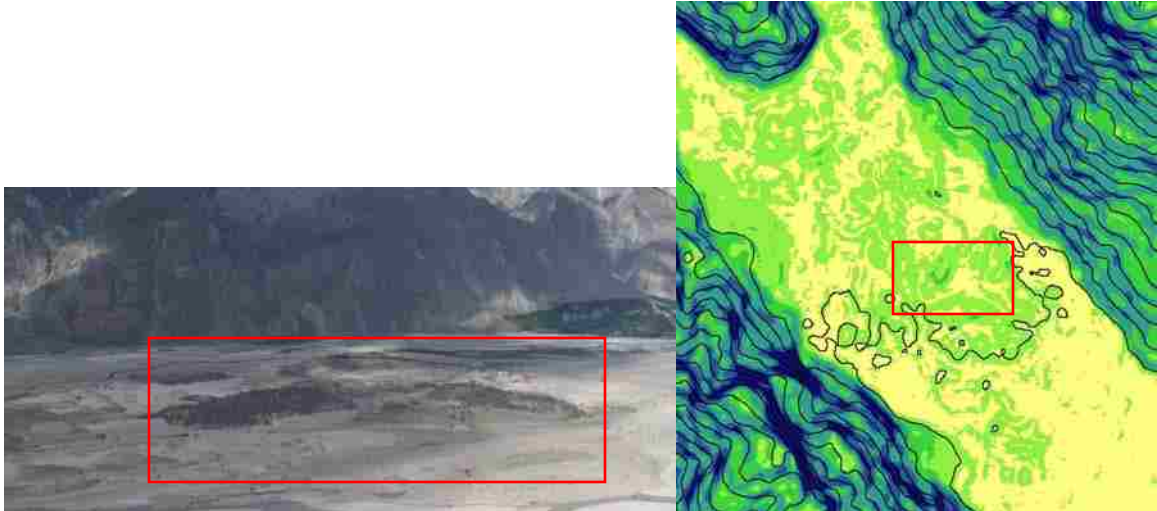


Figure 19. Analysis of geomorphology of the Shigar Valley: field photograph (left), contour and slope angle map (right). The rock avalanche deposit (red box) is visible in the photograph and slope map, but not in the 100 m contour map.

7. Geomorphological Mapping

In addition to the morphometric analysis, results from this GIS database analysis were compared to results derived from the interpretation of the 3D satellite imagery of GoogleEarth. This comparison of data aided the interpretation of landforms. For example, the bench along the left hand side of the GIS map in Figure 20 is also visible in the 3D image. Norin (1925), Owen (1989) and Cronin (1989) identified this bench in the Skardu Basin as lakebeds. The bench on the right hand side is the Bunthang sequence. Using the 3D image, the benches appear to be related geomorphologically.

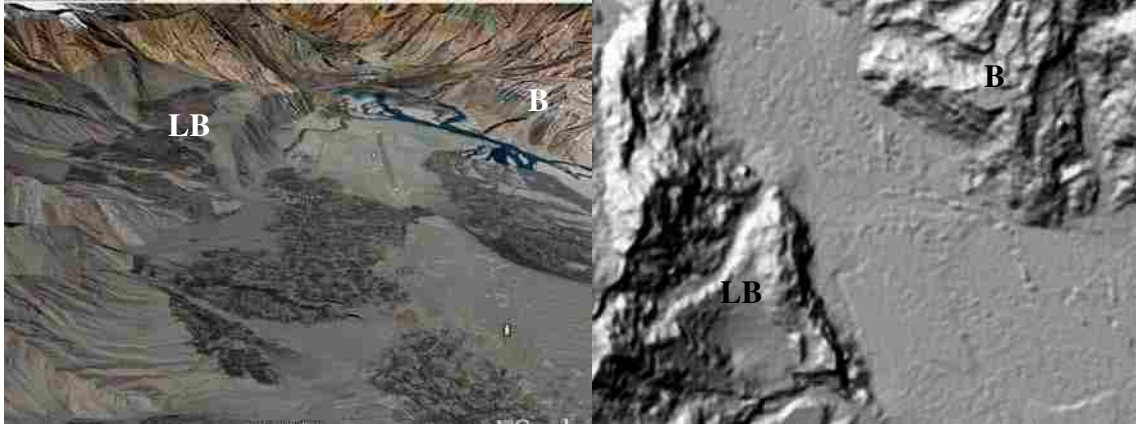


Figure 20. Google Earth image (left) and ASTER/GIS data (right) showing a lakebed bench (LB) and the Bunthang sequence (B) in the Skardu Basin.

The analysis of geomorphology followed an iterative approach: (i) creation of base maps, (ii) overlay of photo orientations, (iii) field note analysis, (iv) visual inspection of photos, and (v) geomorphological mapping. Figure 21 is an example of one of the work maps. Field notes were often used to identify features that were too small to be identified at mapping scale. While digitizing, the map scale was enlarged as necessary to accommodate feature mapping. These features are therefore acknowledged, even if not visible at the published map scale.

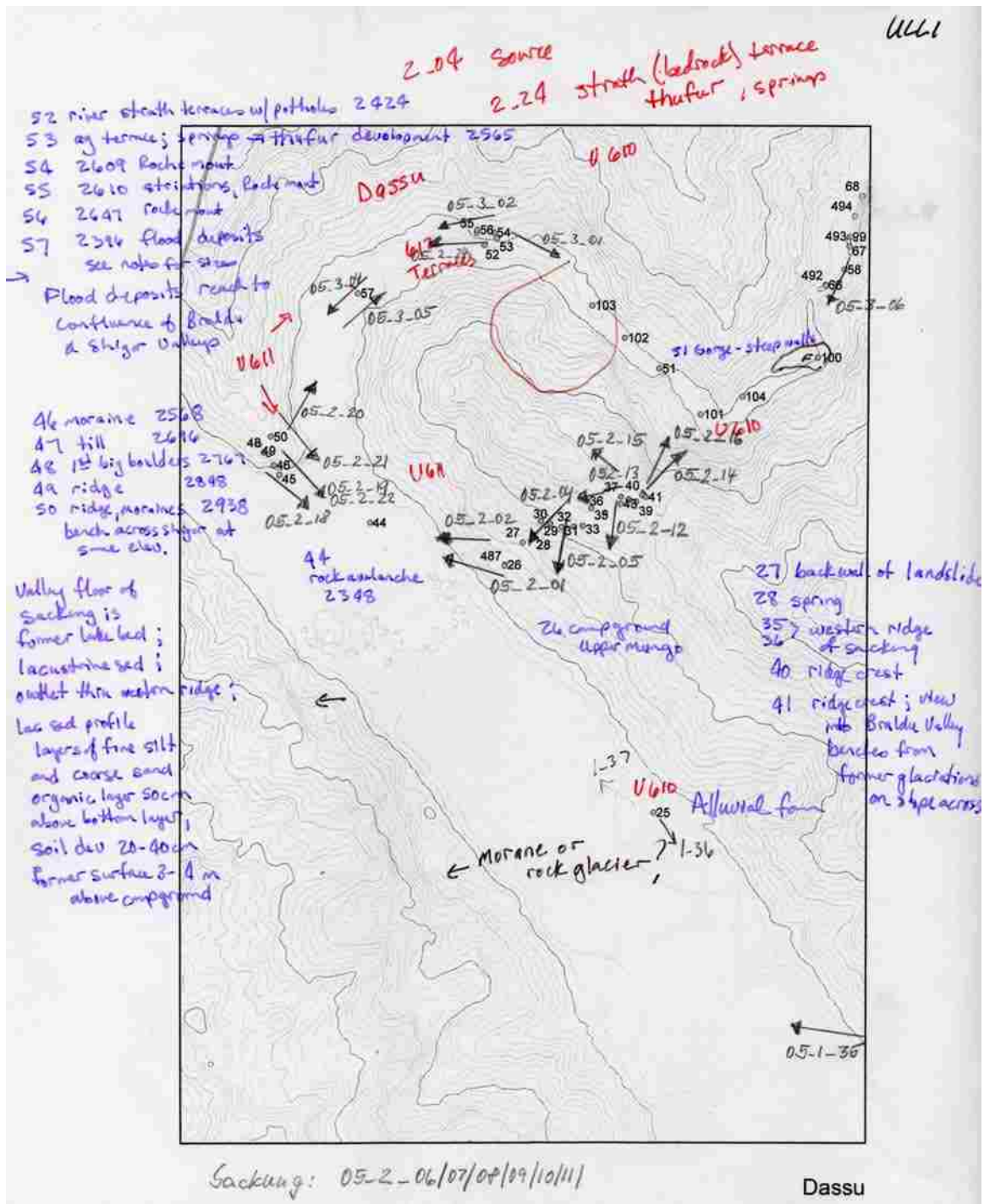


Figure 21. Work map of the Dassu area including GPS locations, view direction of photographs, and notes from field book or GPS entry.

Each of the geomorphology features had a unique signature in the mapping process. Often, several morphometric tools had to be implemented to identify correctly each feature. The attributes for each feature are listed in appendix A.

8. Geomorphological Map Preparation

A series of thirteen geomorphological maps at a scale of 1:100,000 were produced using ArcGIS (appendix F). An additional series of eight detail maps at a scale of 1:50,000 were also produced (appendix F). A feature dataset with feature classes was created in the main geodatabase to facilitate the digitizing of geomorphological features. Including the results from the morphometric analysis and from the interpretation of field notes and work maps, each geomorphological feature was digitized. The digitizing and annotating followed the approach for the geological features. Using a rectangular template, the study area was divided into individual maps with appropriate overlap. The template was based on the final map dimensions with North to the top of the page. Once the ArcGIS database was created, features of specific themes could be displayed as needed on individual maps. All project data are viewable in the *Data View*. In the *Layout View*, the visible data are confined to the specified template size. It is possible to relocate and resize the template or *Data Frame* by using the *pan* feature. The ArcMap Layers include geology, geomorphology, hydrology, settlements, GPS points, contours, hillshade, slope, and ASTER imagery. ASTER data can be viewed as a RGB-composite of bands 1, 2, and 3N, or as an individual band. The final geomorphological maps

include a composite of ASTER imagery draped over the shaded relief map to simulate a three-dimensional image (Figure 22).

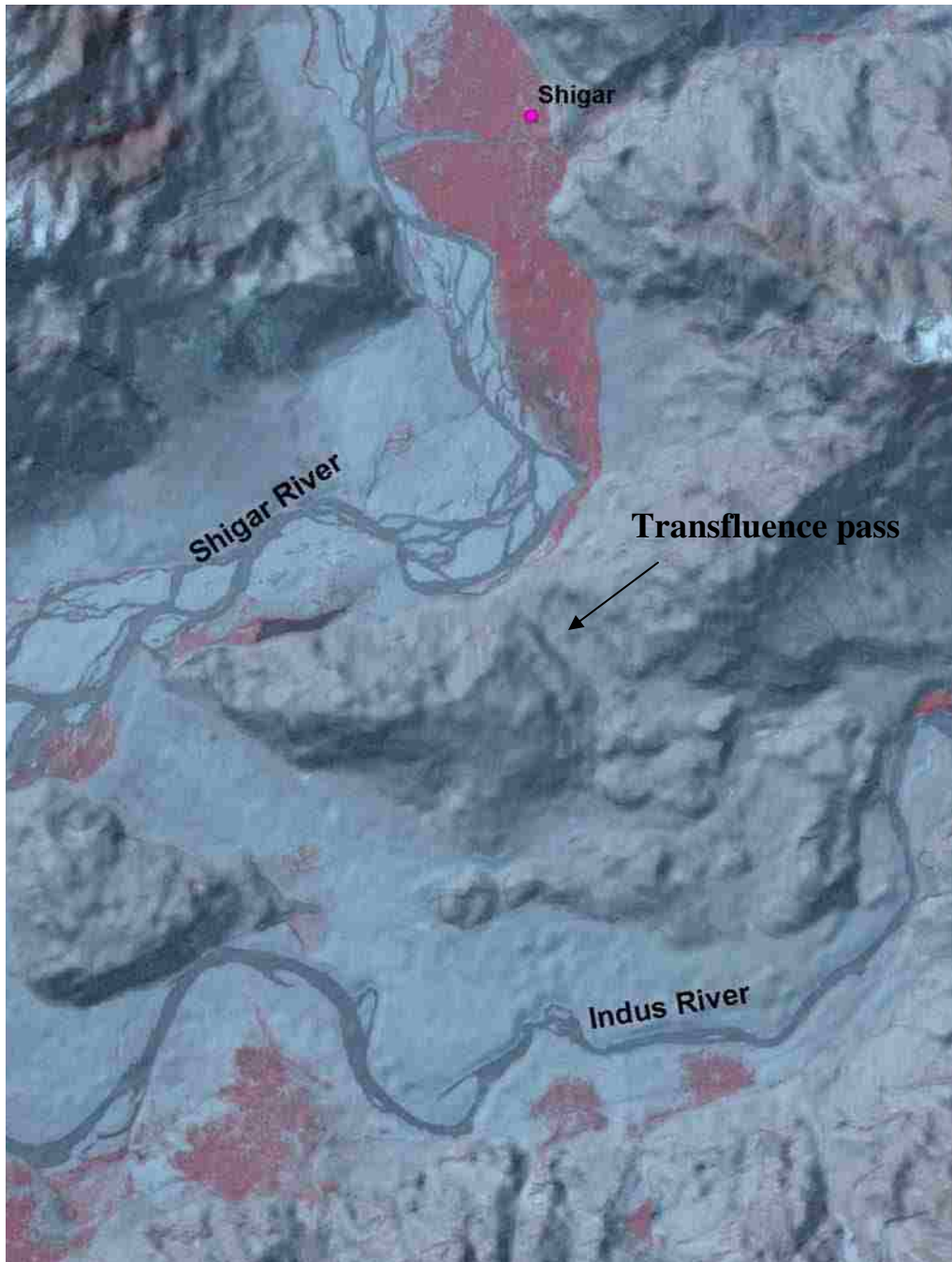


Figure 22. ASTER satellite imagery, 3-2-1 composite, overlain on the ASTER DEM.

IV. RESULTS

The final product of this study is a series of thirteen maps and eight detail maps for the Skardu Basin and the Shigar and Braldu valleys in the Central Karakoram. Each map in the series has three elements: ASTER imagery, Geomorphological map and Slope/ Hillshade map. All maps were made by the author and are presented in appendix F. In the following, landforms are described in relation to geology, geomorphological processes, and altitudinal zones. Each feature will be discussed in context of its presence or absence within the three main regions of analysis, the Skardu Basin, Shigar Valley, and Braldu Valley. For selected case studies, such as flash flood deposits, active landslide areas, sackungen, and rock avalanches, detailed maps allow for a better understanding of localized environmental conditions.

1. Geomorphological Summary

The Skardu Basin has tills preserved on many higher slopes and sand dunes cover wide areas of fluvial sediments from a braided river system. Extensive alluvial and debris fans make up the Shigar Valley, and a sackung follows an anticline on its western ridge. In the narrow Braldu Valley between Dassu and Askole, many fans are deeply dissected, and extensive landsliding is common on the steep slopes. Strath terraces reveal former higher riverbeds and high fluvial erosion rates. Outburst flood deposits from temporary lakes that formed behind former landslides or moraines are located in several locations. Between Askole and K2, tributary glaciers deposited lateral and terminal moraines, and some of the glaciers show characteristics of surging (Hewitt, 1998). Thick

debris covers most of the glaciers; Baltoro Glacier shows a rough topography with countless supra-glacial and para-glacial lakes.

2. Past Glaciations

Past glaciations left their mark in the form of trimlines, terraces, moraines, and roche moutonnées. Seong et al. (2007) presented TCN data that bracket seven advances over at least the last two glacial cycles from ~170-90 ka to 0.8 ka (Table 1). Stages were named for settlement nearest glacial extent. Glaciers have dramatically decreased in length from extensive valley glaciers to restricted tributary glaciers.

Table 1. Glacial history, after Seong et al. (2007).

Glacial stage	Age	Glacial extent
Bunthang	700k +	May have reached past Skardu
Skardu	MIS 6 (~ 150k)	Reached to Skardu
Mungo	MIS 2 (Last Glacial Maximum)	80 km beyond present position
Askole	Holocene	Few km beyond present position

2.1. Moraines and Till Deposits

Till is used to describe any sediment directly deposited from glaciers. Till may be subglacial or supraglacial in origin and may be deposited from meltout or lodgement.

Lateral moraines are formed from debris deposited on top of the glacier by rock fall. The debris or till, forms parallel ridges along the sides of the glacier. When the glacier melts,

the lateral moraines are preserved as high ridges. The tributaries of the Shigar and Braldu valleys have abundant lateral moraines (Figure 23).

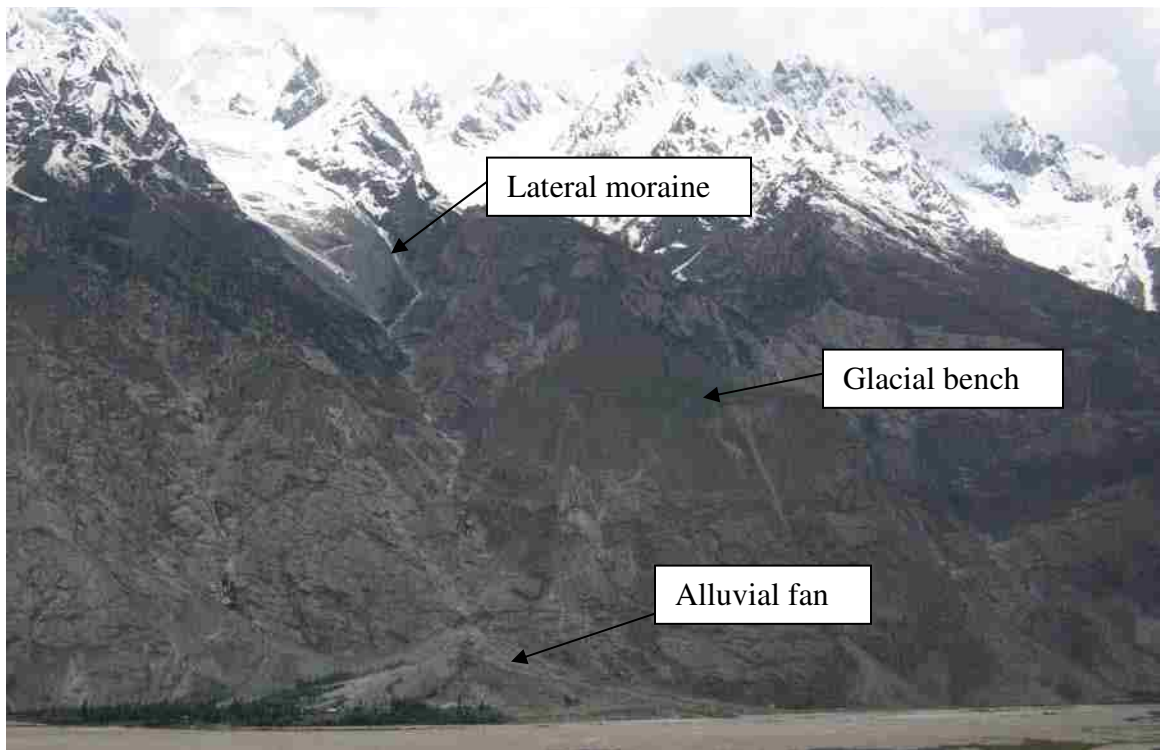


Figure 23. Lateral moraine, alluvial fan and glacial bench in the Shigar Valley.

In the Skardu Basin, the Rock of Skardu, or Karpochi Mesa, has three generations of moraines, indicating three former glacial levels (Figure 24). Till and lateral moraines are recorded in the field notes at elevations 2400 m, 2593 m, and 2707 m. Based on TCN ages, Seong et al. (2007) placed the moraines in the Skardu glacial stage. Based on stratigraphy and similar elevation, Cronin (1989) correlated the moraines with the till at the base of the Bunthang sequence.

Within the Shigar Valley, there are many active lateral moraines. On the southwest side of the valley (Figure 23), the terminus is at elevation 3500 m. Inactive

moraines are at elevation 3100 m and 3900 m. On the northwest side, the active moraine above Alchori has a terminus elevation of 3800 m.



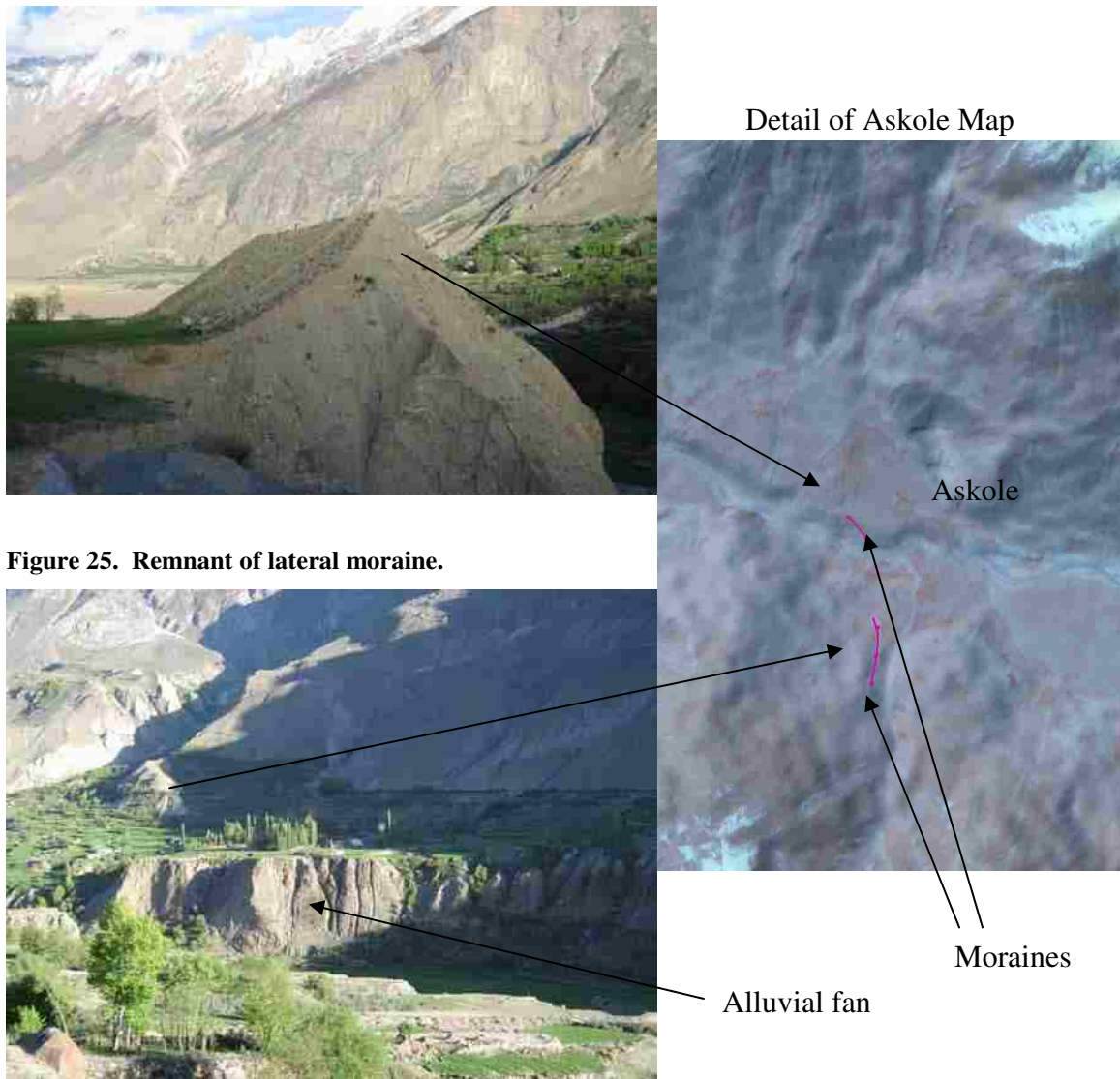
Figure 24. Skardu Basin. (B) Bunthang deposit; (L) lake sediments; (M) three moraine ridges on Karpochi Rock. (R) Shigar River joining the Indus River at Skardu.

Near Askole, in the lower portion of the Braldu Valley, a remnant of a topographic right lateral moraine of a former tributary glacier is preserved on the northern valley side (Figure 25). Other remnants of the lateral moraine are surrounded by younger alluvial fans on the southern valley side (Figure 26).

Terminal moraines are a result of the debris flowing off the surface and by the accumulation of basal till. The size of the moraine is a reflection of the amount of time that the glacier remained in one location and the amount of debris in the system.

Terminal moraines form perpendicular to the drainage, and therefore they are susceptible

to erosion. For example, in Figure 26, the lateral moraines are preserved, while the terminal moraine has been eroded. Terminal moraines are evidence of a standstill and recession of a glacier, and therefore are important indicators of the extent of former glaciations.



Terminal moraines were found in only few locations in the Braldu valley, at the active margins of Baltoro Glacier and Biafo Glacier. As these glaciers have retreated, erosion

has re-deposited former end moraines into the glacial outwash plain. In Figure 27, the lateral moraine is evidence that in the past, Biafo Glacier extended further, and that the former terminal moraine has since been eroded.

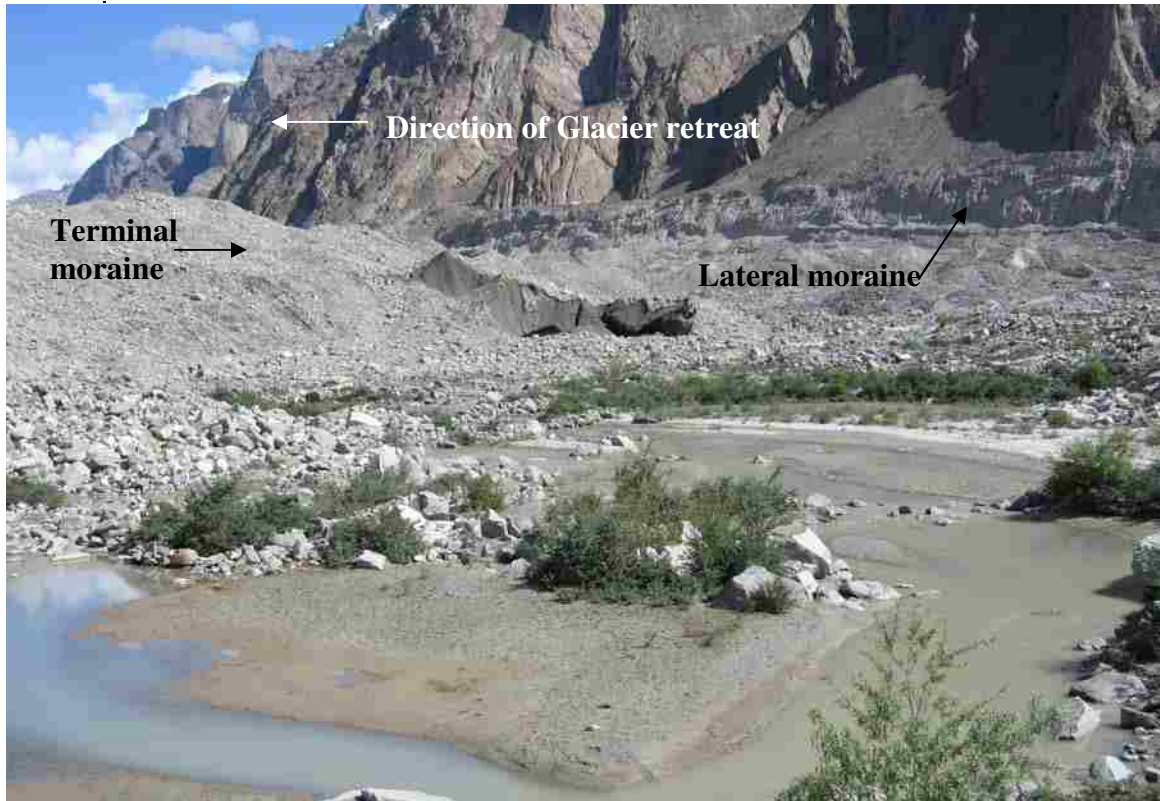


Figure 27. The terminal moraine of Biafo Glacier and remnants of former lateral moraine. Biafo Glacier is to the left of photo.

Many slopes throughout the study area are covered with till. For example, the vegetation on a hillslope near Korophon in the Biafo Glacier snout area is rooted in till (Figure 28). A former longer Baltoro Glacier polished the lower slopes in the Braldu Valley that are now covered with till.

The amount of downwasting of the Biafo Glacier is evident by the higher elevation of the lateral moraine (Figure 29). The lack of a moraine between this surface and the current glacier suggests a rapid ablation, or constant retreat.

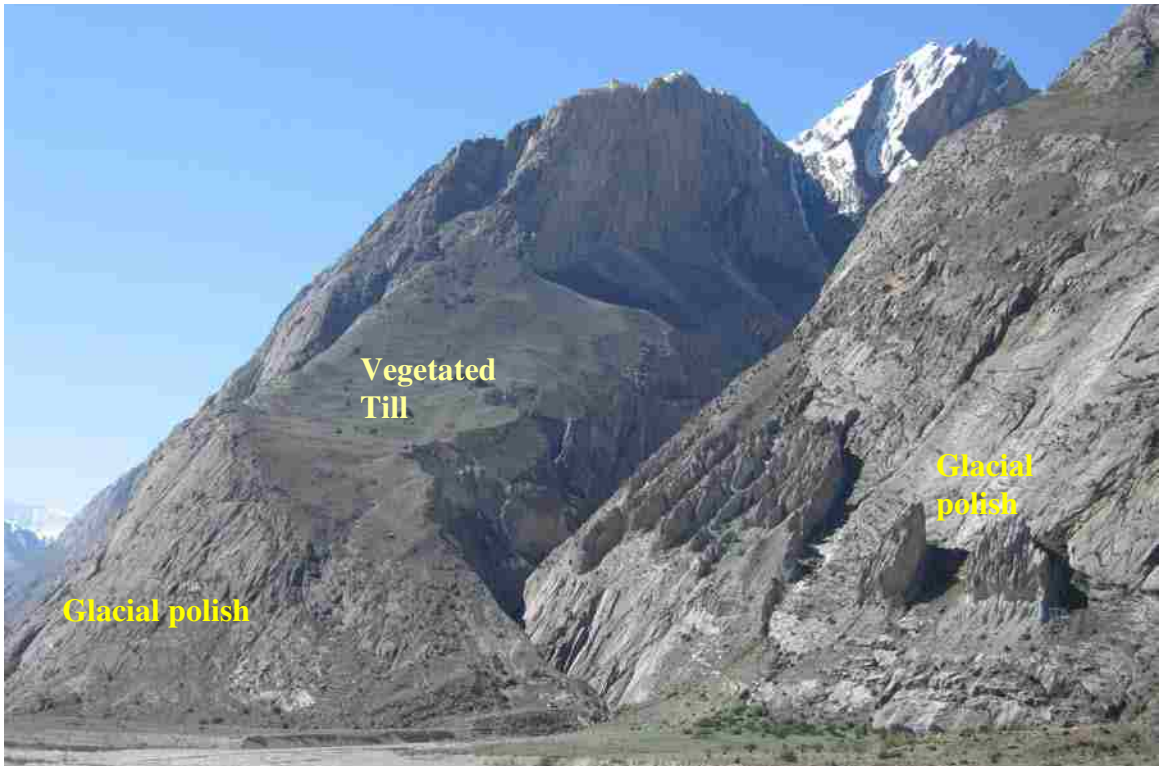


Figure 28. Glacial till and polish on the Braldu Valley slope south of the Biafo Glacier snout.



Figure 29. A lateral moraine along Biafo Glacier is evidence for former higher glacier surface.

The majority of moraines in the Shigar and Braldu valleys are on the S/SW-side of the valley with N/NE-facing slopes. This would indicate that the S/SW side of the valleys had more glaciers. The north facing slopes are shaded by the mountain peaks and therefore have a lower insolation, and therefore a lower ablation rate. This is in agreement with the findings of Naylor and Gabet (2007). They documented valley asymmetry due to glacial and non-glacial erosion in Montana's Bitterroot Range. Their results showed that "solar insolation favored growth of cirque glaciers on the north-facing slopes, while inhibiting them on south-facing slopes." The results also showed that the excavation of cirques on the north-facing slopes was effective in removing more mass and resulted in lateral moraines that were significantly larger than moraines produced on the south facing slopes.

2.2. Trimlines

In the Skardu Basin the thickness of the glaciers are not evident, however the glacial floor can be inferred by features such as passes and benches. From these features, past basin floors were at elevations 2600 m, 3000 m and 4200 m.

There are three sets of trimlines identified in the Shigar and Braldu valleys. Trimlines are demarcations on the valley wall that delineate the maximum thickness of past glaciers. Elevations of trimlines were derived from cross-sections (appendix D). In the landscape, they appear as benches such as the one in Figure 23 and Figure 30. In the Shigar Valley trimlines exist at approximately 3700-3100 m asl, 3250-2700 m asl, and 2900-2500 m asl (Figure 31). The trimlines are more pronounced on the west side of the

valley. The Braldu Valley trimlines are at 5200-4500 m asl, 4500-3700 m asl, and 4000-3200 m asl. The pair of numbers corresponds to the elevation at the upper and lower part of the valley for each of the three trimlines. Only the trimlines at 3200 m and 3700 m carry through both valleys. Therefore, there appears to be four events. At the confluence of the present Baltoro and Liligo glaciers the glacier surface is at 4000 m asl, while a trimline exists at 4700 m asl inferring a former glacier that was 700 m thicker than today. Concordia, near K2, has its present glacier surface at 4500 m asl and a trimline at 5000 m asl, inferring that the former glacier was 500 m thicker.

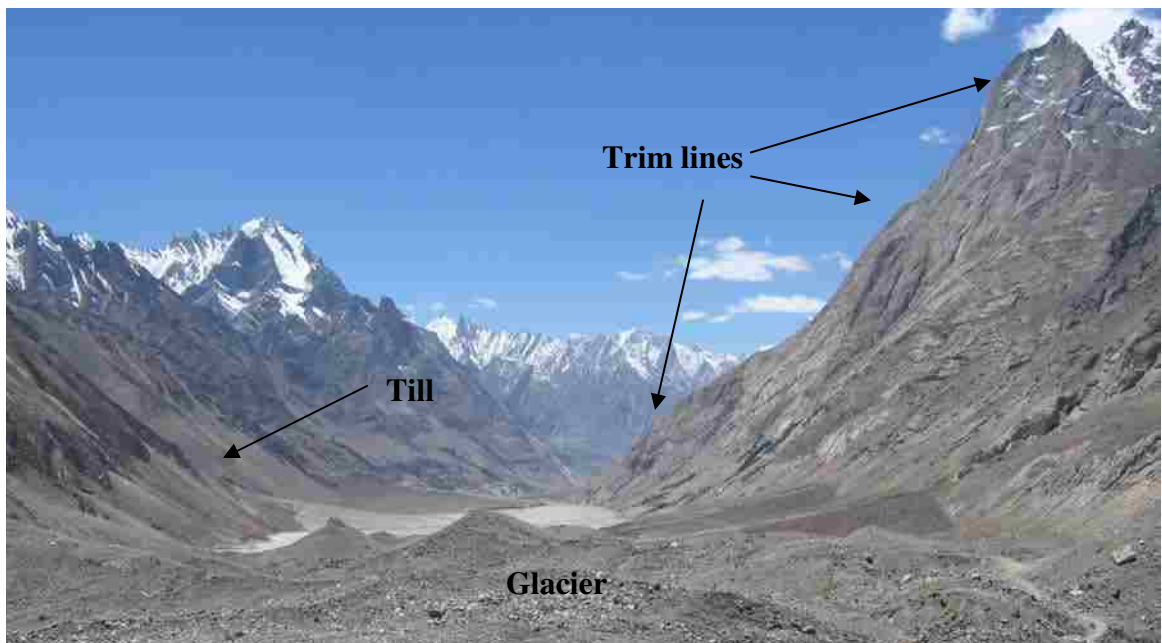


Figure 30. Trimlines on the northern slope of the Braldu Valley in the fore field of Baltoro Glacier. The convex shape sections in the slope indicate former glacial valley walls. Till also indicates former height of glacier.

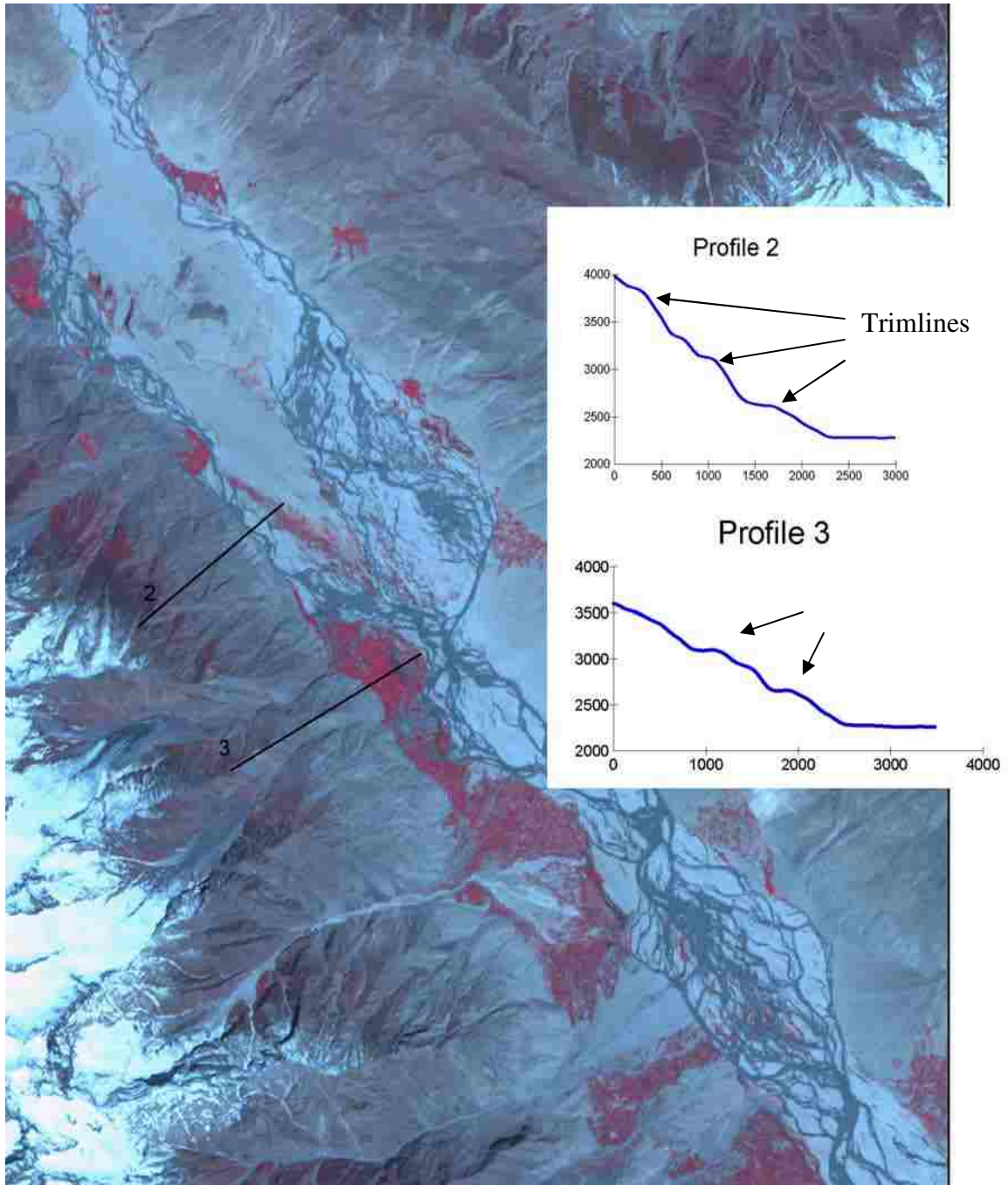


Figure 31. Slope profiles identifying three sets of trimlines (see grade breaks) in the Shigar Valley. Cross-section maps for all valleys are reproduced in appendix D.

2.3. Roche Moutonnée and Transfluence Pass

As the glaciers moved through the valleys, bedrock was eroded by the ice. Roche moutonnées and transfluence passes are evidence of glacier activity and glacial flow direction. Stronodoka Pass is an impressive U-shaped transfluence pass at the eastern side of the Skardu Basin and a relict of a former glacier advance down the Shigar Valley (Figure 32 and appendix F). While the former main Shigar Glacier turned sharply west into the Skardu Basin, parts of the ice were forced to flow across the pass directly south into the Indus Valley (Figure 22). The pass is ~200 m above the present river. The slopes of the pass contain many roche moutonnées that provide evidence for the glacier flow direction from North to South (Figure 33). The sloped side of the roche moutonnées faces up-glacier; the steep side is from the plucking action as the glacier passed over, faces down-glacier. Near Dassu, in the Braldu Valley, roche moutonnées exist at ~200 to 250 m above the present river. Roche moutonnées were not found in the Shigar Valley.



Figure 32. Stronodoka Pass is a U-shaped transfluence pass. It is the result of a former Shigar Valley Glacier. While the main glacier turned west into the Skardu Basin, parts of the ice flowed across the ridge directly south into the Indus Valley.



Figure 33. Roche Moutonnée in the Stronodoka Pass east of the Skardu Basin. The flow direction was north (left) to south (right).

3. Mass Movements

Retreat of the glaciers has exposed over-steepened valley walls that are unstable and subject to mass movement. Mass movement deposits such as rock avalanches, debris flows, erosion gullies, and scree slopes are common throughout the study area.

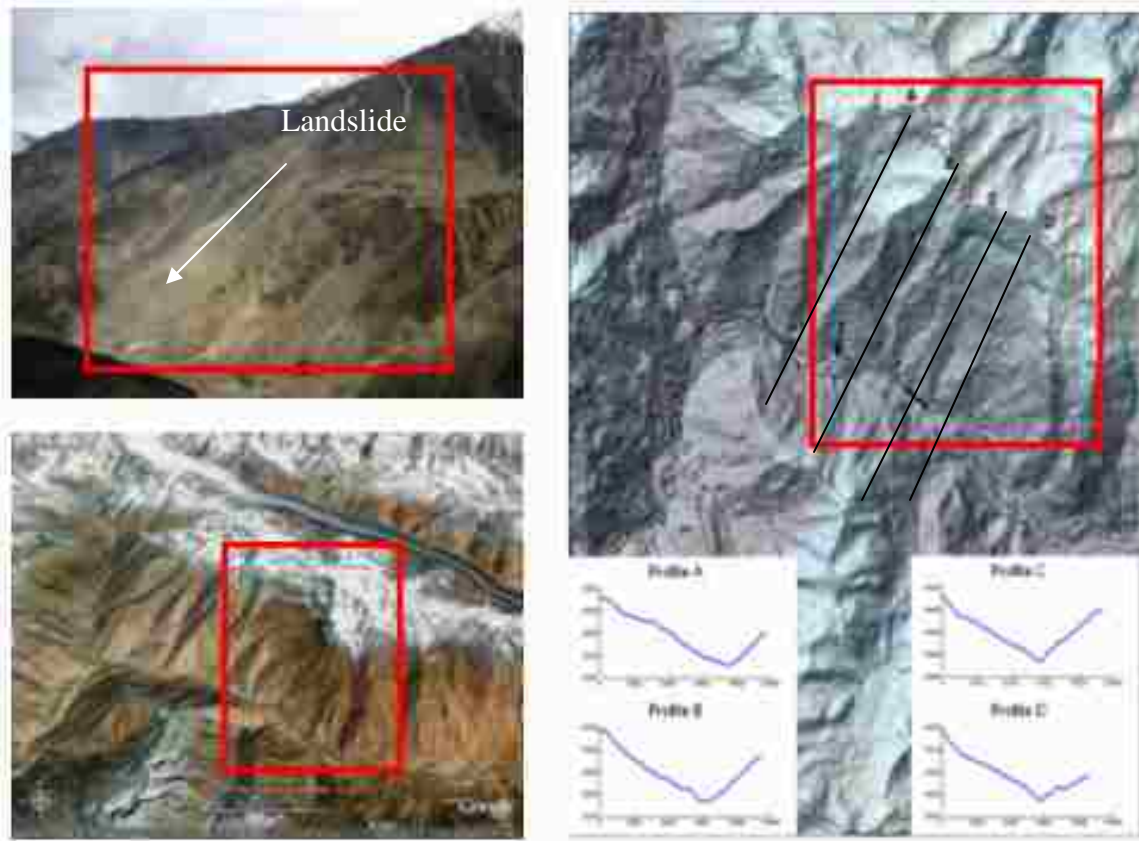


Figure 34. Landsliding in the Chakpo area in Braldu Valley. The red box outlines the landslide area in the three figures. Profiles show the narrow gorge of the here antecedent Braldu River. Cross-sections C and D are through landslide and epigenetic gorge. See appendix D for cross-section maps and appendix F for detail maps.

In the Braldu Valley, between Chakpo and Hoto, scarps are evidence of multiple landslide events (Figure 34). An historic landslide dammed the Braldu River, causing the river to incise a bedrock spur and create an epigenetic gorge (Figure 35). Hewitt (1998) associated this same gorge with the Gomboro Complex Rock Avalanche. Hewitt (1998)

states that in terms of denudation, rivers are doing their work twice to create an epigenetic gorge, and this must be taken into account as a constraint upon the net rate of incision. Because the Braldu River has a stepped profile related to the rock avalanche, net incision of the river into the bedrock seems to be chronically interrupted. In the



Figure 35. Epigenetic gorge associated with an historic landslide near Chakpo in the Braldu Valley.

epigenetic gorge, Seong et al. (2008b) used TCN dating to estimate the strath age of 0.9 ka to 1.2 ka, and the incision rate of 22.9 to 29.0 mm/yr. These incision rates are much higher than the 2.0 to 3.3 mm/yr incision rates for strath terraces upstream and downstream of this point. They attribute the high incision rate to differential uplift that has created a nick point.

The geology of the area, particularly the many faults and fractured rocks, allows water to be an erosional force, both by physical freeze-thaw processes and by lubricating surfaces. The field notes reference several mass movement events associated with precipitation. Near Chongo in the lower Braldu Valley, on a sunny day in the middle of June 2005, the snow-covered mountain was a source of five rock falls in a two-hour span. In the Urdukas area in the upper Braldu Valley, on the Baltoro Glacier there was heavy snow and rainfall the first week of July that led to many rockslides, debris flows and snow avalanches. One week later, a landslide blocked the road between Askole and Chakpo in the Braldu Valley with meter-sized clasts (Figure 36).



Figure 36. A landslide blocked the road between Askole and Chakpo in the Braldu Valley after heavy rainfall in July 2005.

Mass movements are common throughout the study area as the mountains erode to a more stable form. Most such mass movements are merely a process of erosion and slope readjustment. Some result from the erosion of unlithified glacial or fluvial deposits covering the bedrock. Occasionally, tectonic activity is the cause of the mass movement. The talus cones are mundane adjustments, while rock falls are extraordinary events. However, both processes are normal and represent high frequency, low-intensity activity versus low frequency, high-intensity events. The contrast of older lichen-covered boulders and younger lichen-free, sharp-edged boulders in the Dassu gorge is proof of ongoing mass movement activity in the region (Figure 37). Mass movements affect all aspects of the valley topography. Avalanching provides debris cover to the glaciers and affects the ablation rate and meltwater production. Fluvial entrained sediments scour the channels. Landslides block river channels, which can create lakes and resulting break out floods, or occasionally rivers are forced laterally to erode new channels.



Figure 37. Older lichen-covered (A) and younger lichen-free (B) boulders in the Dassu gorge testifying the ongoing mass movement activity.

3.1. Rock Avalanches

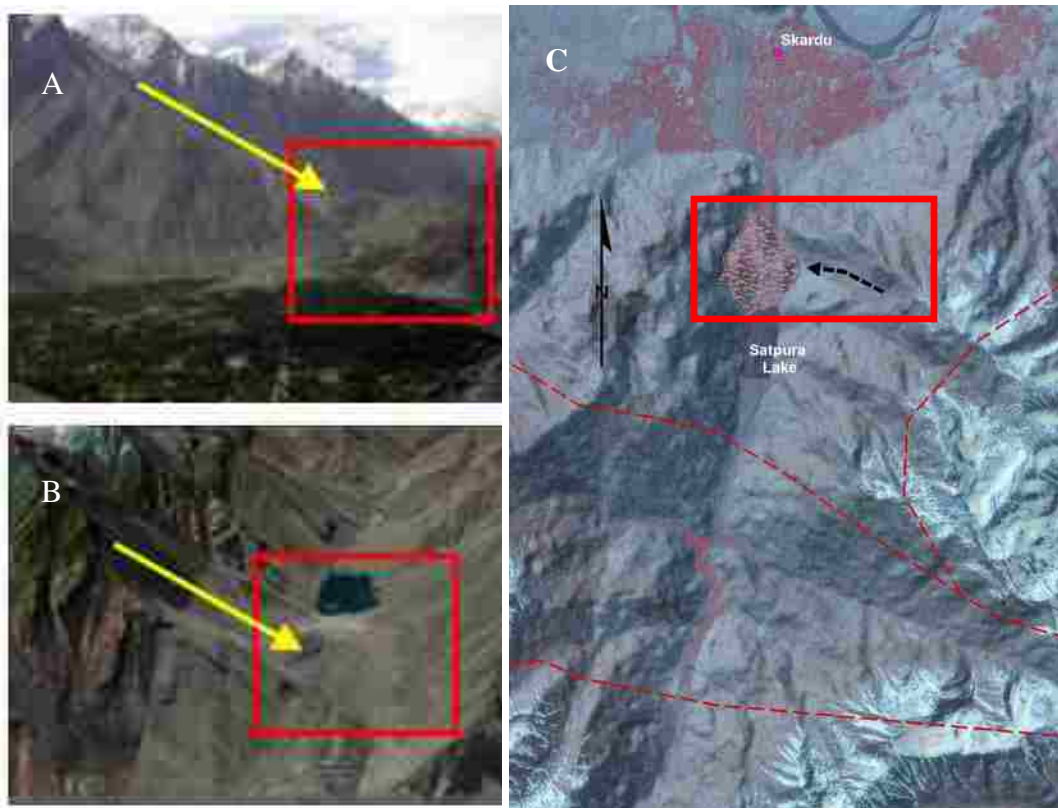


Figure 38. Rock avalanche deposit damming the Satpura River and forming the Satpura Lake south of Skardu. Images A and B are looking south. Red dashed lines on Map C are approximate locations of faults. See appendix F for map legend and large scale map.

Rock avalanches are extreme events during which a substantial amount of material moves in a very short time. There have been several major rock avalanches in the study area. Hewitt (1998) mapped the location of 25 events. South of Skardu, a rock avalanche dammed the Satpura River and created Satpura Lake (Figure 38). Some authors see this deposit as a terminal moraine from a former Satpura Glacier (Norin, 1925; Owen, 1988). Recently, Seong et al. (2008a) measured the TCN on the hummocks in the Skardu area and concluded that the age is incompatible with the required equilibrium-line depression for such a Satpura Glacier, thus supporting Hewitt's (1999)

interpretation of the deposit as a rock avalanche. Evidence for the identification as a rock avalanche is the scarp and the run-out path on the eastern slope of Satpura Valley. The deposit piled up against the western slope forming a brandung, a ridge and a small depression. Both features are parallel with the Satpura River. This interpretation supports the view of Hewitt (1999).

The deposits in the Shigar River at the confluence of the Braldu and Basha Rivers, near Mungo, are the remains of a rock avalanche that spread across the valley from the southern slope above Tsago (Figures 19 and 39). Hewitt (1999) studied this deposit and found woody debris with a ^{14}C age of ~7110 B.P., which suggests a Holocene event.

Rock avalanches and major landslides were found in all valleys.

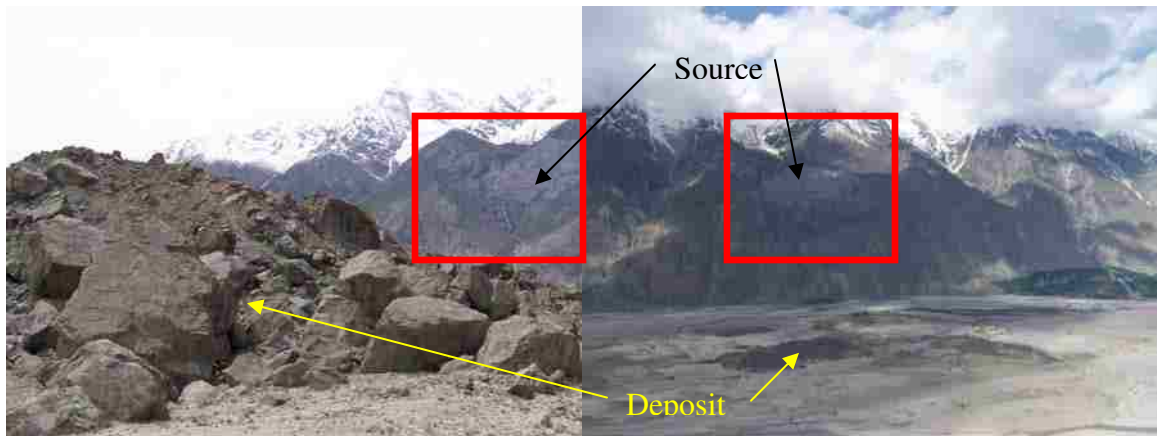


Figure 39. (A), Rock avalanche deposit and source scarp of the avalanche (red box). (B), Rock avalanche deposit in the Shigar Valley near the confluence with the Basha River.

4. Fans

Fans are depositional features at the mouth of a catchment. Debris fans, including talus slopes and scree, are accumulation of rock fragments that fall directly downslope and have a high angle of repose. They are not associated with a stream channel. The debris is generally weathered from freeze-thaw action or stress release and transported by gravity. The rock fragments build upon each other to form a cone extending up the mountainside (Figure 40).



Figure 40. Debris cone in the Braldu Valley.

Alluvial fans develop when a stream flowing from a mountain on to a plain loses gradient, and therefore energy, and deposits a portion of its bedload. The size and gradient of the fan is relative to the coarseness of the grains and the gradient of the mountain stream. There is a direct relationship between the size of the catchment and the size of the fan (Ahnert 1998).

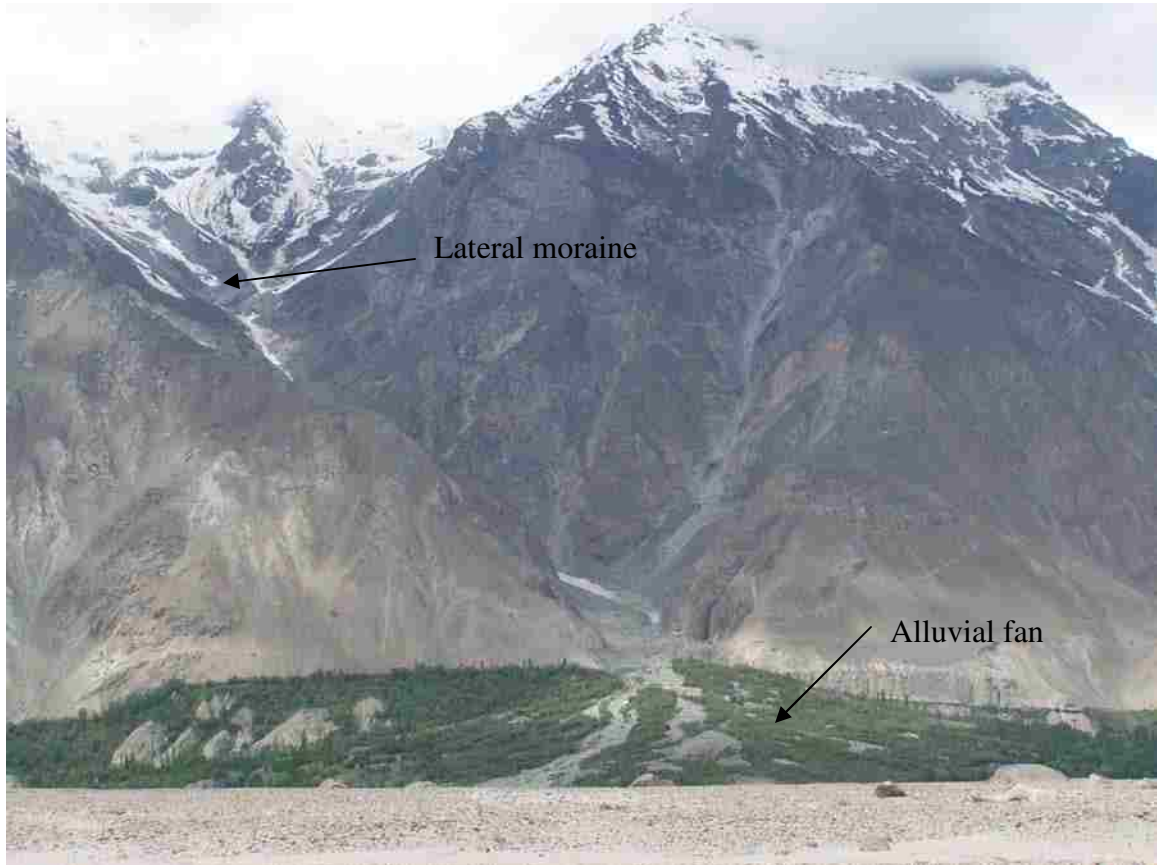


Figure 41. Vegetated alluvial fan, low, broad deposit in the Shigar Valley.

In Figure 41, a vegetated alluvial fan exists on the east side of the Shigar River near the confluence with the Basha River. The fan has a visible gravel streambed. A high runoff event, with a large bedload has overrun the vegetation. Moraines are a source of material for the development of this and other fans. Studies of alluvial fans in British

Columbia showed that the fans were comprised of reworked glaciogenic sediments (Ballantyne, 2003). Owen (*in* Ballantyne, 2003) showed that in the Garwahl Himalaya, glacial retreat was followed by development of fans from reworked morainic debris, and that most have now ceased to accumulate and are exhibiting fan-head encroachment and fluvial erosion (Figure 42).



Figure 42. Alluvial fan in the Braldu River valley, with multiple deposition events and fluvial erosion.

Alluvial fans and debris fans result from different processes, both fluvial action and gravity. In the study area, alluvial fans account for 54% of all fans, while debris fans account for 46%. More than 68% of all alluvial fans are found in the Skardu and Shigar valleys, where alluvial fans were the majority. By contrast, in the Braldu Valley, 60% of

all fans are debris fans. This unequal distribution of fans (Table 2) is due to the difference in properties of the catchment valley, as well as the different processes. This distribution is in agreement with the findings of Ballantyne (2003). The unequal fan distribution is attributable to the time since deglaciation in each of the three valleys (Table 1).

Table 2. Distribution of fans throughout the study area.

Case Study	Number	%
Skardu Basin		
Alluvial fans	24	71
Debris fans	10	29
Total	34	100
Shigar Valley		
Alluvial fans	46	61
Debris fans	29	39
Total	75	100
Braldu Valley		
Alluvial fans	33	40
Debris fans	49	60
Total	82	100
Total fans		
Alluvial fans	103	54
Debris fans	88	46
Total	191	100

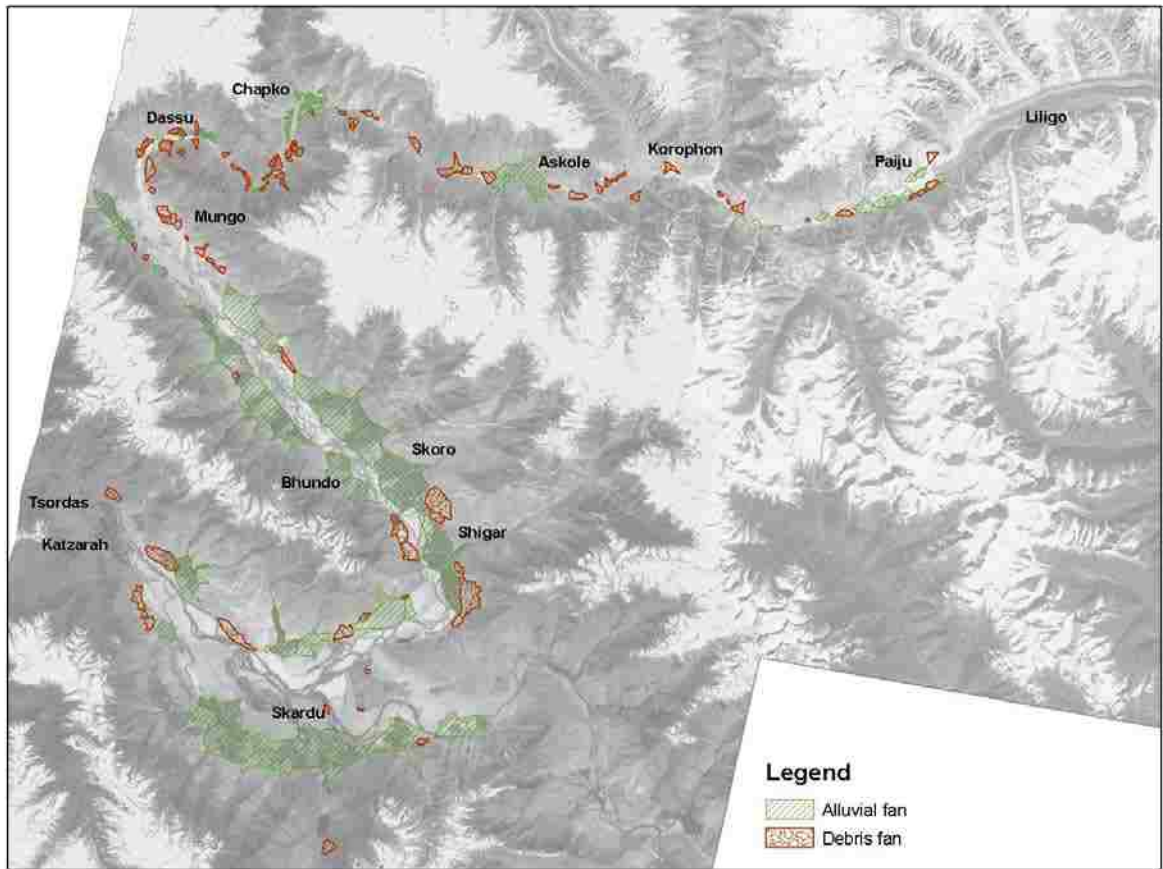


Figure 43. Geographic location of fans.

5. Terraces

5.1. Erosional Terraces

Strath terraces are the result of fluvial erosion into bedrock. They form when the process of vertical erosion, due to downcutting or uplift, creates a bedrock channel and lateral erosion and further vertical erosion leaves a portion of the first channel as a terrace. Such strath terraces are found between Dassu and Tzobu, ~5 m to ~20 m above the present Braldu River. They were not observed in the Skardu Basin, or the Shigar Valley.



Figure 44. Three generations of depositional terraces and one erosional bedrock terrace between Chakpo and Askole in the lower Braldu Valley.

5.2. Depositional Terraces

Depositional terraces were found only in the Braldu Valley. Three generations of river terraces were identified (Figure 44). The terraces formed from a sequence of deposition and incision, where the highest terrace is the oldest. River terraces are the result of four major events: crustal movements, eustatic change in base level, climate variations, and stream capture (Ahnert 1998). Crustal movement, in the form of tectonics or isostatic movement affects the gradient and erosion. Climate fluctuations affect the stream discharge and volume of material transported. Stream capture is a single event

that affects base level and stream velocity and force. The three previous events can be repeated and co-exist. Incision is the result of renewed downcutting from an increase in gradient or during interglacials when glaciers retreated and there was increased fluvial transport with a reduced bedload. Accumulation occurs when speed is reduced and stream bedload is deposited. An abundance of material available from glaciers filled the valleys (Figure 45). Terraces were formed from glacial, fluvial, alluvial, and colluvial deposits. The landforms, not the sediments, are the terrace.



Figure 45. Glacial and alluvial river terrace in the upper Braldu Valley. Note people next to boulders for scale.

6. Flood Deposits

Near Dassu and Chakpo, in the Braldu Valley (Figure 2), there are deposits that record major flood events. The deposits may be due to outburst floods from lakes formed behind landslides or glaciers crossing a valley. Only this narrow valley contained flood deposits.

In the Dassu area, the flood deposits are at an elevation of ~2400 m asl, about 10 m above the recent river (Figure 46). The pegmatite gneiss boulders were measured in three locations. The largest measured boulder was 13.4 m × 9.4 m × 7.5 m, and the average size was 7.5 m × 6.3 m × 5.1 m, equaling 241 m³ of rock. Seong et al. (2008a) calculated a mean discharge of $1.6 \times 10^4 \text{ m}^3 \text{ s}^{-1}$ based on individual boulders and cross-sections. Compare this with the modern average peak discharge for the Indus River, near the confluence with the Arabian Sea, of $5.6 \times 10^4 \text{ m}^3 \text{ s}^{-1}$. Present stream flows for the Braldu River are not available.

The flood deposits near Chakpo are on a terrace that is about 50 m above the recent Braldu River. The largest boulder measured is 7.4 m × 5.4 m × 3.1 m, and the average size is 5.2 m × 4.4 m × 2.7 m, equaling 62 m³. The calculated discharge is $4.5 \times 10^3 \text{ m}^3 \text{ s}^{-1}$ (Seong et al., 2008a). The flood responsible for the Chakpo deposits was significantly weaker than the flood responsible for the Dassu deposits.

Within 3000 m upstream and downstream of Chongo, the oldest terrace generation (T1) includes lacustrine sediments. It is located upstream of the two flood deposits and an epigenetic gorge. The lacustrine deposit records the damming of the valley and the formation of a temporary lake.

Between Askole and Korophon, a further boulder accumulation was analyzed. Seong et al., (2008a) measured five boulders: while the largest was $9.2 \text{ m} \times 7.0 \text{ m} \times 4.2 \text{ m}$ in size, the average size was $7.5 \text{ m} \times 6.3 \text{ m} \times 4.2 \text{ m}$ equaling 198 m^3 . The calculated discharge is $3.6 \times 10^4 \text{ m}^3 \text{ s}^{-1}$, the greatest discharge of the three flood events. Originally, the field notes mentioned it might be a paleoriver deposit; however, Seong et al. (2008a) relates it to a damming of the Braldu Valley by the Biafo Glacier.

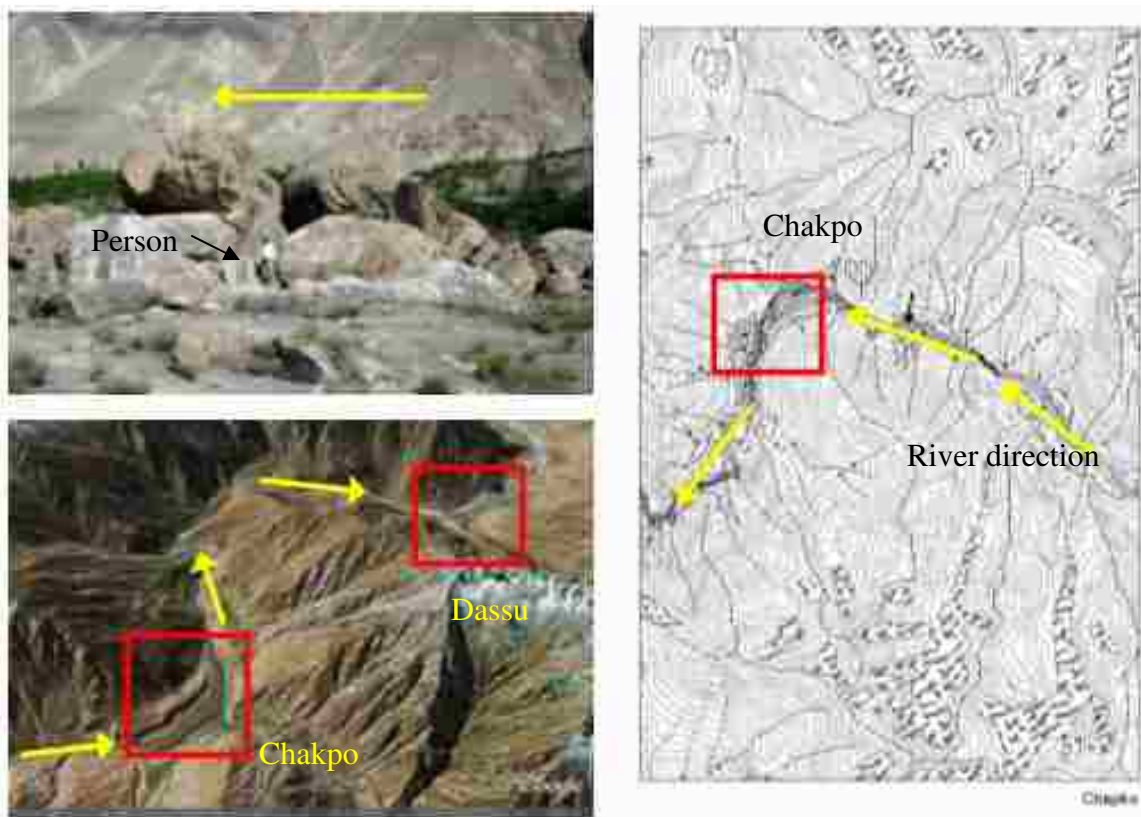


Figure 46. Flood deposits in Chakpo area in the lower Braldu Valley. Note person in photo for scale.

7. Sackungen

A *sackung* (plural: *sackungen*) describes a type of gravitational lateral spreading that is typified by a ridge top trench that parallels the contours of slope. It features an uphill scarp and a convex bulge on the lower slope (Ward, 2003). Sackungen are a form of deep-seated gravitational slope deformation, the slope literally “sags.” A sackung may be considered a high geomorphological risk, because it may initiate rotational-translational slides, with the tendency to evolve into rock avalanches.

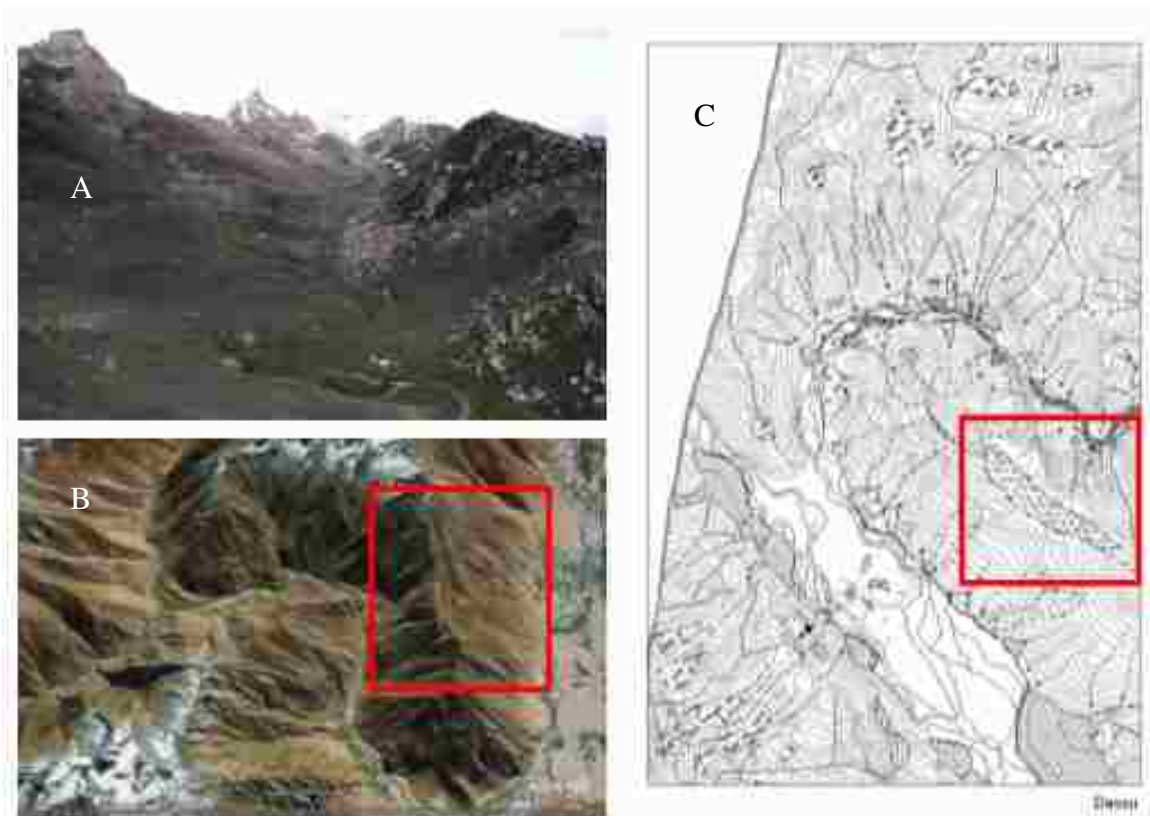


Figure 47. Sackung above Mungo on the ridge separating the Shigar and Braldu valleys. (A) Photo looking down into sackung basin. (B) GoogleEarth image. (C) Geomorphologic map.

An impressive 5200 m long sackung is located on the ridge above Mungo (Figure 47). The graben-type structure is on the ridge that separates the Shigar and Braldu

valleys. The lower western ridge is at ~4000 m asl, while its uphill eastern ridge is at ~4300 m asl creating a substantial trench. The sackung lies over the Main Karakoram Thrust (MKT) on a plunging antiform.

The floor of the sackung is covered with lacustrine sediments indicating the existence of a former lake that later drained through an outlet in the western ridge of the sackung (Figure 48). The lacustrine sediments comprise layers of fine silt and coarse sand piling up 3-4 m above the recent floor. An organic layer 50 cm above the bottom layer and soil development in 20-40 cm from the top was observed.



Figure 48. Lacustrine sediments, soil and organics within the Mungo sackung depression.

Using the typical features of twin ridges and ridge-top depressions, a second sackung was identified near Bhundo, on the west side of the Shigar Valley (Figure 49). This is an example of using the three dimensional view of GoogleEarth to search for patterns on the landscape. The valley on the ridge was atypical, and led to further analysis and identification.

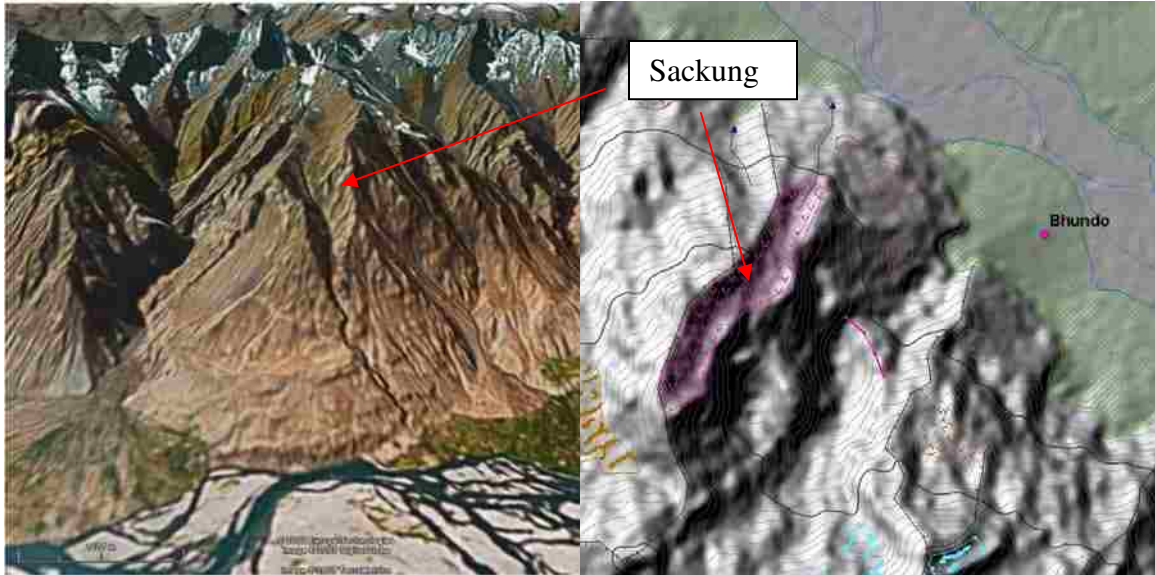


Figure 49. Sackung near Bhundo, GoogleEarth image and detail of Skoro map (appendix F).

Based on Searle's map, the sackung is on a fault line that separates the Kohistan-Ladakh batholith, granites and quartzes, from metasedimentary rocks, greenschist facies slates and phylites. It is 3900 m long and 600 m wide. Unlike the Mungo sackung, it does not have a basin; instead, it has a drainage valley on the ridge.

8. Geologic Fault Lines

Geology and geologic features, such as faults, are instrumental to understanding the geomorphic processes of the study area. Conversely, fault lines and lithologic

discontinuities can be inferred by geomorphic features. Searle (1991) mapped the approximate locations of structural features (Figure 50). The geomorphic mapping has verified some of these locations (Figure 51).

The sackung near Mungo exists on a plunging antiform on or near the Main Karakoram Thrust (MKT) and a lithologic contact. The sackung near Bhundo exists near a lithologic contact. The landslide near Chongo that blocked the Braldu River and created an epigenetic gorge has a fault line near the scarp.

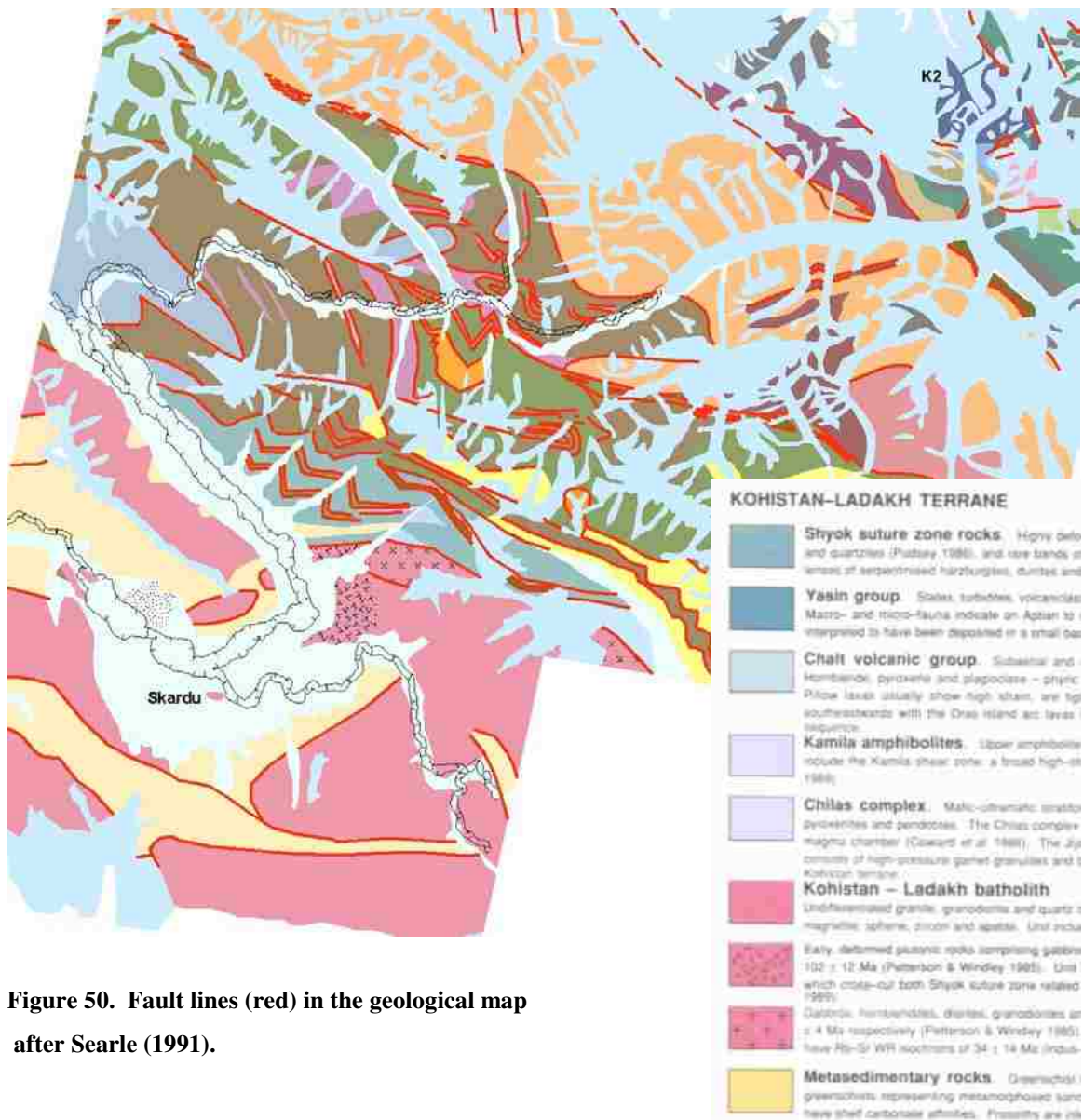


Figure 50. Fault lines (red) in the geological map after Searle (1991).

In the Masherbrum Range, south of the Braldu River, the glaciers have a “hook” shape (Figure 51). This bending of the glaciers is facilitated by a strike-slip fault running perpendicular to the glacier flow. The connection of the bends is the fault line mapped by Searle (1991).

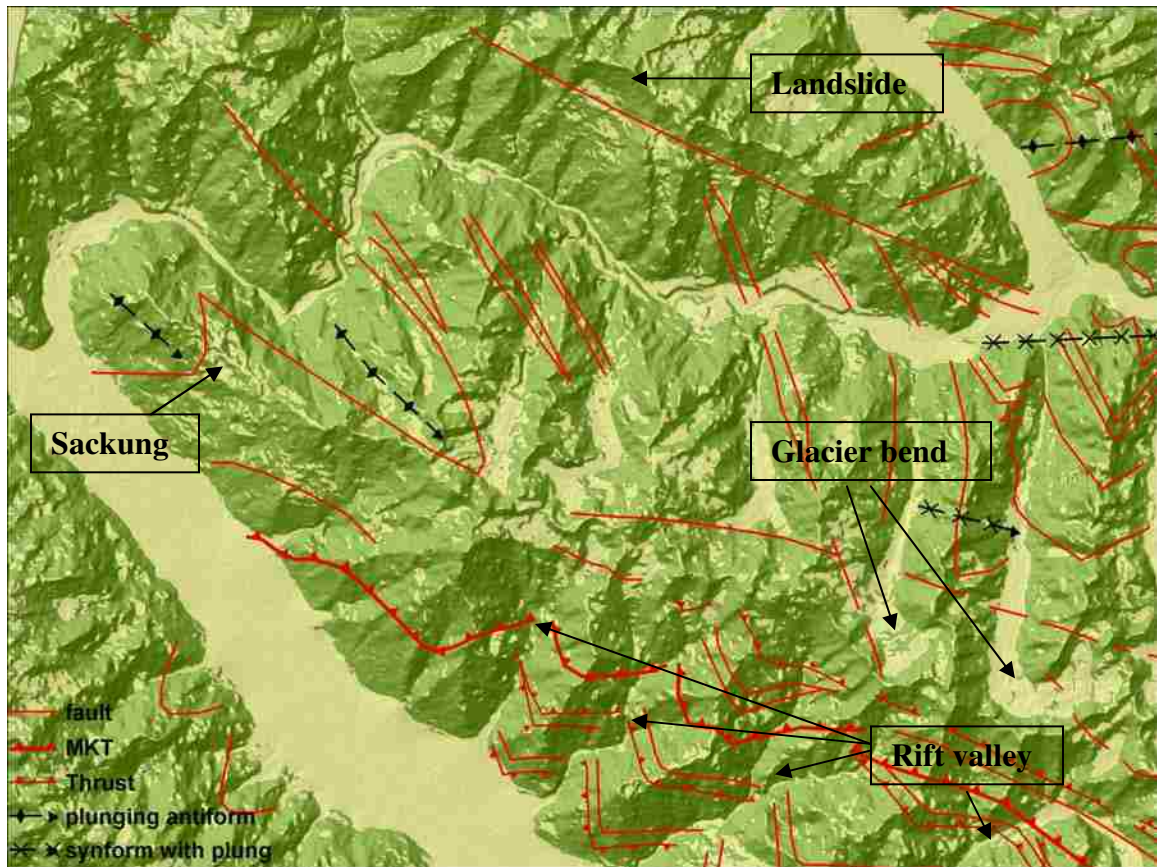


Figure 51. Slope map of the Masherbrum Range in the K2-Karakoram. Light yellow color represents low slope angle. Arrows point to features that are fault related. The red lines are the fault lines after Searle (1991).

Norin (1925) referred to the Bauma-harel Valley, (Figure 51) near Shigar, as a rift valley, as well as the three valleys that parallel it and stated that rift valleys are common within Balistan. The valleys have fault lines and mineral stretching lineations (Searle, 1991) that would support this interpretation.

The Braldu Valley is crossed by several lithologic contacts and fault lines and is an area of high mass movement activity. During the India-Asia collision, the bedrock was uplifted and rotated, such that previously horizontal beds are now at an angle up to vertical. These slopes are unstable and result in mass movements (Figure 52).

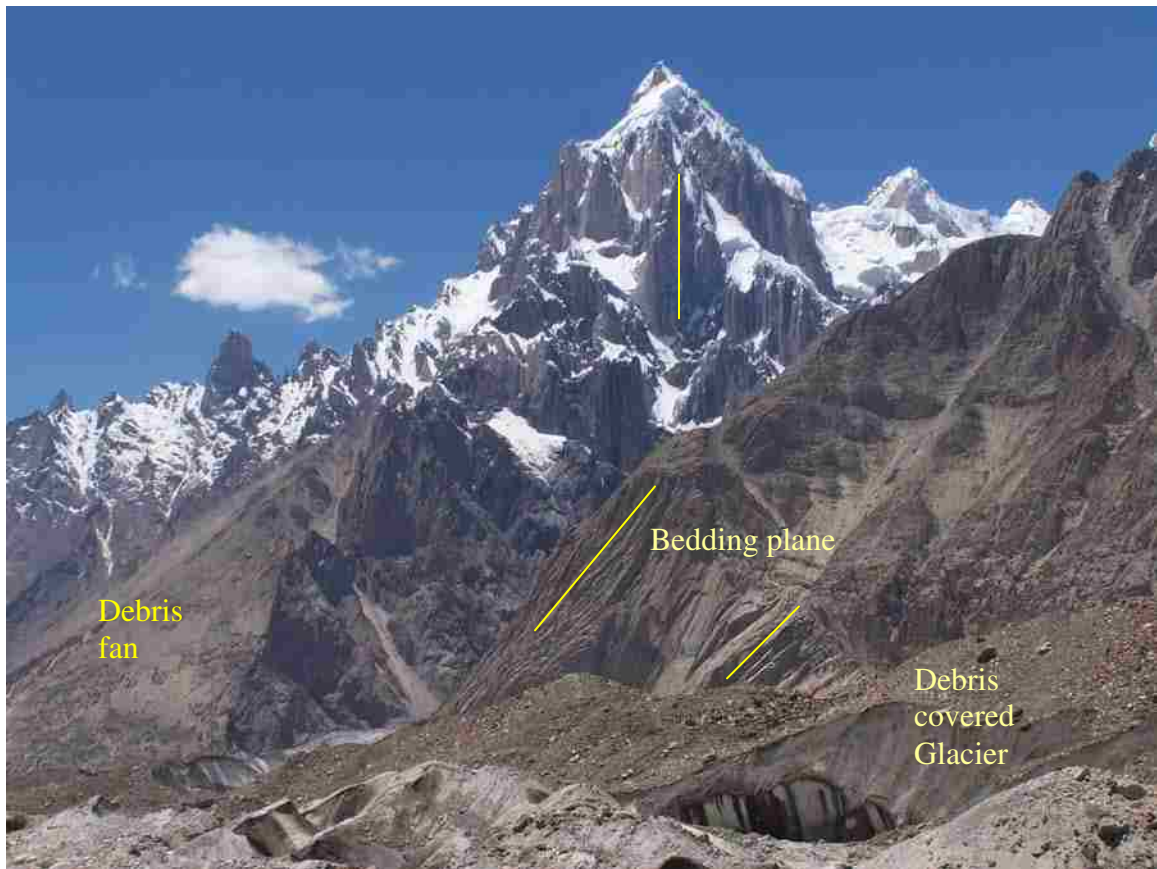


Figure 52. Bedrock bedding planes (yellow lines) between 45 and 90 degree, and debris fans in the Baltoro Valley.

Satpura Lake is flanked by faults to the south and east of the lake (Figure 38). The eastern fault runs through different lithologies and lies near the scarp of the impressive rock avalanche that blocks the valley. Fault lines also parallel the rift valleys south of Satpura Lake. The scarp of a rock avalanche at the north end of the Shigar Valley also occurs in an area of lithology change and a fault line.

V. DISCUSSION

The landscape of the K2-Karakoram, including the Skardu, Shigar, and Braldu valleys, is primarily a result of glacial and paraglacial events. Norin (1925), Cronin (1989), Cronin et al. (1993), and Owen (1988, 1993) have described multiple glacial stages and glacial features of the Central Karakoram. Seong et al. (2007) used surface exposure dating to chronicle the glacial history of the area and identified four glacial stages: Bunthang (> 0.7 Ma), Skardu (70-170 ka), Mungo (11-13 ka), and Askole (0.8-5.7 ka).

Glacial and interglacial periods have distinct signatures. Glaciers left their imprint on the landscape in the form of trimlines, moraines, till, roche moutonnées, transfluence passes, and U-shaped valleys. During each deglaciation, mass movements and fluvial and eolian processes reoccurred and led to the development of fans, terraces and flood deposits. However, glacial and interglacial features are not evenly distributed between Skardu and K2, probably because some features have been subject to subsequent erosion or resedimentation.

1. Skardu Basin

1.1. Satpura Lake

A feature that has been difficult to identify because of the involvement of several geomorphic processes is the dam at Satpura Lake south of Skardu (Figure 38 and Figure 53). While it has been described as a moraine by several authors (e.g. Norin (1925),

Cronin (1989), Cronin et al. (1993), and Owen (1988, 1993), Hewitt (1999) described it as a rock avalanche.

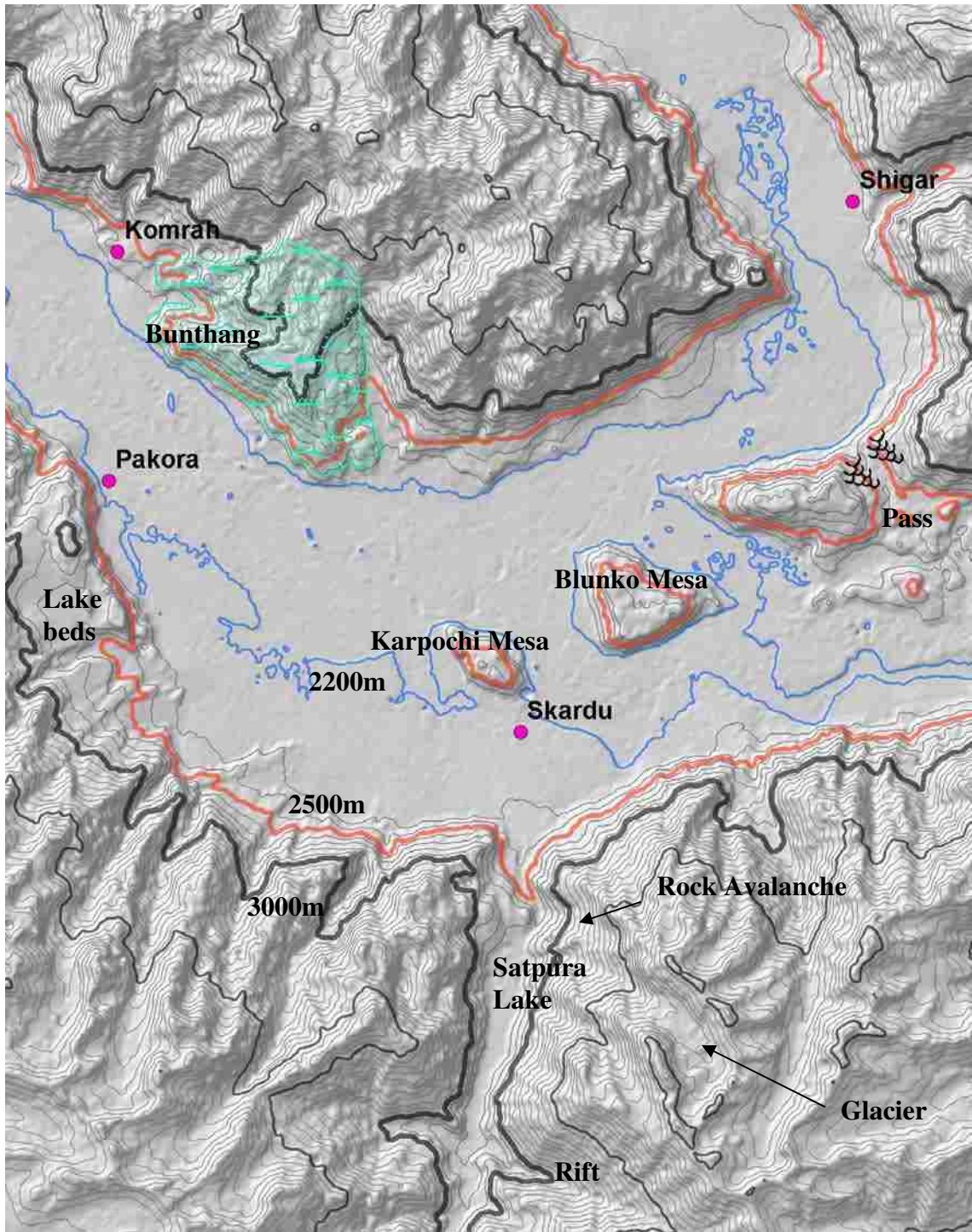


Figure 53. Skardu Basin, showing relative elevations of major features. The Deesai Plateau is south, at the headwaters of the Satpura River.

Owen (1988) noted that the dam deposit includes sediments that appeared to have been deformed by glacial tectonics. Although Seong et al. (2007) support Hewitt's interpretation, they state that the deformation structures still need to be explained. Results of this thesis interpret these sediments as a rock avalanche that occurred on the eastern slope of Satpura Valley. During this mass movement process, glacial sediments were entrained and relocated. Glacial sediments from the glaciers in the Deosai Plateau and the glacier directly south of the landslide would have existed in the valley. The deformation could be either a residual from resedimentation or liquid deformation (i.e. deformation of saturated river sediments by the rock avalanche). This would explain both the lithology and the geomorphology of the feature. The rock avalanche was likely triggered by tectonic activity along the fault that runs through this area (Figure 38). Seismic activity can lead to liquefaction and deformation.

1.2. Faults

Examining the geology map (Figure 54), five unidentified fault lines were discovered. Between the batholith and the metasedimentary rocks there must be a fault that traverses the Skardu Basin. The metasedimentary rocks belong to an antiform that is plunging toward the west. A portion of a fault line is shown at Kachura and again east of the Bunthang sediments, these must connect in the basin. There are lithologic contact zones that are within the Shigar and Indus rivers, and along the ridge of the Haramosh Range. Faults are also implied in these areas. These faults could be influential in the reconstruction of the basin history. The presence of faults would be an explanation for the extraordinary width of these two valleys in comparison to the other valleys in the

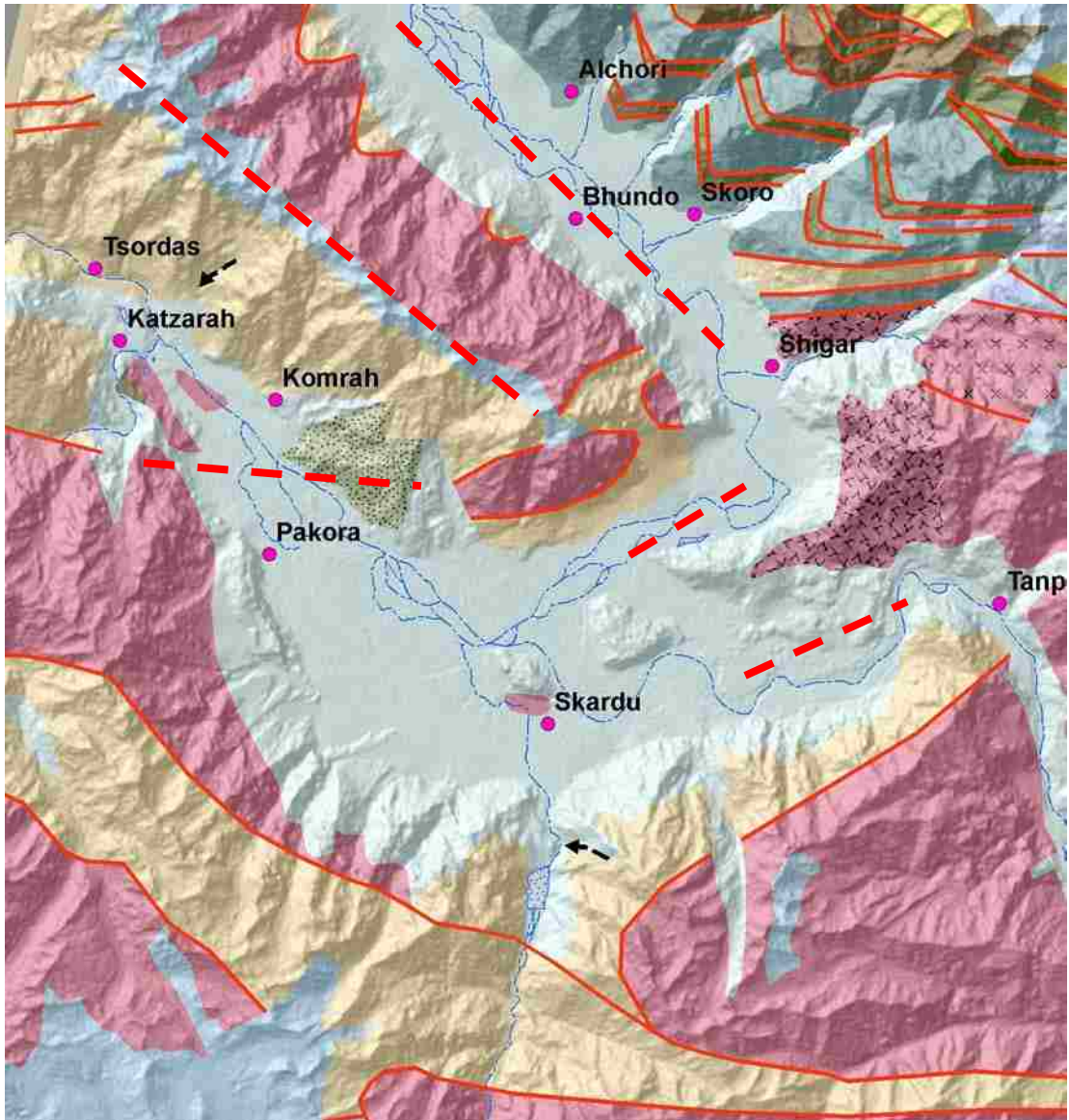


Figure 54. Geology map, each color represents a different rock type. See appendix C for legend. Solid red lines are faults mapped by Searle. Dashed red lines are faults inferred by this study.

area. The presence of a fault line in the Haramosh Range would also account for the high number of scarps located on either side of the range. Scarps are located in the Skardu Basin/Indus River valley above the Katzarah landslide and above the Bunthang deposit. The scarp above the Bunthang is very old, but may date to the glaciation that is preserved in the Bunthang till.

Several hypotheses should be explored. Has tectonic activity displaced features in the basin, such that the correlation of elevations is incorrect? Furthermore, has tectonic activity widened or deepened the basin, such that the apparent glacial and fluvial erosion interpretation is erroneous?

1.3. Bunthang deposit

The Skardu Basin is primarily the work of glaciers (Figure 24 and Figure 55). The base of the Bunthang deposit (Cronin, 1993) is till and the remainder is lacustrine sediments and conglomerates that were deposited when the basin was blocked by either a glacier or a landslide. A portion of the Bunthang deposit is located at the base of a scarp. Lacustrine sediments also exist on the south side of the basin in a terrace at the same elevation as the Bunthang (Figure 20 and 57). The glacier floor is 800 m above the present valley floor at location “F” in Figure 55 and Figure 56.

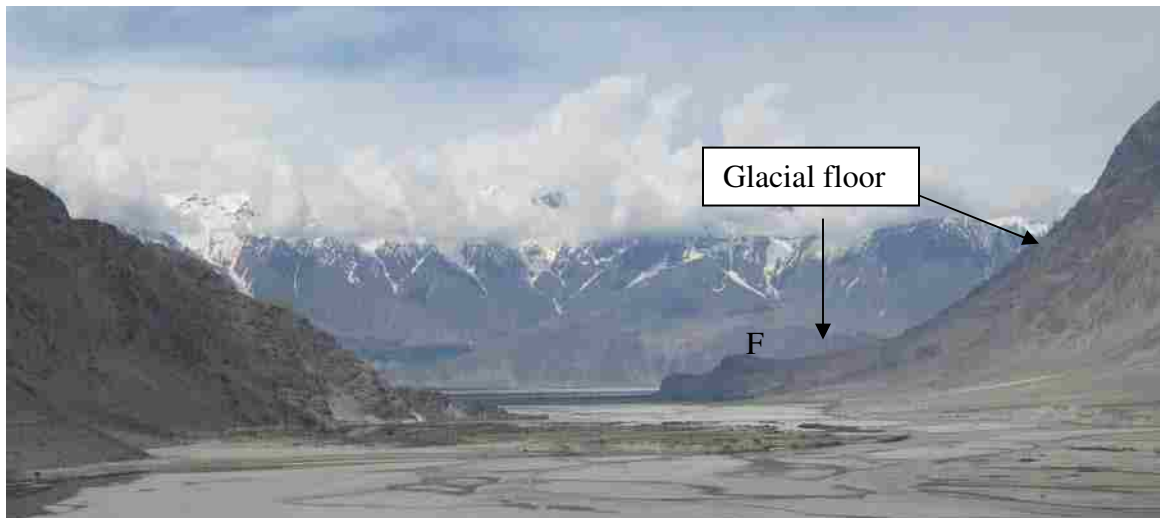


Figure 55. The former glacial valley floor is evidenced by the curve of the bedrock on the right side of the photo. View is from the Shigar Valley, south into the Skardu Basin.

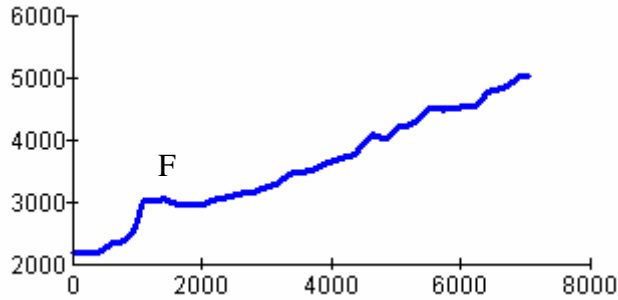


Figure 56. Profile of the glacial valley floor seen in Figure 55.

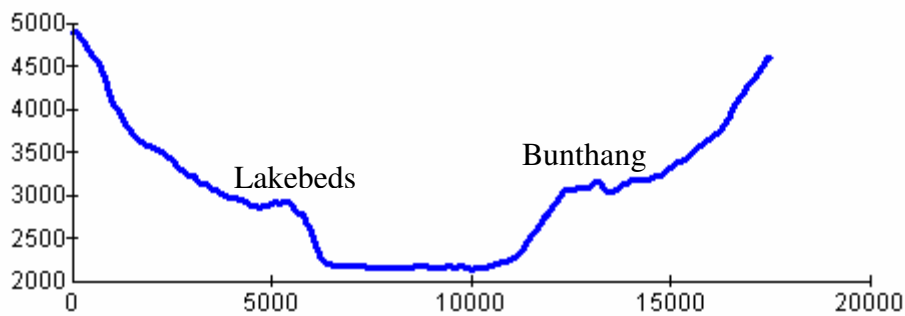


Figure 57. Profile across Skardu Basin, lakebeds, and Bunthang sediments.

A significant observation is the correlation of the surface elevations of point “F”, the Lakebeds, and the Bunthang (Figure 57). At some time in the past, the valley floor was at an elevation of ~3000 m asl (Figure 56 and 57). Profile A, in Figure 58, also has a planar surface at ~3200 m. A second surface that correlates is at elevation ~4200. Owen and Derbyshire (1993) report a “pre-Pleistocene relief” surface at elevation 4100-4200 m in the Hunza Valley. A late Tertiary palaeorelief surface had an elevation of >5200 m. Owen and Derbyshire (1993) also recognized two lower surfaces at ~3000 and 2700 m. These 4200 m and 5200 m planation surfaces are recognized throughout the Karakoram Mountains and Tibet, and are attributed to a combination of climate and tectonics.

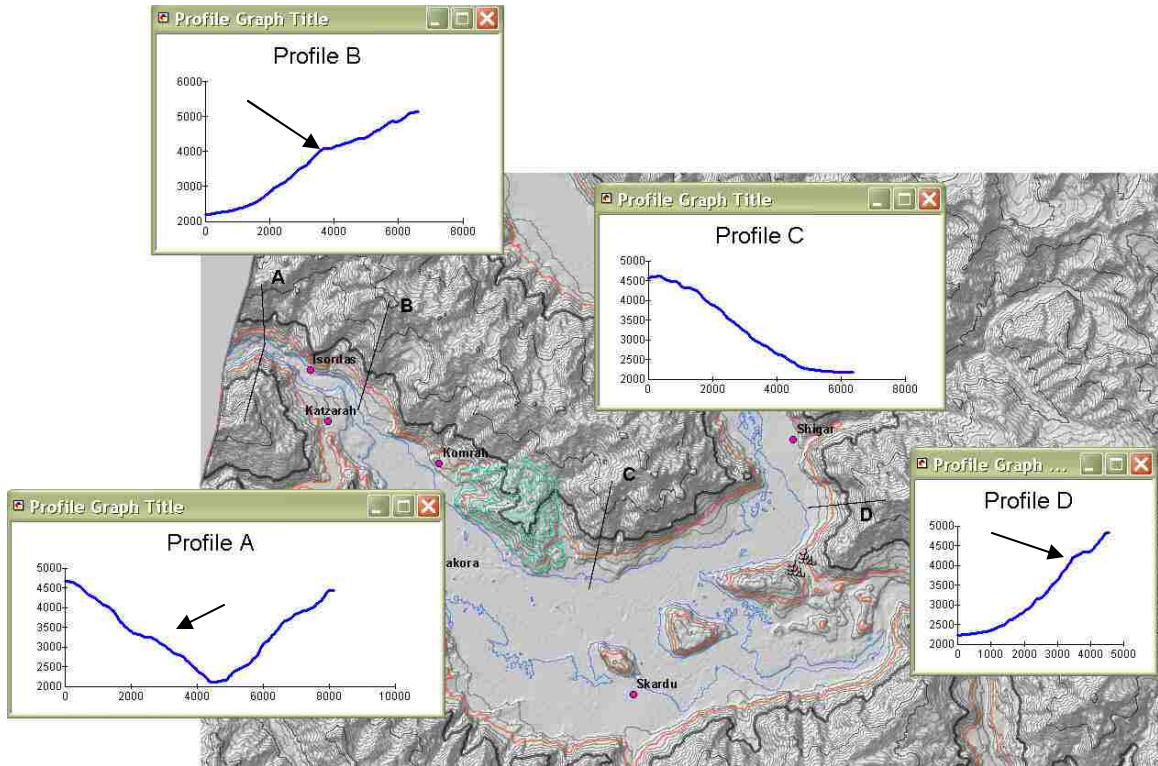


Figure 58. Skardu Basin with trim lines indicated by arrows.

The relative elevations of Karpochi mesa, Blunko mesa, Stronodoka transfluence pass and the base of the Bunthang and Lakebeds are displayed in Figure 53. The transfluence pass on Stronodoka Ridge (Figure 33) and mesas such as Blunko and Karpochi were shaped by a trunk glacier advancing from the Shigar valley. From a stratigraphic view, these features correlate temporally. Cronin (1989) also correlated the Bunthang till with the moraines on Karpochi. However, Seong et al. (2007) placed the Karpochi moraines in the Skardu glacial stage (~150 kya). If the moraine boulders were previously buried by sediments, the TCN age would be a minimum age. In fact, Seong et al. (2007) express that the moraines may actually be much older. Therefore, it is possible that the dates for the Skardu Glacial Stage are incorrect. This would question whether the Skardu Glacial Stage was a distinct event, separate from the Bunthang Stage, in the glacial history. The ice that flowed through the transfluence pass would have also

covered the mesas and removed any previous sediment. Are the mesas, transfluence pass and basal till all features of the same event? The Bunthang till and the Karpochi till can not be of the same age, but associated with different glacial stages.

The Bunthang till is late Cenozoic in age and correlates with the Jalipur till (Cronin and Johnson, 1993). Cronin and Johnson (1993) theorize that glaciation, rapid uplift and slope instability downstream raised the base level of the Indus River allowing the accumulation of sediments. Brookfield (1993) prefers a glacial bedrock basin model to a dammed lake model. He declares that uplift is responsible for the present altitude of the Bunthang. Shroder (1993) describes the Indus River as being deflected north along the Raikot fault zone, before turning abruptly west. In the Indus Valley, near Nanga Parbat, the sediments from the Jalipur till are preserved beneath the Raikot fault (Shroder, 1993). Ages of the Jalipur till and Bunthang till need to be further researched to accurately correlate the two tills. What mechanism is responsible for the till to be visible in the basin, and located beneath a fault?

2. Shigar Valley

The wide Shigar Valley was formed mainly by a former thick trunk glacier. The Baltoro Glacier extended into the valley (Seong et al., 2007) during the Bunthang, Skardu, and Mungo stages. The Chogo Lungma Glacier would have flowed down the Basha River and coalesced with the Baltoro Glacier. The combined glaciers would account for the increased width of the Shigar Valley, as compared to the Braldu or Basha Valleys. Another factor in the oversized valley is the implied fault that passes through

the valley (Figure 50). A fault is delineated between the Kohistan-Ladakh Terrane and batholith on the east side of the valley, but no fault is shown between them in the valley. The Main Karakoram Thrust passes at an angle to the valley and the implied fault. The valley width could be an expression of tectonics as well as glacial and fluvial erosion.

Today the valley is filled with extensive paraglacial alluvial fans (Figure 59). The sediment for the fans originates from mass movement and from the moraines at the head of the catchments. Catchments and moraines are plentiful on the southwest side of the Shigar Valley and the south side of the Braldu Valley. As a result, fans are more plentiful on these respective sides. This is in agreement with the findings of Naylor and Gabet (2007). However, the largest alluvial fans and the largest side valleys are on the northeast side of the Shigar Valley (Figure 43). These valleys include Norin's "rift valleys". This is in agreement with Ahnert (1998) that the size of the fan is in proportion to the size of the catchment. These fans began accumulation after deglaciation.

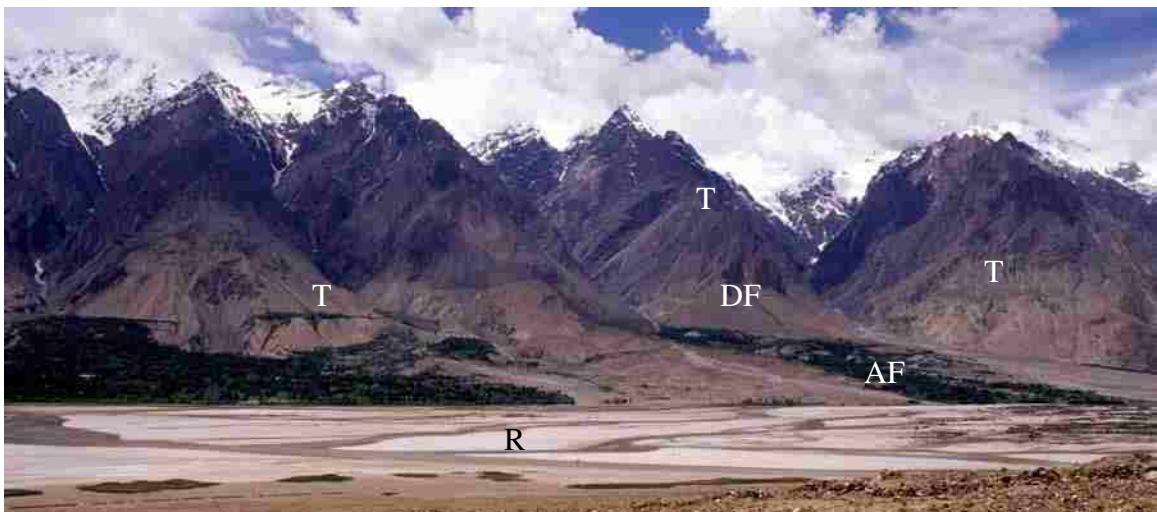


Figure 59. Shigar Valley. (R) Shigar River, (AF) alluvial fan, (DF) debris fan, and (T) trimline.

Observing the cross-sections in appendix D, there are multiple ridges and depressions along the profiles of the west side of the Shigar Valley. This appears to be evidence of a paleovalley.

The geomorphological mapping identified three sets of trimlines at elevations of approximately 1100 m, 675 m, and 425 m above the present valley floor of 2300 m asl. This correlates with the conclusion presented by Seong et al. (2007) that three glacial advances occurred in the Shigar Valley. There is also a surface at ~4700 m asl (Figure 60 and Figure 61) that correlates to the upper surface in the Skardu Basin; this correlates to Owen and Derbyshire's (1993) planation surface.



Figure 60. Shigar Valley, Upper trim line or planation surface.

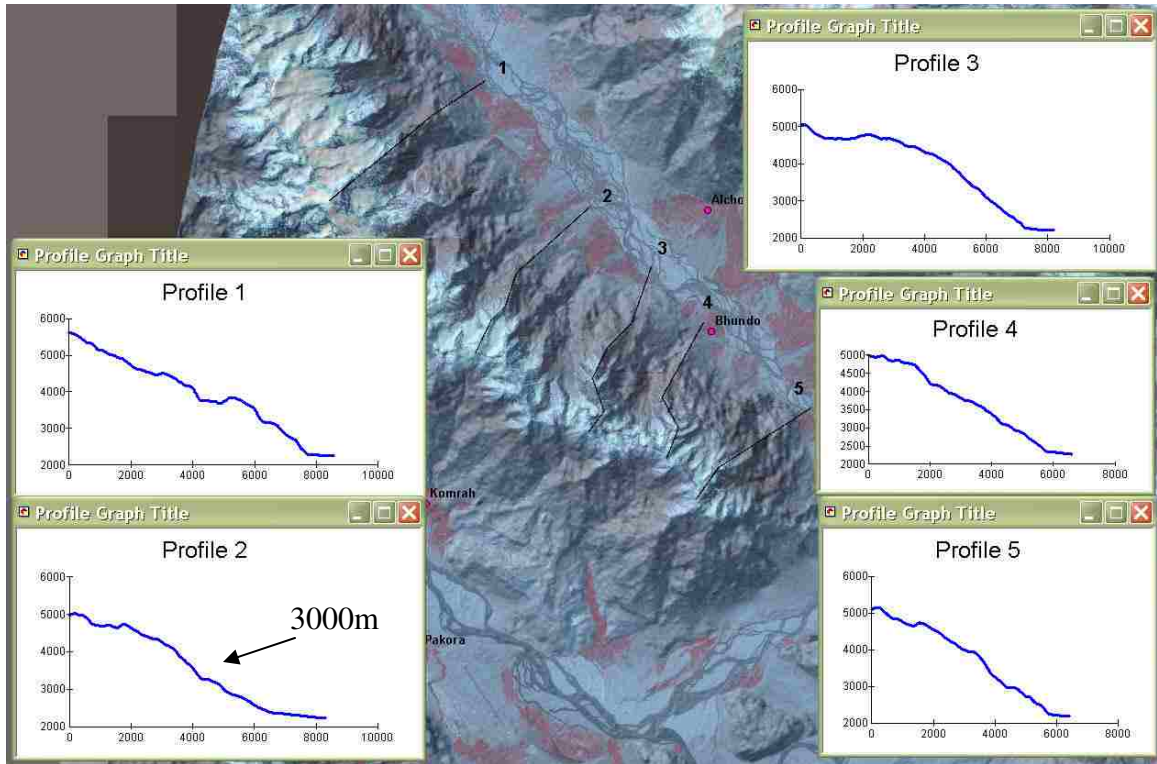


Figure 61. Profiles of west side of Shigar Valley, showing trimlines and upper planar surface.

The contours of the 3000 m asl basin floor and the planation surfaces are shown in Figure 62. The basin, as determined from cross-sections of the downstream end of the Shigar Valley and photo (Figure 55 and Figure 56) would have been very extensive. It is interesting to note the 4200 m planation surface corresponds with the present snowline in the Shigar Valley and lower Braldu Valley and the 5200 m surface corresponds with the present snowline in the upper Braldu Valley and tributaries.

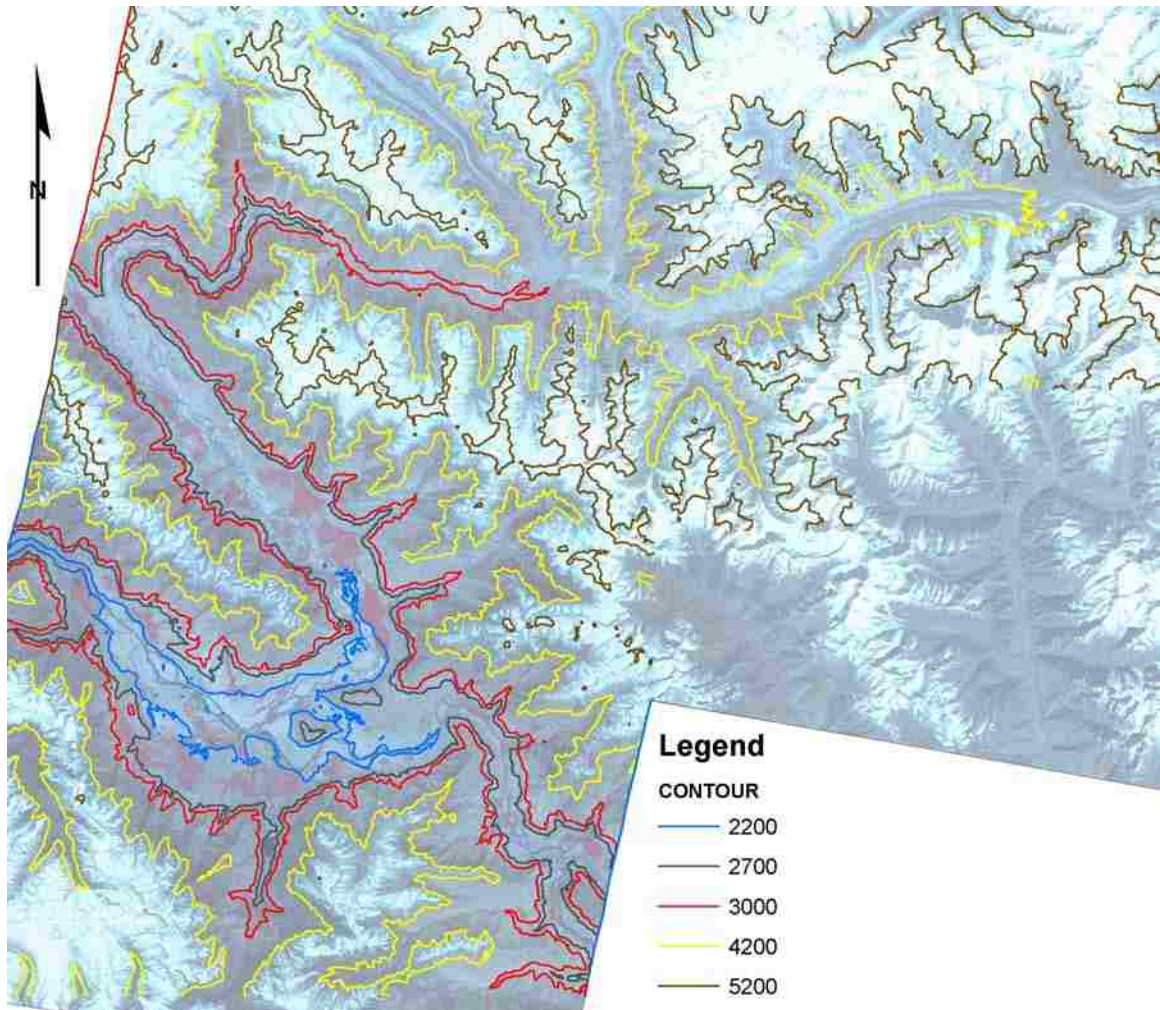


Figure 62. Contours of Planation surfaces at elevations 4200 m and 5200 m. Proposed Basin floor at elevation 3000 m.

3. Braldu Valley

The mostly narrow antecedent Braldu Valley is dominated by a single channel river and evidence of catastrophic flood events (Figure 63). From the confluence of the Shigar and Braldu rivers, between Dassu and Biafo Glacier, the valley follows an incised, sinuous course. Here, the general notion of a wide U-shape glacial valley does not hold true. In the Southern Alps of New Zealand, Brook et al. (2008) studied the cross-profiles



Figure 63. Braldu Valley seen from the ridge of the Mungo sackung. Here, the valley is a gorge with mass movement deposits and debris fans.

of glacial valleys. Their research examined the differences in valley geometry and the duration of glacial occupancy. They found a temporal trend, that valleys become U-shaped with 400 - 600 ka of glacial occupancy. Using this trend, the Braldu Valley was occupied by glaciers for less than 400 ka.

The valley walls are adjusting to deglaciation and the hillside are covered with debris fans. The Western Himalayan Syntaxis, which includes the Kohistan and Ladakh Arcs, contains many actively growing crustal-scale antiforms (Garzanti et al., 2005). The Lower Braldu Valley geometry reflects a combination of the length of glacial occupancy and tectonics, with many mass movements concealing the bedrock form.

The Braldu Valley has three sets of trimlines, two of which correlate to those in the Shigar Valley. The 3700 m asl and 3200 m asl trimlines are the lower limit of the Braldu trimlines and the upper limit of the Shigar trimlines. The third Braldu trimline has a lower elevation of 4500 m asl. There are three terrace generations, which are found only in the Braldu Valley.

The Baltoro Valley (the Braldu Valley upstream from the Biafo Glacier) opens to a wide valley (Figure 64). The braided river indicates a high sediment load issuing from Baltoro Glacier in a sporadic discharge pattern. The valley walls are coated with till, lateral moraines and debris fans. Vegetation is sparse in this area of little soil development and permafrost. Trimlines near Liligo Glacier and Concordia infer former glacial surfaces 700 m and 500 m above today's glacier surface.



Figure 64. Baltoro Glacier and Baltoro Valley with glacial outwash plain.

Erosion has not erased all of the artifacts of the glacial advances. Roche moutonnée, trimlines, moraines, and till are found along the length of the valleys. Roche moutonnées are found in the Dassu area, in the lower Braldu Valley, 200-250 m above the recent river. The only roche moutonnées outside of the Dassu to Askole area are those on the Transfluence Pass, in the Skardu Basin.

Flood deposits are only found in the Braldu Valley. Some of these deposits are located on terraces 10-50 m above the recent river. Lacustrine sediments indicate that first glaciers or landslides initially blocked the trunk valley, followed by the breaching of the dam, which released flash floods capable of carrying huge boulders of the size of a garage. Seong et al. (2008a) calculated a mean discharge of $1.6 \times 10^4 \text{ m}^3 \text{ s}^{-1}$ for the flood near Chakpo. River gages are not available to measure the present river flows. A second flood deposit was identified near Dassu, and a third one is present west of Korophon. These floods scoured the valley, removed many sedimentary features, and left impressive potholes and fluvial polish.

The removal of sediments also undercuts the base of the hillslopes, leading to slope failures, mass movement events, and debris fans. Furthermore, seismic activity might trigger mass movements. Shroder (1998) stated that the maximum denudation by slope failure occurs where major lithologic discontinuities exist, as at terrane boundaries, which are commonly also zones of high seismicity. The Braldu Valley is crossed by many such faults and resulting lithology discontinuities. Debris fans from rock fall and rock avalanches are the dominate fan type. Debris fans make up 60% of all fans in the Braldu Valley, and 39% in the Shigar Valley, contrasted with 47% and 15% by areal measurement, respectively. Historical flood events, and seasonal high water events, erode

and entrain sediments, preventing the formation or growth of many fans. The valleys have been deglaciated for only a relatively short time period and the valley walls are in a state of slope readjustment. Ballantyne et al. (1994) described the similar slope development following recent glacial retreat in Norway.

4. Rivers and Erosion

The rivers of the study area are predominately braided-systems. This is an indication that the carrying capacity of the rivers is insufficient to the amount of sediment load. The sandbars are a storage facility and sediments are transported only during high flows. The implication is that the rivers are mainly a transportation mechanism and not an erosional device. An exception to the braided river systems is in the Braldu Valley between the confluence with the Shigar River and Korophon. Here, the river is confined to a single channel with high incision rates as measured by Seong et al. (2008b). The high incision rate for the epigenetic gorge is partially the result of the river returning to the former base level, after being displaced from the landslide.

Erosion rates of $12,500 \pm 4700$ t/km² year or 4.5 ± 1.7 mm/year were obtained for the Braldu and Shigar catchment (Garzanti et al., 2005). Of the total sediments accumulating in the Tarbela Lake, behind a dam built in 1974, the largest load as determined by petrology studies, is from the Braldu and Shigar River system. They cautioned that erosion patterns deduced from modern sediments might not be extrapolated even to the recent past. There may have been even greater erosion of the active-margin units, such as the Kohistan-Ladakh Arc, in pre-Holocene times.

Gabet et al. (2008) studied the erosion rates in the Himalayas of Nepal. They refer to a current theory that tectonics, climate and erosion are linked. The feedback loop consists of surface uplift, which causes orographic precipitation, which leads to erosion from increased pore-pressure triggered landslides. Denudation rates are high during glacial periods, but during interglacials, the rates of erosion decrease, such that there is a long-term uniform rate. On a time-scale of 10^5 yr, they propose that rock uplift is balanced by erosion. They showed that modern erosion rates parallel rainfall rates.

VI. CONCLUSION

This is the first complete geomorphological map series of the Skardu, Shigar, and Braldu valleys (appendix C and F). The maps created by the author provide a base for further detailed geomorphological mapping in the region. They also confirmed previous work and identified several conflicts of interpretation that need more evaluation.

Geomorphological mapping was used to identify erosional and depositional landforms. Where possible, the process was identified. This study found that the main eroding and transporting media in the K2 study area are glaciers and rivers, with mass movement providing the majority of sediment to the glaciers and rivers. Tectonics has a role in the development of the valleys and the impetus for mass movements.

Mass movements are a result of debuttrressing of valley walls and stress-release. Each is a consequence of the occurrence of glaciers. Mass movements are also triggered by precipitation. Debris is deposited either on glaciers and then to the rivers or directly to the rivers. The sediment has overwhelmed the rivers, creating terraces and sandbars.

Avalanches have blocked the rivers and created dams, leading to outbreak floods or epigenetic gorges. Three historic flood events and annual high water events are responsible for the removal of some of these sediments from the system.

Glacial erosion is evident in the study area from the U-shaped valleys and trim lines, the transfluence pass, *roche moutonnée*, and till deposits. Fluvial erosion is evident from the flood deposits, the alluvial fans, river terraces, epigenetic gorge, potholes and fluvial polish.

Tectonics also contributes to the relief development of the area. Faults are active in the area, as evidenced by the sackungen and bent glacial valleys of the Masherbrum. The antecedent Braldu Valley is the result of river incision during active uplift. The topography of the Skardu Basin and the Shigar Valley are partially the result of faults that transect the valleys. This study identified five previously undisclosed faults within the Skardu and Shigar valleys. The four tributary valleys on the east side of the Shigar Valley are rift valleys. There is also a rift valley perpendicular to the Satpura Valley, south of the lake. Tectonic activity likely produced the rock avalanche that dammed the river and created the lake.

The result of this work does not support Seong et al. (2007 and 2008) and their published four glacial stages. There are three sets of trim lines in each valley, however only two sets correlate, leading to a proposal of four events. These, together with the Bunthang stage would delineate five stages. This would agree with Owen (1988), and Owen and Derbyshire (1988).

This study questions the Cronin and Johnson (1989) theory that the till at the base of the Bunthang is the same as the lateral moraines preserved on top of the Karpochi

Mesa. If the moraines belong to the Skardu stage per Seong et al. (2007), they cannot also belong to the Bunthang stage. However, Seong et al. (2007) state that the age of the moraines might be considerably older. Could they be old enough to belong to the Bunthang stage? Until ages can be collected from the two tills to support a correlation, the assumption hinders the analysis of the basin and restricts the possible geomorphic mechanisms.

This study support Hewitt's conclusion that Satpura Lake is impounded by a rock avalanche and not a moraine as mapped in Seong et al. (2007). The glaciotectonized sediments can be explained by liquid deformation and glacial sediment entrainment during the landslide.

Using slope analysis, a new sackung was discovered in the Shigar Valley above the settlement of Bhundo. Like the sackung above Mungo, this one had geologic origins.

It is difficult to conclude whether glacial, fluvial, or tectonic action is responsible for the greatest relief production. I propose that the relief production of the K2 area is a result of the interplay of all these elements on different temporal scales. No individual element would have the capacity to accomplish the relief without the contribution of the other elements.

REFERENCES

- Ahmed, S., Joyia, M.F., 2003. *Northern Areas strategy for sustainable development background paper: water*. IUCN Pakistan, Northern Areas Programme, Gilgit xiv +67pp.
- Anhert, F., 1998. *Introduction to Geomorphology*. Arnold, London, 352 pp.
- Ballantyne, C.K., Benn, D.I., 1994. Paraglacial slope adjustment and resedimentation following recent glacier retreat, Fåbergstølsdalen, Norway. *Arctic and Alpine Research* 26, p. 255-269.
- Ballantyne, C.K., 2003. Paraglacial Landsystems. In: Evans, D.J. (Ed.), *Glacial Landsystems*. Arnold, London, p. 432-460.
- Bishop, M.P., Shroder, J.F., Bonk, R., Olsenholler, J., 2002. Geomorphic change in high mountains: a western Himalayan perspective. *Global and Planetary Change* 32, p. 311-329.
- Brook, M.S., Kirkbride, M.P., Brock, B.W., 2008. Temporal constraints on glacial valley cross-profile evolution: Two Thumb Range, central Southern Alps, New Zealand. *Geomorphology* 97, p. 24-34.
- Brookfield, M.E., 1993. Miocene to Holocene Uplift and Sedimentation in the Northwestern Himalaya and Adjacent Areas. In: Shroder, J.F. (Ed.), *Himalaya to the Sea: Geology, Geomorphology and the Quaternary*. Routledge, London, p. 43 - 71.

- Cronin, V.S., 1989. Structural setting of the Skardu intermontane basin, Karakoram Himalaya, Pakistan. In: Malinconico, L.L., Lillie, R.J. (Ed.), *Tectonics of the Western Himalayas*. Geological Society of America Special Paper 232, p. 183-202.
- Cronin, V.S., Johnson, G.D., 1993. Revised chronostratigraphy of the Late Cenozoic Bunthang sequence of Skardu intermontane basin, Karakoram Himalaya, Pakistan. In: Shroder, J.F. (Ed.), *Himalaya to the Sea: Geology, Geomorphology and the Quaternary*. Routledge, London, p. 91-107.
- Derbyshire, E., Owen, L.A., 1997. Quaternary glacial history of the Karakoram mountains and northwest Himalayas: a review. *Quaternary International* 38, p. 85-102.
- Fielding, E., 2000. Morphotectonic evolution of the Himalays and Tibetan Plateau. In: Summerfield, M. (Ed.), *Geomorphology and Global Tectonics*. Wiley, Chichester, p. 201-222.
- Foster, D.A., Gleadow, A.J.W., Motimer, G., 1994. Rapid Pliocene exhumation in the Karakoram (Pakistan), revealed by fission-track thermochronology of the K2 gneiss. *Geology* 22, p. 19-22.
- Gabet, E.J., Burbank, D.W., Pratt-Sitaula, B., Putkonen, J., Bookhagen, B., 2008. Modern erosion rates in the High Himalayas of Nepal. *Earth and Planetary Science Letters* 267, p. 482 - 494.
- Garzanti, E., Vezzoli, G., Andò, S., Paparella, P., Clift, P., 2005. Petrology of Indus River sands: a key to interpret erosion history of the Western Himalayan Syntaxis. *Earth and Planetary Science Letters* 229, p. 287 -302.

- Hanson, C.R. 1989. The northern suture in the Shigar valley, Baltistan, northern Pakistan. *Geological Society of America Special Paper 232*, p. 203-215.
- Hewitt, K., 1989. The altitudinal organization of Karakoram geomorphic processes and depositional environments. *Zeitschrift für Geomorphologie N.F.* 76, p. 9-32.
- Hewitt, K., 1998a. Catastrophic landslides and their effects on the Upper Indus streams, Karakoram Himalaya, northern Pakistan. *Geomorphology* 26 p. 47-80.
- Hewitt, K. 1998b. Glaciers receive a surge of attention in the Karakoram Himalaya, *Eos Transactions AGU* 79, 104.
- Hewitt, K., 1999. Quaternary moraines vs catastrophic rock avalanches in the Karakoram Himalaya, northern Pakistan. *Quaternary Research* 51 p. 220-237.
- Khan, T.Z., Cyan, M. R., Tariq, I., Latif, A., Perkin, S, ed. Government of Pakistan and IUCN, 2003. *Northern Areas Strategy for Sustainable Development*. IUCN Pakistan, Karachi xxiii 85pp.
- Kamp, U., 1999. Jungquartäre Geomorphologie und Vergletscherung im östlichen Hindukusch, Chitral, Nordpakistan. *Berliner Geographische Studien* 50. Berlin, 254 pp.
- Kamp, U., Haserodt, K., Shroder, J.F., 2003. Quaternary landscape evolution in the eastern Hindu Kush, Pakistan. *Geomorphology* 57, p. 1-27.
- Kamp, U., Bolch, T., Olsenholler, J., 2003. DEM generation from ASTER satellite data for geomorphometric analysis of Cerro Sillajhuay, Chile/Bolivia. *ASPRS 2003 Annual Proceedings*, May 5-9, 2003, Anchorage, Alaska, U.S.A., 9 pp., CD-ROM.

- Mihalcea, C., Mayer, C., Diolaiuti, G., Lambrecht, A., Smiraglia, C., Tartari, G., 2006. Ice ablation and meteorological conditions on the debris-covered area of Baltoro glacier, Karakoram, Pakistan. *Annals of Glaciology* 43, p. 292-300.
- Naylor, S., Gabet, E., 2007. Valley asymmetry and glacial versus nonglacial erosion in the Bitterroot Range, Montana, USA. *Geology* 35, p. 375-378.
- Norin, Erik, 1925. Preliminary Notes on the Late Quaternary Glaciation of the North-Western Himalaya. *Geografiska Annaler* 7, p. 165-194.
- Owen, L.A., 1988. Wet-sediment deformation of Quaternary and recent sediments in the Skardu Basin, Karakoram Mountains, Pakistan. In: Croot, D. (Ed.), *Galciotectonics: Forms and Processes*. Balkema, Rotterdam, p 123 - 147
- Owen, L.A., Derbyshire, E., 1993. Quaternary and Holocene intermontane basin sedimentation in the Karakoram Mountains. In: Shroder, J.F. (Ed.), *Himalaya to the Sea: Geology, Geomorpholgy and the Quaternary*. Routledge, London, p. 108-131.
- Rao, A. L., Marwat, A. H., 2003. *Northern Areas strategy for sustainable development background paper: forestry*. IUCN Pakistan, Northern Areas Programme, Gilgit xii 66pp.
- Searle, M.P., 1991. *Geology and Tectonics of the Karakoram Mountains*. 1: 250,000. John Wiley & Sons.
- Searle, M.P., Rex, A.J., Tirrul, R., Rex, D.C., Barnicoat, A., Windley, B.F., 1989. Metamorphic, magmatic, and tectonic evolution of the central Karakoram in the Biafo-Baltoro-Hushe regions of northern Pakistan. *Geological Society of America Special Paper* 232, p. 47-73.

Seong, Y.B., Owen, L.A., Bishop, M., Bush, A., Clendon, P., Copland, L., Finkel, R., Kamp, U., Shroder, J.F., 2007. Quaternary glacial history of the Central Karakoram. *Quaternary Science Reviews* 26, p. 3384-3405.

Seong, Y.B., Bishop, M., Bush, A., Clendon, P., Copland, L., Finkel, R., Kamp, U., Owen, L.A., Shroder, J.F., 2008a. Landforms and landscape evolution in the Central Karakoram Mountains. *Geomorphology*, (in press).

Seong, Y.B., Owen, L.A., Bishop, M., Bush, A., Clendon, P., Copland, L., Finkel, R., Kamp, U., Shroder, J.F., 2008b. Rates of fluvial bedrock incision within an actively uplifting orogen: Central Karakoram Mountains, northern Pakistan. *Geomorphology* 94, p. 274-286.

Shroder, J.F., 1993. Himalaya to the sea: geomorphology and the Quaternary of Pakistan in the regional context. In: Shroder, J.F. (Ed.), *Himalaya to the Sea: Geology, Geomorphology and the Quaternary*. Routledge, London, p. 1-42.

Shroder, J.F., Bishop, M.P., 2000. Unroofing of the Nanga Parbat Himalaya. In: Khan, M.A. et al. (Ed.), *Tectonics of the Nanga Parbat Syntaxis and the Western Himalaya*. Geological Society, London, Special Publications, 163-179.

Shroder, J.F., Owen, L.A., Derbyshire, E., 1993. Quaternary glaciation of the Karakoram and Nanga Parbat Himalaya. In: Shroder, J.F. (Ed.), *Himalaya to the Sea: Geology, Geomorphology and the Quaternary*. Routledge, London, p. 132-158.

Shroder, J.F., 1998. Slope failure and denudation in the western Himalaya. *Geomorphology* 26, p. 81-105.

Shroder, J.F., Bishop, M.P., 1998. Mass movement in the Himalaya: new insights and research directions. *Geomorphology* 26, p. 13-35.

Shroder, J.F., Bishop, M.P., Copland, L., Sloan, V.F., 2000. Debris-covered glaciers and rock glaciers in the Nanga Parbat Himalaya, Pakistan. *Geografiska Annaler Series A, Physical Geography*, 82/1, p. 17-31.

van der Beek, P., Bourbon, P. 2008. A quantification of the glacial imprint on relief development in the French western Alps. *Geomorphology* 97, p. 52-72.

Ward, S., 2003. Sackung. In: Goudie, A.S. (ed.), *Encyclopedia of Geomorphology*. Routledge, London, p. 890-891.

APPENDIX A

Identification Methods

Each of the features on the map was identified by different characteristics. Following is a list of the attributes used for identification and mapping.

Fan

- arc outline in contour
- low slope angle
- fans often vegetated
- alluvial: mouth of drainage
- debris: erosion, no drainage
- photo identification

Scarp and cirque

- substantial slope break on slope map and hillshade map

Moraine

- ridge parallel or perpendicular to glacier path
- hillshade map or slope map

River bank

- historic: slope break on hillshade map
- current: satellite image
- Shigar active system mapped bank-full, delineated stream to show braided channels

Bedrock terrace

- flat spots on hillshade map
- photos

Flood deposits

GPS points, field notes, photos

too small to be identified in DEM, raster size 15-meters

Avalanche path

contour lines; arcuate, flow path

field notes and GPS

literature, historic paths

Trimlines

grade break; slope, hillshade, contour maps

valley cross-sections

photos

Terrace sequence

field notes

photos

valley cross-sections

Strath terraces

field notes and GPS

valley cross-sections

Till

field notes

photos

GoogleEarth satellite images

Old channel, incised channel, gorge

field notes and GPS

photos

Paleo Lake sediments

previous maps, i.e. Owen and Cronin

Sand

slope, hillshade, contour maps

ASTER satellite image

Avalanche deposit

slope, hillshade, contour maps

location opposite landslide

photos

satellite image

Drainage

V-shape contours, “point” is upstream

Ridge

V-shape contours, “point” is downhill

Sackung,

drainage pattern, depression, on a ridge

slope and hillshade maps

photos

field notes and GPS

satellite images

Proglacial lake

GPS points, field notes, photos

too small to be identified in DEM, raster size 15-meters

Roche moutonnées

GPS points, field notes, photos

too small to be identified in DEM, raster size 15-meters

Erosion path

contours

source for debris fan or cone

visual; scree slopes often lighter color than surrounding slope in ASTER

Appendix B

Coordinate Systems

Personal Geodatabase

Projected Coordinate System:

Name: WGS_1984_UTM_Zone_43N

Projection: Transverse_Mercator

Parameters:

False_Easting: 500000.000000

False_Northing: 0.000000

Central_Meridian: 75.000000

Scale_Factor: 0.999600

Latitude_Of_Origin: 0.000000

Linear Unit: Meter (1.000000)

Geographic Coordinate System:

Name: GCS_WGS_1984

Angular Unit: Degree (0.017453292519943299)

Prime Meridian: Greenwich (0.000000000000000000)

Datum: D_WGS_1984

Spheroid: WGS_1984

Semimajor Axis: 6378137.000000000000000000

Semiminor Axis: 6356752.314245179300000000

Inverse Flattening: 298.257223563000030000

X/Y Domain:

Min X: 0.000000

Min Y: 3000000.000000

Max X: 21474836.450000

Max Y: 24474836.450000

Precision: 100.000000

M Domain:

Min: 0.000000

Max: 21474.836450

Scale: 100000.000000

Z Domain:

Min: 0.000000

































Max: 21474.836450

Scale: 100000.000000

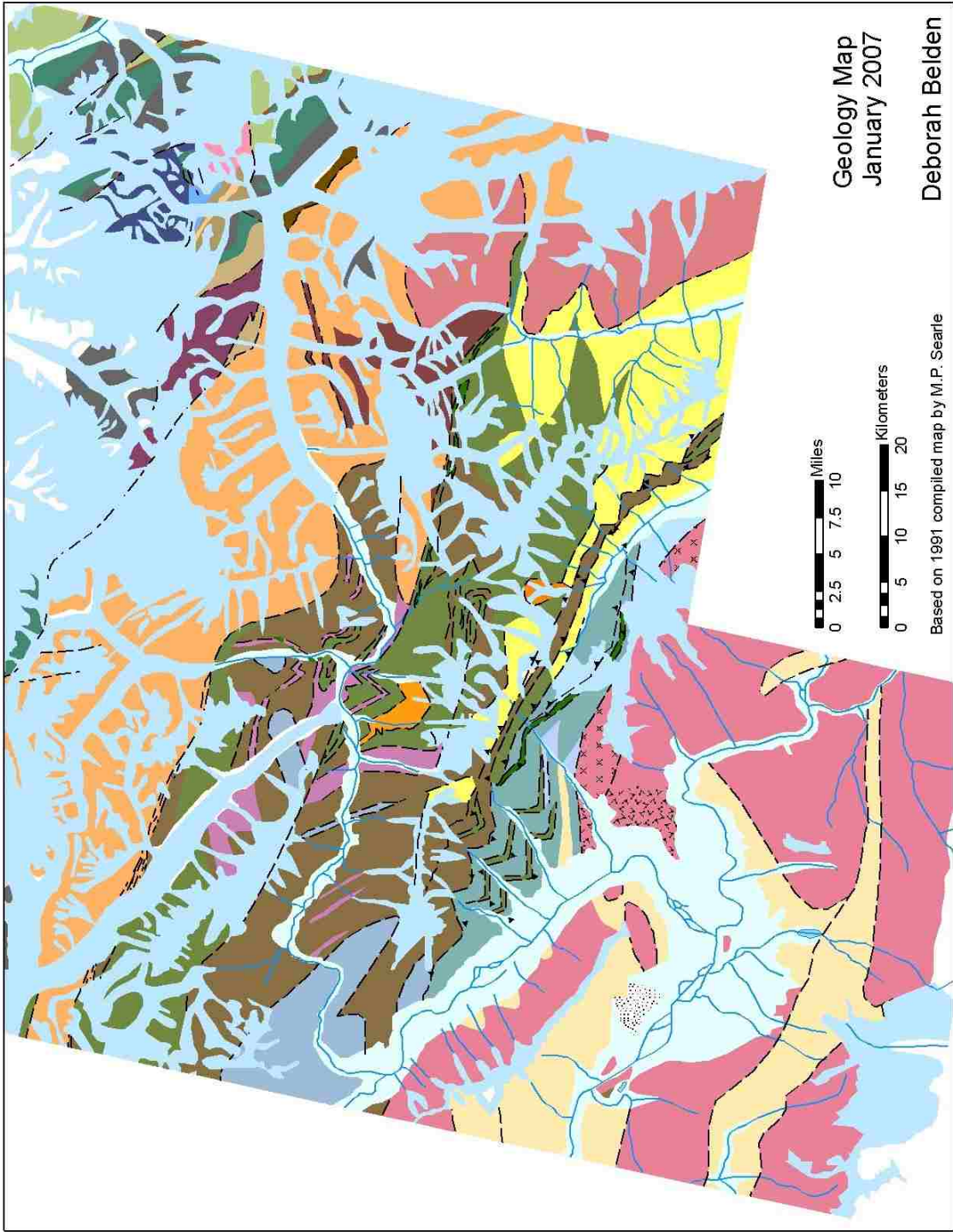
Appendix C

Geology

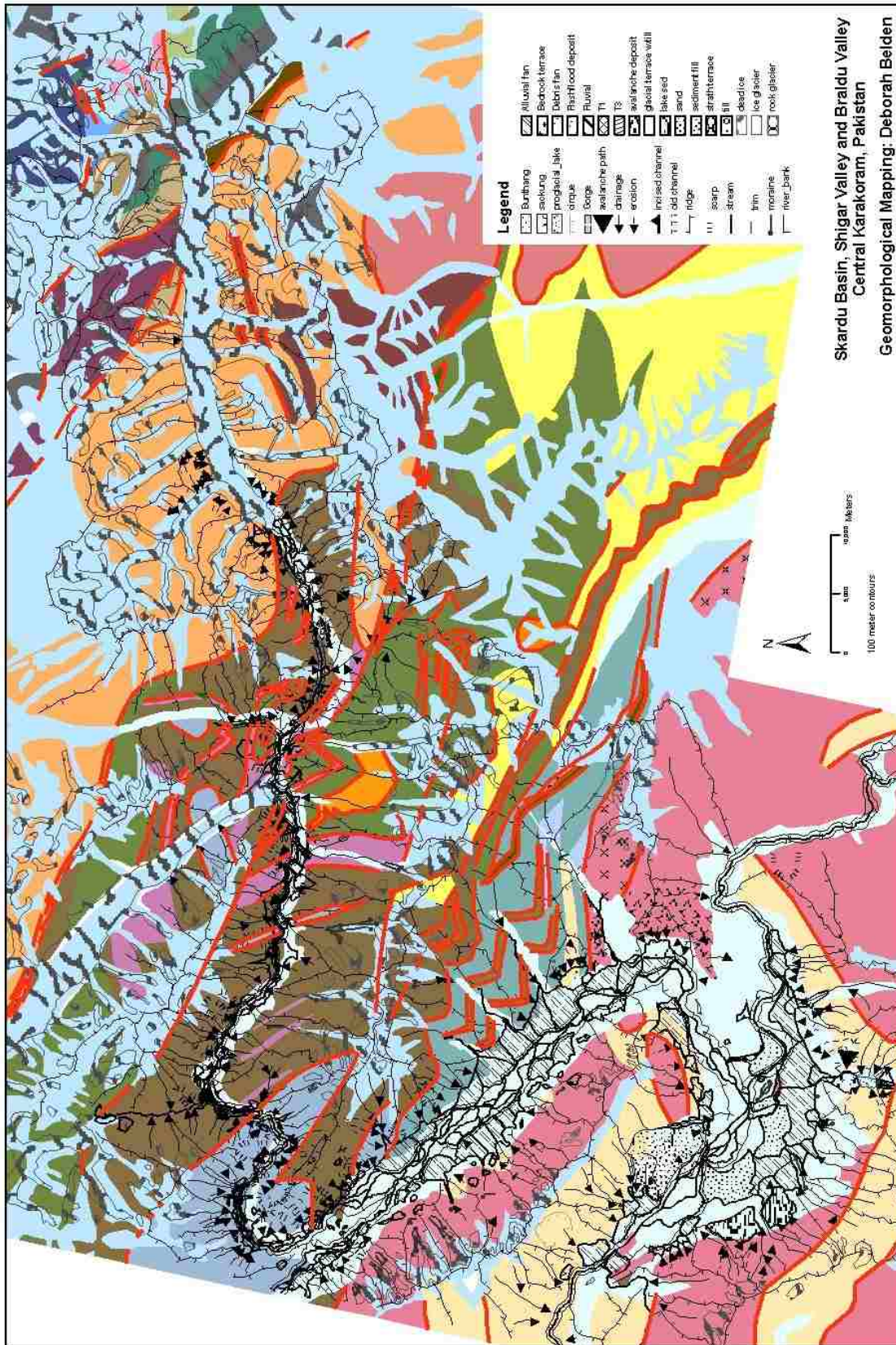
Geology Legend

<u>Map ID</u>	<u>Formation</u>
 AF	Aghil formation
 Ash	Ash-flow tuffs
 AU	Askole unit
 BF	Baltoro formation
 BPU	Baltoro plutonic unit
 BPQD	Broad Peak quartz diorites
 Bunthang	Bunthang sequence
 CL	Chalt volcanic group
 CV	Chingkang-la pluton
 DG	Dassu gneiss
 DS	Doksam sequence
 DU	Dumordu unit
 GU	Ganschen unit
 HG	Hushe gneiss
 K2G	K2 gneiss
 KPC	Kande plutonic complex
 KF	Khalkhal formation
 KLG	Kohistan-Ladakh batholith Gabbros
 KLP	Kohistan-Ladakh batholith Plutonic
 KLU	Kohistan-Ladakh batholith Undifferentiated granite
 MG	Mango Gusar pluton
 MC	Masherbrum complex
 MS	Metasedimentary rocks
 MCA	Mitre contact aureole
 MTU	Muztagh Tower unit
 PUMU	Panmah ultramafic-mafic unit
 QA	Quaternary and Recent alluvium
 Savoia	Savoia formation
 SF	Shaksgam formation
 SSZ	Shyok suture zone rocks
 UF	Urdok formation
 ice	permanent snow and ice cover
NO_ID	Not identified by Searle

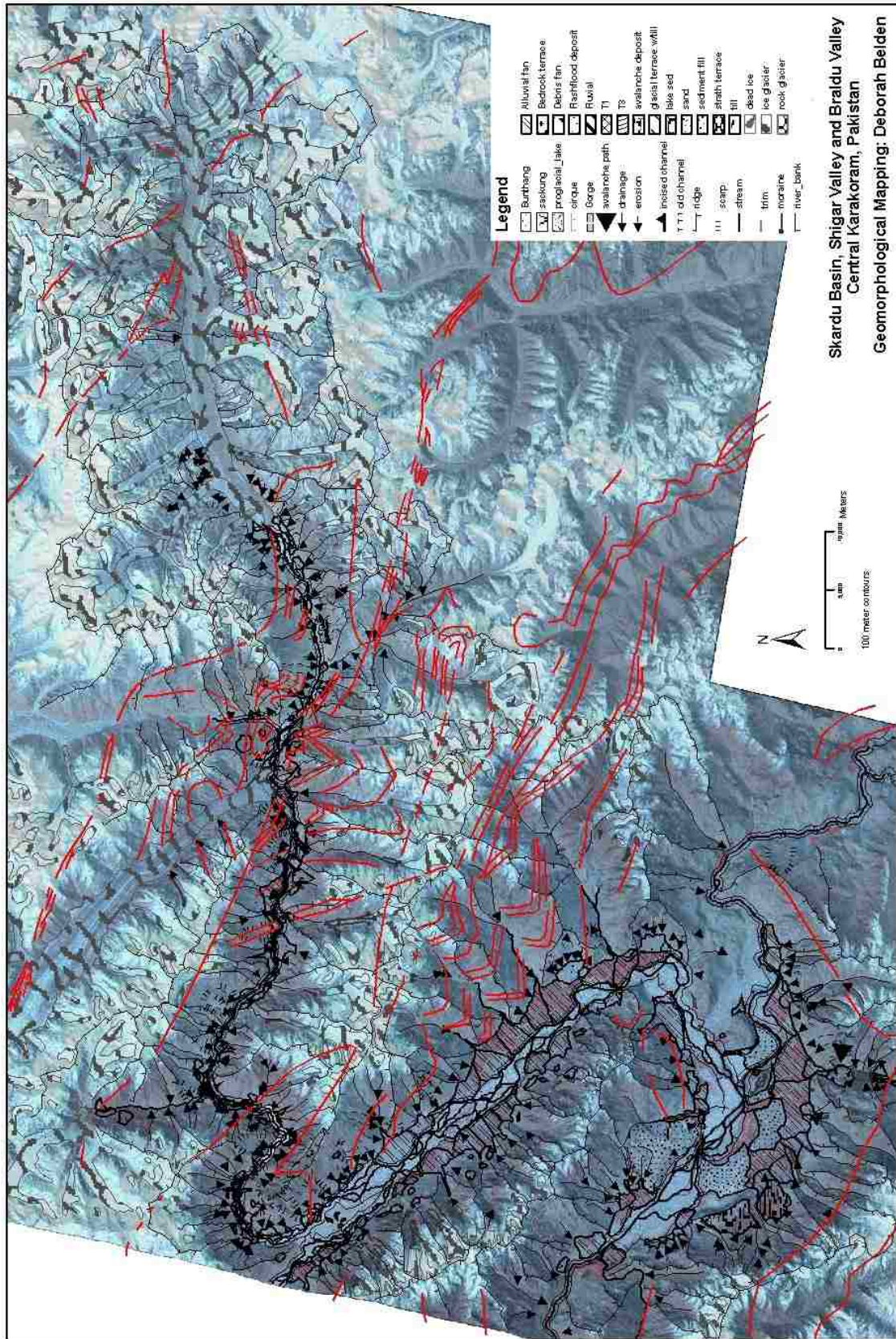
Geology 1. Geology legend after Searle 1991.



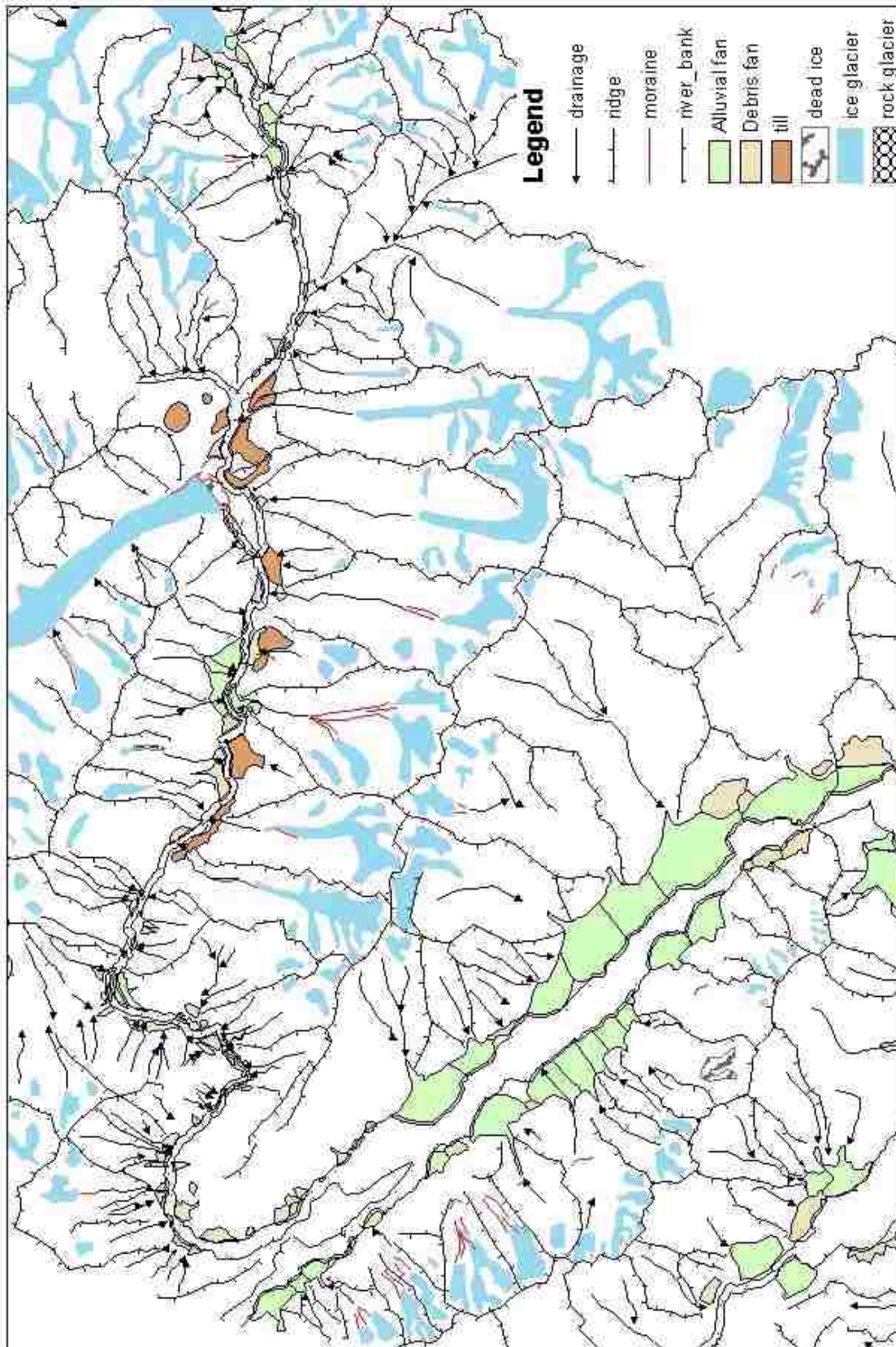
Geology 2. Geology map based on Searle.



Geology 3. Geology and Geomorphology.



Geology 4. Faults Geomorphology and ASTER.

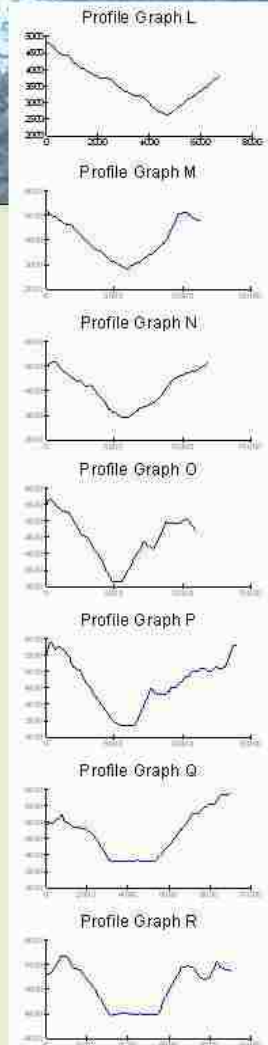
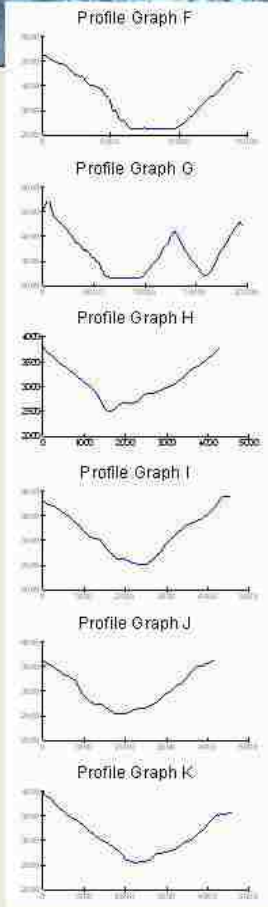
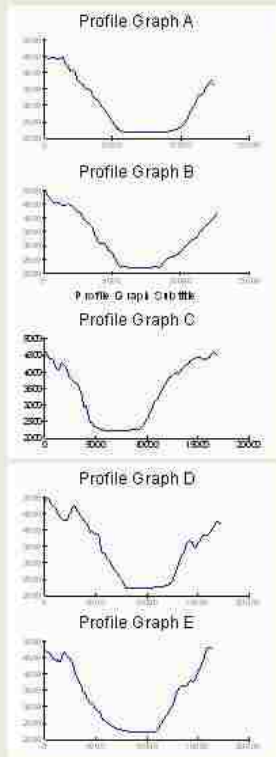
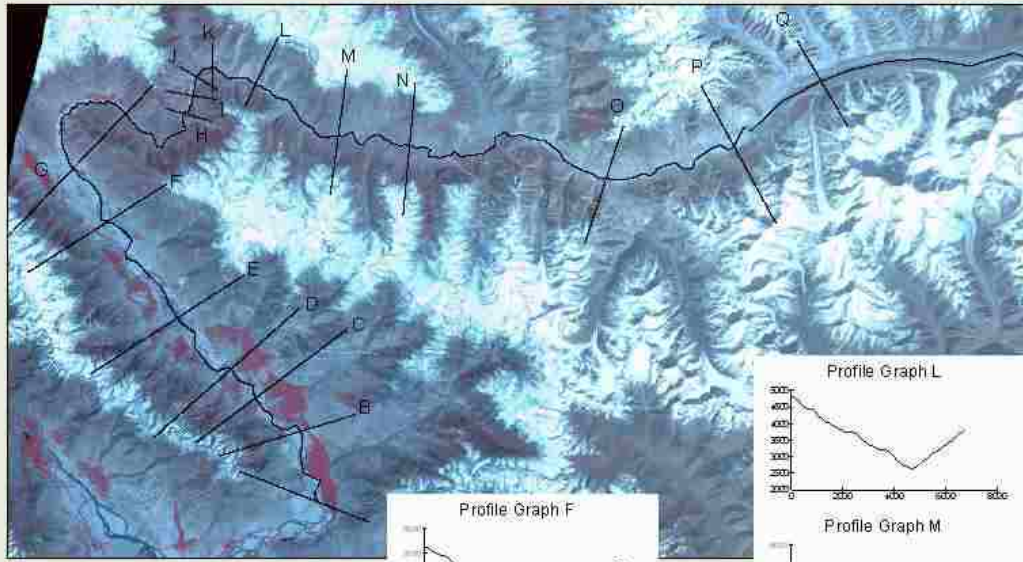


Geology 5. Glaciers, moraines and fans.

D. Belden 2008

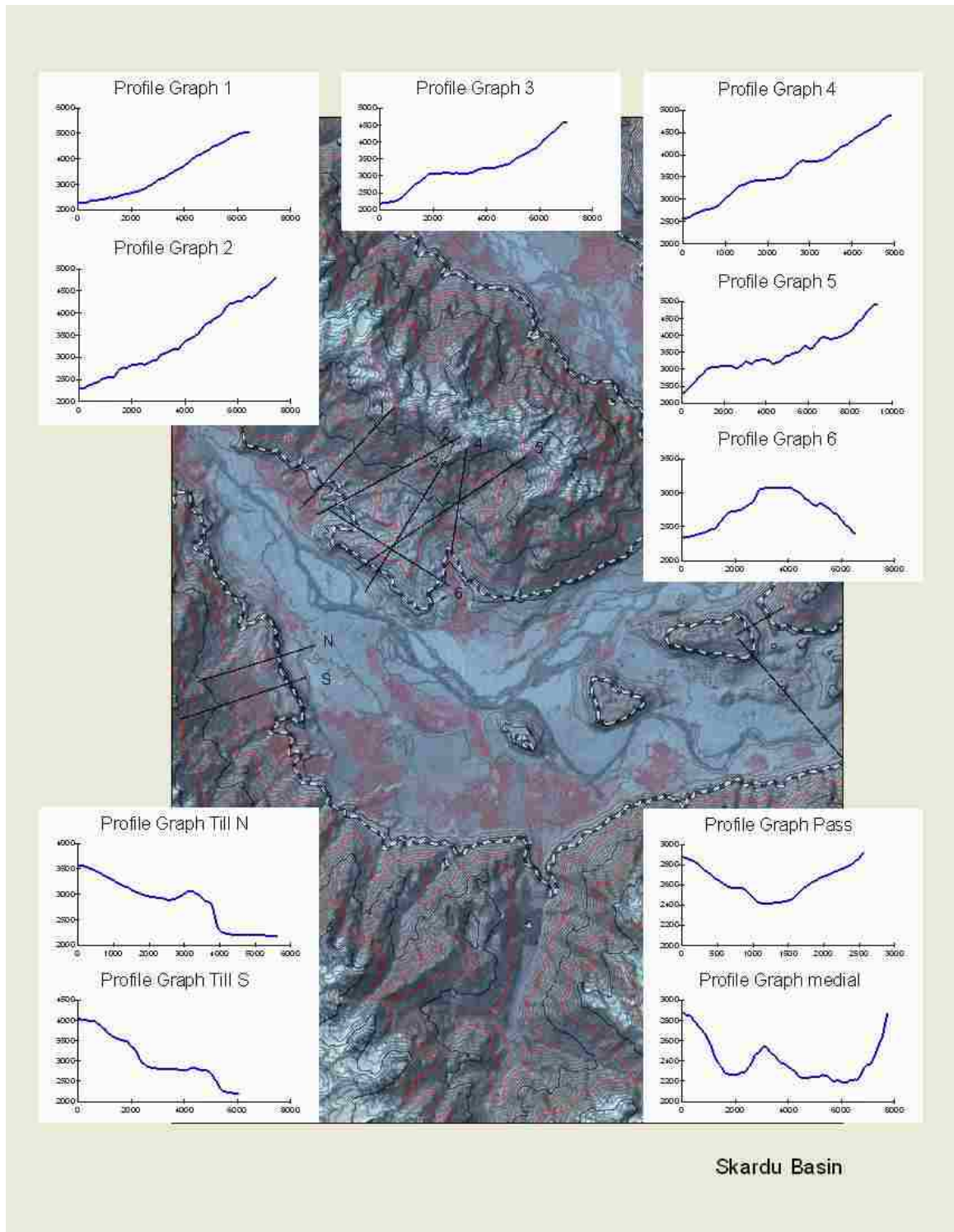
Appendix D

Cross-sections



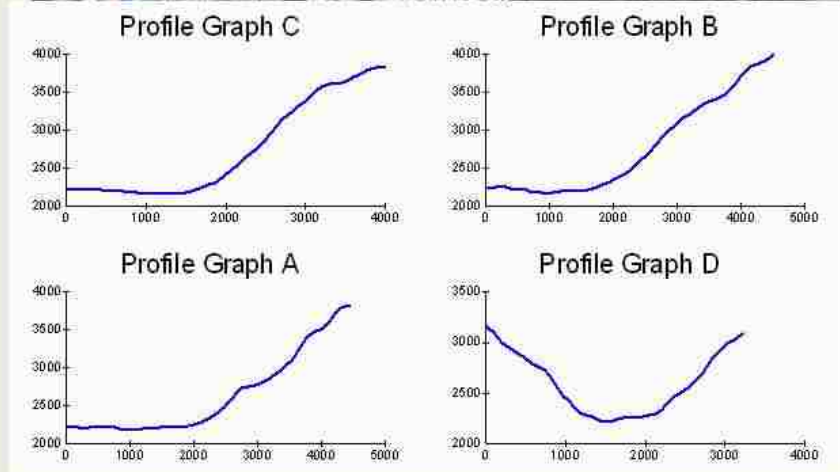
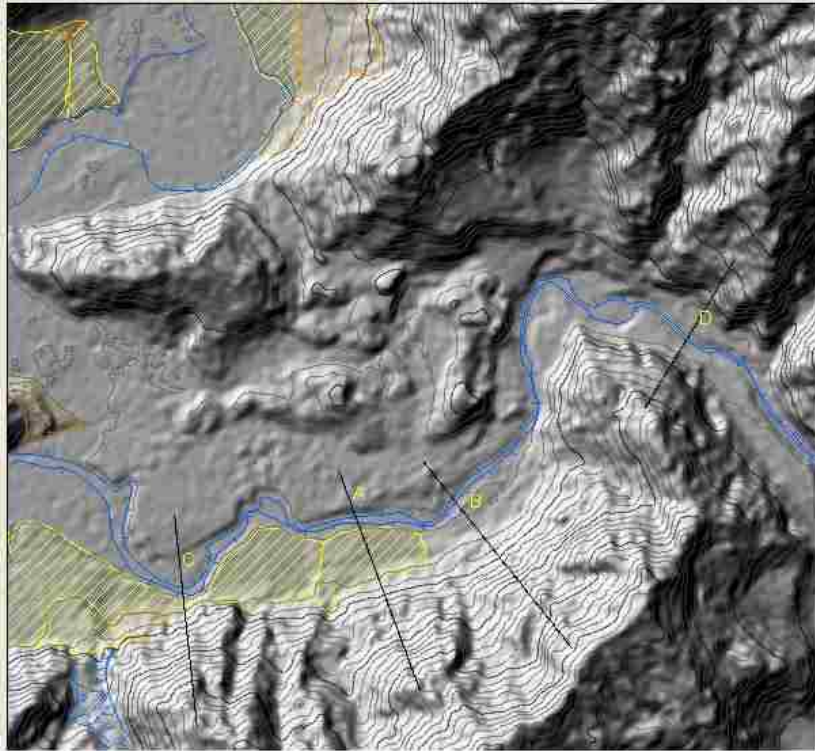
Cross-section 1. Project area.

D. Belden 2008



Cross-section 2. Skardu Basin.

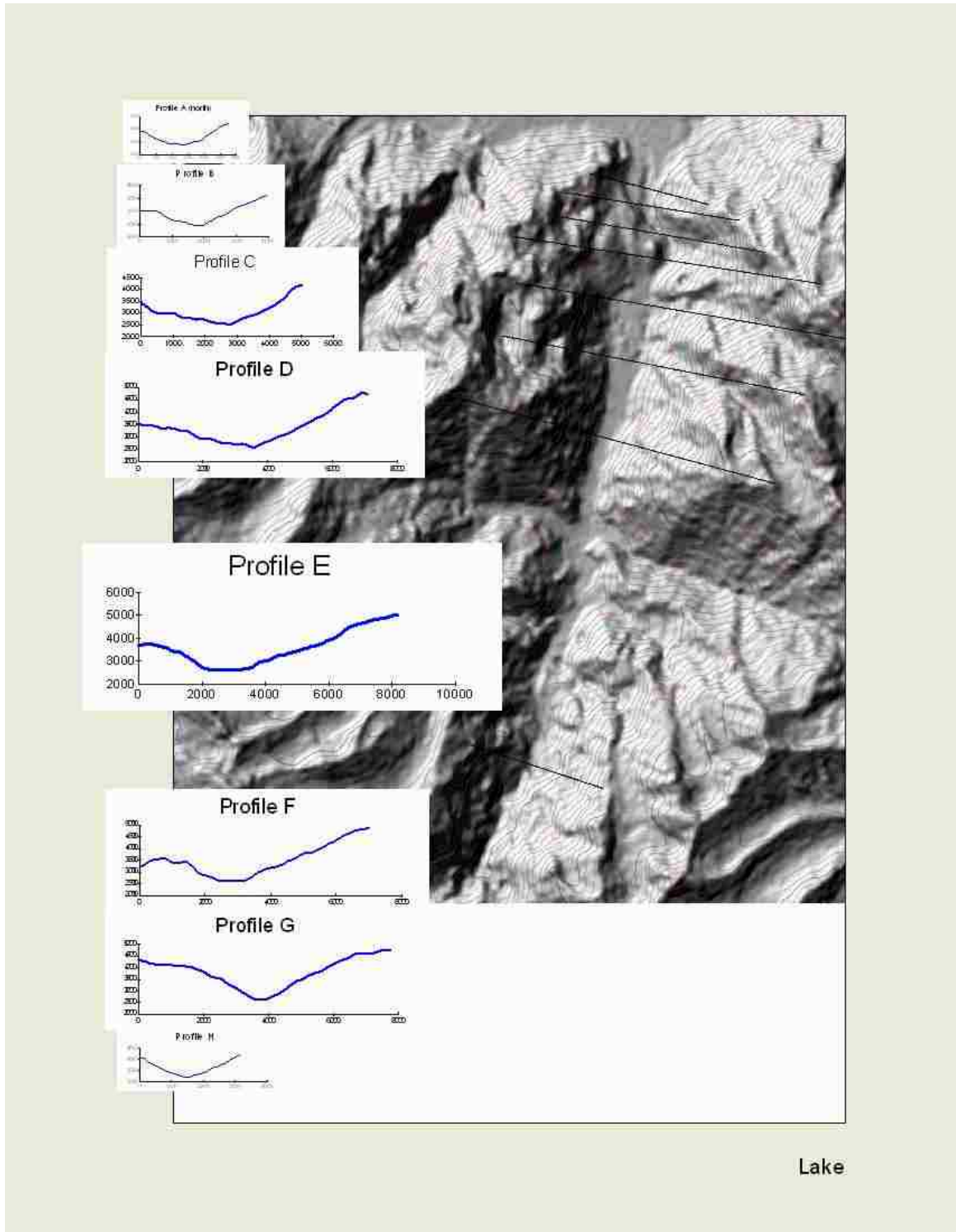
D. Belden 2008



Skardu Basin
Trim Line

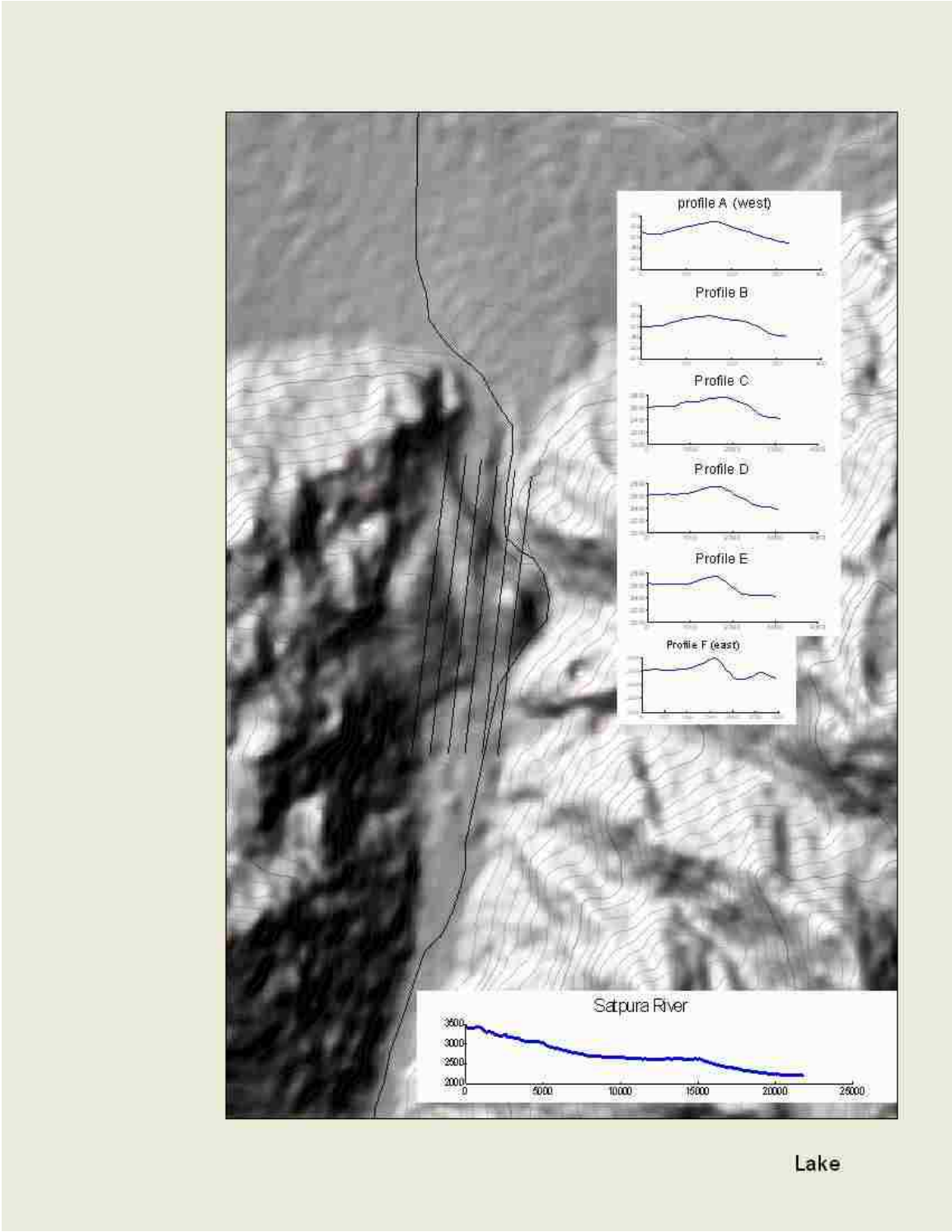
Cross-section 3. Skardu Basin trim lines.

D. Belden 2008



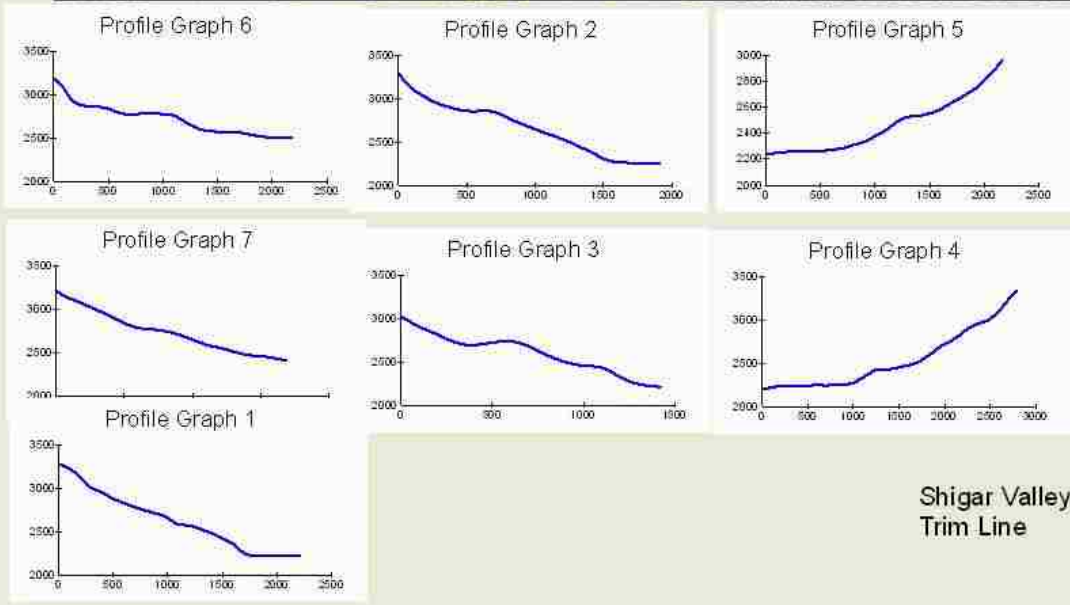
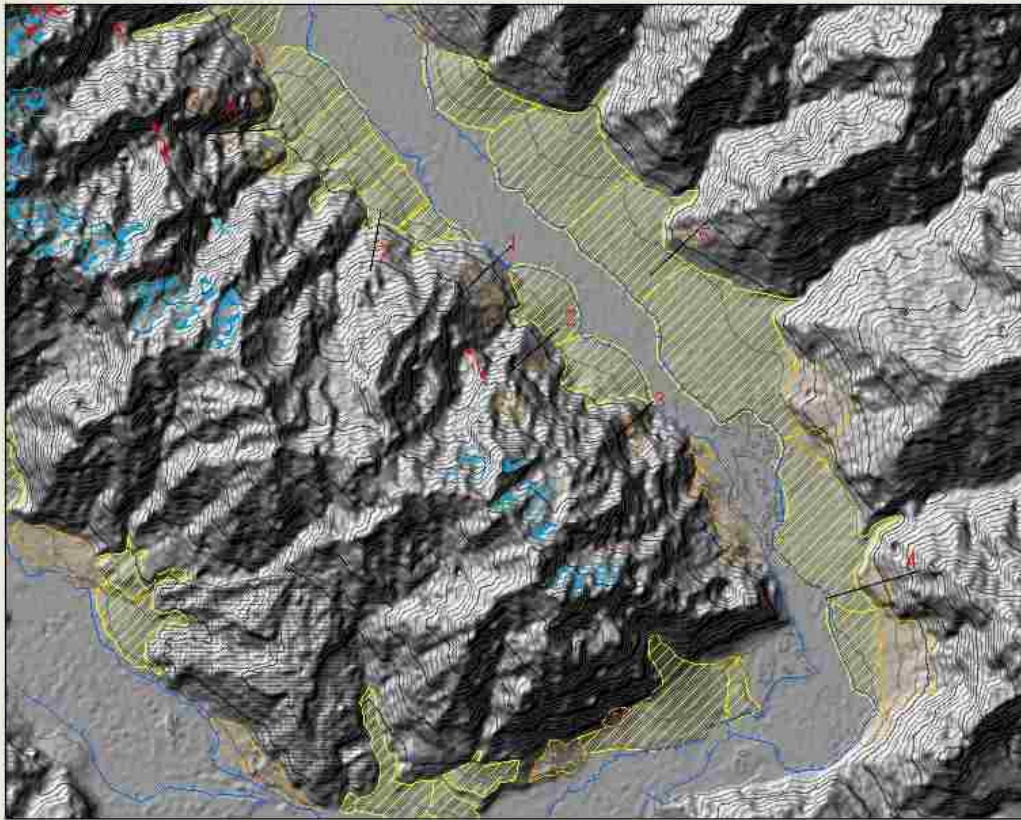
Cross-section 4. Satpura Lake.

D. Belden 2008



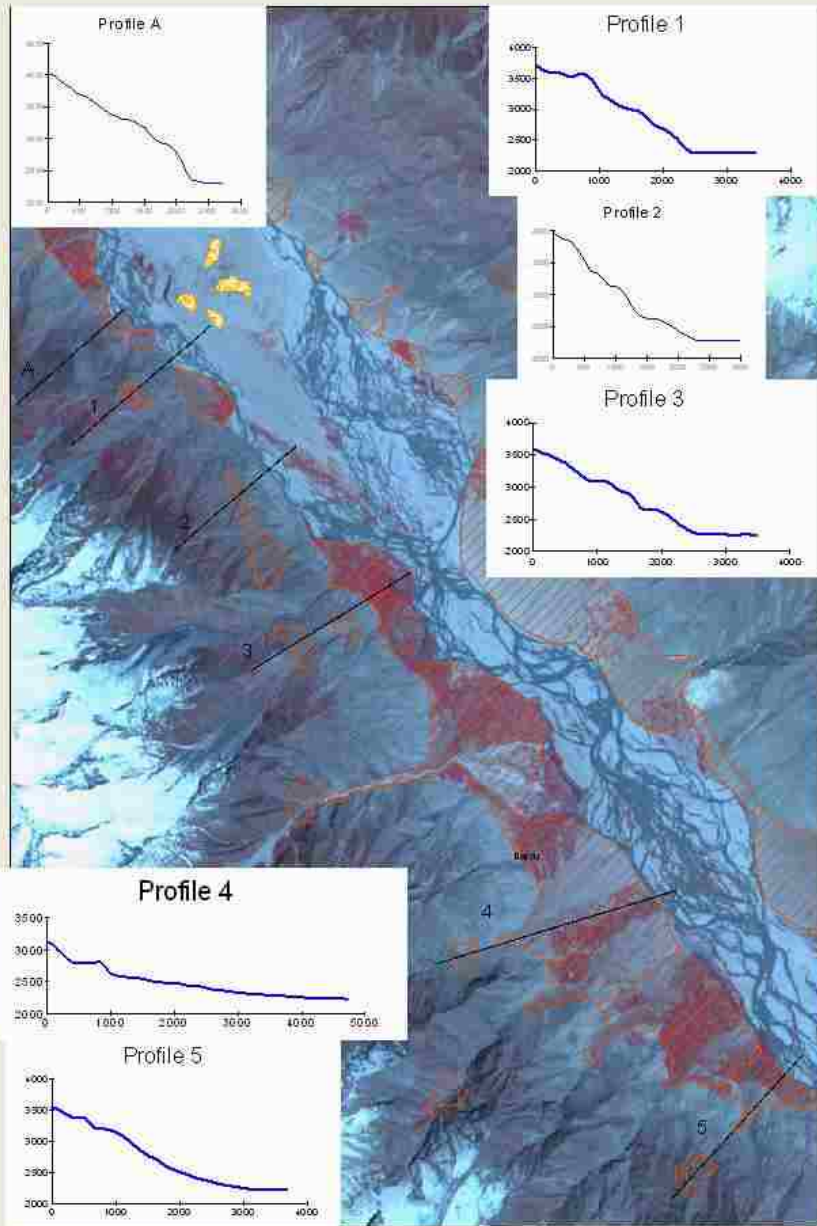
Cross-section 5. Satpura Lake impoundment.

D. Belden 2008



Cross-section 6. Shigar valley trim lines.

D. Belden 2008

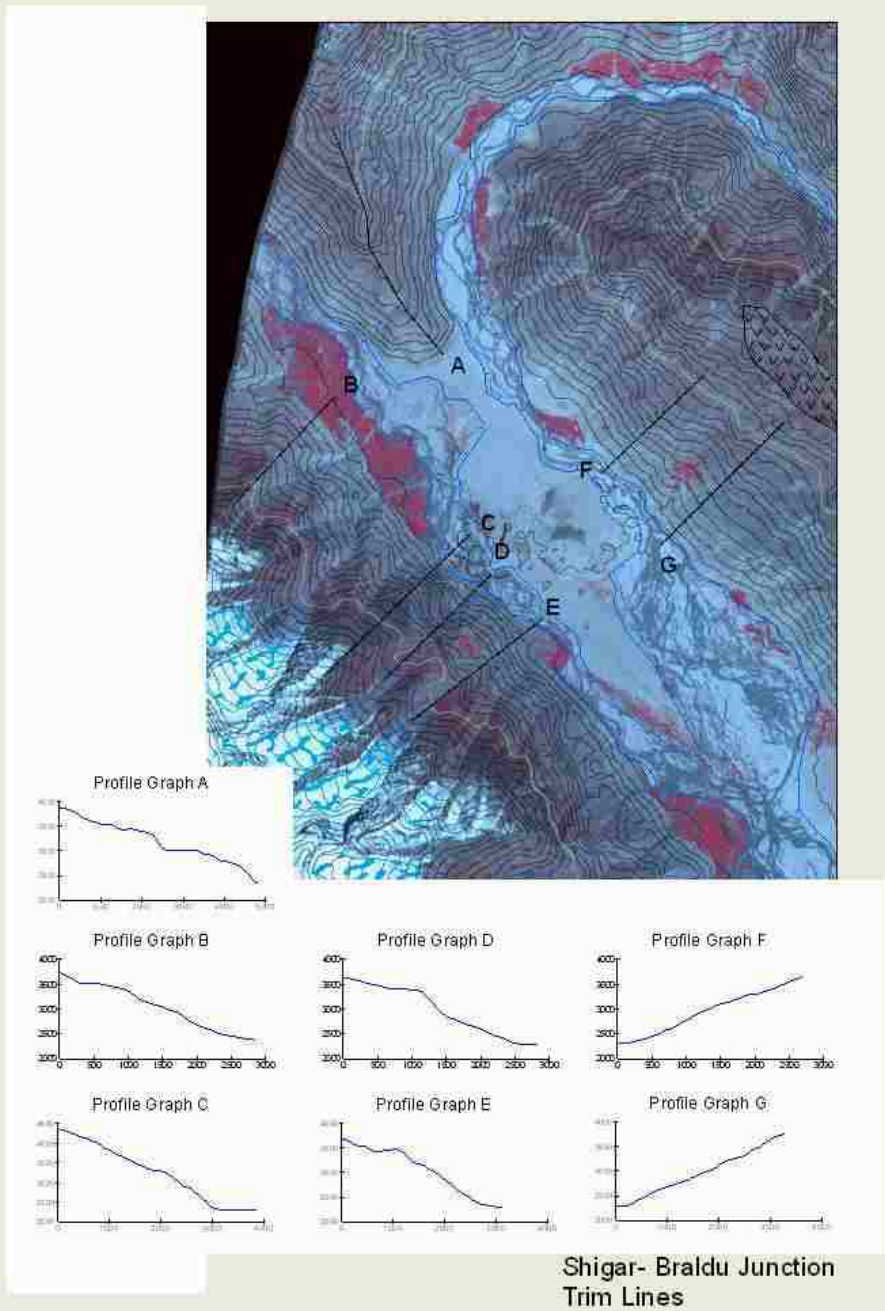


Shigar Bedrock Terraces

2/7/07 DJB

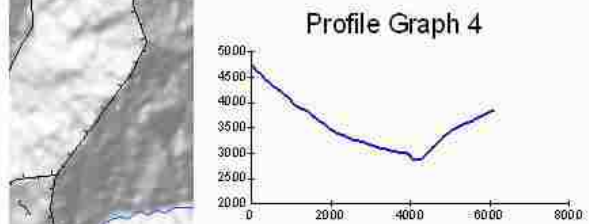
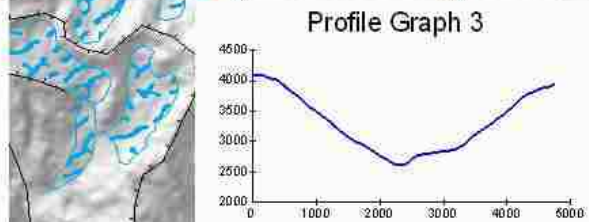
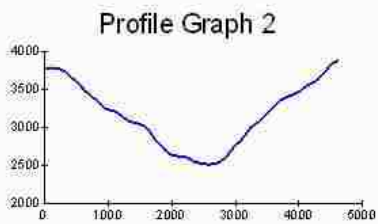
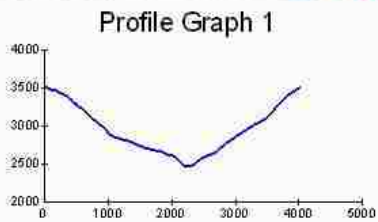
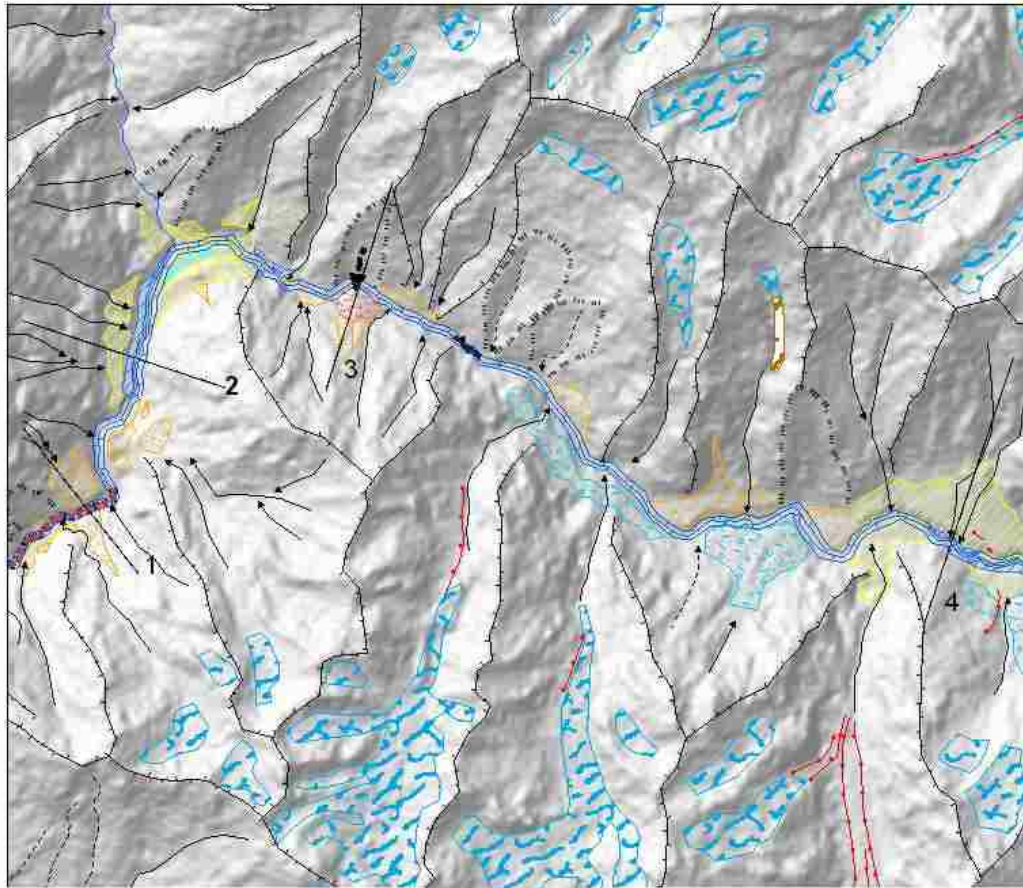
Cross-section 7. Skoro area trim lines.

D. Belden 2008



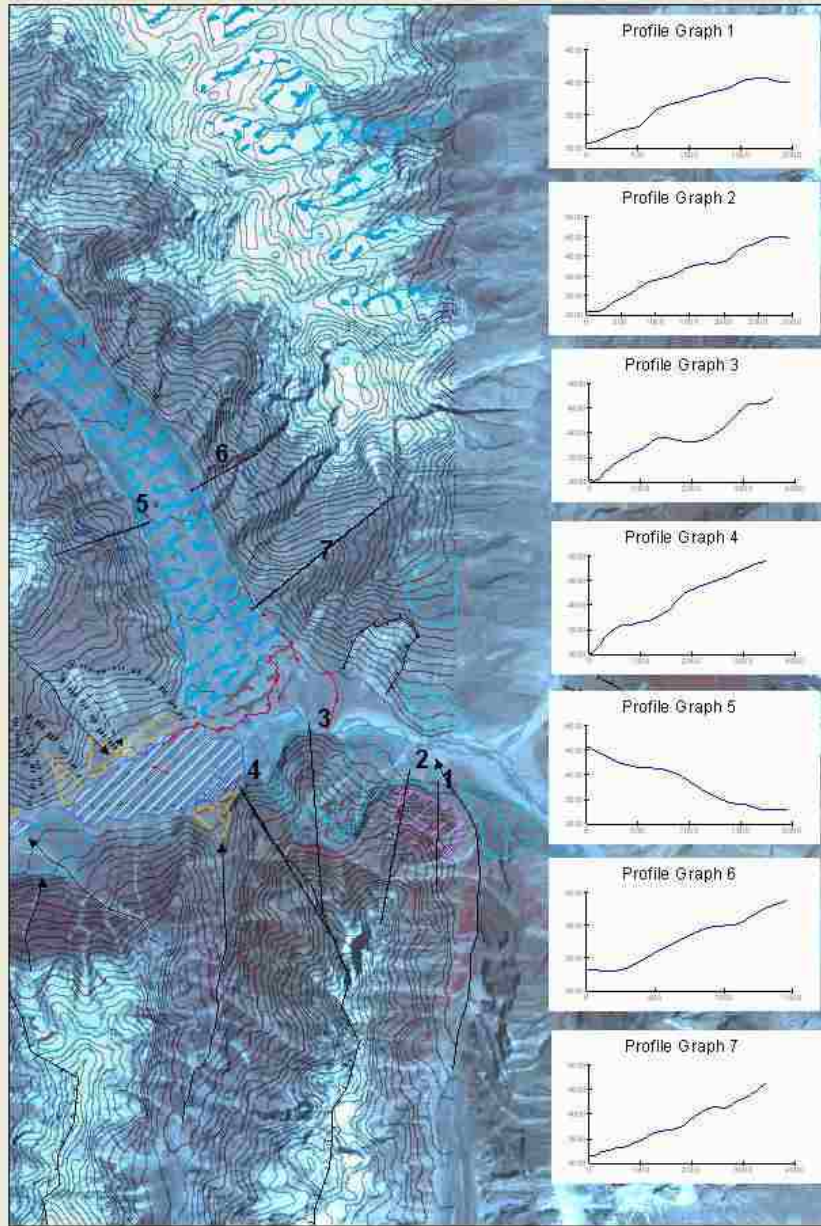
Cross-section 8. Mungo area trim lines.

D. Belden 2008



D. Belden 2008

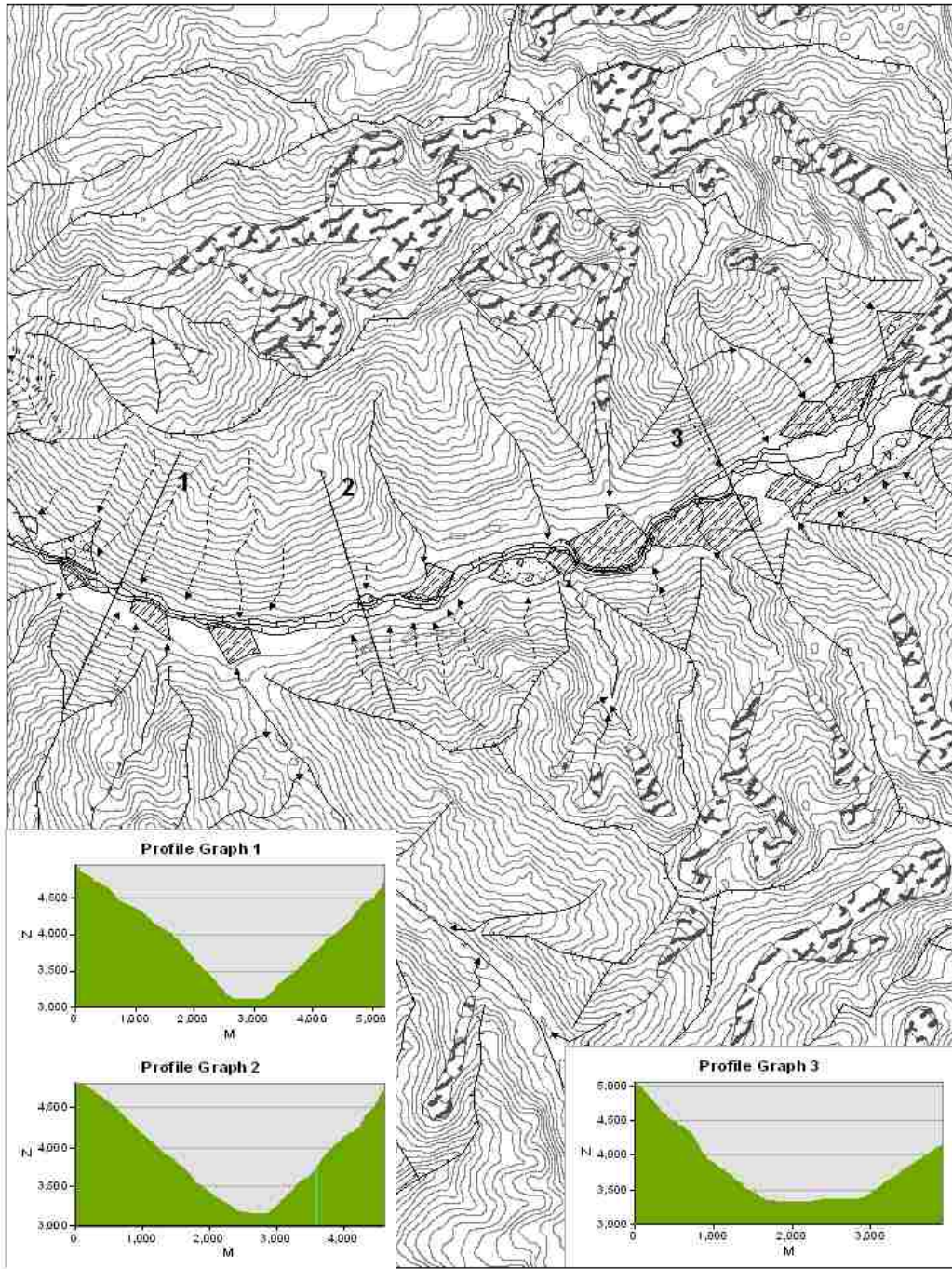
Cross-section 9. Chakpo area.



Biafo Glacier Trim Lines

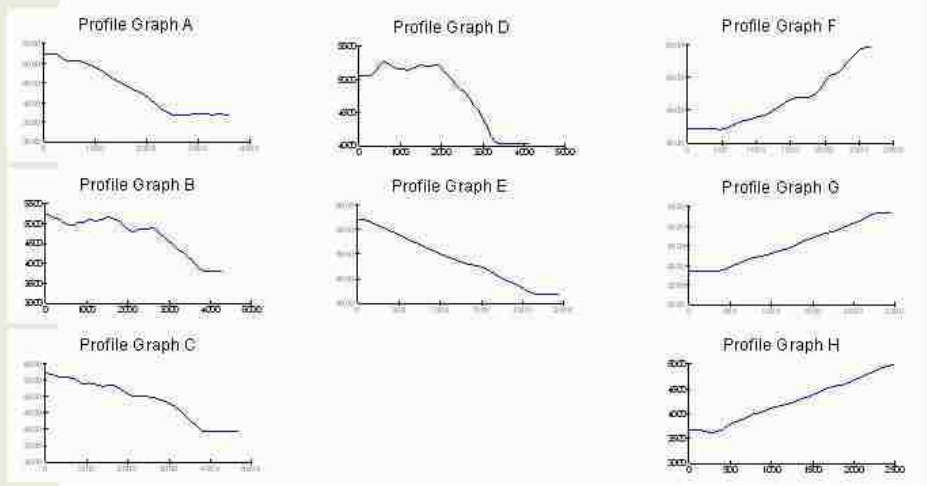
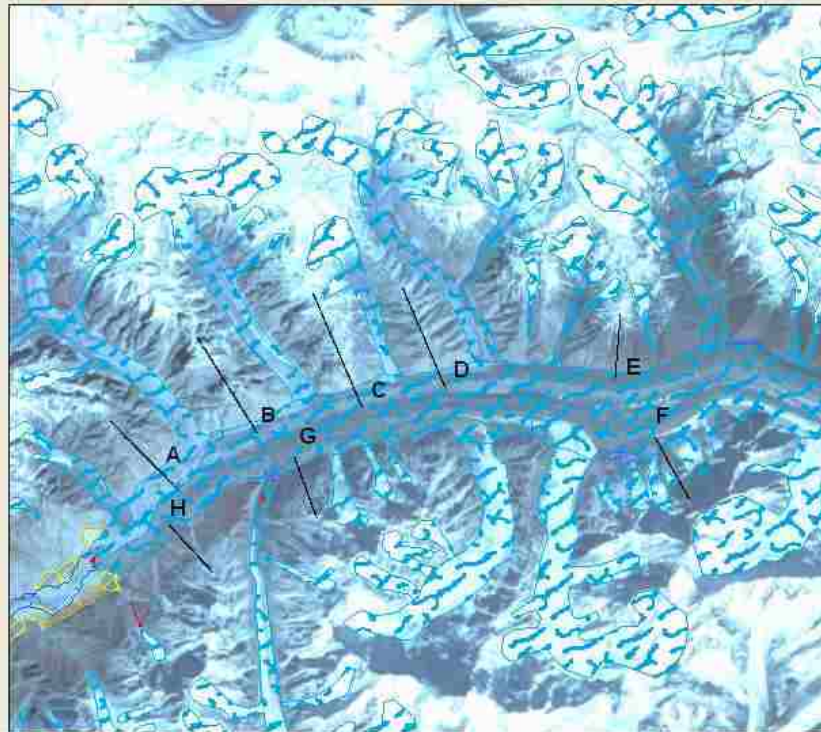
Cross-section 10. Biafo Glacier trim lines.

D. Belden 2008



D. Belden 2008

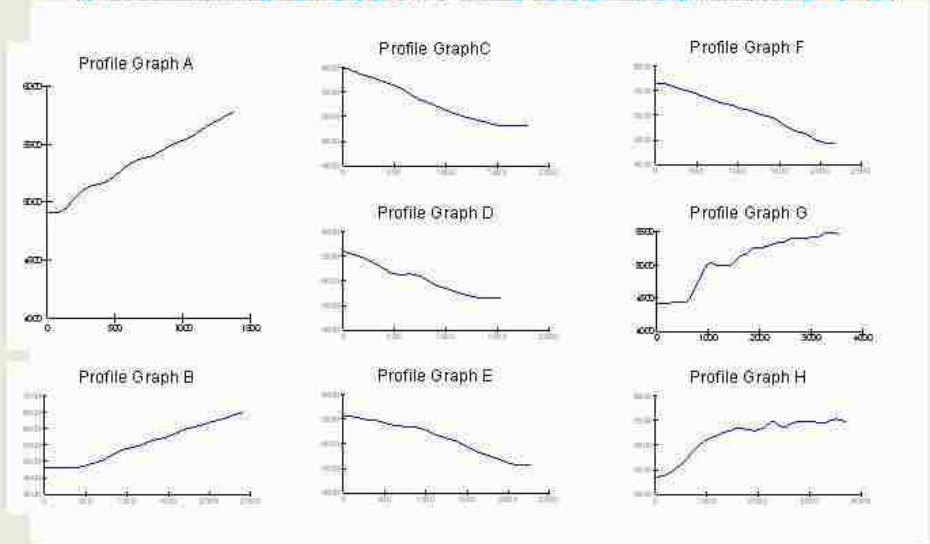
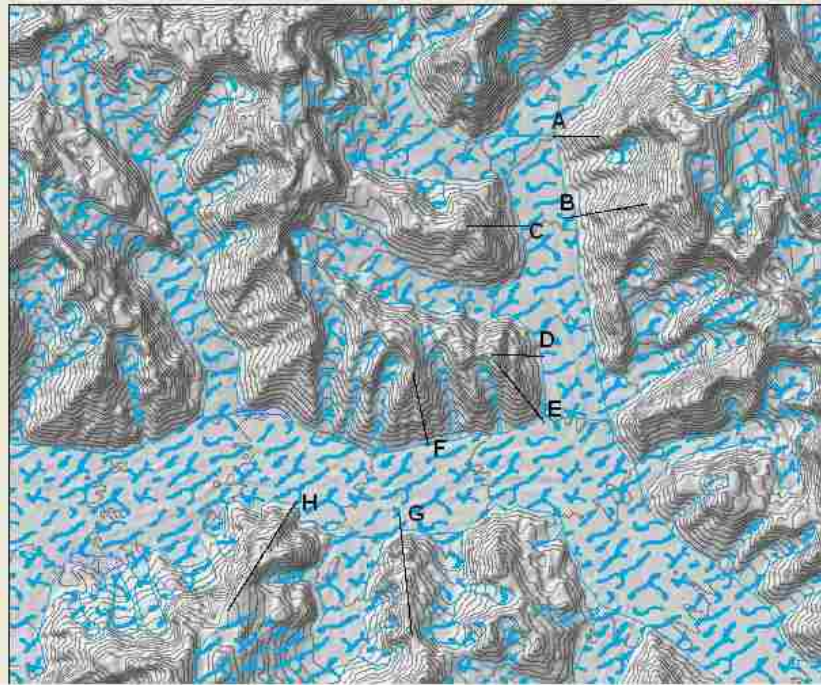
Cross-section 11. Paiju area.



Baltoro Glacier near Lilligo

Cross-section 12. Baltoro Glacier.

D. Belden 2008



Concordia Trim Lines

Cross-section 13. Concordia trim lines.

D. Belden 2008

Appendix E

GPS data, coordinates, elevations, reference to photos.

K2 Project - GPS Data and Pictures

WP	New #	Description	Date	Position		Altitude	Pics Ulli	Pics Ulli_Geoff	Pics Luke (date, not always location!)
				Decimal Degree North	Decimal Degree East				
11	11	Skardu Hotel	6/5/05	35.315889	75.609528	2226	(1.9-1.11)		(1617-1622)
12	12	Skardu Area; Ridge	6/6/05	35.321472	75.613222	2337	(1.12-1.15)	(27-51)	
13	13	Skardu Area; Ridge	6/6/05	35.320556	75.615028	2423	(1.12-1.15)	(27-51)	
14	14	Skardu Area; Ridge	6/6/05	35.317778	75.616861	2540	(1.12-1.15)	(27-51)	
15	15	Skardu Area; Ridge	6/6/05	35.313361	75.622222	2644	(1.12-1.15)	(27-51)	
16	16	Skardu Area; Ridge; Top	6/6/05	35.3105	75.627028	2709	(1.12-1.15)	(27-51)	
17	17	Skardu Area; Ridge	6/6/05	35.314972	75.626083	2597	(1.12-1.15)	(27-51)	
18	18	Skardu Area; Ridge	6/6/05	35.403639	75.526806	2456	(1.12-1.15)	(27-51)	
19	19	Rioclas Valley; Kumra; Bunthang Till	6/7/05	35.403444	75.528667	2339	(1.16-1.21)	(55-78)	(1623-1627)
20	20	Rioclas Valley; Kumra; Bunthang Till	6/7/05	35.396556	75.553694	2718	(1.16-1.21)	(55-78)	(1623-1627)
21	21	Skardu Valley Mouth	6/7/05	35.363861	75.653694	2232	(1.22-1.23)	(80-93)	(1623-1627)
22	22	Skardu Valley Mouth	6/7/05	35.397833	75.713583	2200	(1.22-1.23)	(80-93)	(1623-1627)
23	23	Skardu - Mungo; Shigar	6/8/05	35.413056	75.740806	2276	(1.24-1.37; 2.1-2.3)	(94-118)	(1628-1633)
25	25	Skardu - Mungo; Shigar	6/8/05	35.599833	75.562389	2410	(1.24-1.37; 2.1-2.3)	(94-118)	(1628-1633)
26	26	Skardu - Mungo; Camp	6/8/05	35.650472	75.526389	2807	(1.24-1.37; 2.1-2.3)	(94-118)	(1628-1633)
27	27	Mungo Camp - Sackung	6/9/05	35.655028	75.530806	3095	(2.4-2.10)		(1634-1663)
28	28	Mungo Camp - Sackung	6/9/05	35.656083	75.533194	3213	(2.4-2.10)		(1634-1663)
29	29	Mungo Camp - Sackung	6/9/05	35.659222	75.535	3373	(2.4-2.10)		(1634-1663)

30	30	Mungo Camp - Sackung	6/9/05	35.658694	75.537222	3463	(2.4-2.10)	(1634-1663)
31	31	Mungo Camp - Sackung	6/9/05	35.658028	75.540028	3562	(2.4-2.10)	(1634-1663)
32	32	Mungo Camp - Sackung	6/9/05	35.658111	75.543	3625	(2.4-2.10)	(1634-1663)
33	33	Mungo Camp - Sackung	6/9/05	35.65825	75.545167	3736	(2.4-2.10)	(1634-1663)
34	34	Mungo Camp - Sackung	6/9/05	35.660889	75.550583	3836	(2.4-2.10)	(1634-1663)
35	35	Mungo Camp - Sackung	6/9/05	35.661833	75.547278	3905	(2.4-2.10)	(1634-1663)
36	36	Mungo Camp - Sackung	6/9/05	35.663278	75.546111	3964	(2.4-2.10)	(1634-1663)
37	37	Mungo Sackung - Ridge	6/10/05	35.664111	75.554528	4004	(2.11-2.16)	(129-140) (1664-1672)
38	38	Mungo Sackung - Ridge	6/10/05	35.663611	75.556444	4083	(2.11-2.16)	(129-140) (1664-1672)
39	39	Mungo Sackung - Ridge	6/10/05	35.663167	75.558278	4145	(2.11-2.16)	(129-140) (1664-1672)
40	40	Mungo Sackung - Ridge	6/10/05	35.664444	75.559806	4260	(2.11-2.16)	(129-140) (1664-1672)
41	41	Mungo Sackung - Ridge	6/10/05	35.664056	75.560583	4313	(2.11-2.16)	(129-140) (1664-1672)
42	42	Mungo Sackung - Ridge	6/10/05	35.663167	75.557361	4123	(2.11-2.16)	(129-140) (1664-1672)
43	43	Mungo Sackung - Ridge	6/10/05	35.662694	75.5545	3981	(2.11-2.16)	(129-140) (1664-1672)
44	44	Shigar Valley and Ridge near Mungo	6/11/05	35.659194	75.49325	2348	(2.17-2.23)	
45	45	Shigar Valley and Ridge near Mungo	6/11/05	35.669139	75.470972	2443	(2.17-2.23)	
46	46	Shigar Valley and Ridge near Mungo	6/11/05	35.671083	75.469583	2568	(2.17-2.23)	
47	47	Shigar Valley and Ridge near Mungo	6/11/05	35.673278	75.468333	2696	(2.17-2.23)	
48	48	Shigar Valley and Ridge near Mungo	6/11/05	35.673694	75.467111	2774	(2.17-2.23)	
49	49	Shigar Valley and Ridge near Mungo	6/11/05	35.675361	75.466	2848	(2.17-2.23)	
50	50	Shigar Valley and Ridge near Mungo	6/11/05	35.676861	75.468889	2938	(2.17-2.23)	

51	51	Dasu; Strath Terrace	6/12/05	35.690194	75.563944	2979	(2.24; 3.1- 3.3)		(1673- 1684)
52	52	Dasu; Strath Terrace	6/12/05	35.715361	75.521583	2424	(2.24; 3.1- 3.3)		(1673- 1684)
53	53	Dasu; Strath Terrace	6/12/05	35.716639	75.524639	2565	(2.24; 3.1- 3.3)		(1673- 1684)
54	54	Dasu; Strath Terrace	6/12/05	35.717833	75.523972	2609	(2.24; 3.1- 3.3)		(1673- 1684)
55	55	Dasu; Strath Terrace	6/12/05	35.717778	75.519694	2610	(2.24; 3.1- 3.3)		(1673- 1684)
56	56	Dasu; Strath Terrace	6/12/05	35.718361	75.519806	2647	(2.24; 3.1- 3.3)		(1673- 1684)
57	57	Dasu; Flood Deposits	6/12/05	35.705778	75.490389	2396	(3.4- 3.5)		(1673- 1684)
58	58	Mungo - Askole; Apo Ali Ghon	6/13/05	35.710083	75.609278	2498	3.6		(1685- 1712)
59	59	Mungo - Askole; Chakpo; Flood Deposits	6/13/05	35.732583	75.617278	2569	3.7		(1685- 1712)
60	60	Mungo - Askole; Huge Landslide	6/13/05	35.729056	75.664528	2802	(3.8- 3.15)		(1685- 1712)
61	61	Mungo - Askole; Huge Landslide	6/13/05	35.729222	75.667806	2664	(3.8- 3.15)		(1685- 1712)
62	62	Mungo - Askole; Strath Terrace	6/13/05	35.719639	75.688861	2882			(1685- 1712)
63	63	Mungo - Askole	6/13/05	35.698639	75.715833	2877	3.16		(1685- 1712)
900	64	Huge Landslide	6/14/05	35.720767	75.676283	3163	-3.17	(147-164)	(1713- 1724)
901	65	Huge Landslide	6/14/05	35.7228	75.667083	3015	-3.17	(147-164)	(1713- 1724)
902	66	Huge Landslide	6/14/05	35.729467	75.6633	2830	-3.17	(147-164)	(1713- 1724)
64	67	Askole; Camp; Weather Station	6/15/05	35.683111	75.817167	3066		(165-232)	(1725- 1743); Movie Glacier Outlet
65	68	Askole - Chakpo; Mapping; Pakora Area	6/15/05	35.695917	75.721306	2860		(165-232)	(1725- 1743); Movie Glacier Outlet
66	69	Askole - Chakpo; Mapping	6/15/05	35.706972	75.604667	2525		(165-232)	(1725- 1743); Movie Glacier Outlet

67	70	Askole - Chakpo; Mapping; Chakpo Area	6/15/05	35.714833	75.6105	2554	(165-232)	(1725-1743); Movie Glacier Outlet
68	71	Askole - Chakpo; Mapping	6/15/05	35.724889	75.613583	2579	(165-232)	(1725-1743); Movie Glacier Outlet
69	72	Askole - Chakpo; Mapping	6/15/05	35.735389	75.620694	2608	(165-232)	(1725-1743); Movie Glacier Outlet
70	73	Askole - Chakpo; Mapping	6/15/05	35.7305	75.648917	2652	(165-232)	(1725-1743); Movie Glacier Outlet
71	74	Askole - Chakpo; Mapping; Huge Landslide	6/15/05	35.730111	75.660639	2796	(165-232)	(1725-1743); Movie Glacier Outlet
72	75	Askole - Chakpo; Mapping; Huge Landslide	6/15/05	35.728611	75.665917	2793	(165-232)	(1725-1743); Movie Glacier Outlet
73	76	Askole - Chakpo; Mapping; Huge Landslide	6/15/05	35.707583	75.708861	2803	(165-232)	(1725-1743); Movie Glacier Outlet
74	77	Askole - Chakpo; Mapping; Pakora Area	6/15/05	35.701111	75.714583	2846	(165-232)	(1725-1743); Movie Glacier Outlet
75	78	Askole - Chakpo; Mapping	6/15/05	35.689917	75.729861	2880	(165-232)	(1725-1743); Movie Glacier Outlet
76	79	Askole - Chakpo; Mapping	6/15/05	35.686694	75.746306	2871	(165-232)	(1725-1743); Movie Glacier Outlet
77	80	Askole - Chakpo; Mapping	6/15/05	35.68725	75.751722	2932	(165-232)	(1725-1743); Movie Glacier Outlet

78	81	Askole - Chakpo; Mapping	6/15/05	35.687472	75.754	2936	(165-232)	(1725-1743); Movie Glacier Outlet
79	82	Askole - Chakpo; Mapping	6/15/05	35.689861	75.766083	2969	(165-232)	(1725-1743); Movie Glacier Outlet
80	83	Askole - Chakpo; Mapping	6/15/05	35.687472	75.790722	2998	(165-232)	(1725-1743); Movie Glacier Outlet
81	84	Askole - Chakpo; Mapping	6/15/05	35.681667	75.806944	2983	(165-232)	(1725-1743); Movie Glacier Outlet
82	85	Askole - Chakpo; Mapping; Askole; Hummocky Moraine	6/15/05	35.68325	75.8095	3051	(165-232)	(1725-1743); Movie Glacier Outlet
83	86	Askole - Chakpo; Mapping; Askole; Endmoraine	6/15/05	35.680194	75.812722	3051	(165-232)	(1725-1743); Movie Glacier Outlet
84	87	Askole - Chakpo; Mapping; Askole; Endmoraine	6/15/05	35.6795	75.813472	3049	(165-232)	(1725-1743); Movie Glacier Outlet
85	88	Askole; Camp; Kitchen Tent	6/16/05	35.682861	75.817472	3061	(1-23)	(1744-1747)
86	89	Askole - Chakpo; Mapping; Surungo	6/16/05	35.682333	75.804222	2939	(1-23)	(1744-1747)
87	90	Askole - Chakpo; Mapping; Sino	6/16/05	35.685528	75.783944	2898	(1-23)	(1744-1747)
88	91	Askole - Chakpo; Mapping	6/16/05	35.689111	75.767028	2924	(1-23)	(1744-1747)
89	92	Askole - Chakpo; Mapping; Chongo	6/16/05	35.686333	75.745583	2874	(1-23)	(1744-1747)
90	93	Askole - Chakpo; Mapping; Chongo	6/16/05	35.689778	75.739639	2966	(1-23)	1748-1768; Movie Rockfall

91	94	Askole - Chakpo; Mapping; Chongo	6/16/05	35.689444	75.742	2966	(1-23)	(1769- 1782)
92	95	Askole - Chakpo; Mapping; Huge Landslide	6/17/05	35.729611	75.664583	2789	(8-77)	
93	96	Askole - Chakpo; Mapping; Chakpo Area; Flood Deposits	6/17/05	35.738389	75.624806	2608	(8-77)	
94	97	Askole - Chakpo; Mapping; Chakpo Area; Flood Deposits	6/17/05	35.738333	75.624722	2610	(8-77)	
95	98	Askole - Chakpo; Mapping; Chakpo Area; Flood Deposits	6/17/05	35.739139	75.626944	2628	(8-77)	
96	99	Askole - Chakpo; Mapping; Chakpo Area; Flood Deposits	6/17/05	35.739667	75.628167	2630	(8-77)	
97	100	Askole - Chakpo; Mapping; Chakpo Area; Flood Deposits	6/17/05	35.739417	75.627361	2625	(8-77)	
98	101	Askole - Chakpo; Mapping; Chakpo Area; Flood Deposits	6/17/05	35.739306	75.626806	2615	(8-77)	
99	102	Askole - Chakpo; Mapping; Apo Ali Ghon	6/17/05	35.716694	75.610472	2657	(8-77)	
100	103	Askole - Chakpo; Mapping; Miasa	6/17/05	35.692306	75.602833	2698	(8-77)	
101	104	Askole - Chakpo; Mapping	6/17/05	35.680833	75.574056	2693	(8-77)	

102	105	Askole - Chakpo; Mapping; "Dasu Gorge"	6/17/05	35.696444	75.555528	2482	(8-77)	
103	106	Askole - Chakpo; Mapping	6/17/05	35.703	75.547444	2489	(8-77)	
104	107	Askole - Chakpo; Mapping	6/17/05	35.684417	75.584333	2510	(8-77)	
105	108	Askole - Chakpo; Mapping	6/17/05	35.726167	75.679889	2546	(8-77)	
106	109	Askole - Chakpo; Mapping	6/17/05	35.697167	75.717444	2831	(8-77)	
107	110	Askole - Korophong/Biafo Glacier	6/18/05	35.678972	75.828417	3006	(78-137)	(1785- 1820)
108	111	Askole - Korophong/Biafo Glacier	6/18/05	35.678861	75.838333	3066	(78-137)	(1785- 1820)
109	112	Askole - Korophong/Biafo Glacier	6/18/05	35.672944	75.852611	3007	(78-137)	(1785- 1820)
110	113	Askole - Korophong/Biafo Glacier	6/18/05	35.670778	75.861194	2985	(78-137)	(1785- 1820)
111	114	Askole - Korophong/Biafo Glacier	6/18/05	35.672139	75.864694	3012	(78-137)	(1785- 1820)
112	115	Askole - Korophong/Biafo Glacier	6/18/05	35.676194	75.877778	3015	(78-137)	(1785- 1820)
113	116	Askole - Korophong/Biafo Glacier	6/18/05	35.67575	75.900583	3033	(78-137)	(1785- 1820)
114	117	Askole - Korophong/Biafo Glacier	6/18/05	35.684361	75.908694	3072	(78-137)	(1785- 1820)
115	118	Korophong; Biafo Glacier; Camp	6/19/05	35.689639	75.914417	3064	(4-52)	(1821- 1830)
116	119	Korophong; Biafo Glacier; Glacier Portal	6/19/05	35.692583	75.914111	3068	(4-52)	(1821- 1830)
117	120	Korophong; Biafo Glacier; Glacier Portal	6/19/05	35.692667	75.914389	3078	(4-52)	(1821- 1830)
118	121	Korophong; Biafo Glacier	6/19/05	35.693083	75.914222	3072	(4-52)	(1821- 1830)
119	122	Korophong; Biafo Glacier	6/19/05	35.693167	75.912194	3107	(4-52)	(1821- 1830)
120	123	Korophong; Biafo Glacier	6/19/05	35.693278	75.913861	3117	(4-52)	(1821- 1830)
121	124	Korophong; Biafo Glacier	6/19/05	35.693722	75.914222	3068	(4-52)	(1821- 1830)

122	125	Korophong; Biafo Glacier	6/19/05	35.694083	75.91425	3073	(4-52)	(1821- 1830)
123	126	Korophong; Biafo Glacier	6/19/05	35.694306	75.913889	3084	(4-52)	(1821- 1830)
124	127	Korophong; Biafo Glacier	6/19/05	35.694583	75.913889	3076	(4-52)	(1821- 1830)
125	128	Korophong; Biafo Glacier	6/19/05	35.695194	75.913806	3072	(4-52)	(1821- 1830)
126	129	Korophong; Biafo Glacier	6/19/05	35.695556	75.913889	3077	(4-52)	(1821- 1830)
127	130	Korophong; Biafo Glacier	6/19/05	35.696028	75.913667	3061	(4-52)	(1821- 1830)
128	131	Korophong; Biafo Glacier; Small Meltwater Stream	6/19/05	35.696528	75.913389	3091	(4-52)	(1821- 1830)
129	132	Korophong; Biafo Glacier	6/19/05	35.696528	75.912861	3085	(4-52)	(1821- 1830)
130	133	Korophong; Biafo Glacier	6/19/05	35.696167	75.912222	3108	(4-52)	(1821- 1830)
131	134	Korophong; Biafo Glacier	6/19/05	35.696778	75.912722	3132	(4-52)	(1821- 1830)
132	135	Korophong; Biafo Glacier	6/19/05	35.697611	75.913194	3083	(4-52)	(1821- 1830)
133	136	Korophong; Biafo Glacier	6/19/05	35.69775	75.913972	3116	(4-52)	(1821- 1830)
134	137	Korophong; Biafo Glacier	6/19/05	35.698472	75.914472	3102	(4-52)	(1821- 1830)
135	138	Korophong; Biafo Glacier	6/19/05	35.698111	75.915667	3110	(4-52)	(1821- 1830)
136	139	Korophong; Biafo Glacier	6/19/05	35.698528	75.91625	3134	(4-52)	(1821- 1830)
137	140	Korophong; Biafo Glacier; Contact Margin - Lateral Moraine	6/19/05	35.699083	75.916667	3134	(4-52)	(1821- 1830)
138	141	Korophong; Biafo Glacier	6/19/05	35.696333	75.917917	3099	(4-52)	(1821- 1830)
139	142	Korophong; Biafo Glacier; Weather Station	6/19/05	35.6925	75.911806	3134	(4-52)	(1821- 1830)
140	143	Korophong; Biafo Glacier; Moraine behind Camp	6/20/05	35.69	75.914083	3098	54	(1831- 1838)
141	144	Korophong; Biafo Glacier; Glacier Portal	6/20/05	35.692667	75.913861	3082		(1831- 1838)
142	145	Korophong; Biafo Glacier; Glacier Portal	6/20/05	35.6925	75.913361	3079		(1831- 1838)
143	146	Korophong; Biafo Glacier	6/20/05	35.692028	75.912806	3126		(1831- 1838)

144	147	Korophong; Biafo Glacier	6/20/05	35.691139	75.912472	3083		(1831- 1838)
145	148	Korophong; Biafo Glacier	6/20/05	35.691	75.912528	3048		(1831- 1838)
146	149	Korophong; Biafo Glacier	6/20/05	35.69075	75.912222	3081		(1831- 1838)
147	150	Korophong; Biafo Glacier	6/20/05	35.690583	75.912361	3057		(1831- 1838)
148	151	Korophong; Biafo Glacier	6/20/05	35.690194	75.911833	3073		(1831- 1838)
149	152	Korophong; Biafo Glacier	6/20/05	35.689889	75.911972	3098		(1831- 1838)
150	153	Korophong; Biafo Glacier	6/20/05	35.689528	75.912083	3069		(1831- 1838)
151	154	Korophong; Biafo Glacier	6/20/05	35.68925	75.912139	3058		(1831- 1838)
152	155	Korophong; Biafo Glacier	6/20/05	35.688694	75.912417	3061		(1831- 1838)
153	156	Korophong; Biafo Glacier	6/20/05	35.688222	75.912056	3061	56	(1831- 1838)
154	157	Korophong; Biafo Glacier; Proglacial Lake 1	6/20/05	35.687833	75.911306	3052		(1831- 1838)
155	158	Korophong; Biafo Glacier	6/20/05	35.687778	75.910917	3044		(1831- 1838)
156	159	Korophong; Biafo Glacier	6/20/05	35.687389	75.910306	3059		(1831- 1838)
157	160	Korophong; Biafo Glacier	6/20/05	35.687639	75.910333	3058		(1831- 1838)
158	161	Korophong; Biafo Glacier	6/20/05	35.687611	75.909583	3065		(1831- 1838)
159	162	Korophong; Biafo Glacier	6/20/05	35.687306	75.90875	3057		(1831- 1838)
160	163	Korophong; Biafo Glacier	6/20/05	35.687361	75.908361	3044	58	(1831- 1838)
161	164	Korophong; Biafo Glacier; Proglacial Lake 2	6/20/05	35.687444	75.90775	3053	57	(1831- 1838)
162	165	Korophong; Biafo Glacier	6/20/05	35.687056	75.907278	3050		(1831- 1838)
163	166	Korophong; Biafo Glacier	6/20/05	35.686472	75.906611	3051		(1831- 1838)
164	167	Korophong; Biafo Glacier	6/20/05	35.685972	75.906194	3047		(1831- 1838)
165	168	Korophong; Biafo Glacier	6/20/05	35.685556	75.905722	3060		(1831- 1838)
166	169	Korophong; Biafo Glacier	6/20/05	35.685333	75.905111	3064	59	(1831- 1838)
167	170	Korophong; Biafo Glacier	6/20/05	35.685444	75.904444	3064		(1831- 1838)
168	171	Korophong; Biafo Glacier	6/20/05	35.685167	75.904111	3069		(1831- 1838)
169	172	Korophong; Biafo Glacier	6/20/05	35.685111	75.903833	3066	60	(1831- 1838)

170	173	Korophong; Biafo Glacier	6/20/05	35.685167	75.903944	3056		(1831-1838)
171	174	Korophong; Biafo Glacier	6/20/05	35.685167	75.902889	3070		(1831-1838)
172	175	Korophong; Biafo Glacier	6/20/05	35.685111	75.902417	3079		(1831-1838)
173	176	Korophong; Biafo Glacier	6/20/05	35.684861	75.901722	3072		(1831-1838)
174	177	Korophong; Biafo Glacier	6/20/05	35.684639	75.901333	3069		(1831-1838)
175	178	Korophong; Biafo Glacier	6/20/05	35.684611	75.900861	3067		(1831-1838)
176	179	Korophong; Biafo Glacier	6/20/05	35.685028	75.900111	3061		(1831-1838)
177	180	Korophong; Biafo Glacier	6/20/05	35.685083	75.899944	3061		(1831-1838)
178	181	Korophong; Biafo Glacier	6/20/05	35.685222	75.899556	3066		(1831-1838)
179	182	Korophong; Biafo Glacier	6/20/05	35.685278	75.899222	3064		(1831-1838)
180	183	Korophong; Biafo Glacier	6/20/05	35.685361	75.898861	3065		(1831-1838)
181	184	Korophong; Biafo Glacier	6/20/05	35.685611	75.898528	3061		(1831-1838)
182	185	Korophong; Biafo Glacier	6/20/05	35.686	75.898083	3063		(1831-1838)
183	186	Korophong; Biafo Glacier; Main Meltwater Stream	6/20/05	35.686167	75.897806	3069	61-69	(1831-1838)
184	187	Korophong; Biafo Glacier	6/20/05	35.686222	75.897833	3061		(1831-1838)
185	188	Korophong; Biafo Glacier	6/20/05	35.675806	75.901083	3066		(1831-1838)
186	189	Korophong; Biafo Glacier; Proglacial Lake 1	6/21/05	35.685722	75.908306	3047		(1839-1851)
187	190	Korophong; Biafo Glacier; Proglacial Lake 1	6/21/05	35.685944	75.908472	3051		(1839-1851)
188	191	Korophong; Biafo Glacier; Proglacial Lake 1	6/21/05	35.686222	75.908361	3053		(1839-1851)
189	192	Korophong; Biafo Glacier; Proglacial Lake 1	6/21/05	35.686417	75.908389	3050		(1839-1851)
190	193	Korophong; Biafo Glacier; Proglacial Lake 1	6/21/05	35.686889	75.908028	3050		(1839-1851)

191	194	1	Korophong; Biafo Glacier; Proglacial Lake	6/21/05	35.687278	75.907972	3048	(1839-1851)
192	195	1	Korophong; Biafo Glacier; Proglacial Lake	6/21/05	35.687444	75.907722	3045	(1839-1851)
193	196	1	Korophong; Biafo Glacier; Proglacial Lake	6/21/05	35.686833	75.907028	3043	(1839-1851)
194	197	1	Korophong; Biafo Glacier; Proglacial Lake	6/21/05	35.686611	75.90675	3046	(1839-1851)
195	198	1	Korophong; Biafo Glacier; Proglacial Lake	6/21/05	35.686083	75.906806	3047	(1839-1851)
196	199	1	Korophong; Biafo Glacier; Proglacial Lake	6/21/05	35.685917	75.907111	3048	(1839-1851)
197	200	1	Korophong; Biafo Glacier; Proglacial Lake	6/21/05	35.68575	75.906833	3051	(1839-1851)
198	201	1	Korophong; Biafo Glacier; Proglacial Lake	6/21/05	35.685389	75.907278	3050	(1839-1851)
199	202	1	Korophong; Biafo Glacier; Proglacial Lake	6/21/05	35.685556	75.907833	3071	(1839-1851)
200	203	1	Korophong; Biafo Glacier; Proglacial Lake	6/21/05	35.685556	75.907889	3057	(1839-1851)
201	204	1	Korophong; Biafo Glacier; Main Paleo- Meltwater Stream; E-Side	6/21/05	35.67475	75.901611	3037	(71-74) (1839-1851)
202	205	1	Korophong; Biafo Glacier; Main Paleo- Meltwater Stream; E-Side	6/21/05	35.675417	75.901417	3042	(71-74) (1839-1851)

203	206	Korophong; Biafo Glacier; Main Paleo- Meltwater Stream; E-Side	6/21/05	35.675861	75.9015	3040	(71-74)	(1839- 1851)
204	207	Korophong; Biafo Glacier; Main Paleo- Meltwater Stream; E-Side	6/21/05	35.676333	75.901361	3042	(71-74)	(1839- 1851)
205	208	Korophong; Biafo Glacier; Main Paleo- Meltwater Stream; E-Side	6/21/05	35.677278	75.901667	3047	(71-74)	(1839- 1851)
206	209	Korophong; Biafo Glacier; Main Paleo- Meltwater Stream; E-Side	6/21/05	35.678167	75.902333	3045	(71-74)	(1839- 1851)
207	210	Korophong; Biafo Glacier; Moraine/Till	6/21/05	35.678444	75.902056	3047	(75-84)	(1839- 1851)
208	211	Korophong; Biafo Glacier; Moraine/Till	6/21/05	35.677806	75.901083	3036	(75-84)	(1839- 1851)
209	212	Korophong; Biafo Glacier; Main Paleo- Meltwater Stream; W-Side	6/21/05	35.677083	75.900611	3048	(85-87)	(1839- 1851)
210	213	Korophong; Biafo Glacier; Main Paleo- Meltwater Stream; W-Side	6/21/05	35.676278	75.900139	3076	(85-87)	(1839- 1851)
211	214	Korophong; Biafo Glacier; Main Paleo- Meltwater Stream; W-Side	6/21/05	35.675694	75.900083	3091	(85-87)	(1839- 1851)
212	215	Korophong; Biafo Glacier; Main Paleo- Meltwater Stream; W-Side	6/21/05	35.67525	75.9	3048	(85-87)	(1839- 1851)

213	216	Korophong; Biafo Glacier; Main Paleo- Meltwater Stream; W-Side	6/21/05	35.674167	75.8995	3045	(85-87)	(1839- 1851)
214	217	Korophong; Biafo Glacier; Main Paleo- Meltwater Stream; W-Side	6/21/05	35.672694	75.897	3041	(85-87)	(1839- 1851)
215	218	Korophong; Biafo Glacier; Irrigation Channel	6/21/05	35.678333	75.889583	3042	(88-98)	(1839- 1851)
216	219	Korophong; Biafo Glacier; Irrigation Channel	6/21/05	35.681	75.89	3036	(88-98)	(1839- 1851)
217	220	Korophong; Biafo Glacier; Irrigation Channel	6/21/05	35.681639	75.890639	3032	(88-98)	(1839- 1851)
218	221	Korophong; Biafo Glacier; Irrigation Channel	6/21/05	35.682333	75.889889	3036	(88-98)	(1839- 1851)
219	222	Korophong; Biafo Glacier; Irrigation Channel	6/21/05	35.682694	75.890472	3046	(88-98)	(1839- 1851)
220	223	Korophong; Biafo Glacier; Irrigation Channel	6/21/05	35.683167	75.891056	3050	(88-98)	(1839- 1851)
221	224	Korophong; Biafo Glacier; Irrigation Channel	6/21/05	35.683583	75.891306	3049	(88-98)	(1839- 1851)
222	225	Korophong; Biafo Glacier; Irrigation Channel	6/21/05	35.683611	75.892	3055	(88-98)	(1839- 1851)
223	226	Korophong; Biafo Glacier; Irrigation Channel	6/21/05	35.684083	75.892528	3059	(88-98)	(1839- 1851)
224	227	Korophong; Biafo Glacier; Irrigation Channel	6/21/05	35.684556	75.893472	3059	(88-98)	(1839- 1851)
225	228	Korophong; Biafo Glacier; Irrigation Channel	6/21/05	35.68475	75.893417	3057	(88-98)	(1839- 1851)

226	229	Korophong; Biafo Glacier; Irrigation Channel	6/21/05	35.684944	75.893944	3055	(88-98)	(1839-1851)
227	230	Korophong; Biafo Glacier; Irrigation Channel	6/21/05	35.684944	75.895389	3068	(88-98)	(1839-1851)
228	231	Korophong; Biafo Glacier; Irrigation Channel	6/21/05	35.685306	75.896167	3070	(88-98)	(1839-1851)
229	232	Korophong; Biafo Glacier; Irrigation Channel	6/21/05	35.685528	75.896917	3067	(88-98)	(1839-1851)
230	233	Korophong; Biafo Glacier; Irrigation Channel	6/21/05	35.68575	75.897528	3065	(88-98)	(1839-1851)
231	234	Korophong - Tzobu; Moraine SE of Camp	6/22/05	35.688278	75.925306	3092	(3.18- 3.24)	99-111 (1852-1878)
232	235	Korophong - Tzobu	6/22/05	35.685278	75.938944	3125	(3.18- 3.24)	112-114; (115-118) (1852-1878)
233	236	Korophong - Tzobu; Confluence Braldu and Tributary Rivers	6/22/05	35.682639	75.955417	3129	(3.18- 3.24)	119-125; (126-127) (1852-1878)
234	237	Korophong - Tzobu	6/22/05	35.694778	75.97175	3153	(3.18- 3.24)	128-133; (134-136) (1852-1878)
235	384	Korophong - Tzobu; Active Rockfall	6/22/05	35.698278	75.973444	3177	(3.18- 3.24)	137-138; (139)
236	385	Korophong - Tzobu	6/22/05	35.661556	75.9845	3170	(3.18- 3.24)	140-149; (150-159) (1879-1889)
237	386	Korophong - Tzobu; Camp	6/22/05	35.657694	75.993222	3153	(3.18- 3.24)	160-161 (1879-1889)
PIA1	387	Tzobu - Paiju	6/23/05	35.6545	76.002139	3192	(3.35; 4.1- 4.10)	(163-176)
PIA2	388	Tzobu - Paiju; West of Confluence Braldu and Tributary Rivers	6/23/05	35.650417	76.013556	3182	(3.35; 4.1- 4.10)	(163-176)
PIA3	389	Tzobu - Paiju; East of Confluence Braldu and Tributary Rivers	6/23/05	35.649583	76.029083	3194	(3.35; 4.1- 4.10)	(177-230)
PIA4	390	Tzobu - Paiju	6/23/05	35.653722	76.054972	3233	(3.35; 4.1- 4.10)	(177-230)

							4.10)	
							(3.35; 4.1- 4.10)	(177-230)
PIA5	391	Tzobu - Paiju	6/23/05	35.658167	76.065944	3259	(3.35; 4.1- 4.10)	(177-230)
PIA6	392	Tzobu - Paiju	6/23/05	35.661417	76.077333	3263	(3.35; 4.1- 4.10)	(177-230)
PIA7	238	Tzobu - Paiju	6/23/05	35.658611	76.094194	3309	(3.35; 4.1- 4.10)	(177-230)
PIA8	239	Tzobu - Paiju	6/23/05	35.662222	76.101222	3362	(3.35; 4.1- 4.10)	(177-230)
PIA9	240	Tzobu - Paiju	6/23/05	35.668639	76.11025	3385	(3.35; 4.1- 4.10)	(177-230)
242	241	Baltoro Glacier; Margin	6/25/05	35.692694	76.154667	3441		1-13
243	242	Baltoro Glacier; Margin	6/25/05	35.693694	76.159056	3516		(14-21)
244	243	Baltoro Glacier; Margin	6/25/05	35.691361	76.159833	3510		(14-21)
245	244	Baltoro Glacier; Margin	6/25/05	35.689694	76.15875	3503		(14-21)
246	245	Baltoro Glacier; Margin	6/25/05	35.689111	76.149389	3447		(14-21)
247	246	Baltoro Glacier; Margin; Small Moraine 1	6/26/05	35.68575	76.154722	3412		(28-37)
248	247	Baltoro Glacier; Margin; Small Moraine 1	6/26/05	35.686028	76.154333	3410		(28-37)
249	248	Baltoro Glacier; Margin; Small Moraine 1	6/26/05	35.6865	76.15425	3407		(28-37)
250	249	Baltoro Glacier; Margin; Small Moraine 1	6/26/05	35.686556	76.15425	3397		(28-37)
251	250	Baltoro Glacier; Margin; Small Moraine 1	6/26/05	35.687028	76.1545	3401		(28-37)
252	251	Baltoro Glacier; Margin; Small Moraine 1	6/26/05	35.687361	76.154694	3406		(28-37)
253	252	Baltoro Glacier; Margin; Small Moraine 1	6/26/05	35.687639	76.154639	3409		(28-37)

254	253	Baltoro Glacier; Margin; Small Moraine 1	6/26/05	35.687861	76.154389	3409	(28-37)
255	254	Baltoro Glacier; Margin; Small Moraine 1	6/26/05	35.687972	76.154361	3406	(28-37)
256	255	Baltoro Glacier; Margin; Small Moraine 2	6/26/05	35.688333	76.154528	3408	(28-37)
257	256	Baltoro Glacier; Margin; Small Moraine 2	6/26/05	35.688083	76.154444	3407	(28-37)
258	257	Baltoro Glacier; Margin; Small Moraine 2	6/26/05	35.687917	76.154583	3408	(28-37)
259	258	Baltoro Glacier; Margin; Small Moraine 2	6/26/05	35.687806	76.154639	3405	(28-37)
260	259	Baltoro Glacier; Margin; "Desio Boulder"	6/26/05	35.687889	76.152889	3395	38-40
261	260	Baltoro Glacier; Margin	6/26/05	35.690861	76.154833	3408	(41-48)
262	261	Baltoro Glacier; Margin	6/26/05	35.690556	76.15475	3404	(41-48)
263	262	Baltoro Glacier; Margin	6/26/05	35.69025	76.154722	3403	(41-48)
264	263	Baltoro Glacier; Margin	6/26/05	35.689972	76.154611	3402	(41-48)
265	264	Baltoro Glacier; Margin	6/26/05	35.689694	76.154222	3401	(41-48)
266	265	Baltoro Glacier; Margin	6/26/05	35.689361	76.154028	3400	(41-48)
267	266	Baltoro Glacier; Margin	6/26/05	35.688667	76.154083	3403	(41-48)
268	267	Baltoro Glacier; Margin	6/26/05	35.688333	76.154472	3409	(41-48)
269	268	Baltoro Glacier; Margin	6/26/05	35.688	76.154694	3411	(41-48)

270	269	Baltoro Glacier; Margin	6/26/05	35.687639	76.154806	3412	(41-48)
271	270	Baltoro Glacier; Margin	6/26/05	35.687333	76.154861	3414	(41-48)
272	271	Baltoro Glacier; Margin	6/26/05	35.687111	76.154806	3408	(41-48)
273	272	Baltoro Glacier; Margin	6/26/05	35.686167	76.15475	3406	(41-48)
274	273	Baltoro Glacier; Margin	6/26/05	35.685889	76.155056	3417	(41-48)
275	274	Baltoro Glacier; Margin	6/26/05	35.685639	76.155583	3414	(41-48)
276	275	Baltoro Glacier; Margin	6/26/05	35.685361	76.156361	3421	(41-48)
277	276	Baltoro Glacier; Margin	6/26/05	35.685167	76.156806	3424	(41-48)
278	277	Baltoro Glacier; Margin	6/26/05	35.685222	76.157722	3430	(41-48)
279	278	Baltoro Glacier; Margin	6/26/05	35.685389	76.158361	3433	(41-48)
280	279	Baltoro Glacier; Margin	6/26/05	35.685722	76.158694	3436	(41-48)
281	280	Baltoro Glacier; Margin	6/26/05	35.685306	76.159444	3440	(41-48)
282	281	Baltoro Glacier; Margin	6/26/05	35.684917	76.16025	3442	(41-48)
283	282	Baltoro Glacier; Margin	6/26/05	35.6845	76.161333	3444	(41-48)
284	283	Baltoro Glacier; Margin	6/26/05	35.683889	76.162222	3452	(41-48)
285	284	Baltoro Glacier; Margin	6/26/05	35.6835	76.163722	3464	(41-48)
286	285	Baltoro Glacier; Margin	6/26/05	35.683694	76.164306	3470	(41-48)
287	286	Baltoro Glacier; Margin	6/26/05	35.683667	76.164861	3470	(41-48)
288	287	Baltoro Glacier; Margin	6/26/05	35.683361	76.1655	3475	(41-48)

289	288	Baltoro Glacier; Margin	6/26/05	35.68325	76.166111	3466	(41-48)
290	289	Baltoro Glacier; Margin	6/26/05	35.683611	76.166472	3469	(41-48)
291	290	Baltoro Glacier; Surface	6/26/05	35.69525	76.183833	3626	(49-53)
292	291	Baltoro Glacier; Proglacial Lake	6/26/05	35.699083	76.190833	3718	54-55
293	292	Baltoro Glacier; Meltwater Stream between Glacier and Valley Slope	6/26/05	35.707806	76.202611	3739	56
294	293	Liligo Glacier; Western Moraine	6/26/05	35.714861	76.225639	3781	(57-62)
295	294	Liligo Glacier; Terminus	6/26/05	35.714806	76.226139	3826	63-73; (74-77)
296	295	Liligo Glacier; Eastern Margin	6/26/05	35.714694	76.228167	3853	78
297	296	Liligo Glacier; Meltwater Stream	6/26/05	35.713361	76.229889	3892	
298	297	Liligo Camp - Dunge Glacier crossing Baltaro Glacier	6/27/05	35.718778	76.234139	3933	(79-97)
299	298	Liligo Camp - Dunge Glacier crossing Baltaro Glacier	6/27/05	35.72825	76.237056	3897	(79-97)
300	299	Liligo Camp - Dunge Glacier crossing Baltaro Glacier	6/27/05	35.732861	76.238194	3904	(79-97)
301	300	Liligo Camp - Dunge Glacier crossing Baltaro Glacier	6/27/05	35.738111	76.23725	3911	(79-97)
302	301	Liligo Camp - Dunge Glacier crossing Baltaro Glacier	6/27/05	35.726444	76.236833	3941	(79-97)

303	302	Liligo Glacier; Camp	6/28/05	35.716139	76.232833	3844	(98-135)
304	303	Liligo Glacier; Medial Moraine	6/28/05	35.709278	76.225333	3922	(98-135)
305	304	Liligo Glacier; Margin	6/28/05	35.712139	76.230333	3858	(98-135)
306	305	Liligo Glacier; Margin	6/28/05	35.713028	76.230444	3838	(98-135)
307	306	Liligo Glacier; Margin	6/28/05	35.713389	76.230194	3837	(98-135)
308	307	Liligo Glacier; Margin	6/28/05	35.713833	76.229528	3850	(98-135)
309	308	Liligo Glacier; Margin	6/28/05	35.714611	76.229472	3834	(98-135)
310	309	Liligo Glacier; Margin	6/28/05	35.714583	76.229083	3846	(98-135)
311	310	Liligo Glacier; Margin	6/28/05	35.714333	76.228778	3842	(98-135)
312	311	Liligo Glacier; Margin	6/28/05	35.714556	76.2285	3839	(98-135)
313	312	Liligo Glacier; Margin	6/28/05	35.714806	76.228472	3836	(98-135)
314	313	Liligo Glacier; Margin	6/28/05	35.714694	76.228278	3839	(98-135)
315	314	Liligo Glacier; Margin	6/28/05	35.714806	76.227972	3832	(98-135)
316	315	Liligo Glacier; Margin	6/28/05	35.714639	76.227361	3832	(98-135)
317	316	Liligo Glacier; Margin	6/28/05	35.714694	76.226972	3834	(98-135)
318	317	Liligo Glacier; Margin	6/28/05	35.714667	76.226778	3832	(98-135)
319	318	Liligo Glacier; Margin	6/28/05	35.714222	76.226694	3833	(98-135)
320	319	Liligo Glacier; Margin	6/28/05	35.714472	76.226417	3831	(98-135)
321	320	Liligo Glacier; Margin	6/28/05	35.714417	76.226194	3835	(98-135)
322	321	Liligo Glacier; Margin	6/28/05	35.714278	76.225944	3834	(98-135)
323	322	Liligo Glacier; Margin	6/28/05	35.71425	76.225861	3835	(98-135)
324	323	Liligo Glacier; Margin	6/28/05	35.714194	76.225194	3844	(98-135)
325	324	Liligo Glacier; Margin	6/28/05	35.714083	76.224972	3842	(98-135)
326	325	Liligo Glacier; Margin	6/28/05	35.713861	76.224944	3843	(98-135)
327	326	Liligo Glacier; "Dry Lakes"	6/28/05	35.714667	76.225778	3828	(98-135)
328	327	Liligo Glacier; "Dry Lakes"	6/28/05	35.7145	76.226361	3830	(98-135)
329	328	Liligo Glacier; "Dry Lakes"	6/28/05	35.714722	76.22675	3830	(98-135)
330	329	Liligo Glacier; "Dry Lakes"	6/28/05	35.714639	76.227389	3831	(98-135)

331	330	Liligo Glacier; "Dry Lakes"	6/28/05	35.714833	76.227944	3833	(98-135)
332	331	Liligo Glacier; "Dry Lakes"	6/28/05	35.714722	76.228278	3833	(98-135)
333	332	Liligo Glacier; "Dry Lakes"	6/28/05	35.714778	76.2285	3833	(98-135)
334	333	Liligo Glacier; "Dry Lakes"	6/28/05	35.714306	76.228833	3822	(98-135)
335	334	Liligo Glacier; "Dry Lakes"	6/28/05	35.714417	76.228944	3828	(98-135)
336	335	Liligo Glacier; "Dry Lakes"	6/28/05	35.714583	76.228972	3830	(98-135)
337	336	Liligo Glacier; "Dry Lakes"	6/28/05	35.715056	76.228861	3832	(98-135)
338	337	Liligo Glacier; "Dry Lakes"	6/28/05	35.715306	76.229361	3835	(98-135)
339	338	Liligo Glacier; "Dry Lakes"	6/28/05	35.716056	76.229056	3833	(98-135)
340	339	Liligo Glacier; "Dry Lakes"	6/28/05	35.715972	76.228583	3833	(98-135)
341	340	Liligo Glacier; "Dry Lakes"	6/28/05	35.715722	76.2285	3833	(98-135)
342	341	Liligo Glacier; "Dry Lakes"	6/28/05	35.715889	76.227917	3824	(98-135)
343	342	Liligo Glacier; "Dry Lakes"	6/28/05	35.716306	76.227139	3832	(98-135)
344	343	Liligo Glacier; "Dry Lakes"	6/28/05	35.716583	76.227083	3837	(98-135)
345	344	Liligo Glacier; "Dry Lakes"	6/28/05	35.716889	76.226639	3839	(98-135)
346	345	Liligo Glacier; "Dry Lakes"	6/28/05	35.717083	76.226139	3838	(98-135)
347	346	Liligo Glacier; "Dry Lakes"	6/28/05	35.717306	76.225944	3839	(98-135)
348	347	Liligo Glacier; "Dry Lakes"	6/28/05	35.717333	76.225833	3840	(98-135)
349	348	Liligo Glacier; "Dry Lakes"	6/28/05	35.71725	76.225528	3838	(98-135)
350	349	Liligo Glacier; "Dry Lakes"	6/28/05	35.71725	76.225333	3835	(98-135)
351	350	Liligo Glacier; "Dry Lakes"	6/28/05	35.71675	76.225472	3821	(98-135)
352	351	Liligo Glacier; "Dry Lakes"	6/28/05	35.716583	76.225361	3830	(98-135)
353	352	Liligo Glacier; "Dry Lakes"	6/28/05	35.716722	76.225583	3832	(98-135)
354	353	Liligo Glacier; "Dry Lakes"	6/28/05	35.717222	76.226	3837	(98-135)
355	354	Liligo Glacier; "Dry Lakes"	6/28/05	35.716889	76.225972	3836	(98-135)
356	355	Liligo Glacier; "Dry Lakes"	6/28/05	35.716694	76.22575	3838	(98-135)
357	356	Liligo Glacier; "Dry Lakes"	6/28/05	35.715583	76.227528	3828	(98-135)
358	357	Liligo Glacier; Actual Lake	6/28/05	35.713722	76.229694	3848	(98-135)

359	358	Liligo Glacier; Actual Lake	6/28/05	35.713333	76.230278	3842	(98-135)
360	359	Liligo Glacier; Actual Lake	6/28/05	35.713417	76.230639	3836	(98-135)
361	360	Liligo Glacier; Actual Lake	6/28/05	35.714194	76.231611	3831	(98-135)
362	361	Liligo Glacier; Actual Lake	6/28/05	35.714472	76.231861	3836	(98-135)
363	362	Liligo Glacier; Actual Lake	6/28/05	35.715722	76.232111	3843	(98-135)
364	363	Liligo Glacier; Actual Lake	6/28/05	35.716111	76.232583	3835	(98-135)
365	364	Liligo Glacier; Actual Lake	6/28/05	35.71575	76.232028	3828	(98-135)
366	365	Liligo Glacier; Actual Lake	6/28/05	35.716528	76.232806	3826	(98-135)
367	366	Liligo Glacier; Actual Lake	6/28/05	35.716056	76.231694	3828	(98-135)
368	367	Liligo Glacier; Actual Lake	6/28/05	35.715833	76.230889	3832	(98-135)
369	368	Liligo Glacier; Actual Lake	6/28/05	35.716917	76.230667	3842	(98-135)
370	369	Liligo Glacier; Actual Lake	6/28/05	35.717611	76.230278	3842	(98-135)
371	370	Liligo - Urdokas	6/29/05	35.722139	76.247528	3926	(136-162)
372	371	Liligo - Urdokas; Tributary Glacier 1	6/29/05	35.723111	76.252694	3953	(136-162)
373	372	Liligo - Urdokas; Tributary Glacier 2	6/29/05	35.726806	76.268111	3971	(136-162)
374	373	Liligo - Urdokas; Tributary Glacier 3	6/29/05	35.727278	76.276889	4034	(136-162)
375	374	Urdokas; Camp	6/29/05	35.727194	76.284639	4069	163-164
376	375	Urdokas	6/30/05	35.725806	76.286472	4149	(165-190)
377	376	Urdokas	6/30/05	35.724361	76.286694	4236	(165-190)
378	377	Urdokas	6/30/05	35.723833	76.286778	4289	(165-190)
379	378	Urdokas; Landslide	7/1/05	35.728389	76.288889	4046	
380	379	Urdokas; Landslide	7/1/05	35.728056	76.286806	4069	
381	380	Urdokas; Landslide	7/1/05	35.727472	76.286361	4137	
382	381	Urdokas; Landslide	7/1/05	35.728167	76.285556	4058	
383	382	Baltoro Glacier; Gore II Camp	7/6/05	35.746278	76.404556	4331	
500	383	Baltoro Glacier; Concordia	7/7/05	0	0		4.15- 4.20

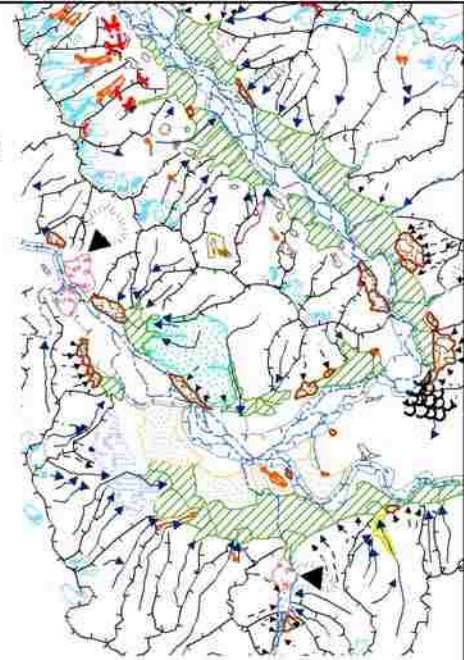
501	393	Baltoro Glacier; Concordia - Gore II	7/7/05	0	0
502	394	Baltoro Glacier; Concordia - Gore II	7/7/05	0	0
503	395	Baltoro Glacier; Concordia - Gore II	7/7/05	0	0
504	396	Baltoro Glacier; Concordia - Gore II	7/7/05	0	0
505	397	Baltoro Glacier; Concordia - Gore II	7/7/05	0	0
506	398	Baltoro Glacier; Concordia - Gore II	7/7/05	0	0
507	399	Baltoro Glacier; Concordia - Gore II	7/7/05	0	0
508	400	Baltoro Glacier; Concordia - Gore II	7/7/05	0	0
509	401	Baltoro Glacier; Concordia - Gore II	7/7/05	0	0
510	402	Baltoro Glacier; Concordia - Gore II	7/7/05	0	0
511	403	Baltoro Glacier; Concordia - Gore II	7/7/05	0	0
600	404	Baltoro Glacier; Gore II - Urdokas	7/8/05	0	0
601	405	Baltoro Glacier; Gore II - Urdokas	7/8/05	0	0
602	406	Baltoro Glacier; Gore II - Urdokas	7/8/05	0	0
603	407	Baltoro Glacier; Gore II - Urdokas	7/8/05	0	0

604	408	Baltoro Glacier; Gore II - Urdokas	7/8/05	0	0		
605	409	Baltoro Glacier; Gore II - Urdokas	7/8/05	0	0		
606	410	Baltoro Glacier; Gore II - Urdokas	7/8/05	0	0		
607	411	Baltoro Glacier; Urdokas; Camp	7/8/05	0	0		
608	412	Askole - Skardu; Active Landslide and Roadblock	7/12/05	35.7118	75.705933	3033	4.23- 4.25; 5.1- 5.2; (5.4- 5.5) (5.06-5.22)
609	413	Skardu	7/13/05	35.363733	75.739867	2441	























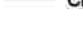












APPENDIX F

Maps

**GEOMORPHOLOGICAL MAPPING
OF THE K2 AREA, PAKISTAN
USING GIS AND REMOTE SENSING**

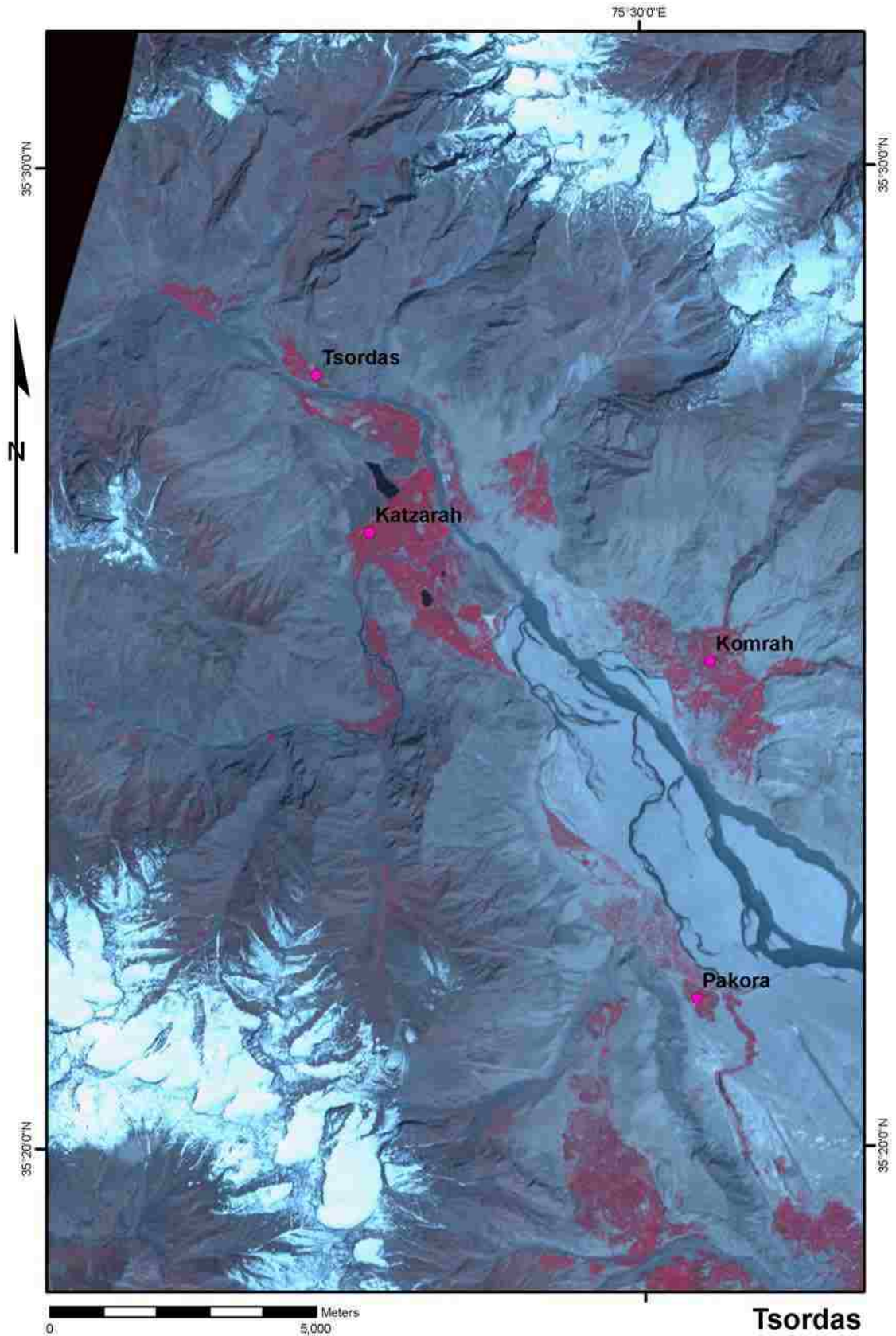


Legend

- | | |
|---|--|
|  roche moutonnees |  Alluvial fan |
|  Gorge |  Bedrock terrace |
|  avalanche path |  Debris fan |
|  drainage |  Flood deposit |
|  erosion |  Fluvial |
|  incised channel |  T1 |
|  old channel |  T3 |
|  ridge |  avalanche deposit |
|  scarp |  glacial terrace w/till |
|  stream |  lake sediment |
|  trim |  sand |
|  cirque |  sediment fill |
|  moraine |  strath terrace |
|  river_bank |  till |
|  ice glacier |  lake |
|  dead ice |  Bunthang |
|  rock glacier |  sackung |
|  rock or receded glacier | |

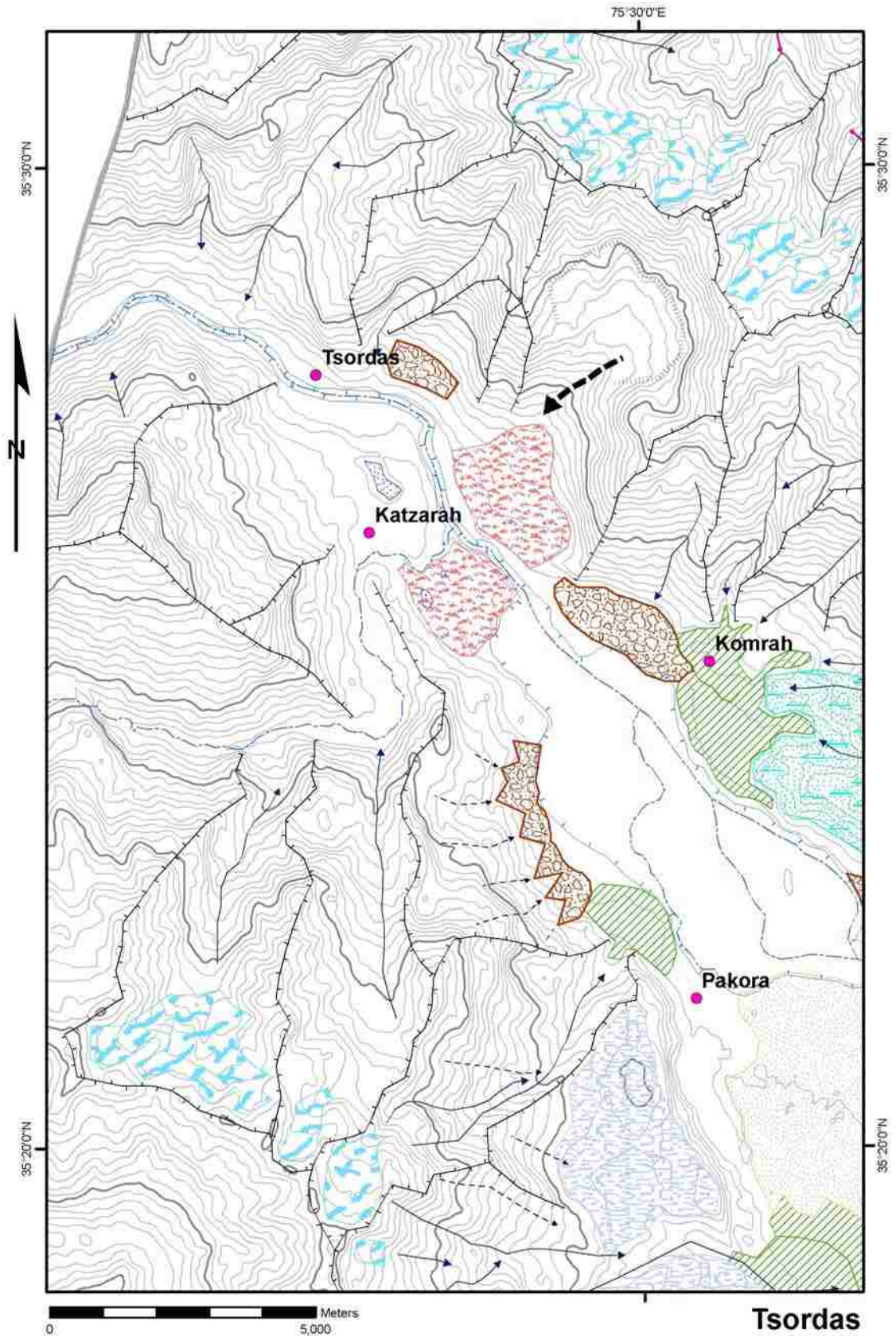
D. Belden 2008

Map 1. Legend.



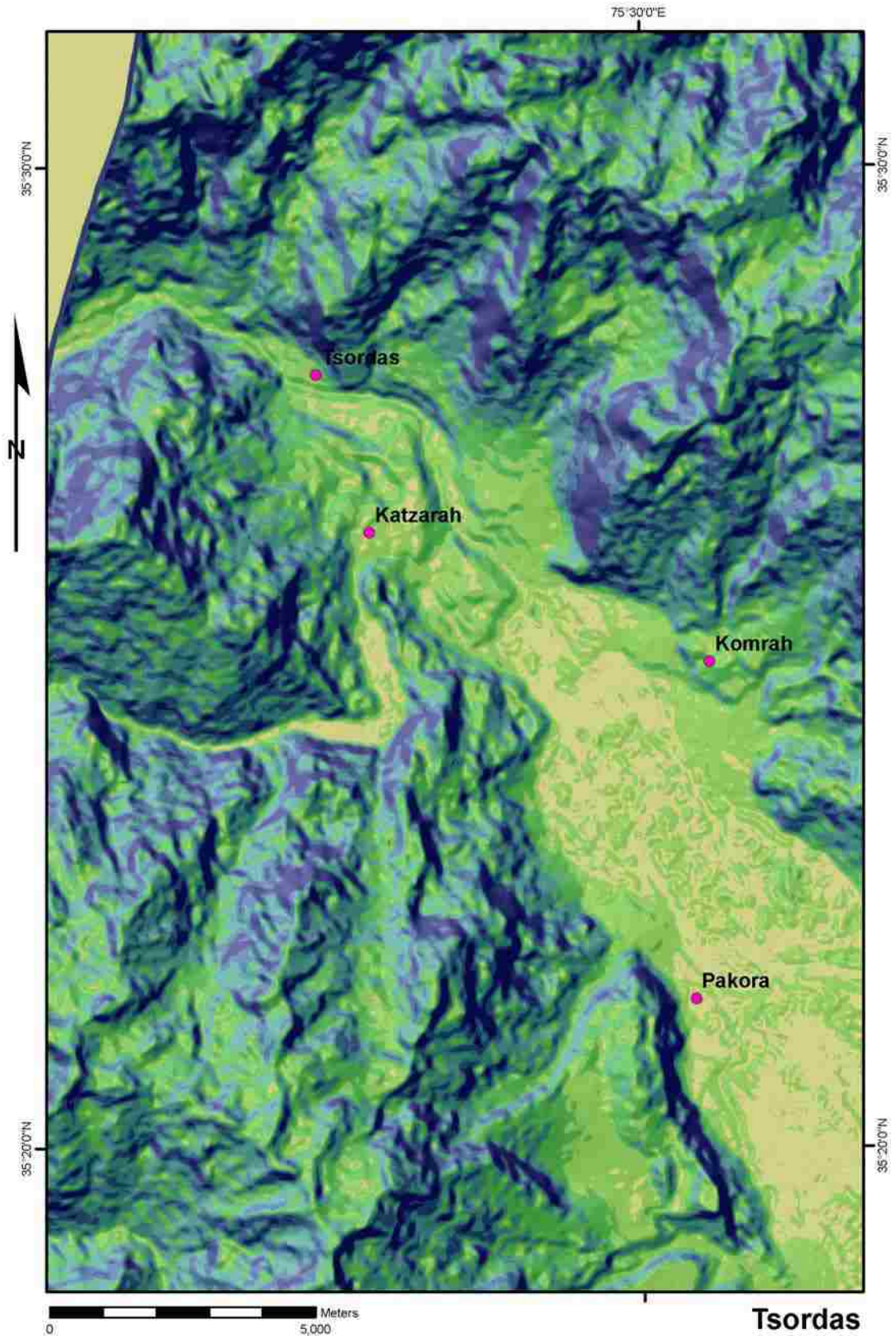
Map 2. Tsordas: ASTER imagery.

Tsordas
D. Belden 2008



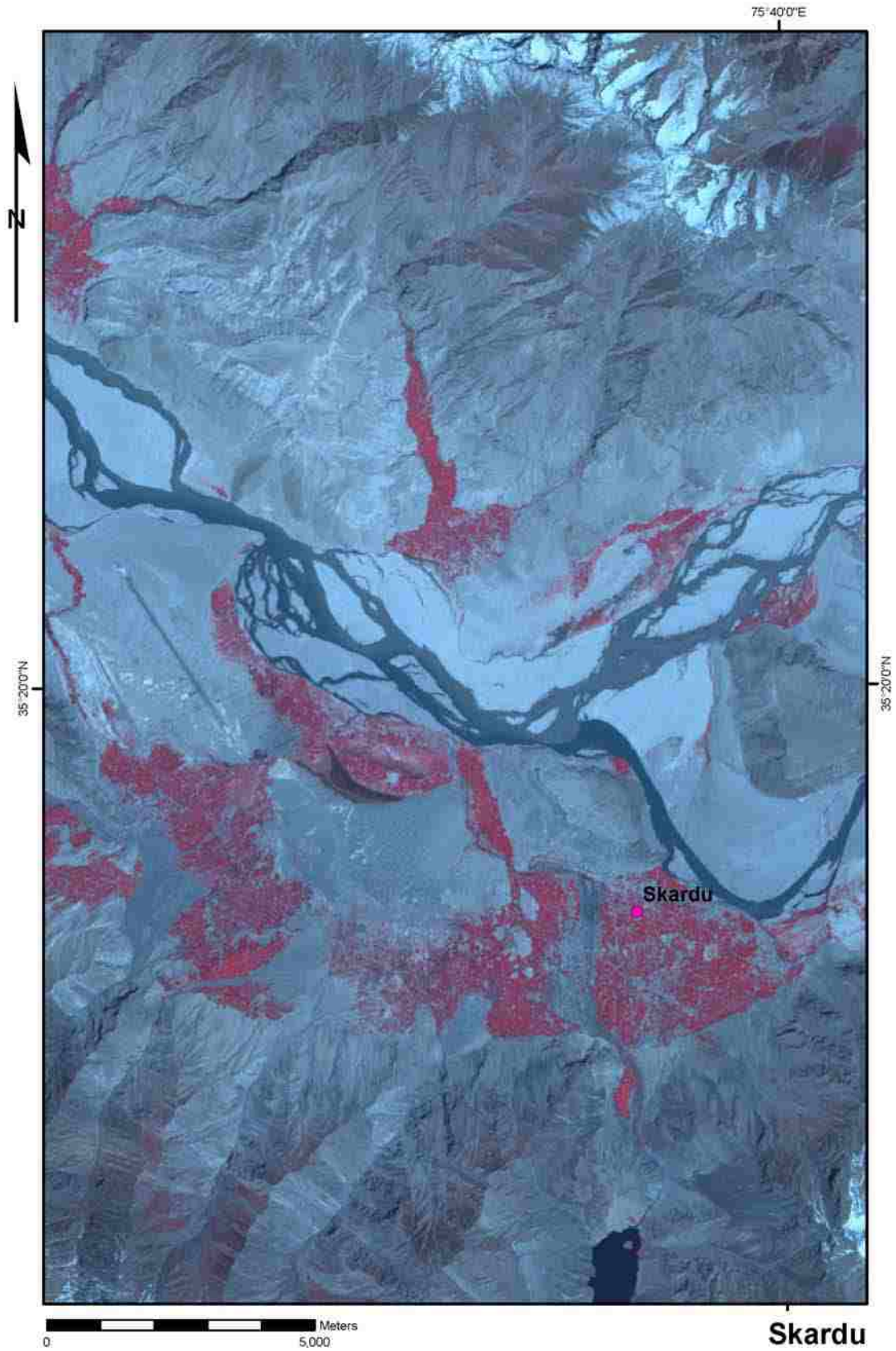
Map 3. Tsordas: geomorphological map.

Tsordas
D. Belden 2008



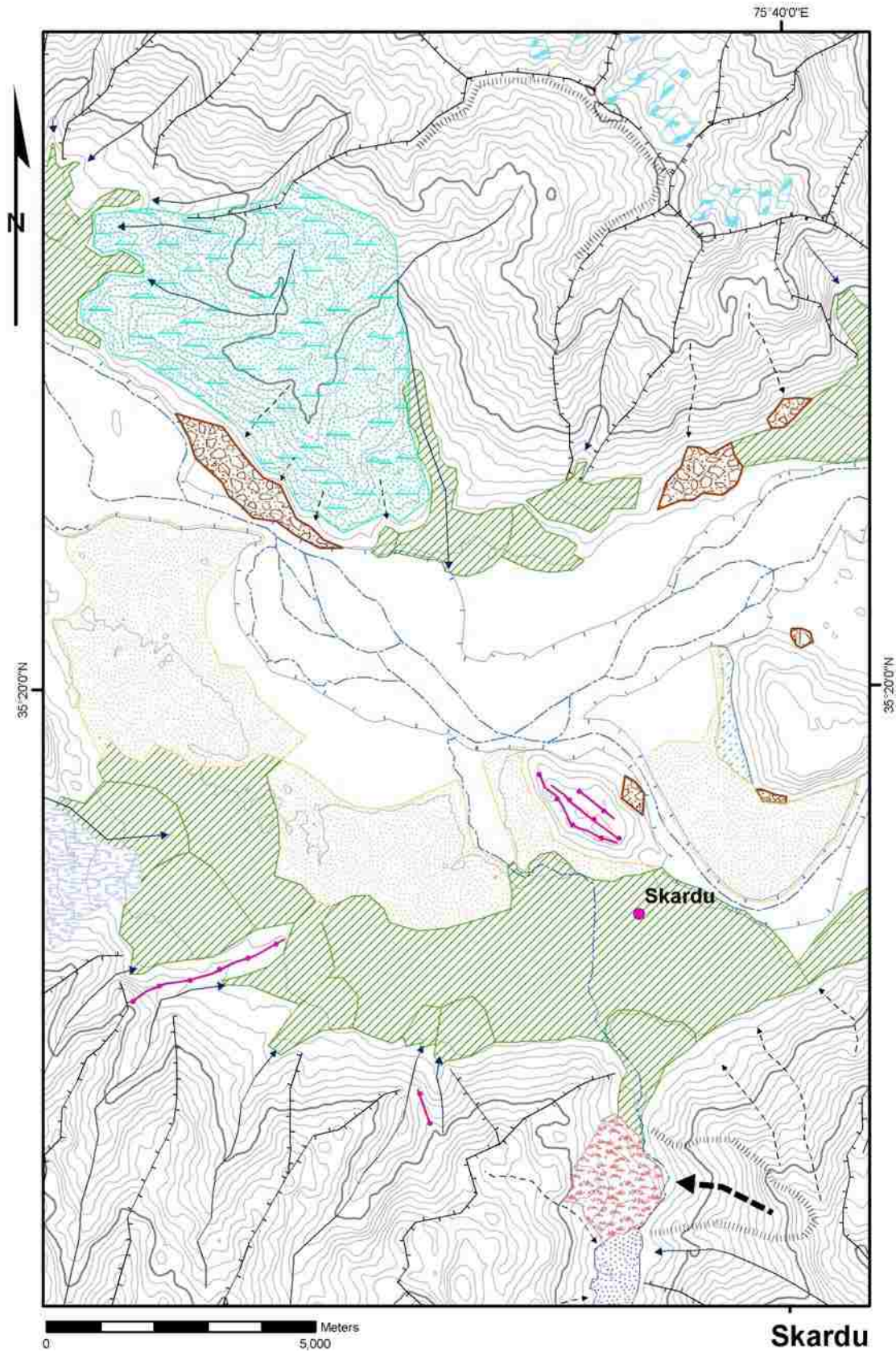
Map 4. Tsordas: slope map.

Tsordas
D. Belden 2008



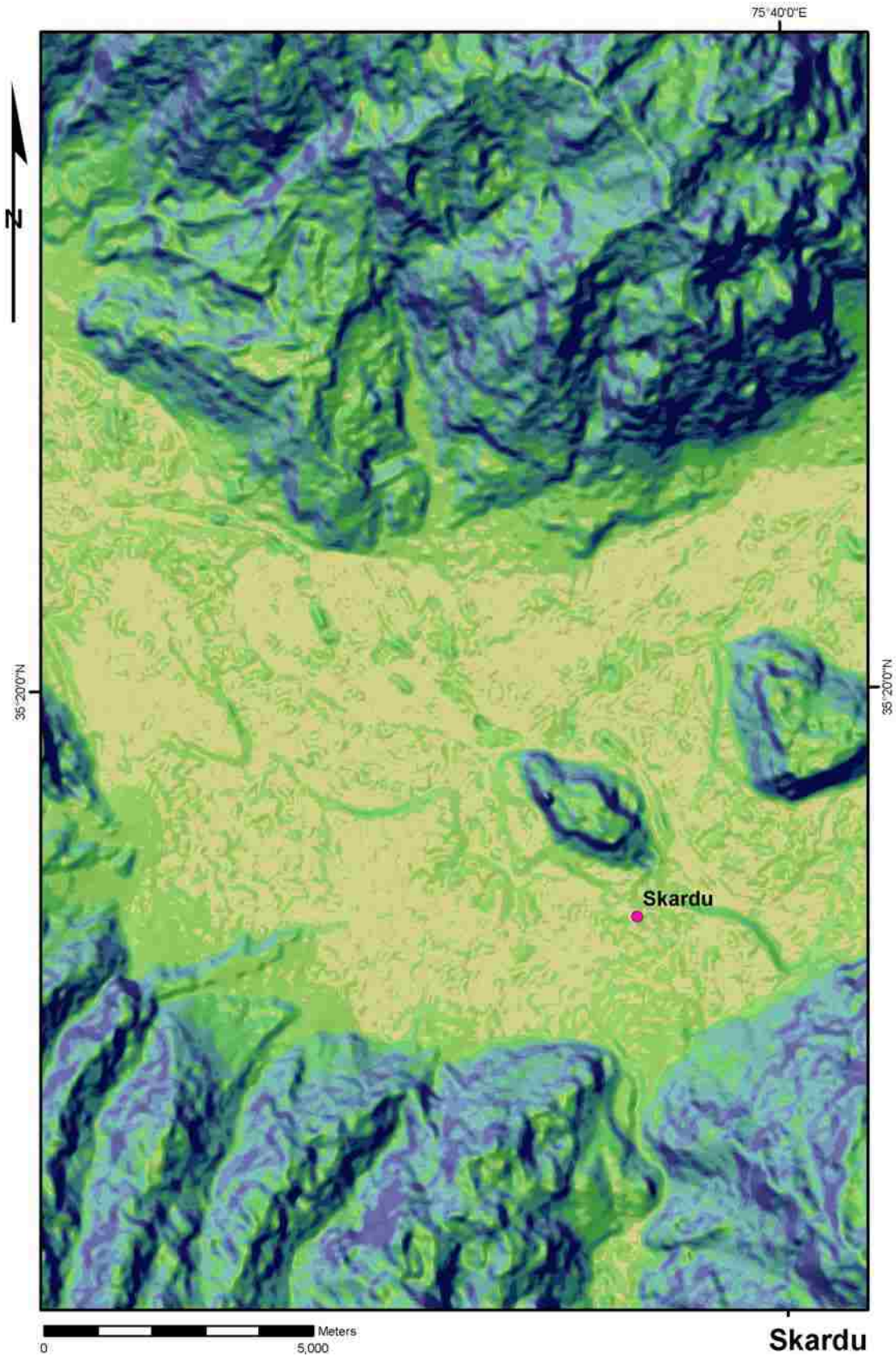
Map 5. Skardu: ASTER imagery.

Skardu
D. Belden 2008



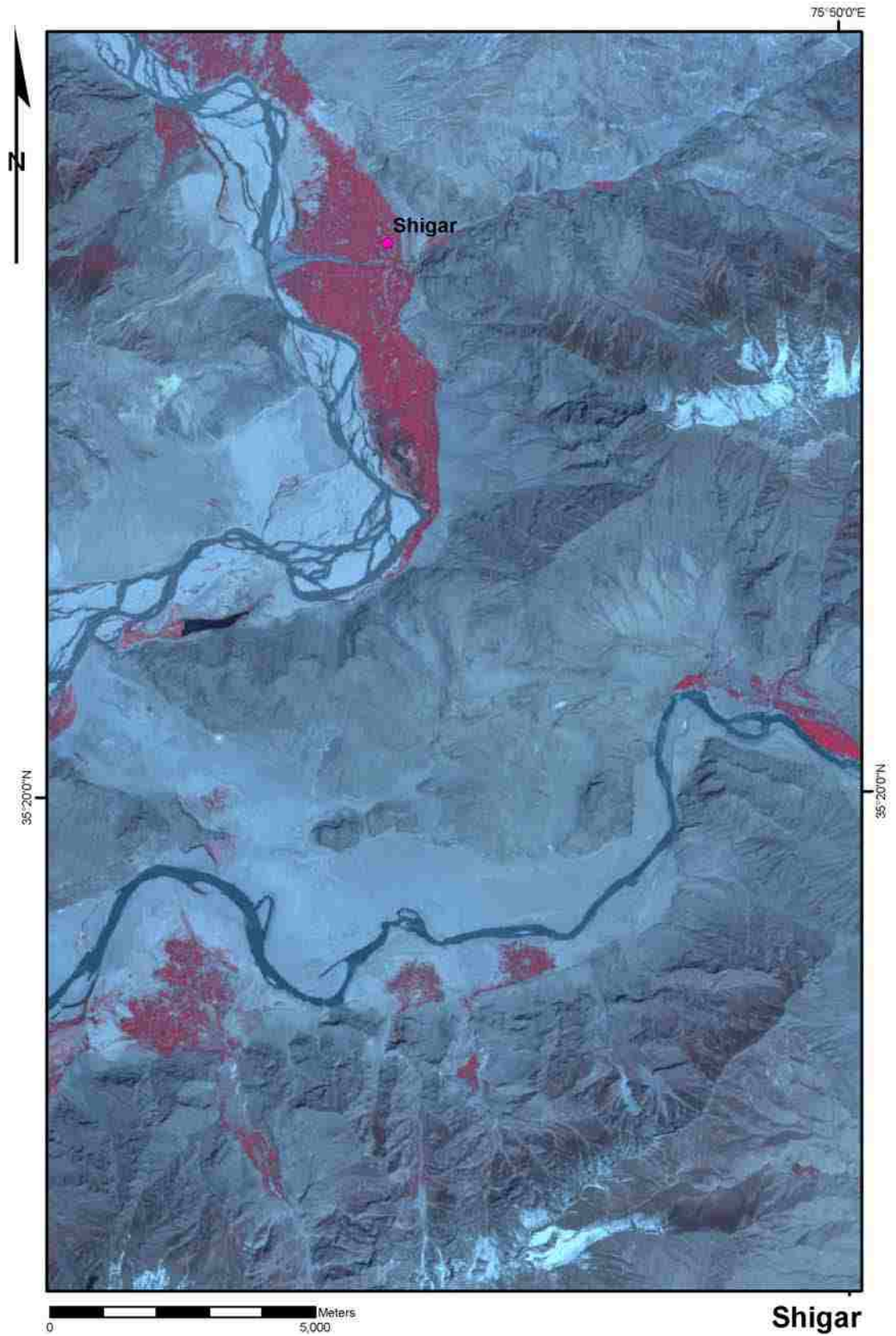
Map 6. Skardu: geomorphological map.

Skardu
D. Belden 2008



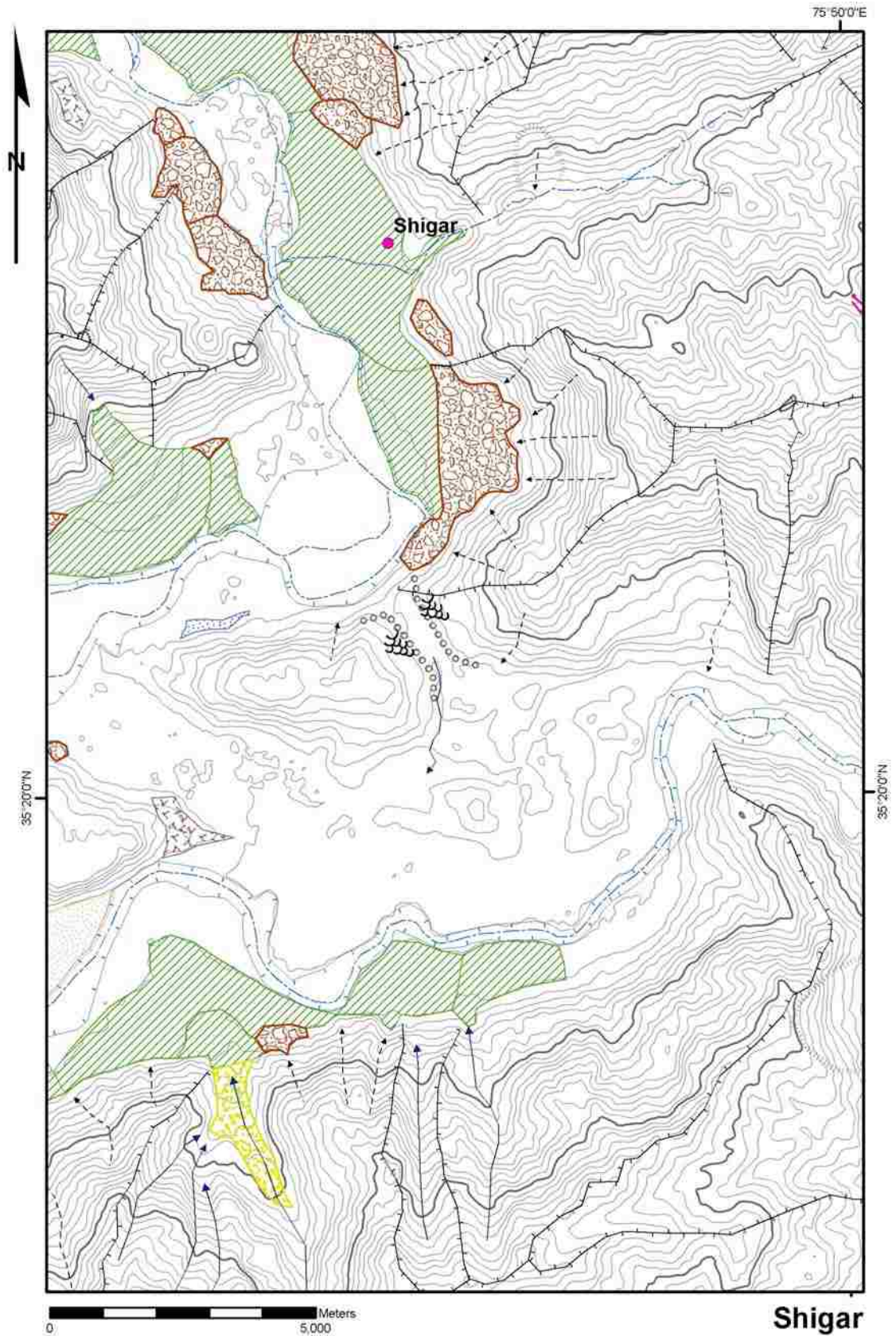
Map 7. Skardu: slope map.

Skardu
D. Belden 2008



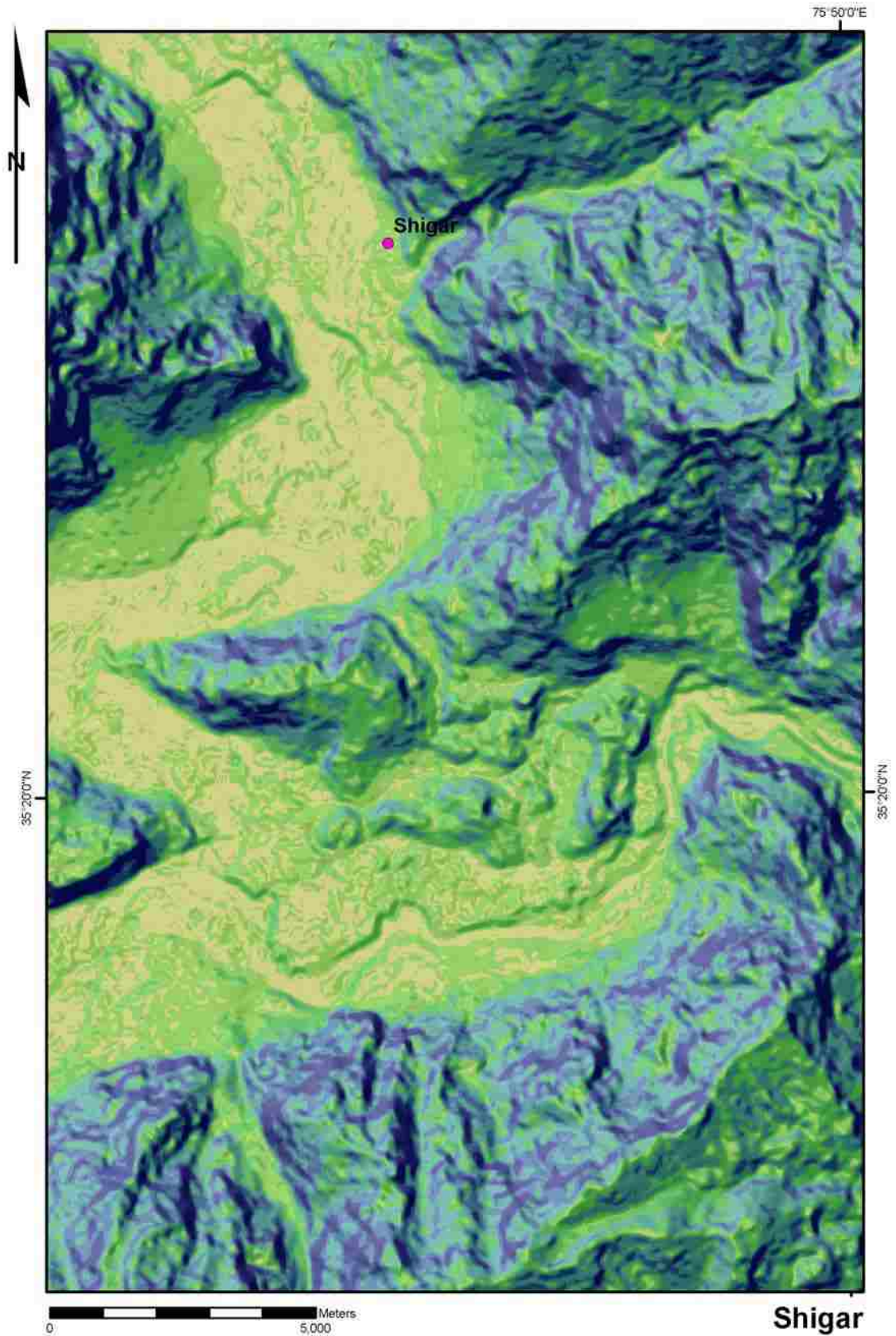
Map 8. Shigar: ASTER imagery.

D. Belden 2008



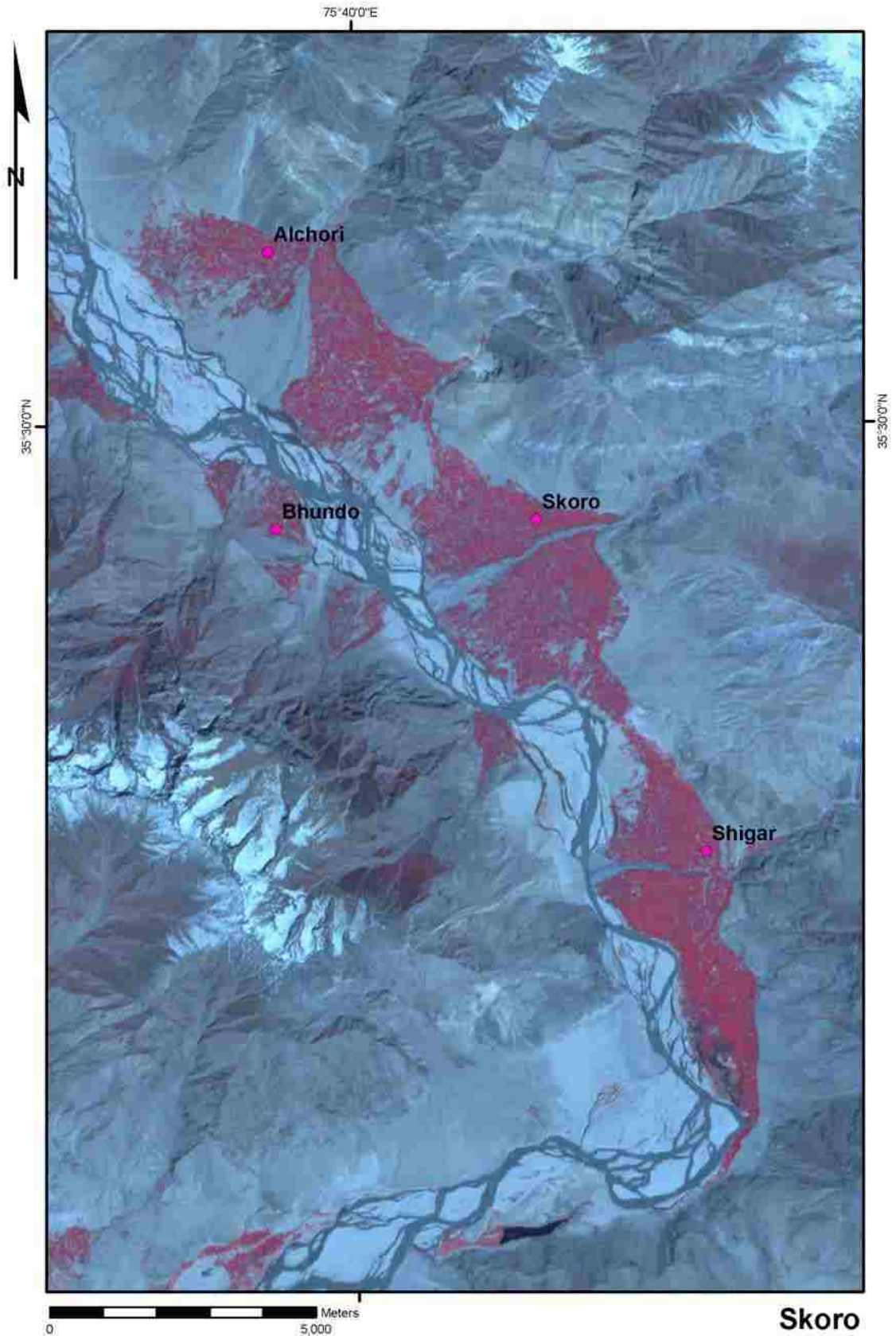
Map 9. Shigar: geomorphological map.

Shigar
D. Belden 2008



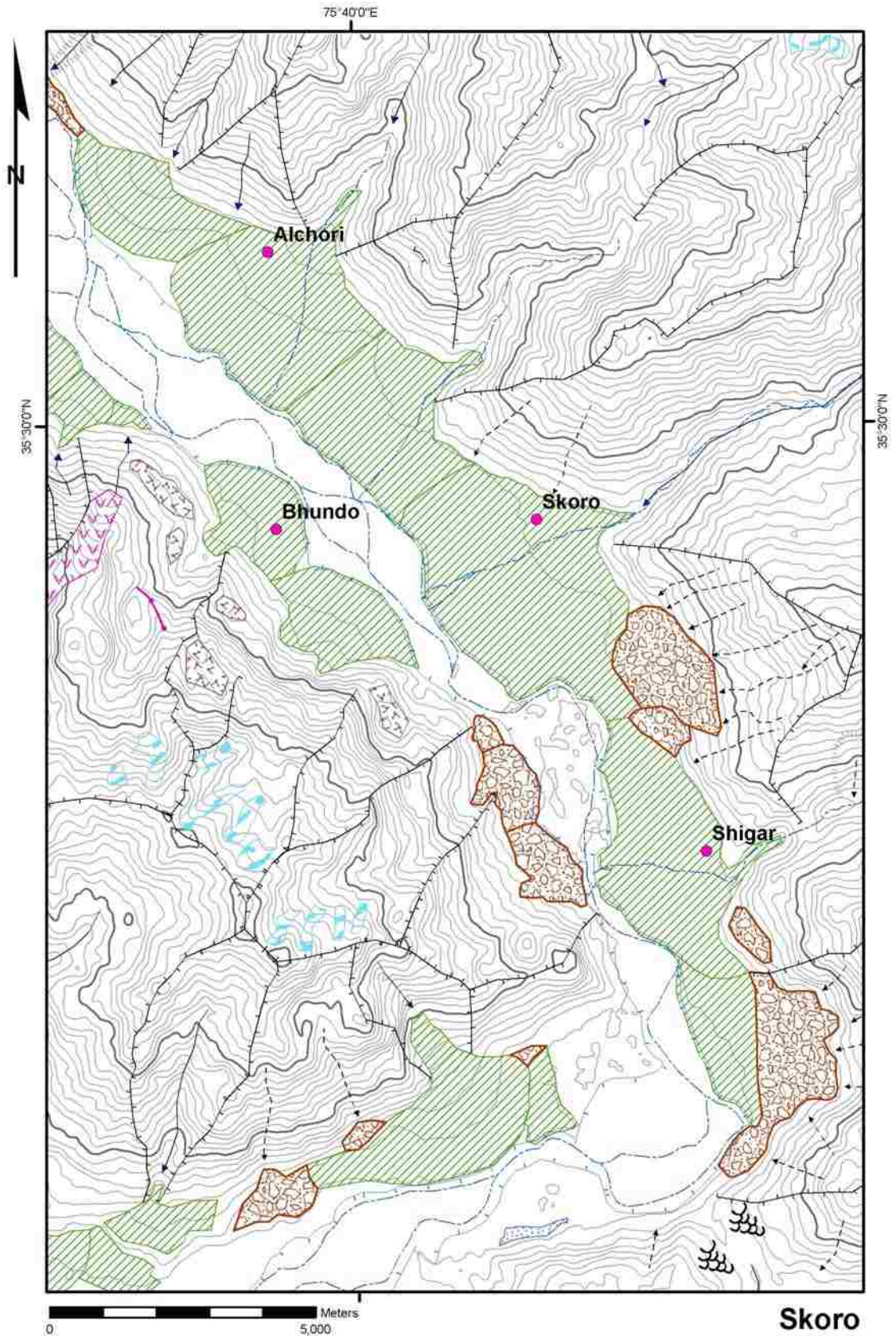
Map 10. Shigar: slope map.

Shigar
D. Belden 2008



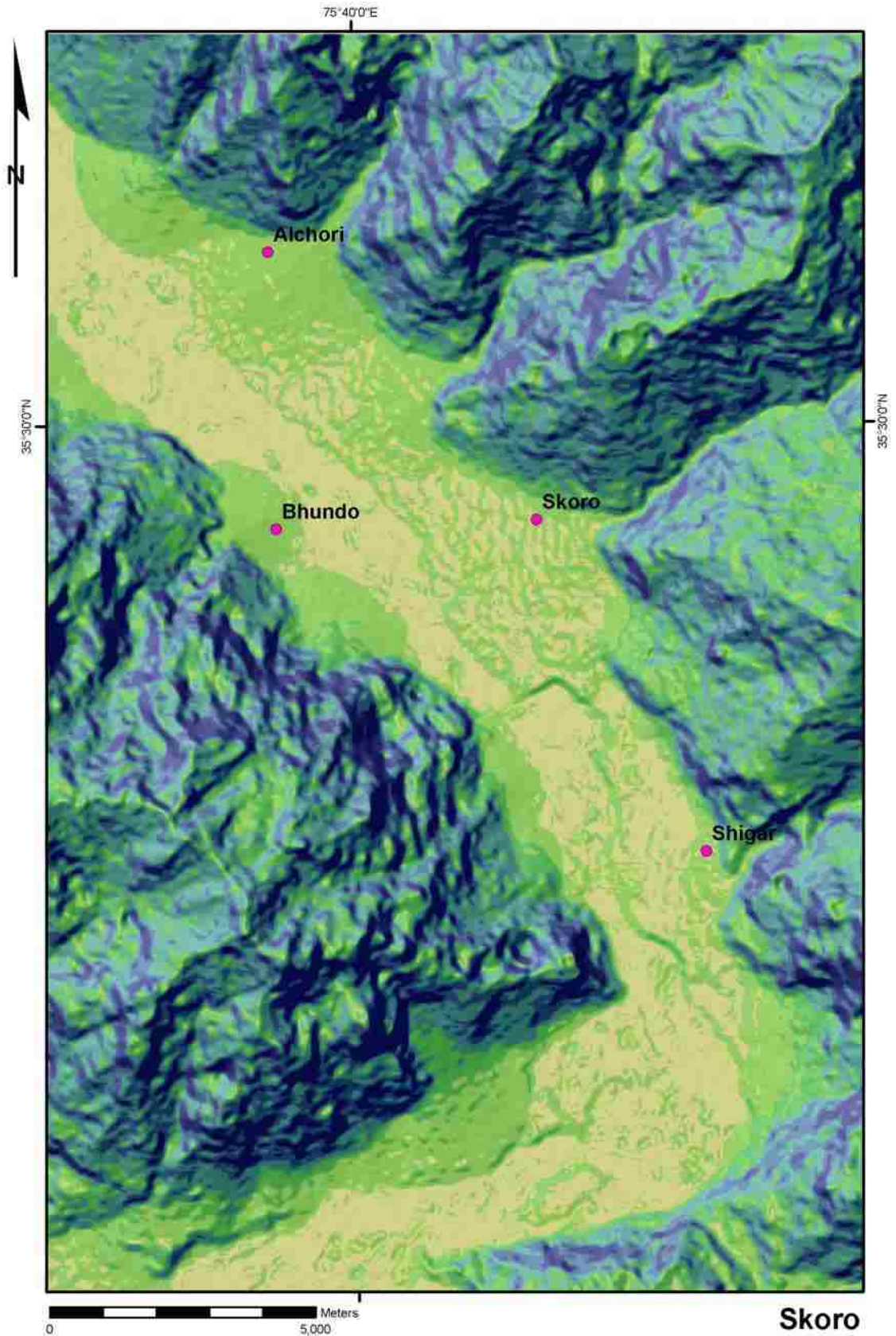
Map 11. Skoro: ASTER imagery.

Skoro
D. Belden 2008



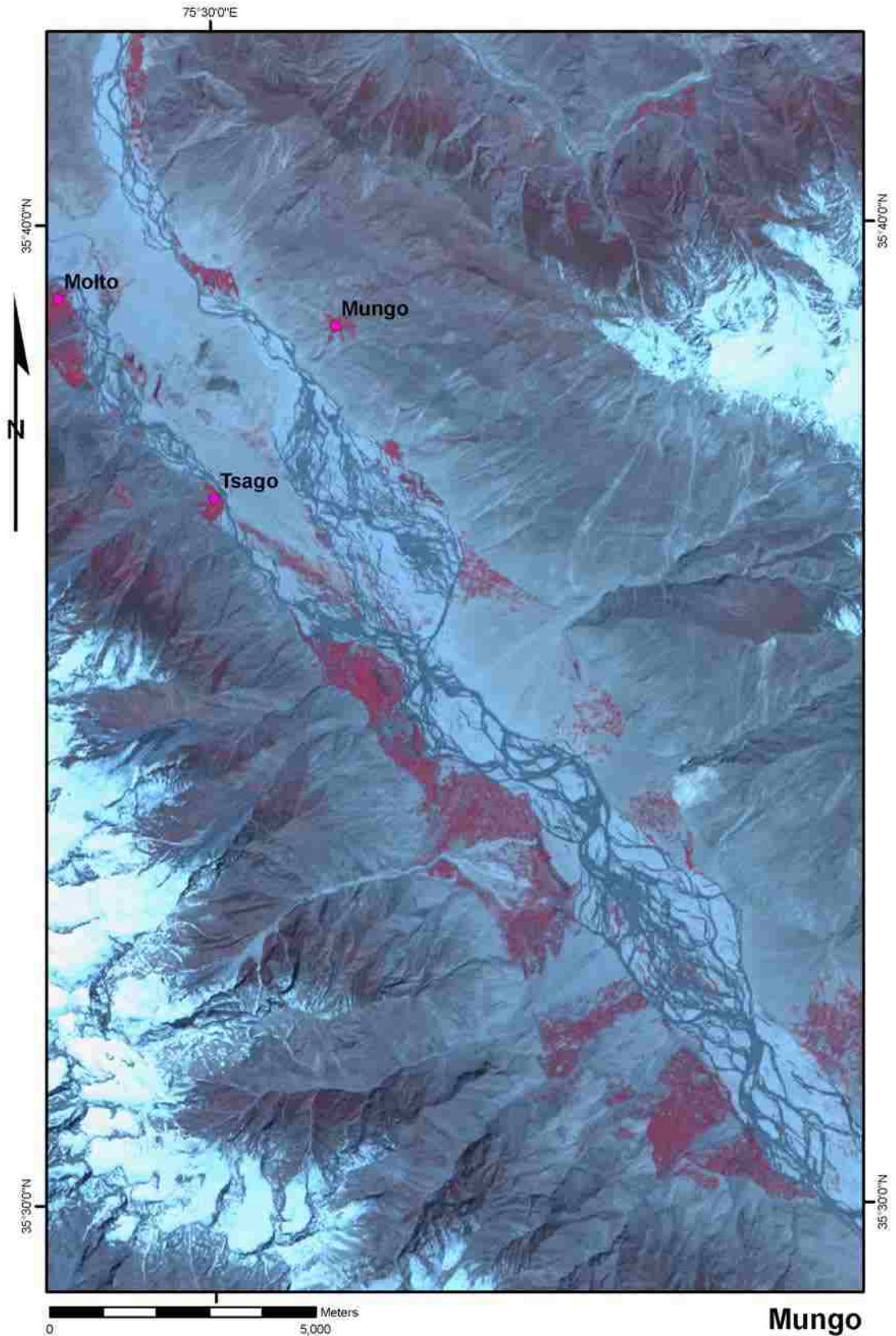
Map 12. Skoro: geomorphological map.

Skoro
D. Belden 2008



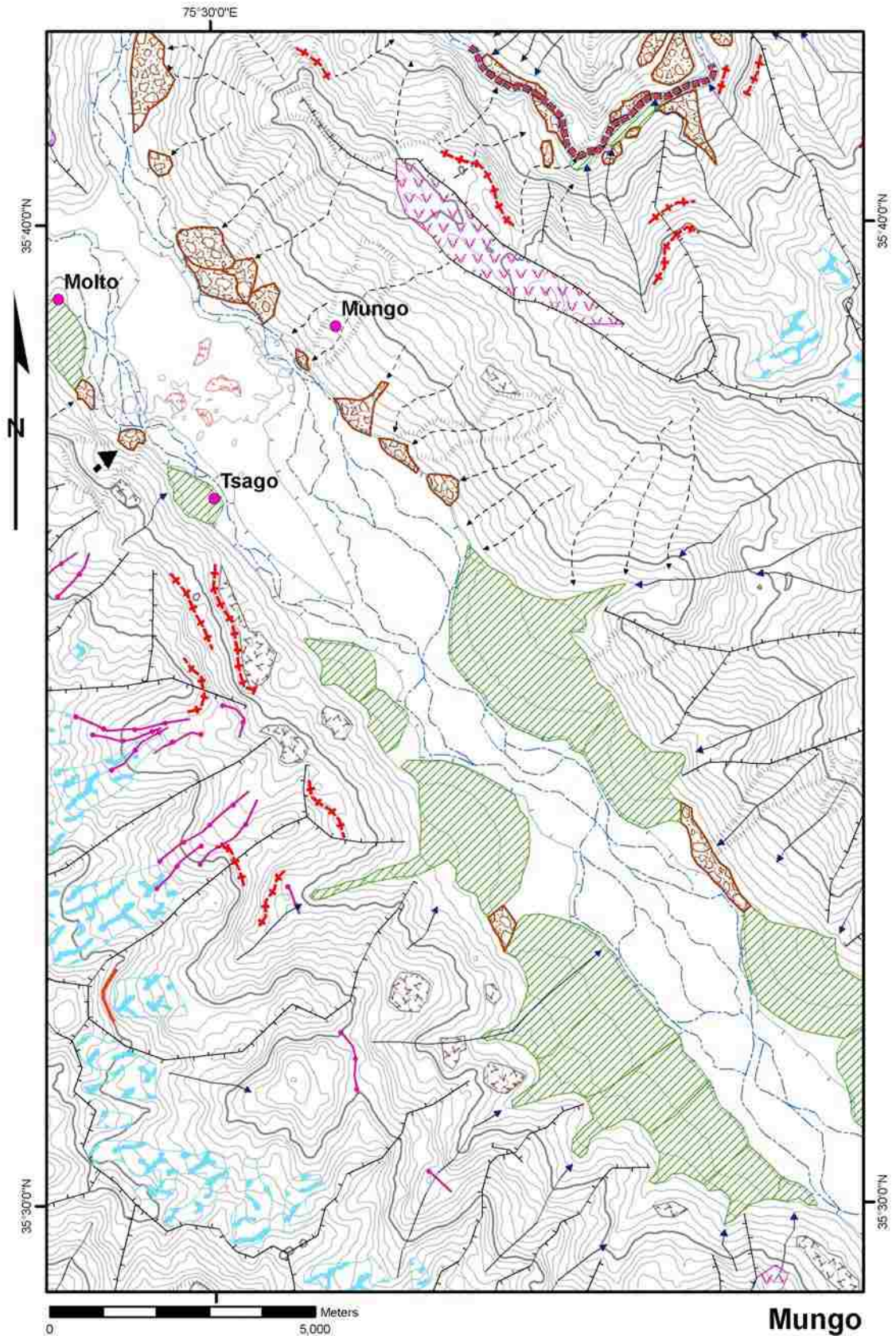
Map 13. Skoro: slope map.

D. Belden 2008



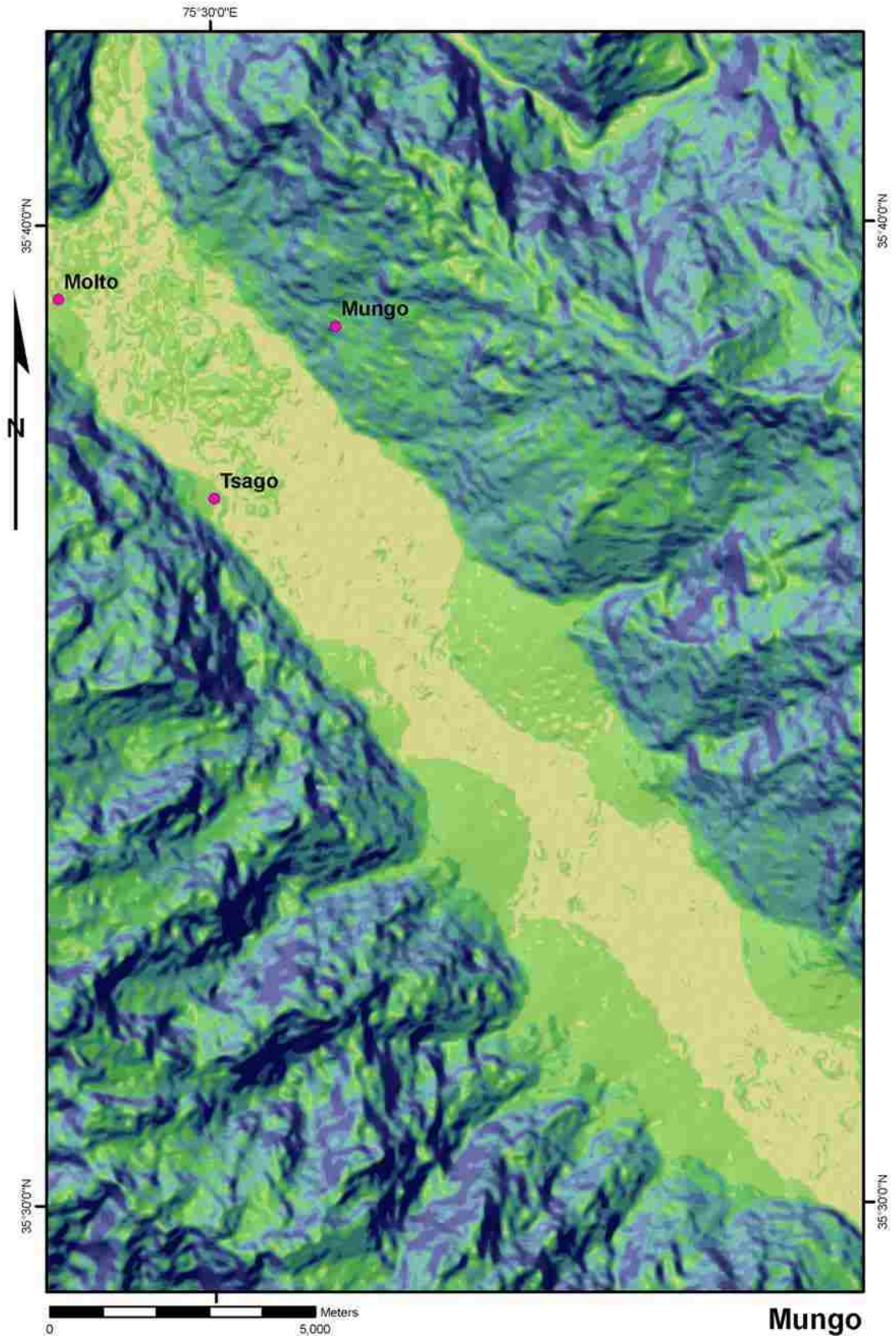
Map 14. Mungo: ASTER imagery.

Mungo
D. Belden 2008



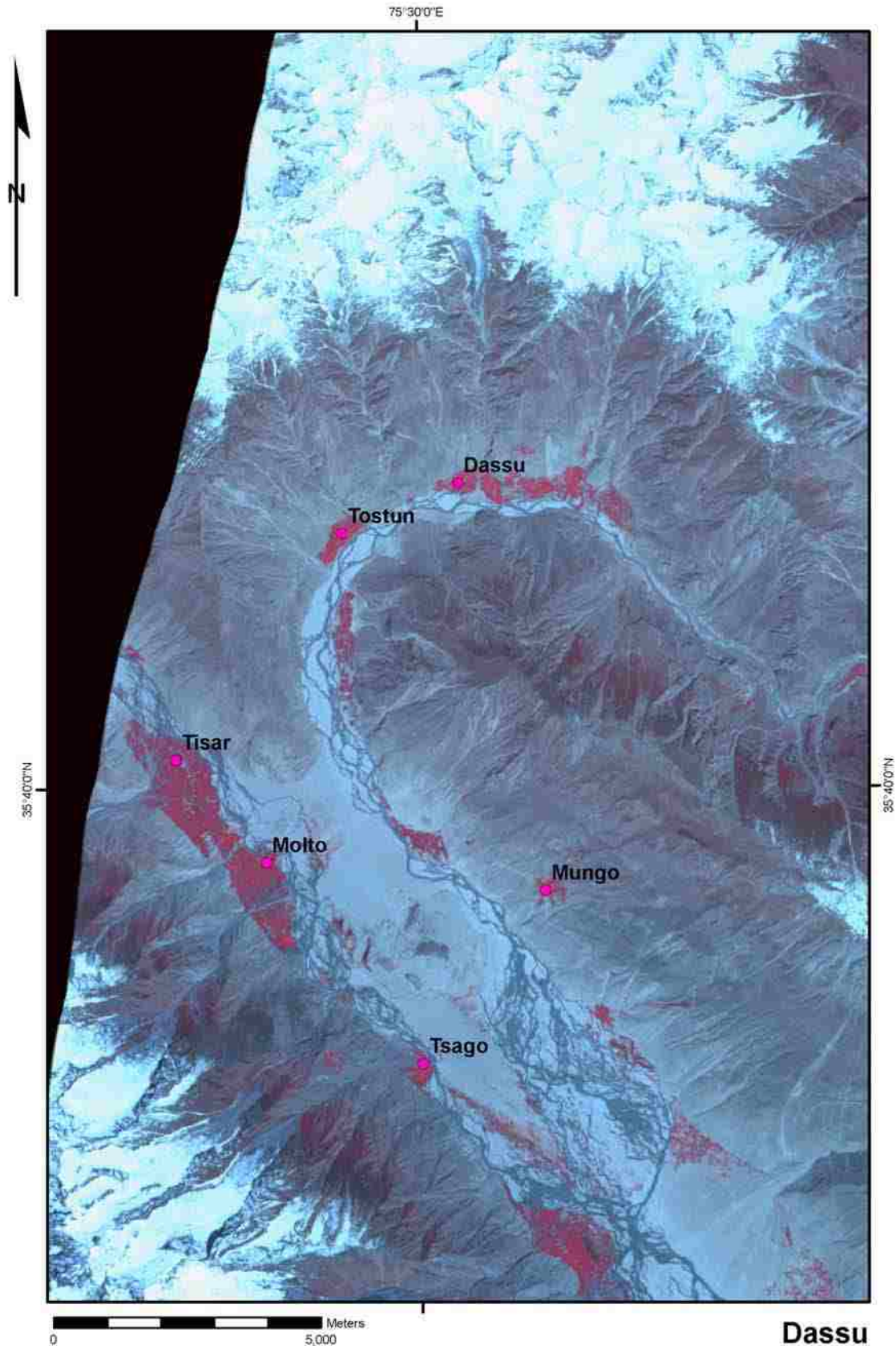
Map 15. Mungo: geomorphological map.

Mungo
D. Belden 2008



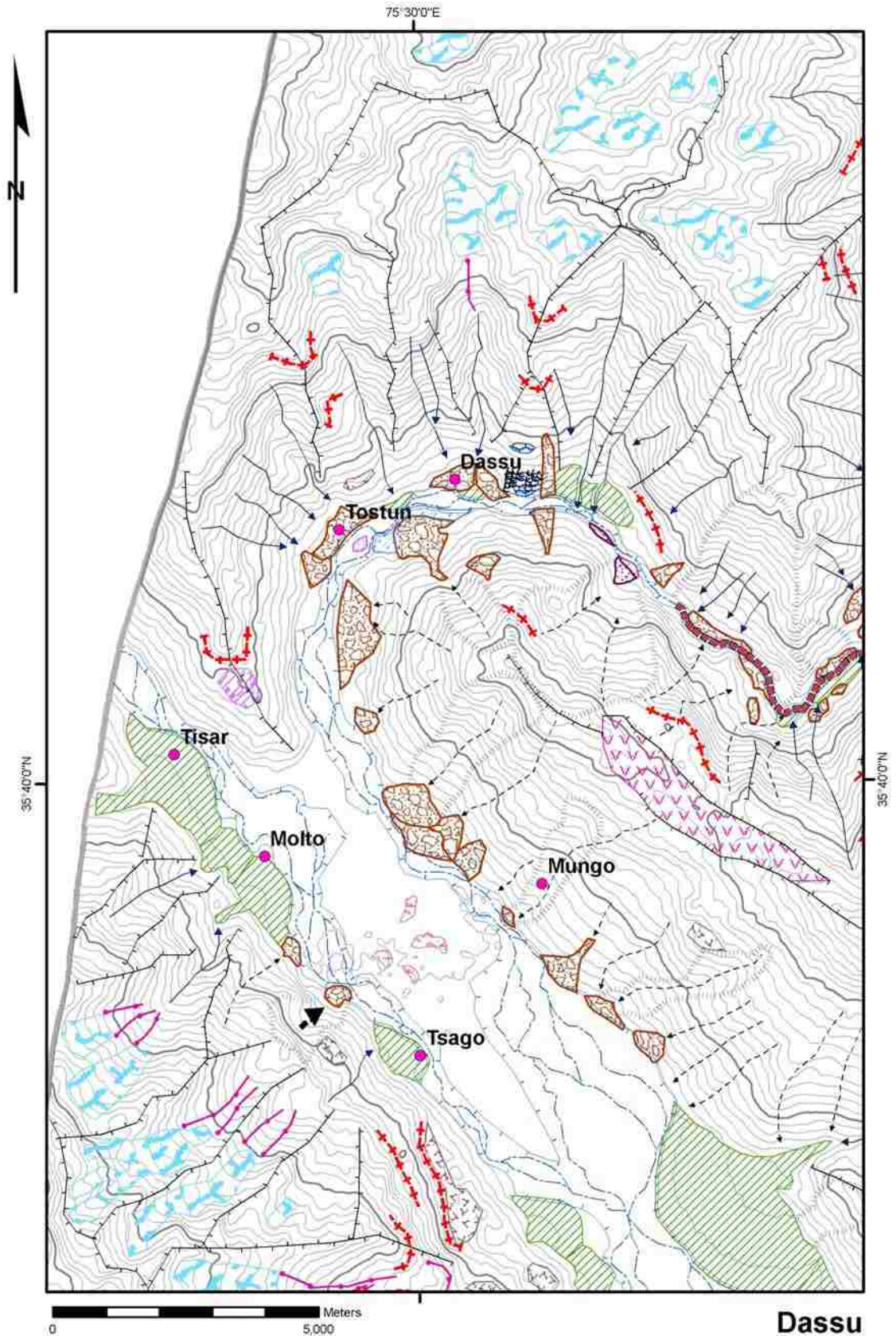
Map 16. Mungo: slope map.

Mungo
D. Belden 2008



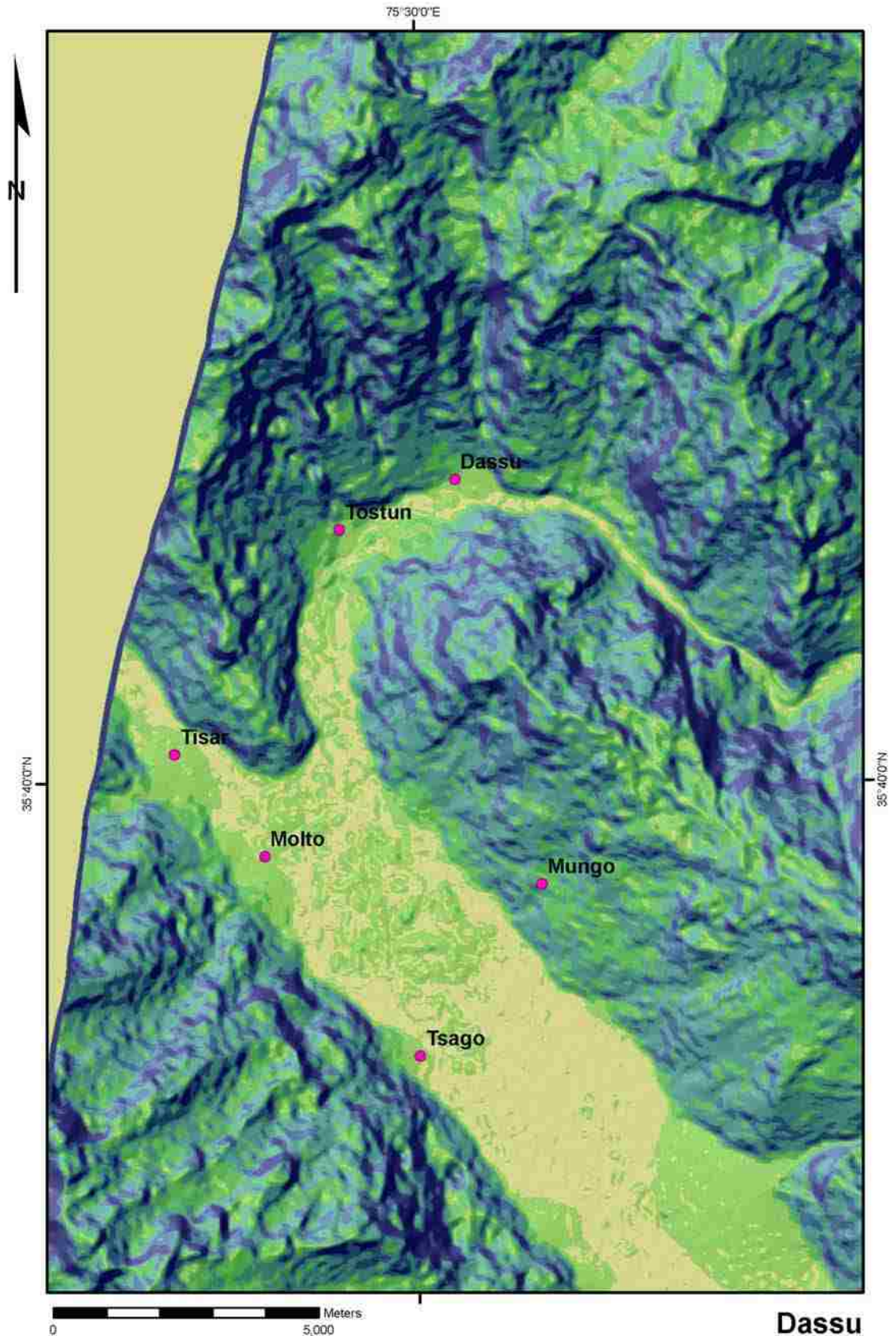
Map 17. Dasso: ASTER imagery.

Dassu
D. Belden 2008



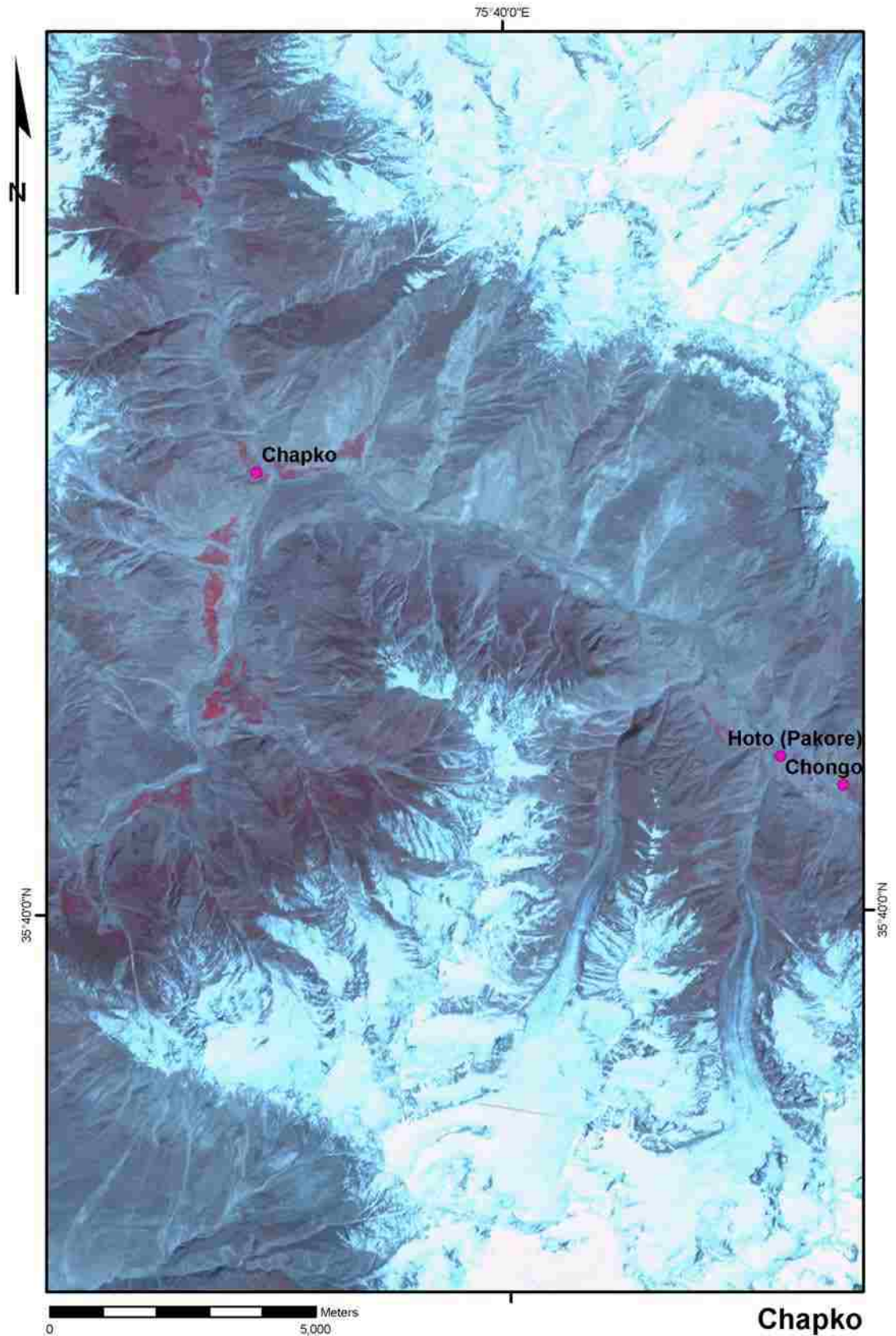
Map 18. Dasso geomorphological map.

D. Belden 2008



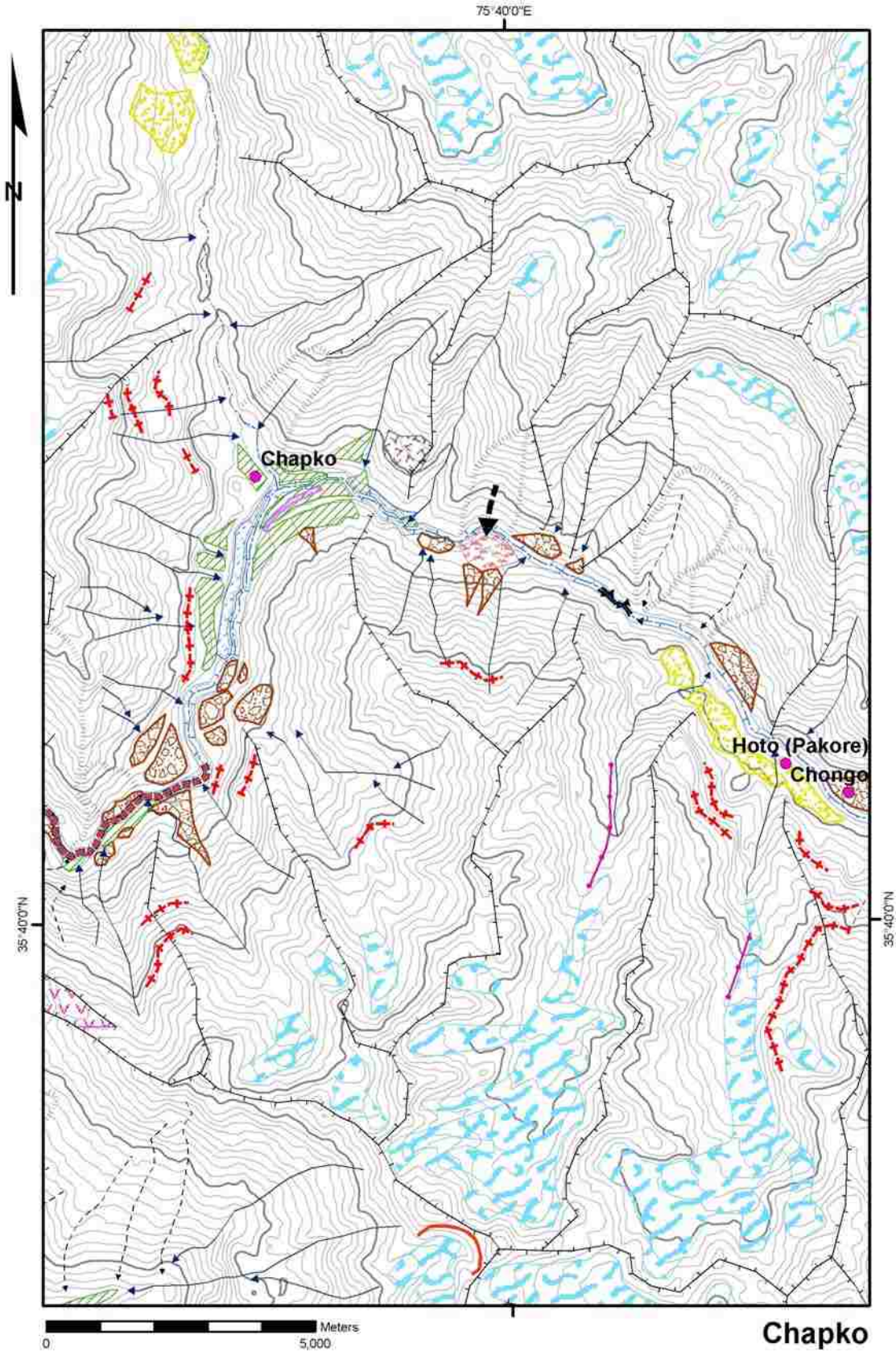
Map 19. Dassu slope map.

Dassu
D. Belden 2008



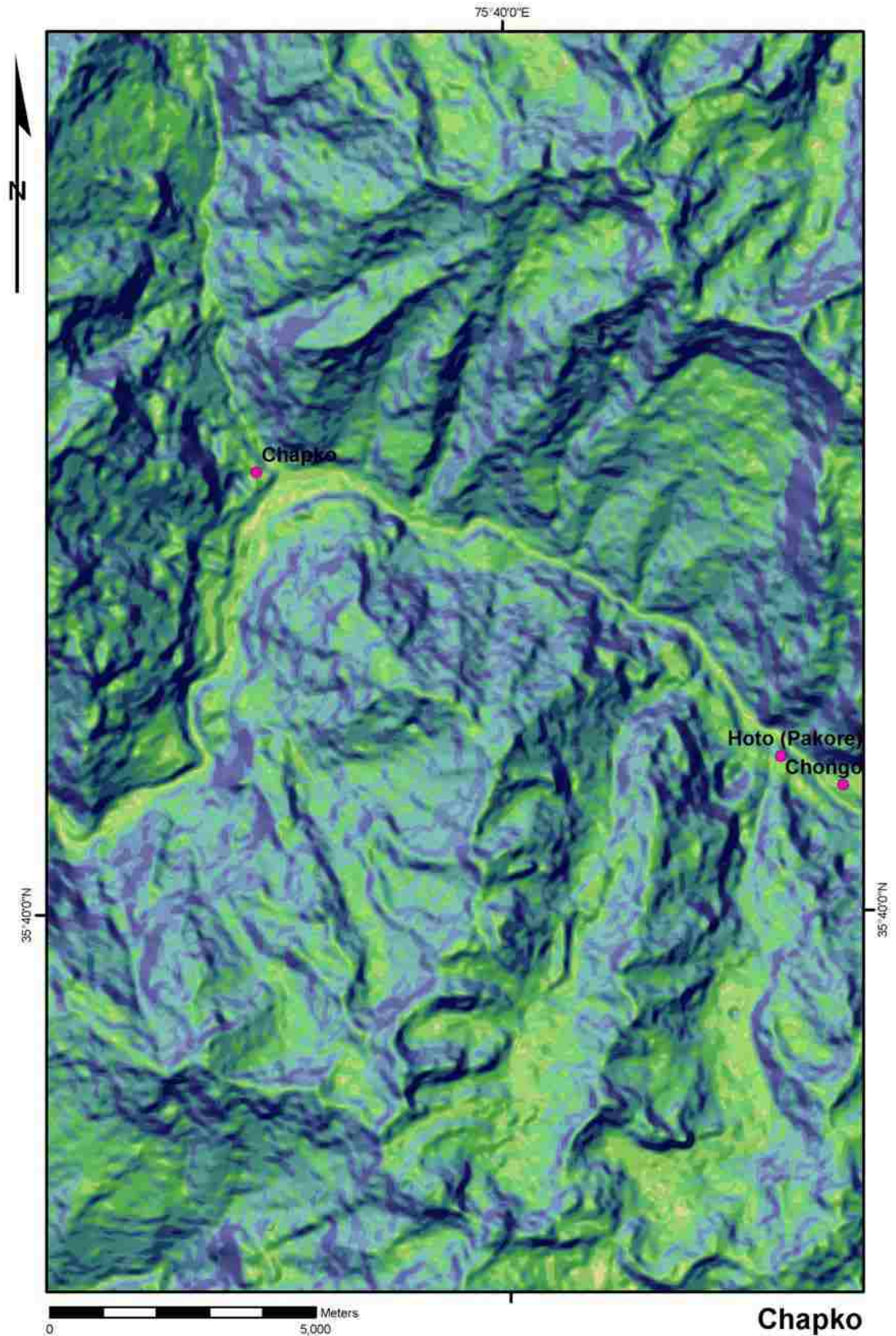
Map 20. Chakpo: ASTER imagery.

Chapko
D. Belden 2008



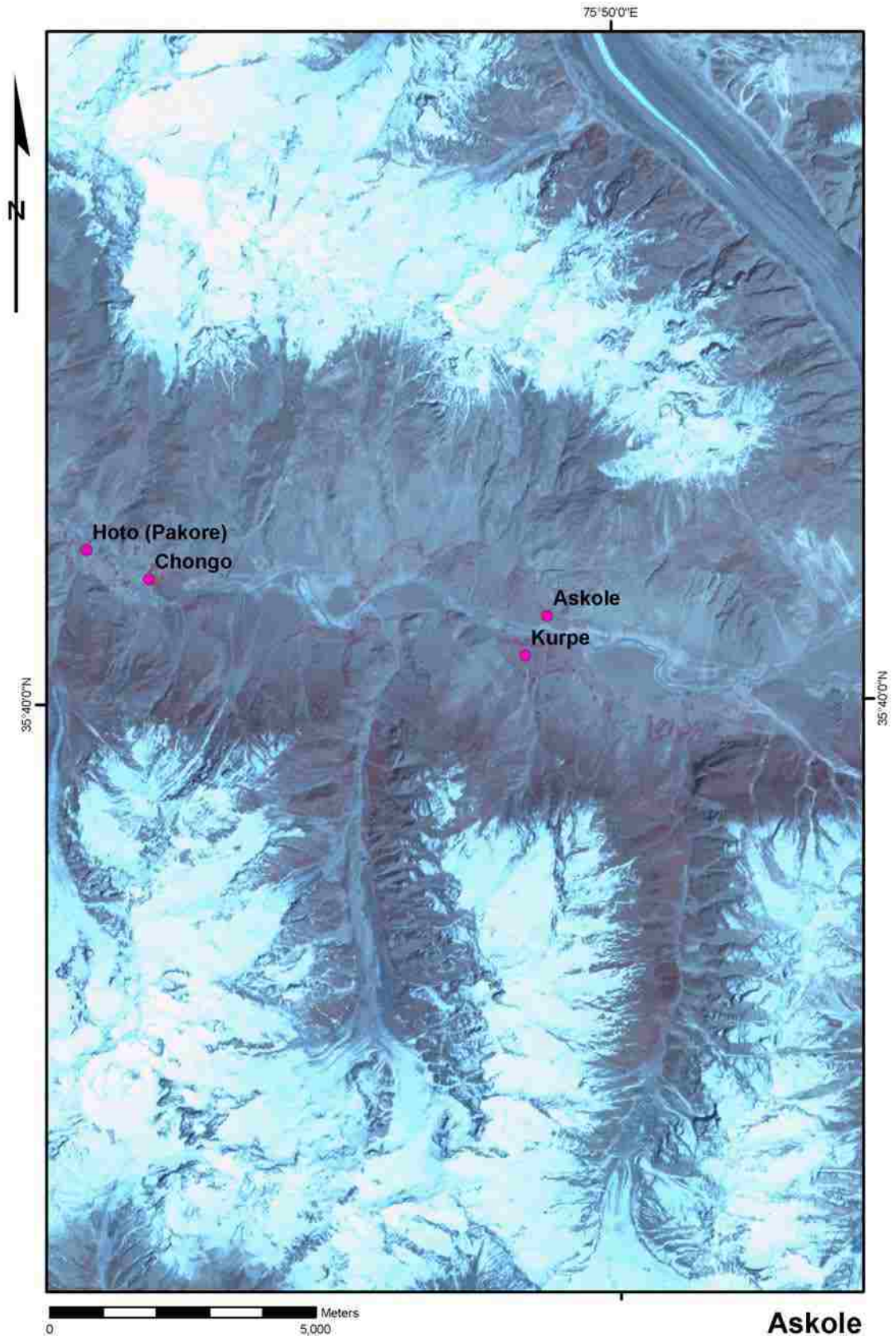
Map 21. Chakpo: geomorphological map.

Chapko
D. Belden 2008



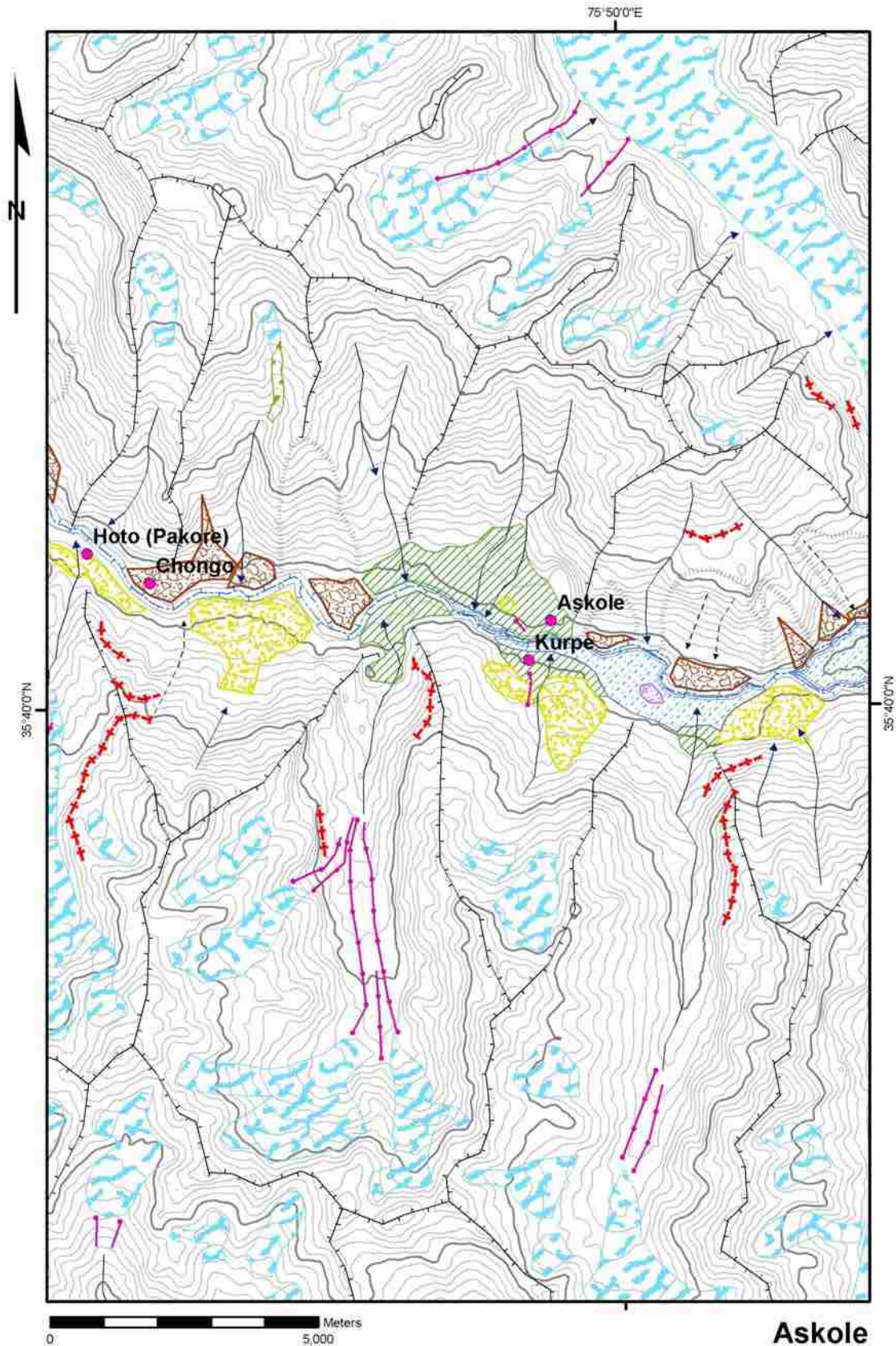
Map 22. Chakpo: slope map.

Chapko
D. Belden 2008



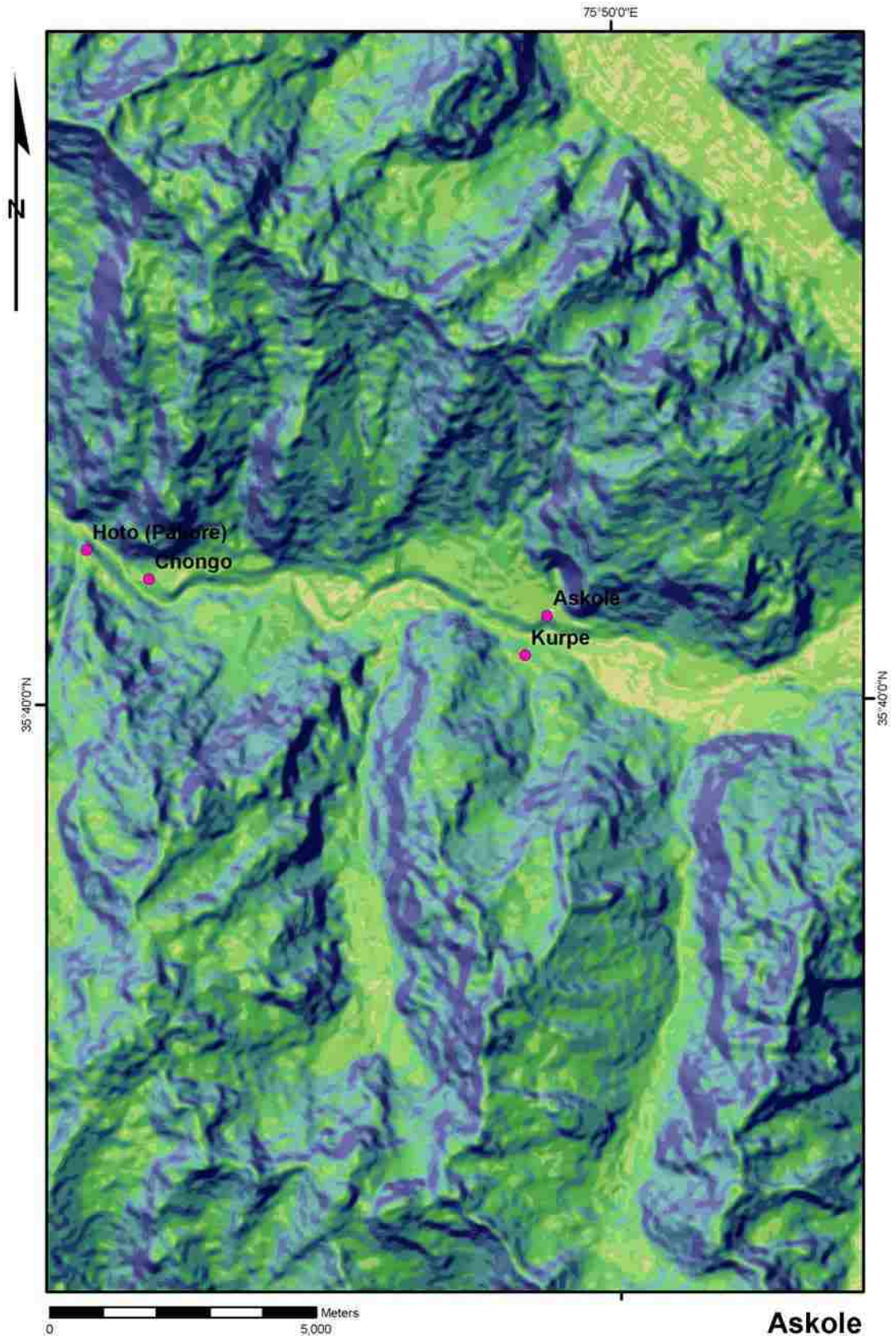
Map 23. Askole: ASTER imagery.

Askole
D. Belden 2008



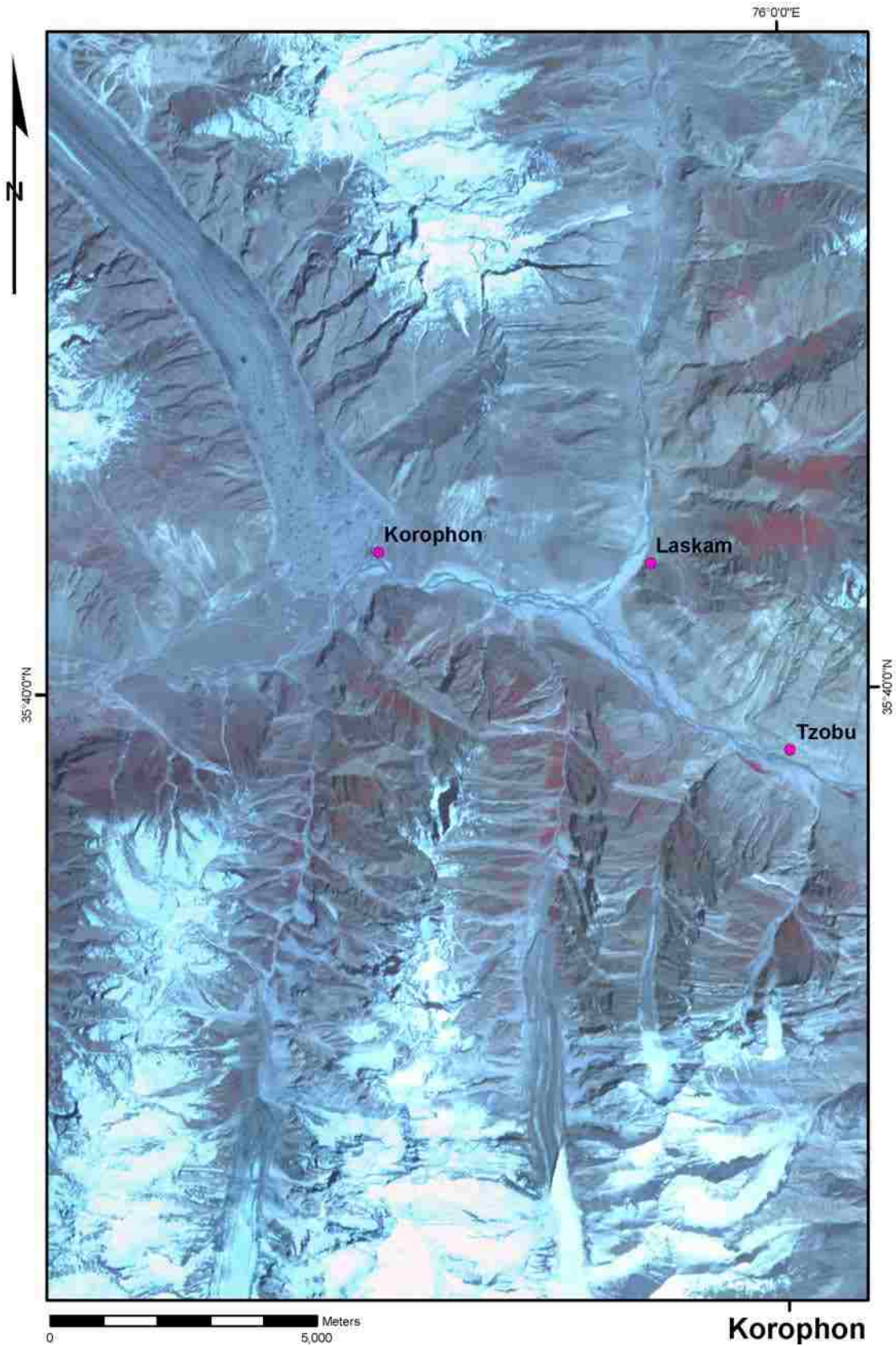
Map 24. Askole: geomorphological map.

Askole
D. Belden 2008



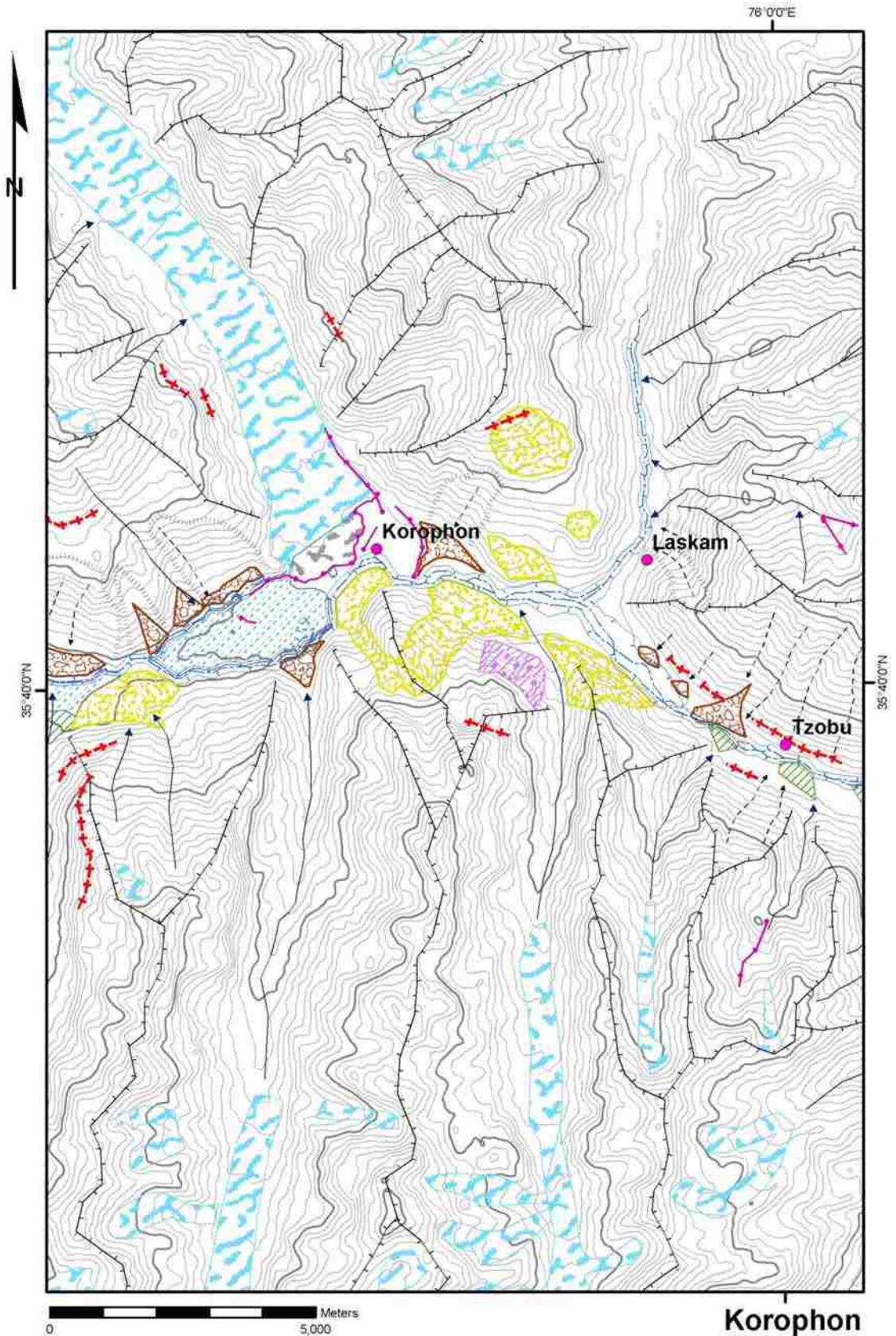
Map 25. Askole: slope map.

Askole
D. Belden 2008



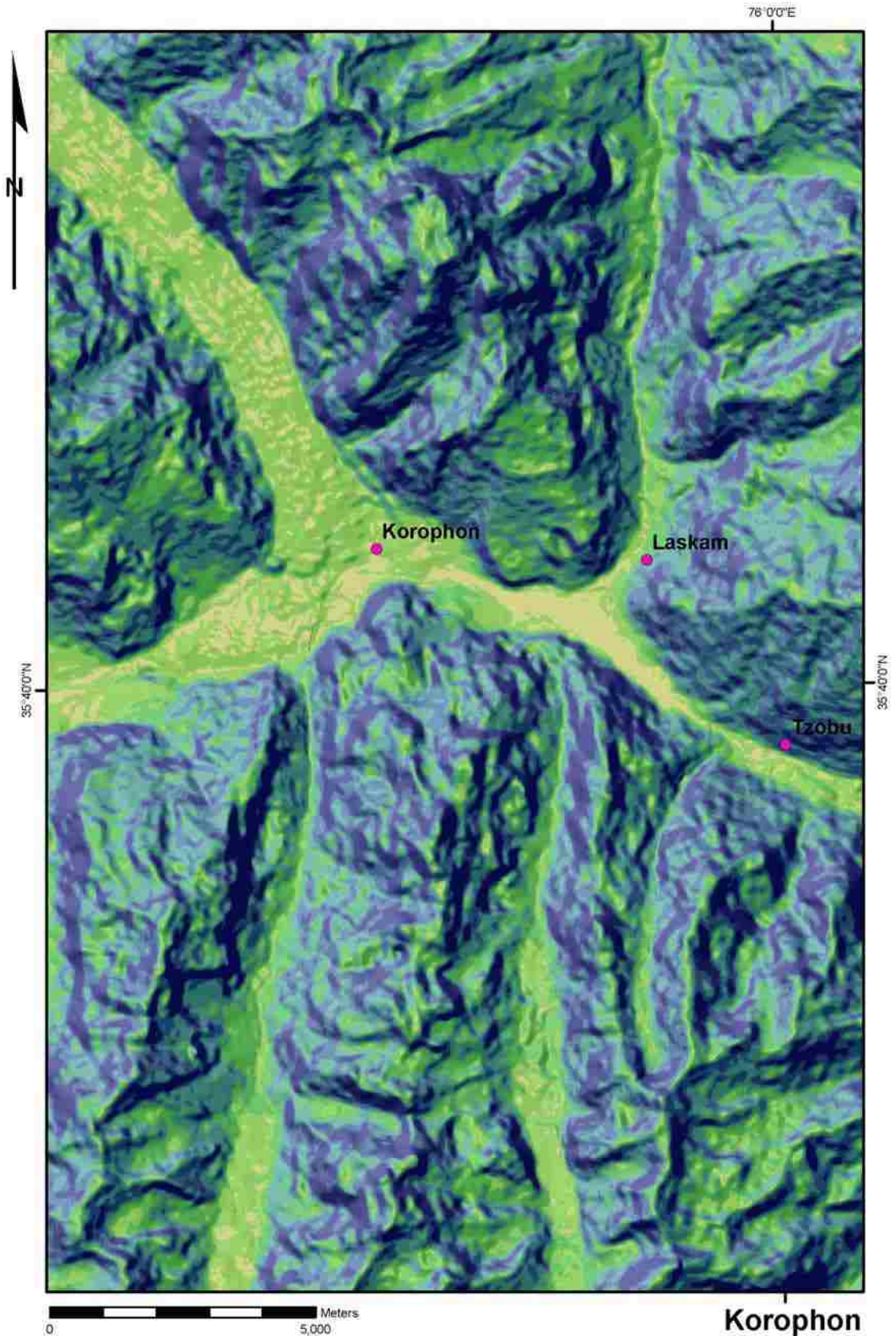
Map 26. Korophon: ASTER imagery.

Korophon
D. Belden 2008



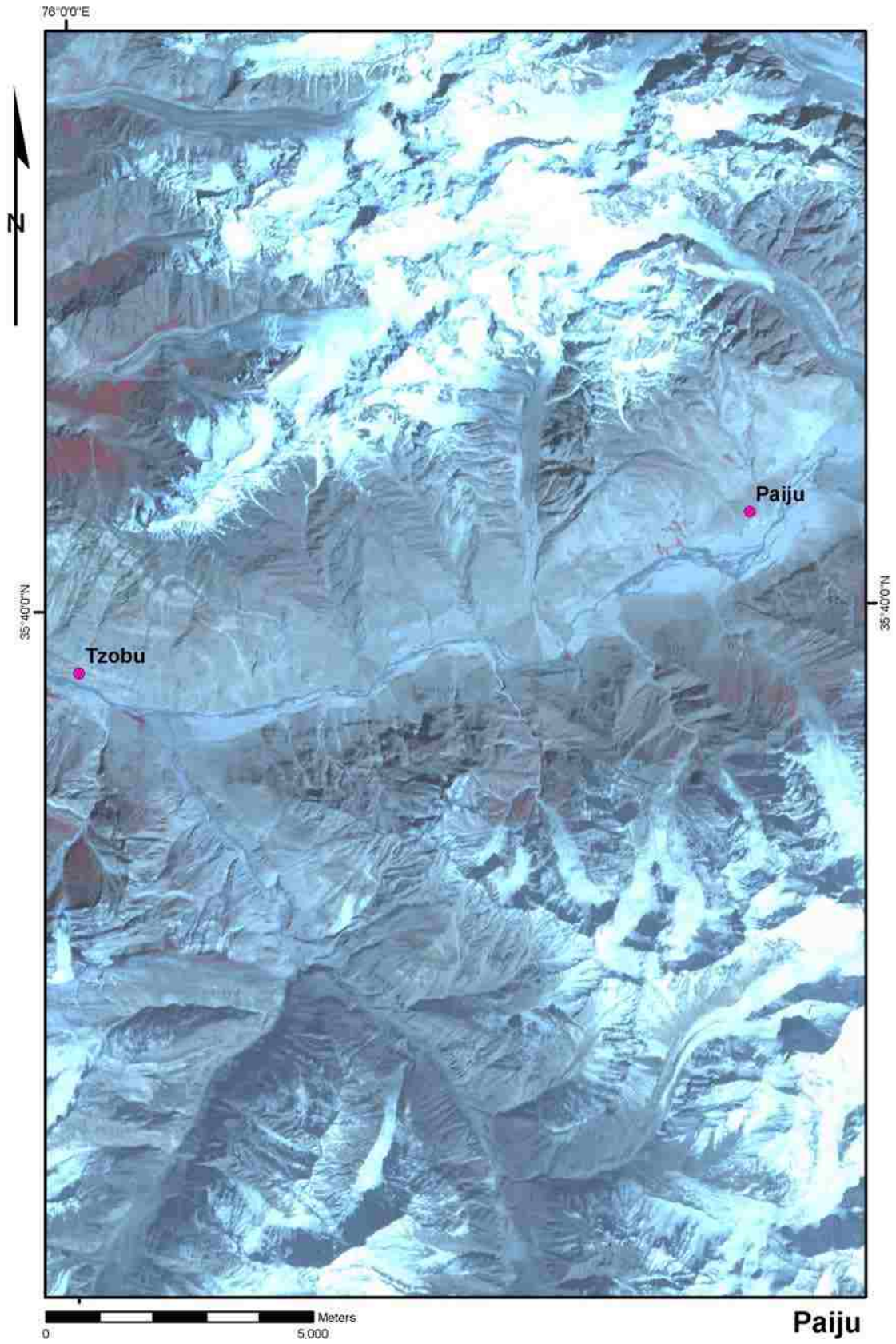
Map 27. Korophon: geomorphological map.

Korophon
D. Belden 2008



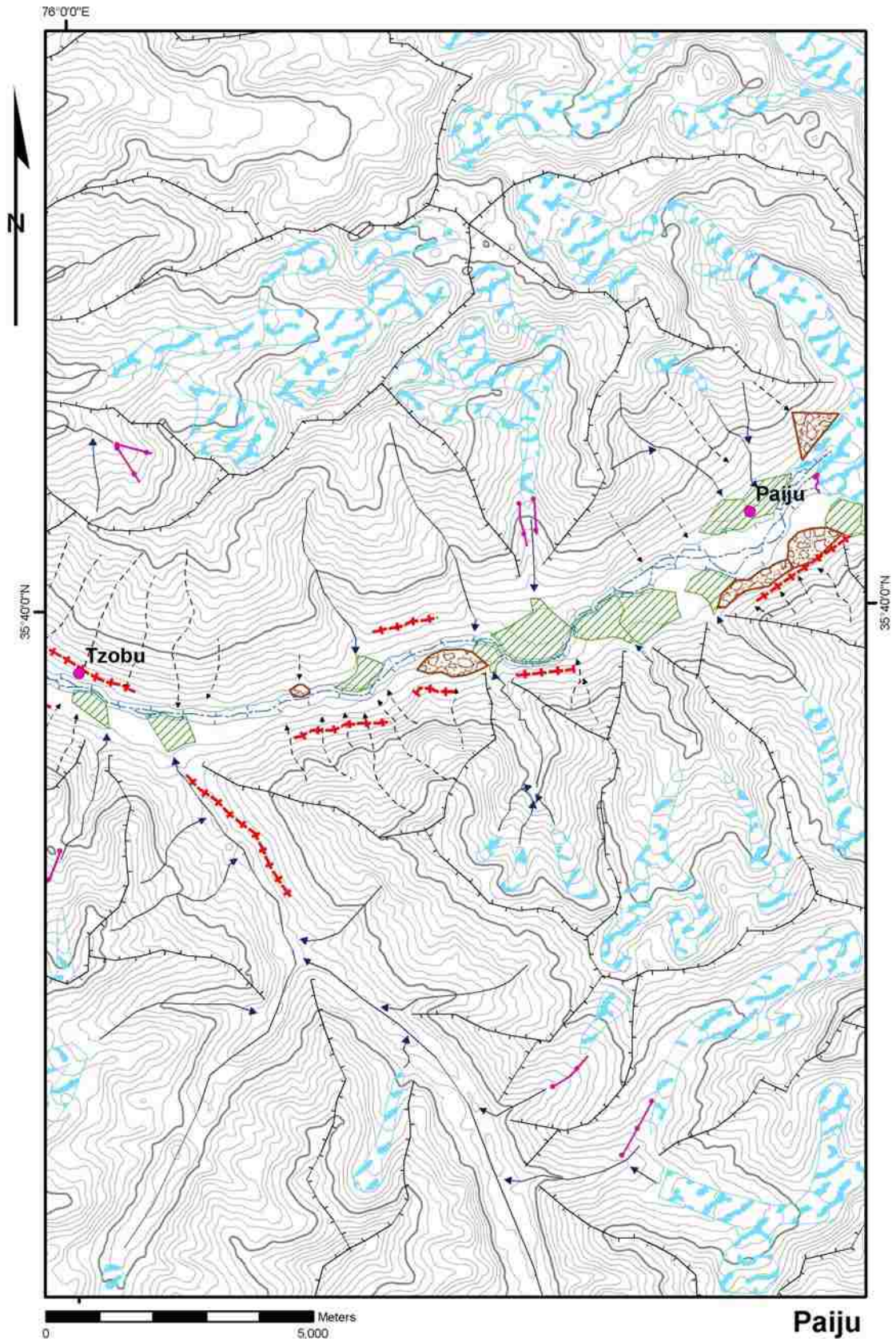
Map 28. Korophon: slope map.

Korophon
D. Belden 2008



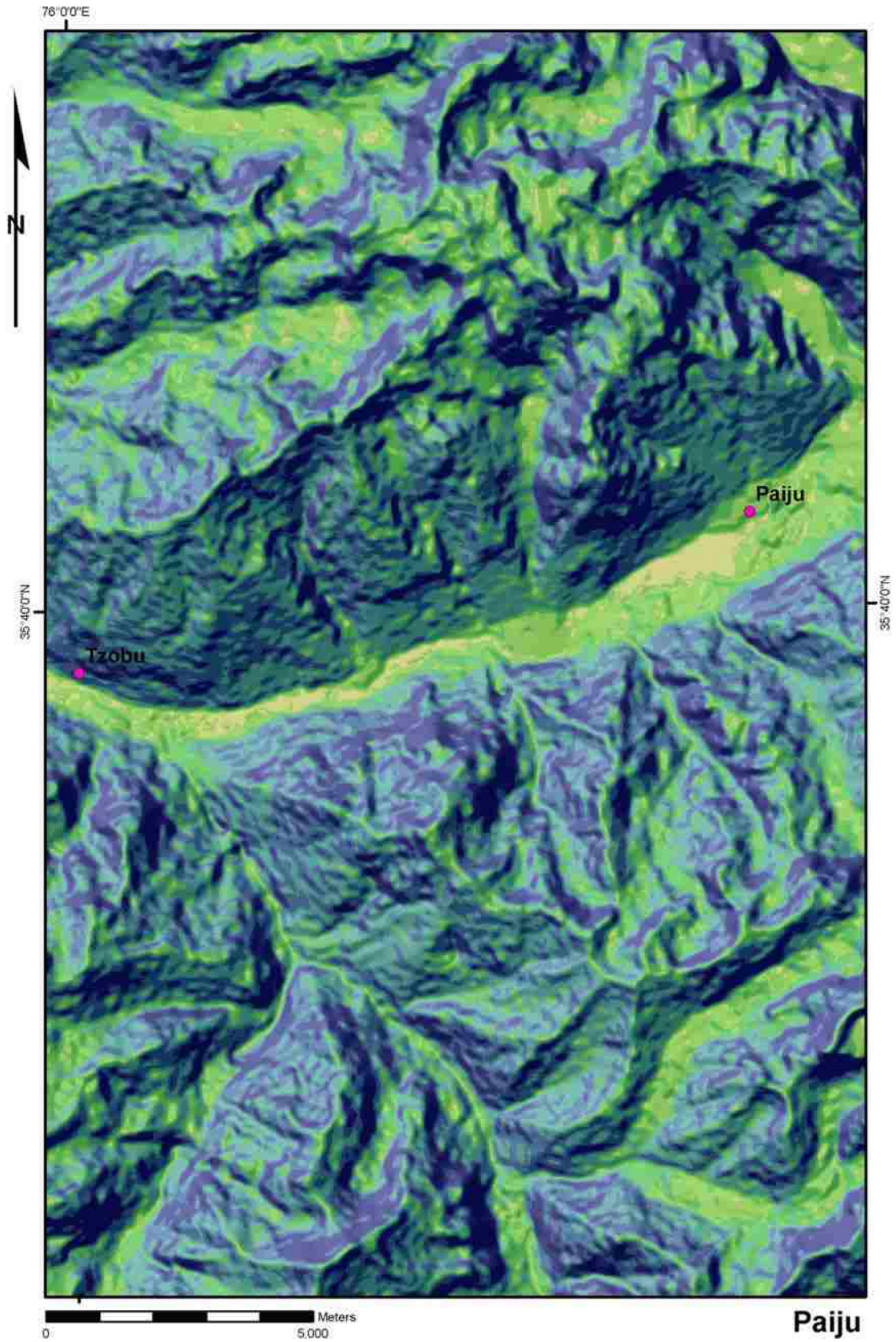
Map 29. Paiju: ASTER imagery.

D. Belden 2008



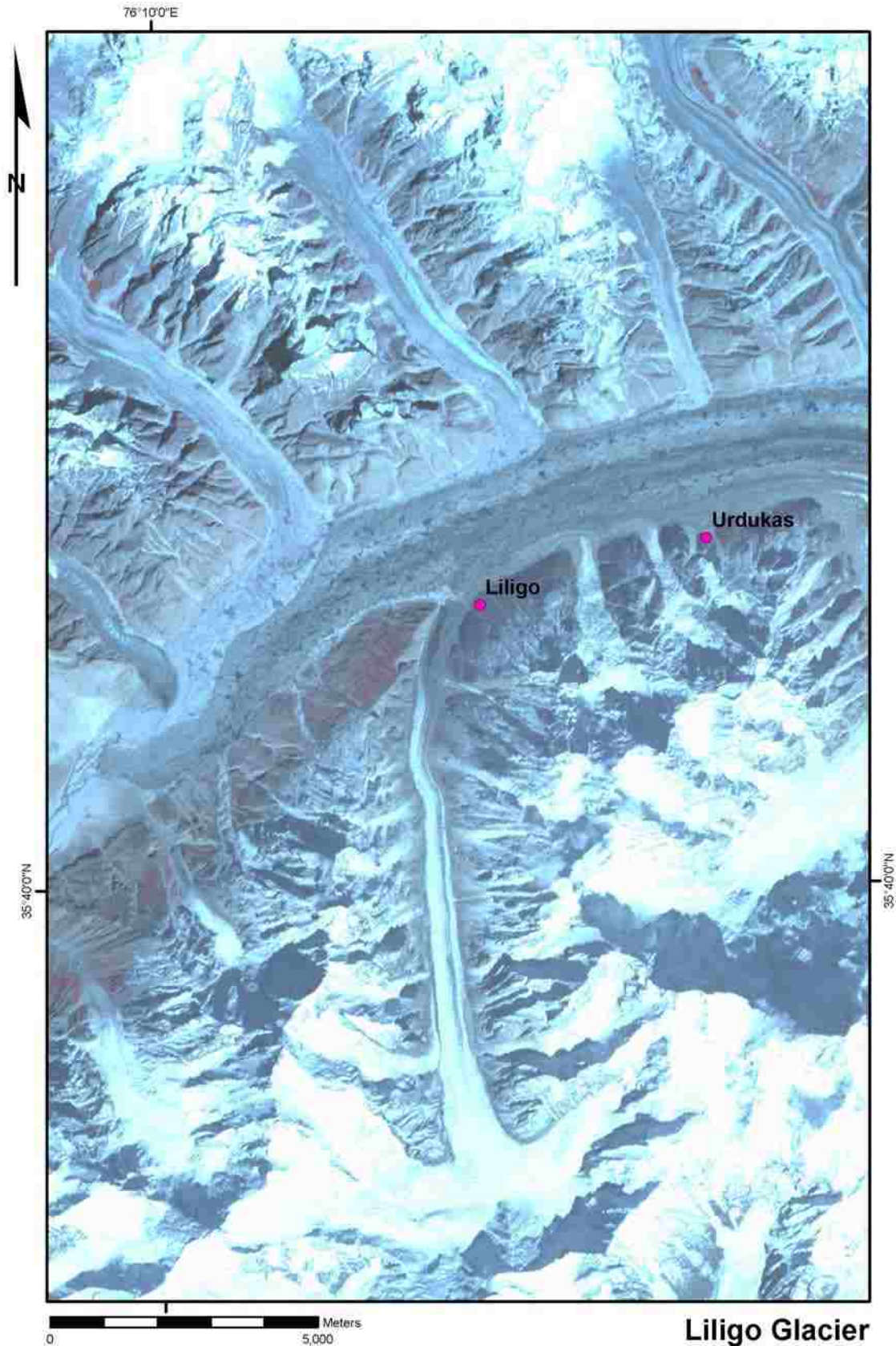
Map 30. Paiju: geomorphological map.

D. Belden 2008



Map 31. Paiju: slope map.

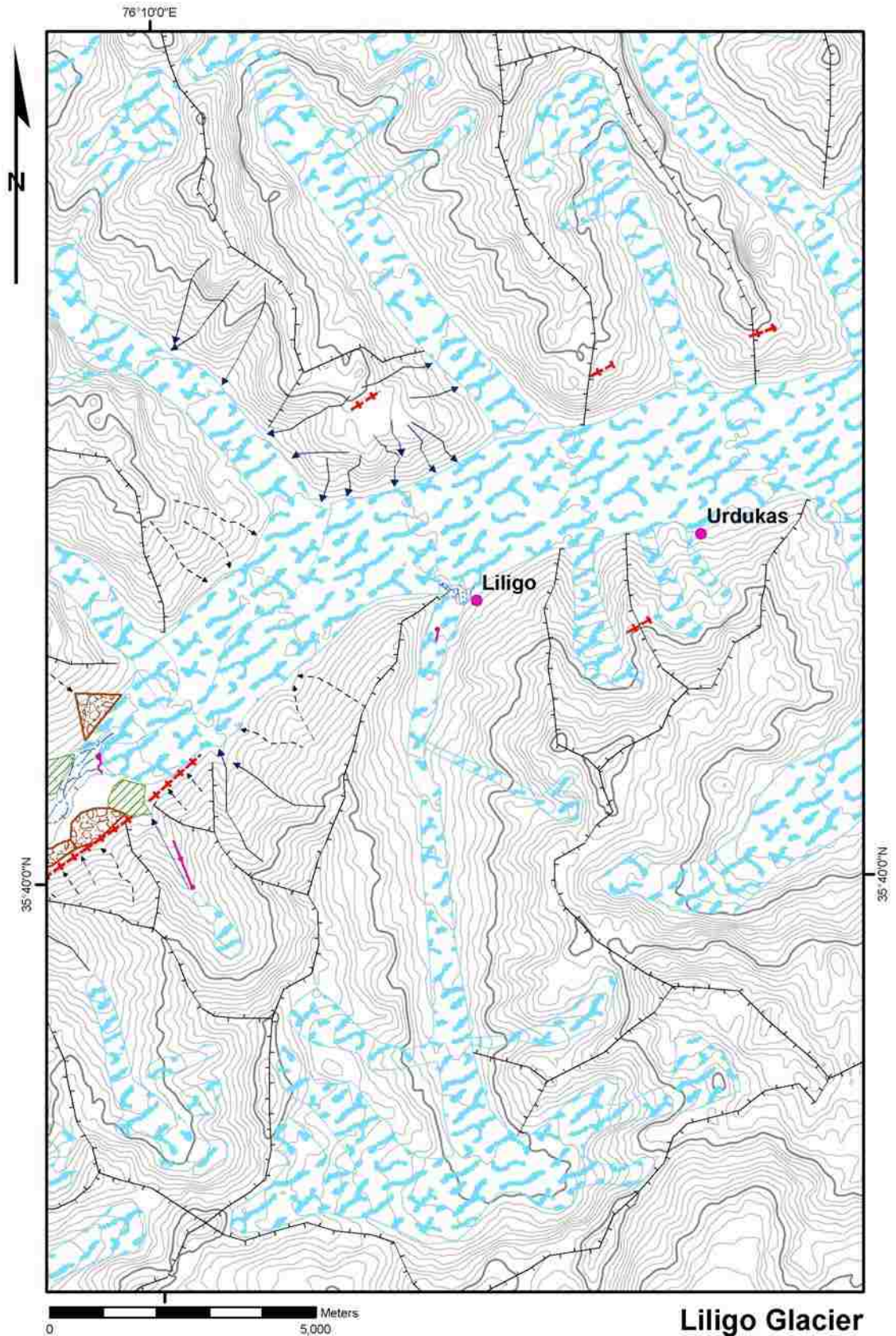
Paiju
D. Belden 2008



Map 32. Liligo Glacier: ASTER imagery.

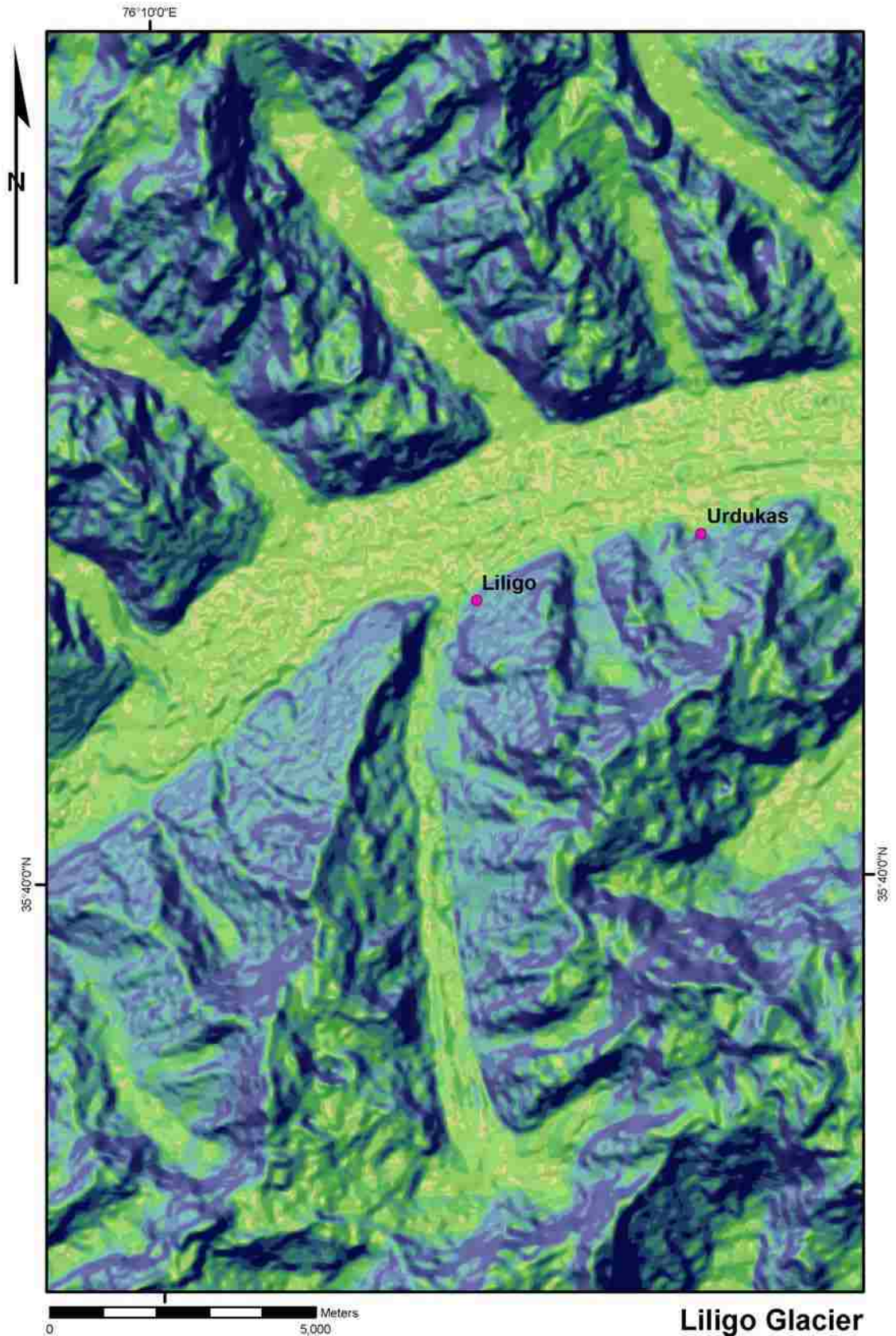
Liligo Glacier

D. Belden 2008



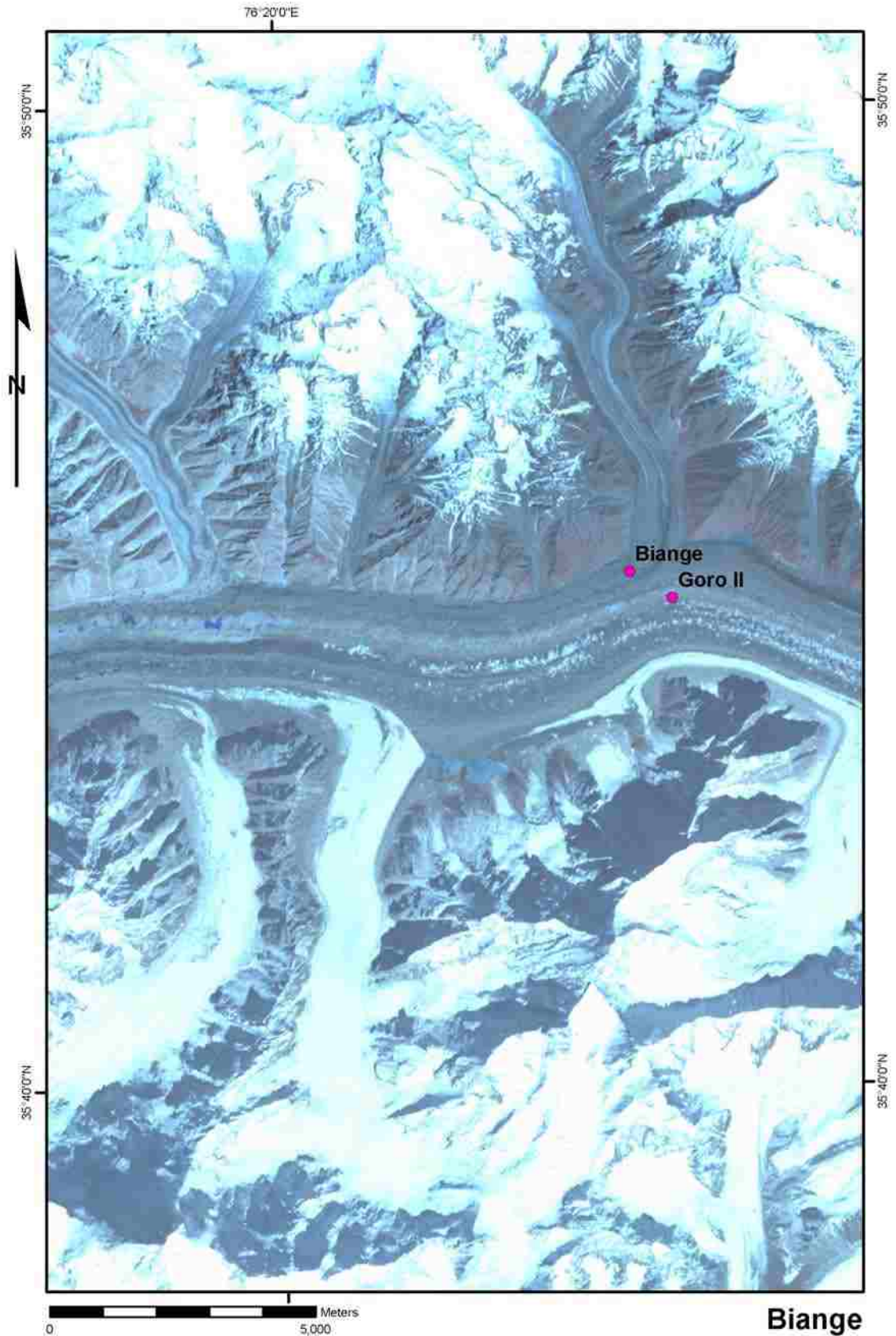
Map 33. Liligo Glacier: geomorphological map.

Liligo Glacier
D. Belden 2008



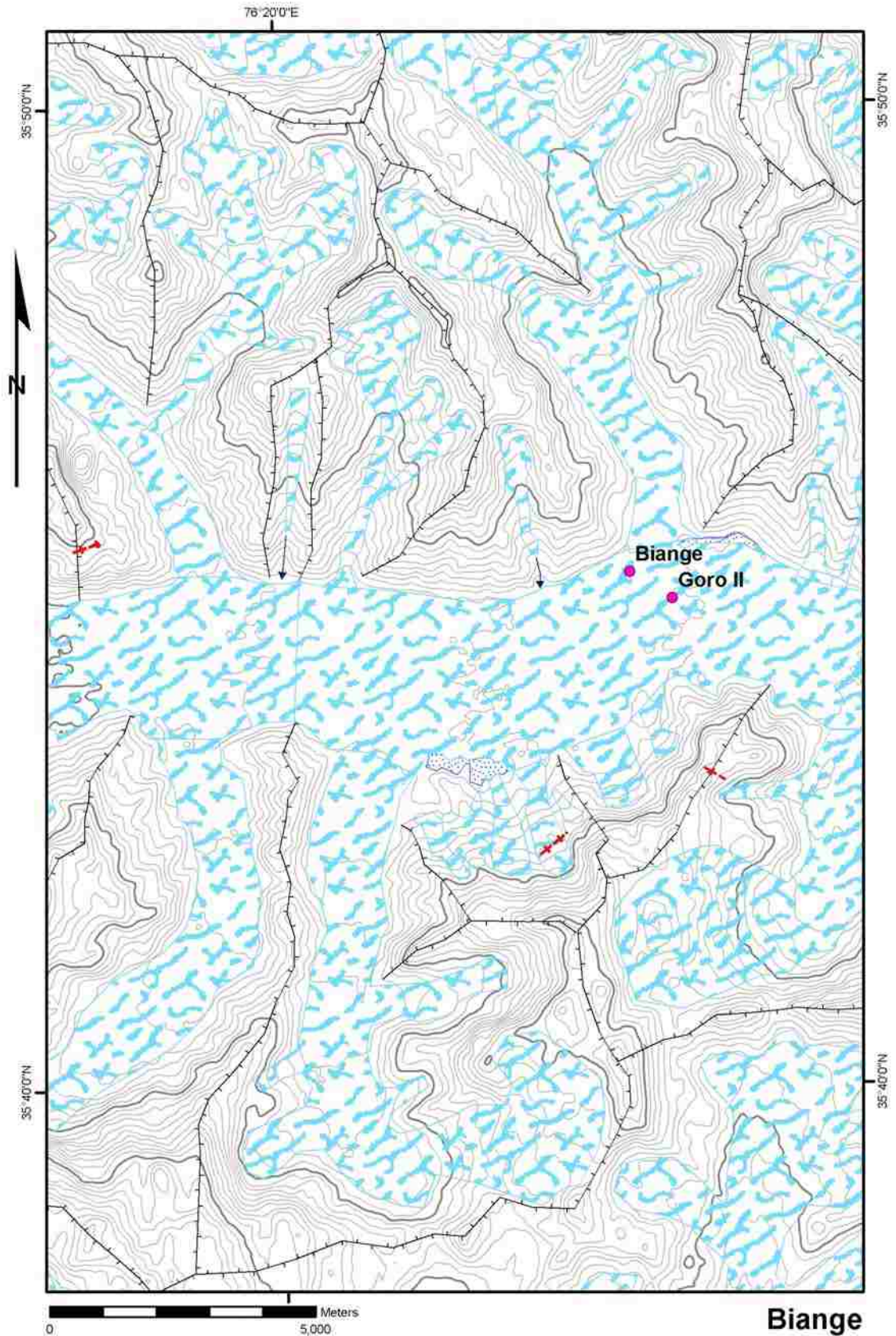
Map 34. Liligo Glacier: slope map.

Liligo Glacier
D. Belden 2008



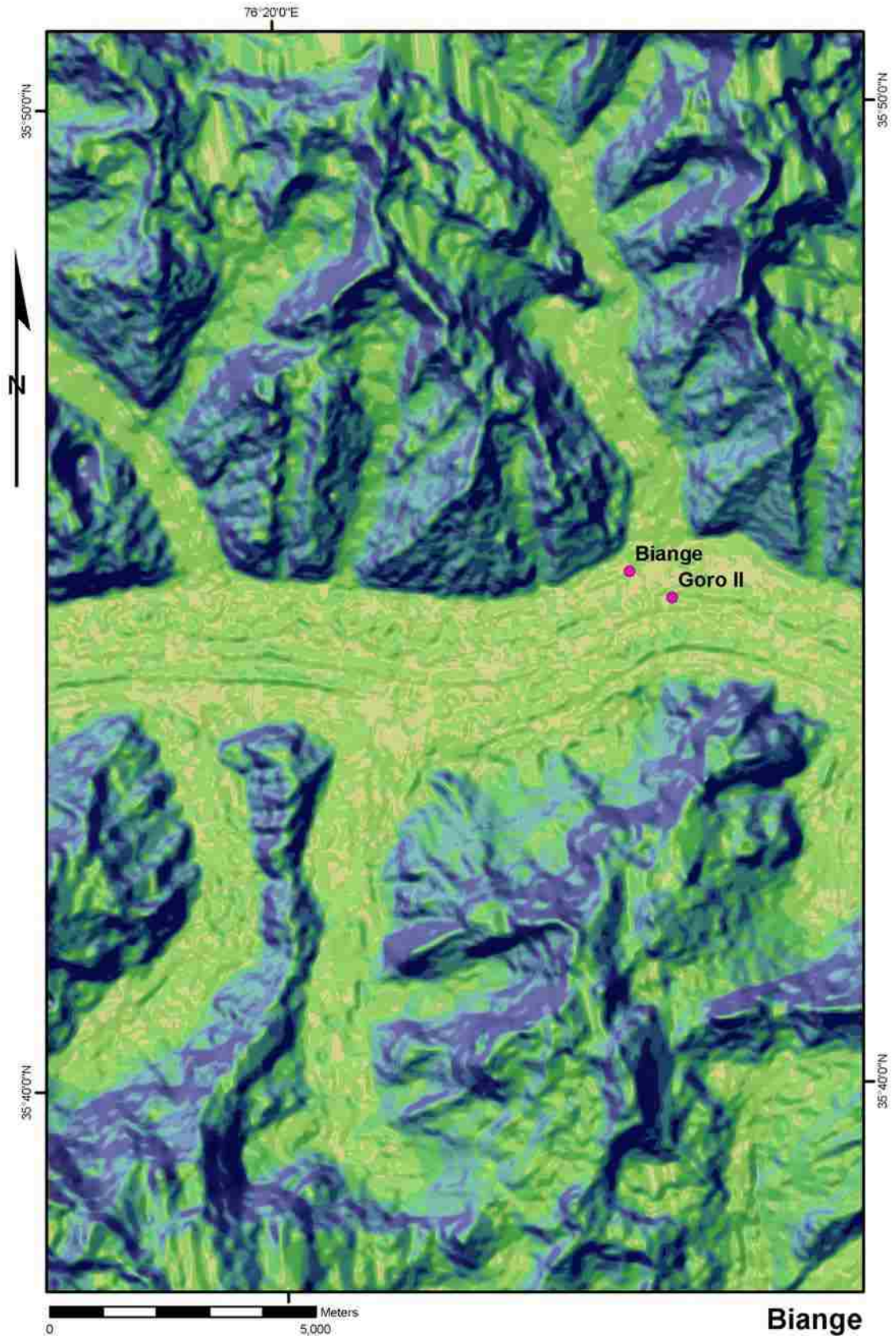
Map 35. Biange: ASTER imagery.

Biange
D. Belden 2008



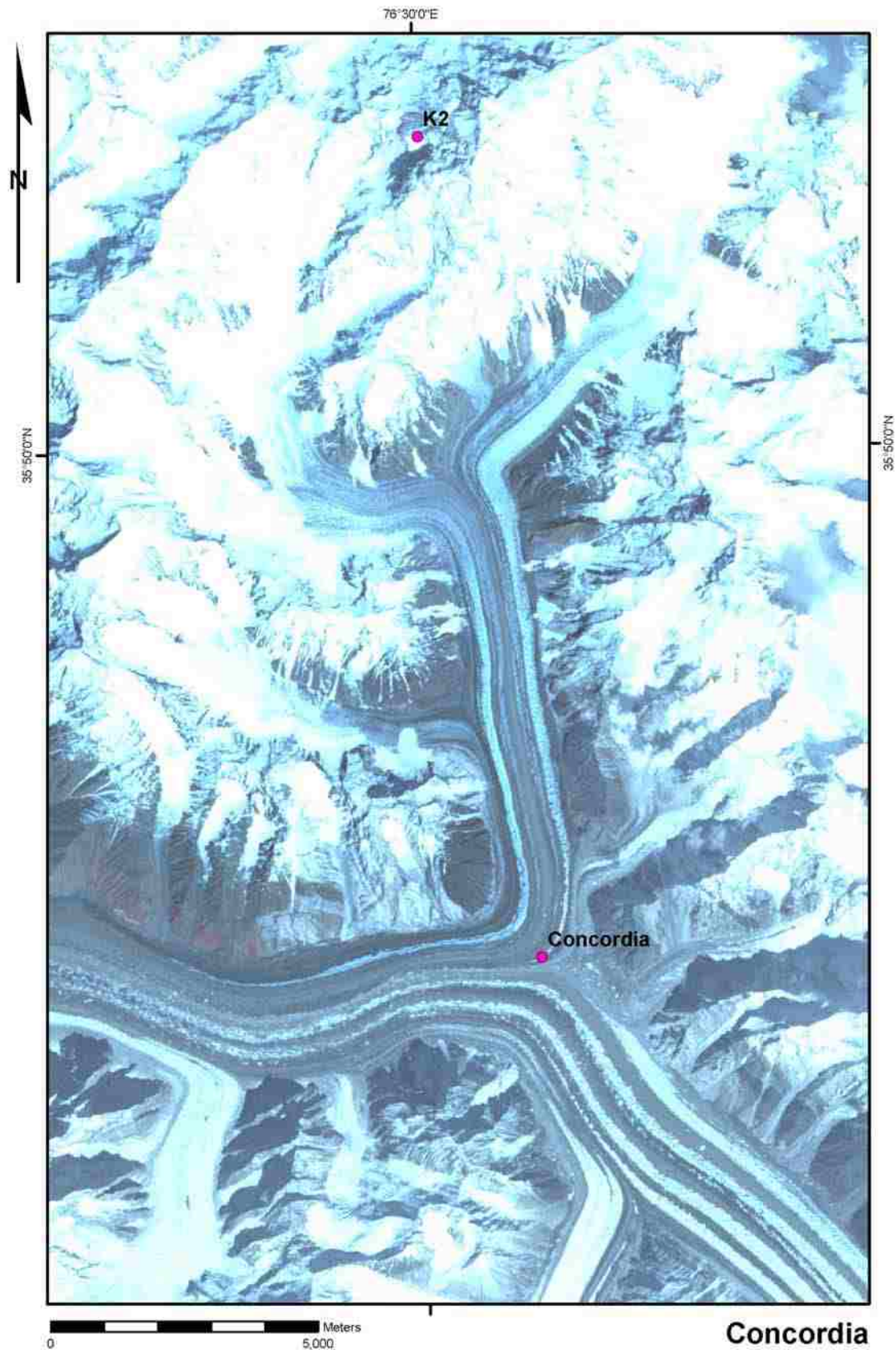
Map 36. Biange: geomorphological map.

Biange
D. Belden 2008

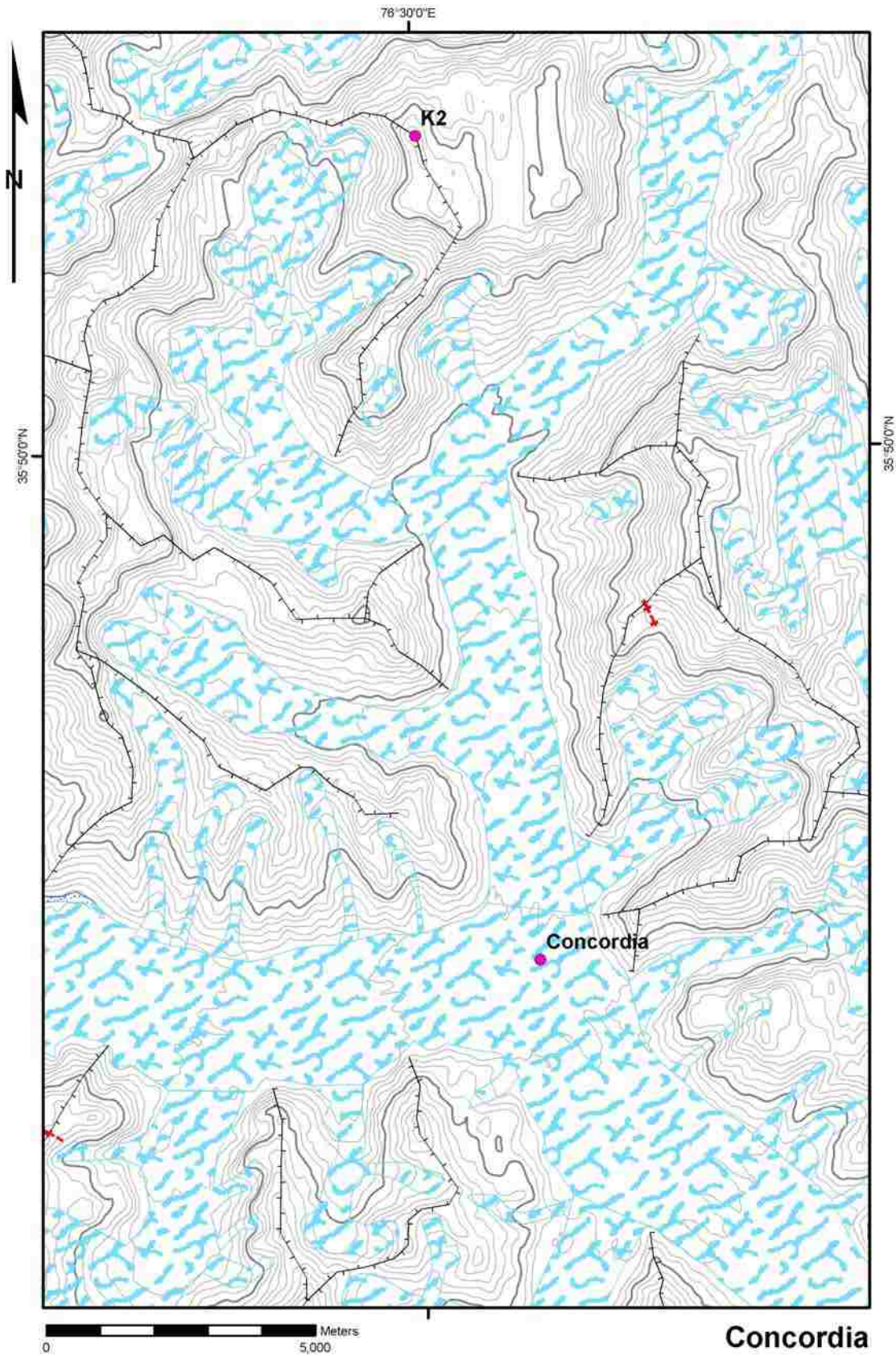


Map 37. Biange: slope map.

Biange
D. Belden 2008



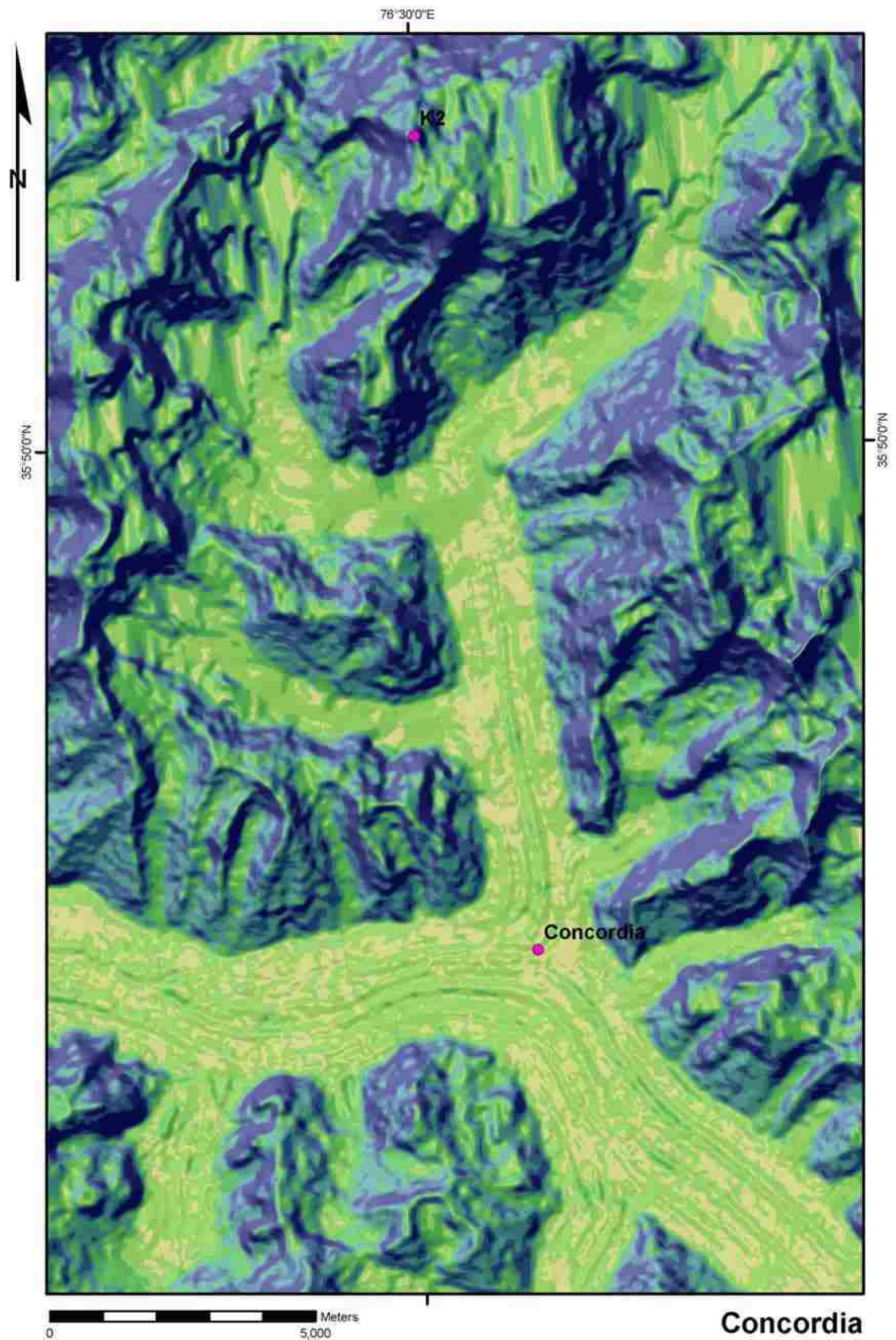
Map 38. Concordia: ASTER imagery.



Map 39. Concordia: geomorphological map.

Concordia

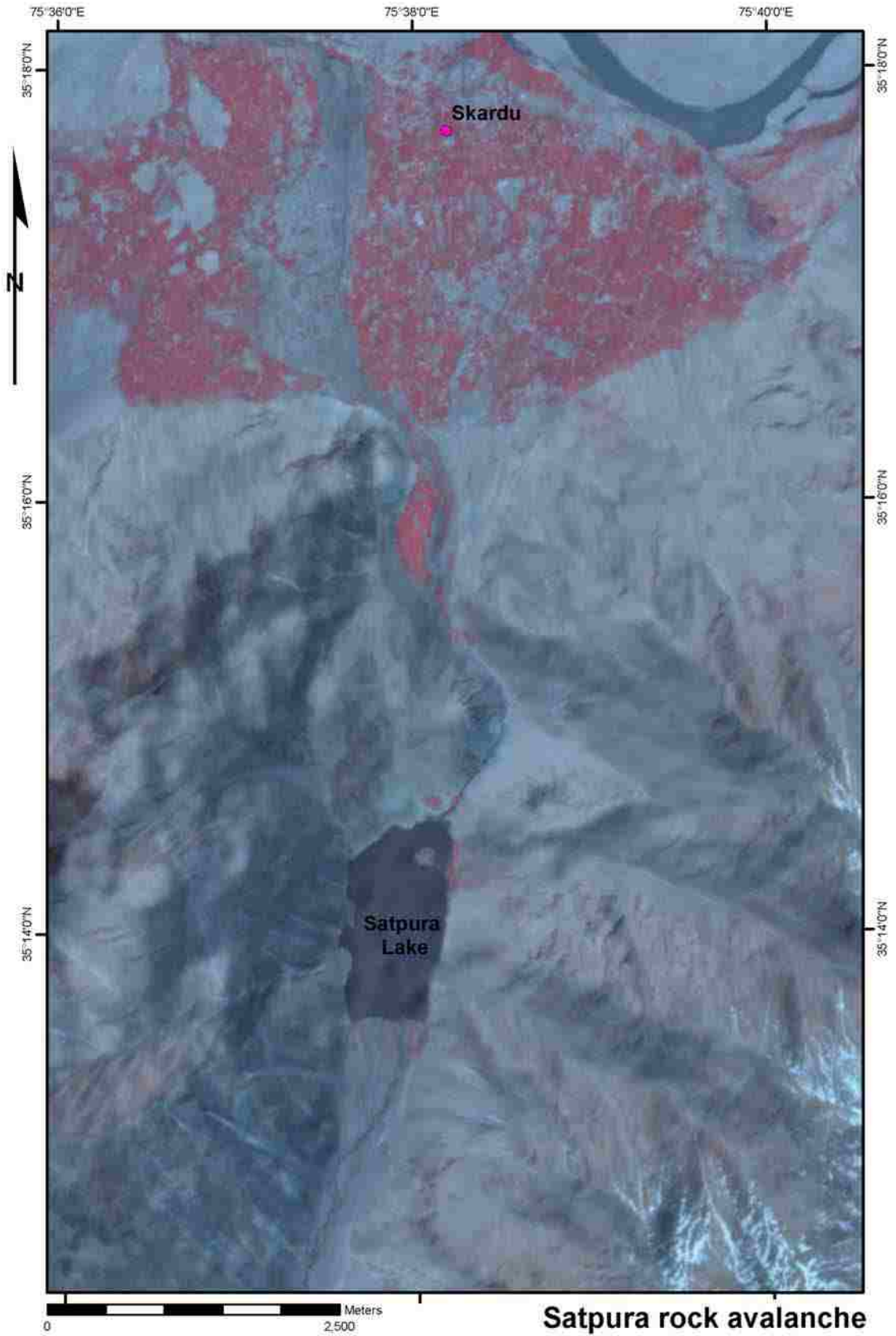
D. Belden 2008



Map 40. Concordia: slope map.

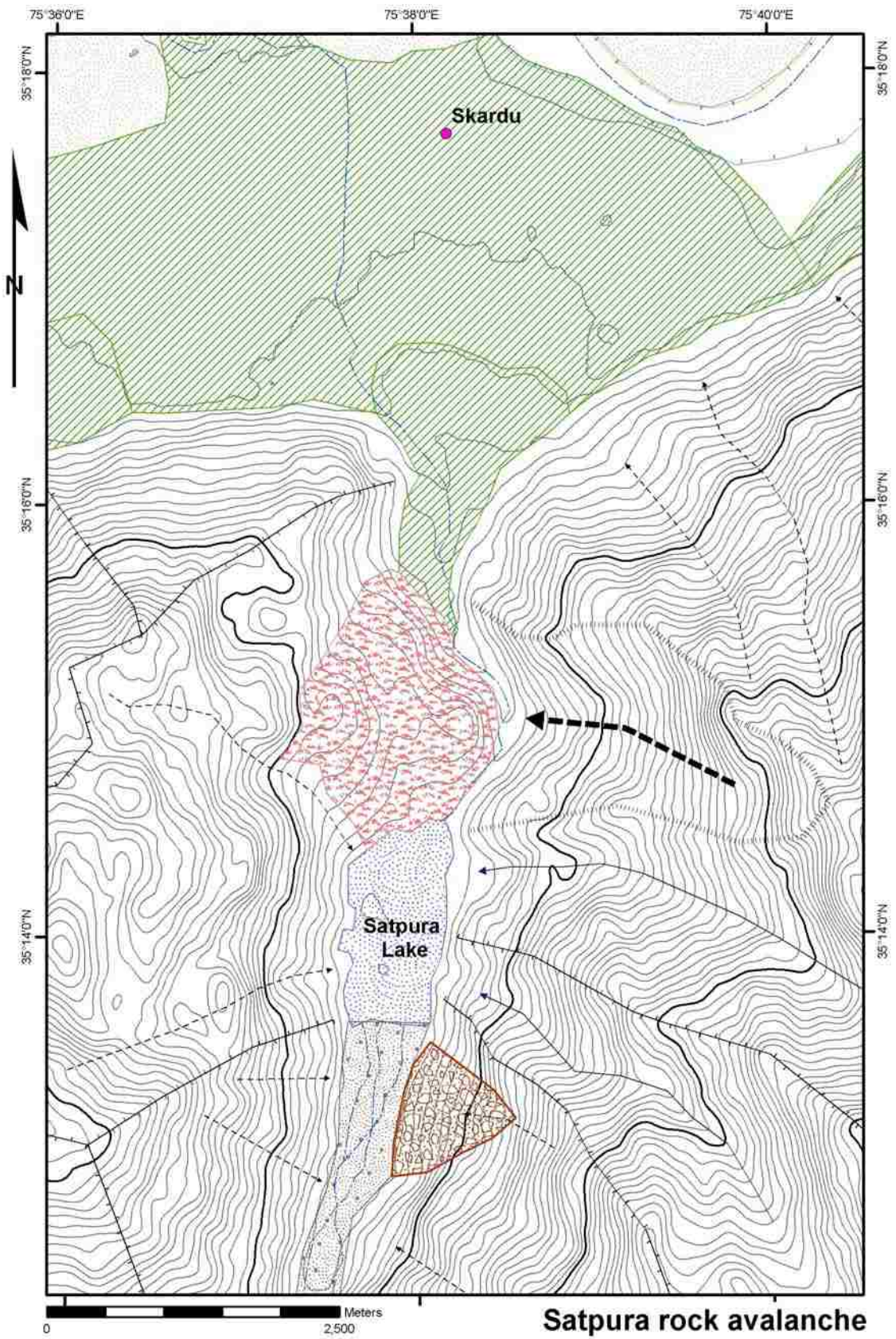
Concordia

D. Belden 2008



Map 41. Satpura rock avalanche: ASTER imagery.

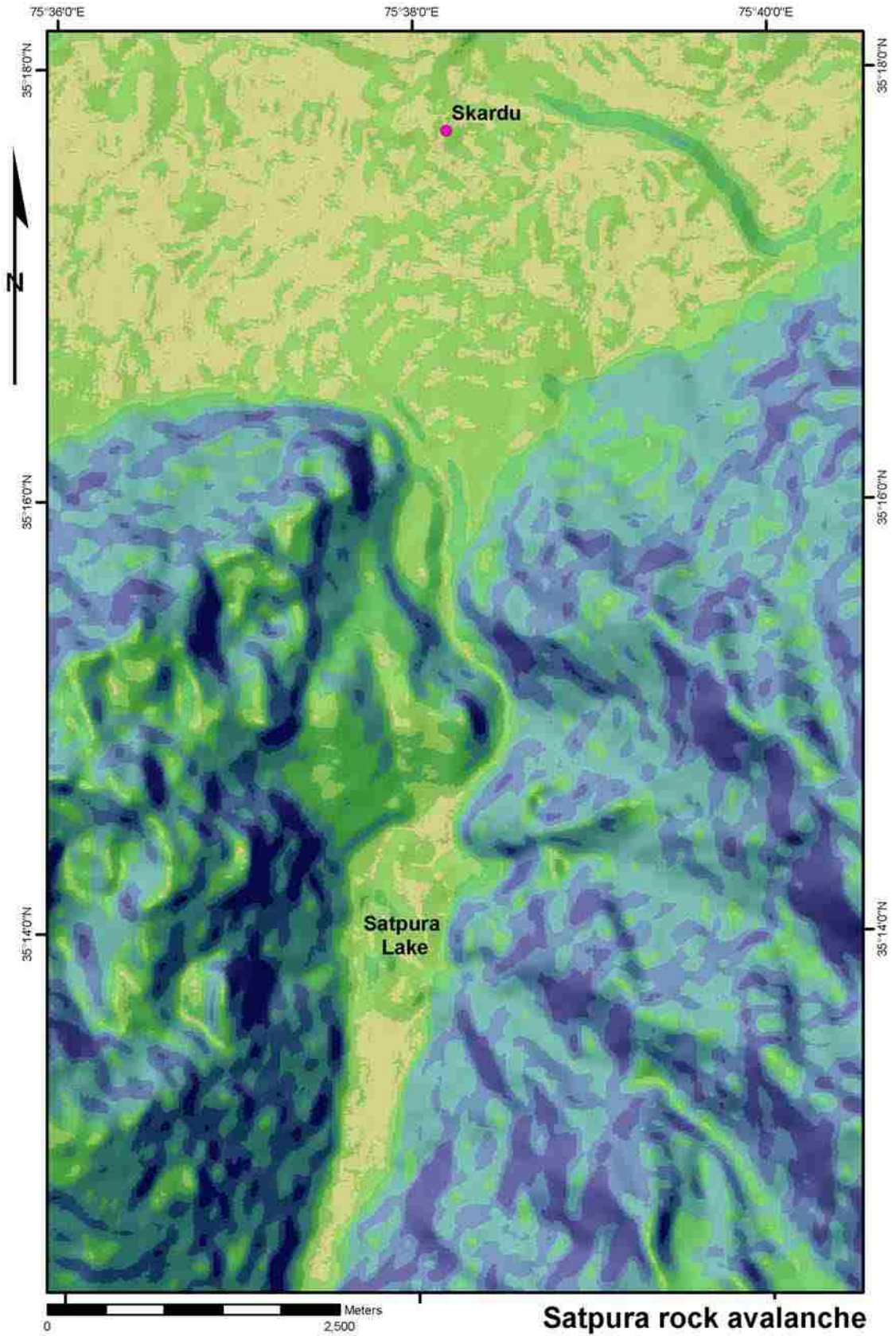
D. Belden 2008



Satpura rock avalanche

Map 42. Satpura rock avalanche: geomorphological map.

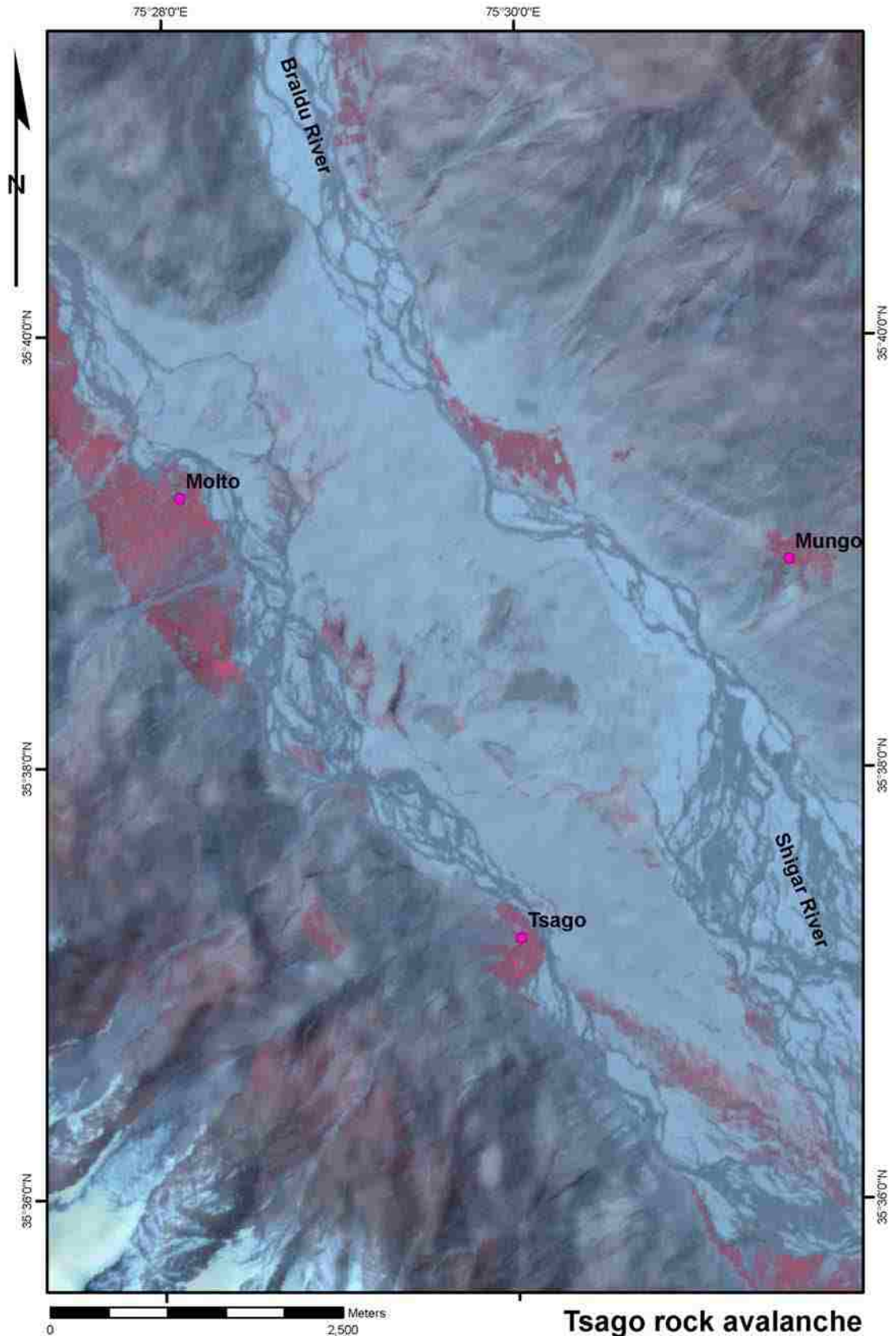
D. Belden 2008



Map 43. Satpura rock avalanche: slope map.

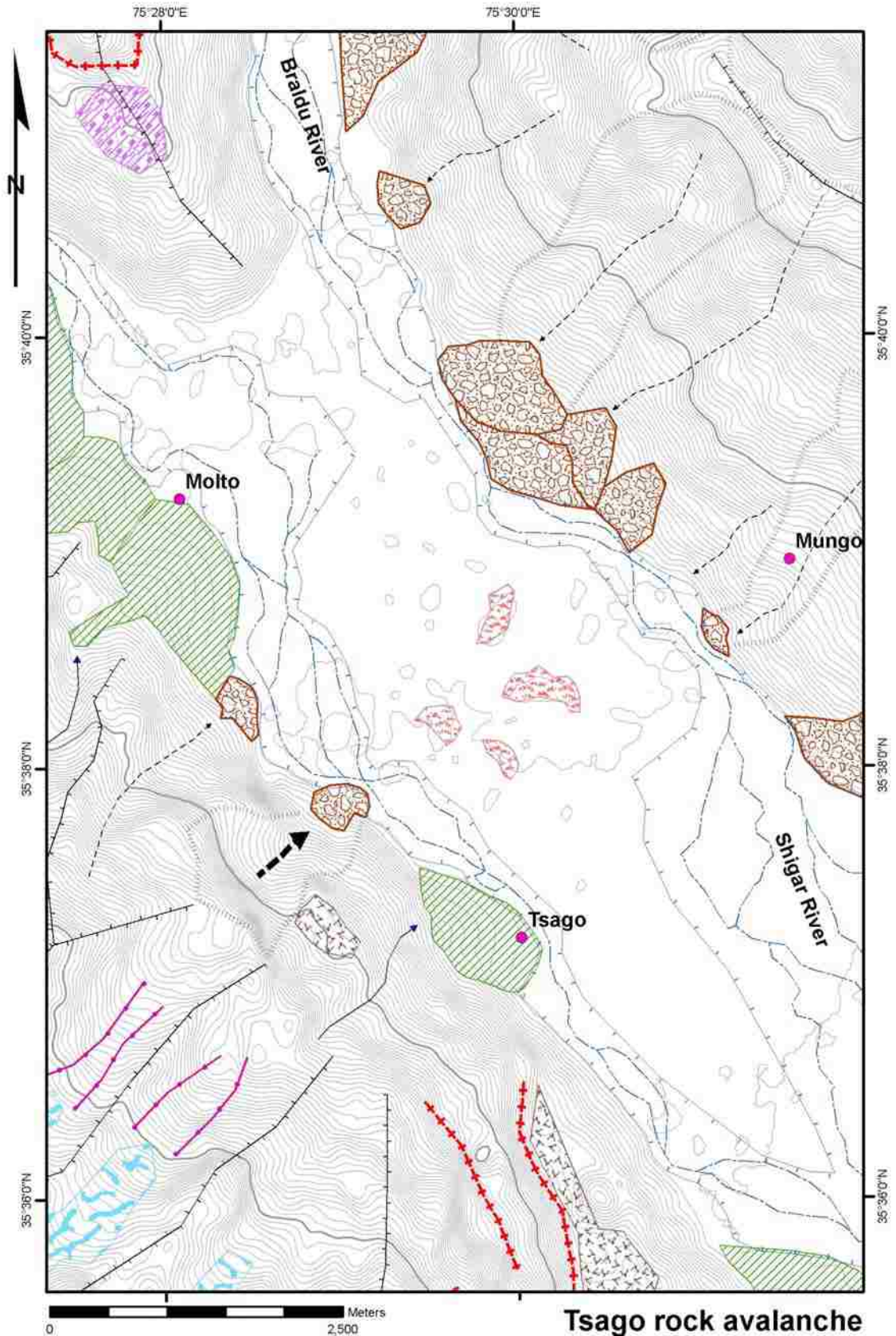
Satpura rock avalanche

D. Belden 2008



Map 44. Tsago rock avalanche: ASTER imagery.

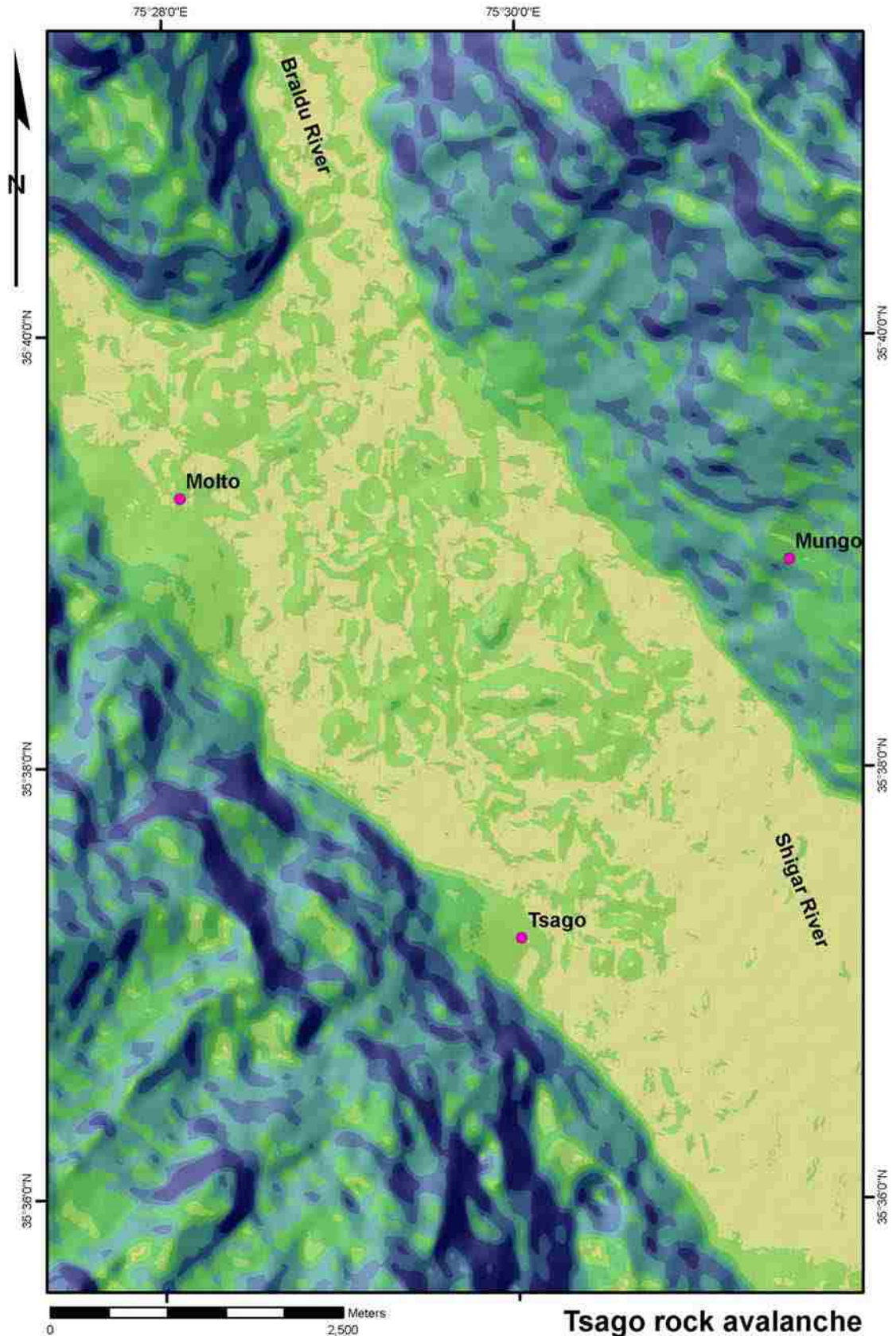
Tsago rock avalanche
D. Belden 2008



Tsago rock avalanche

Map 45. Tsago rock avalanche: geomorphological map.

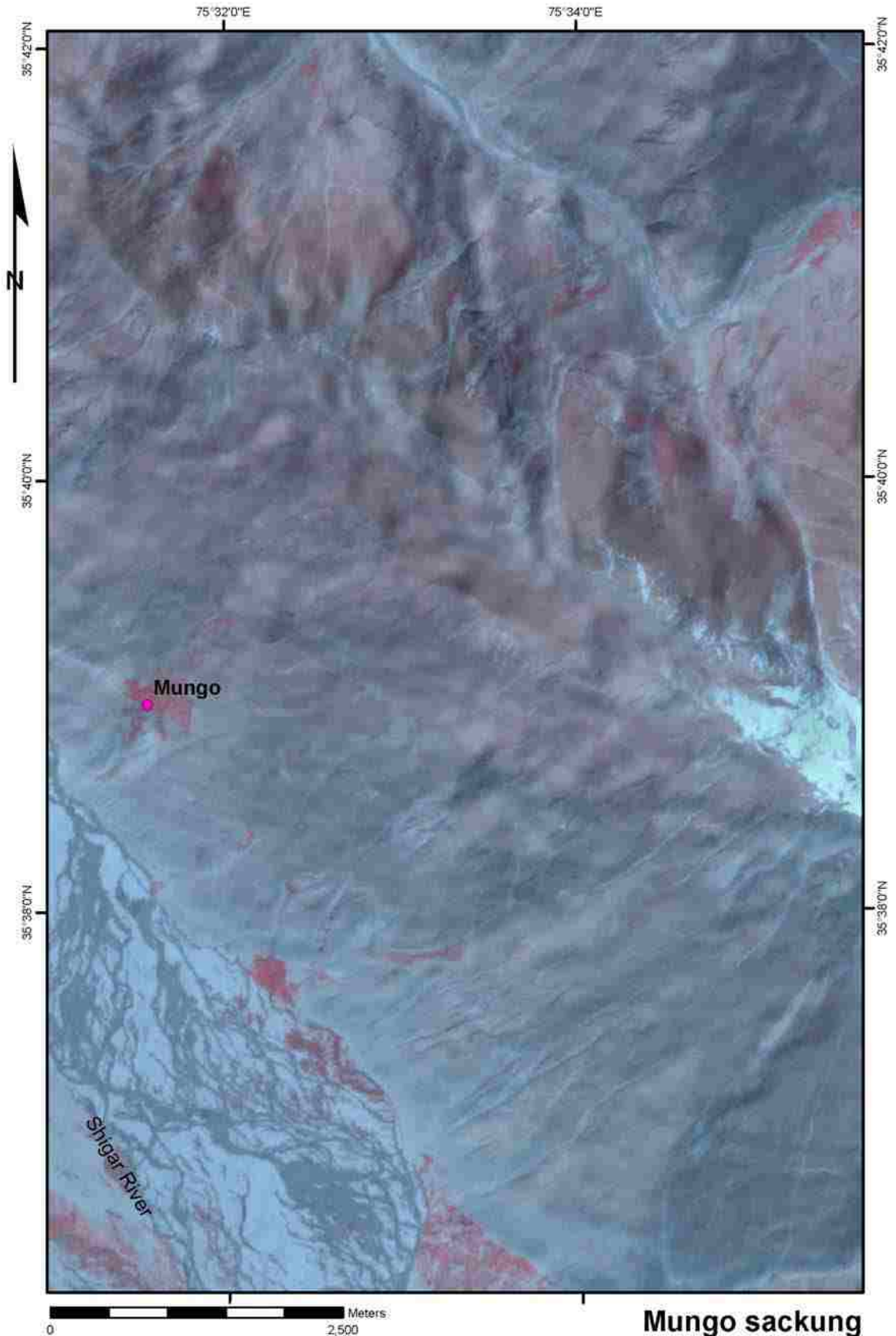
D. Belden 2008



Tsago rock avalanche

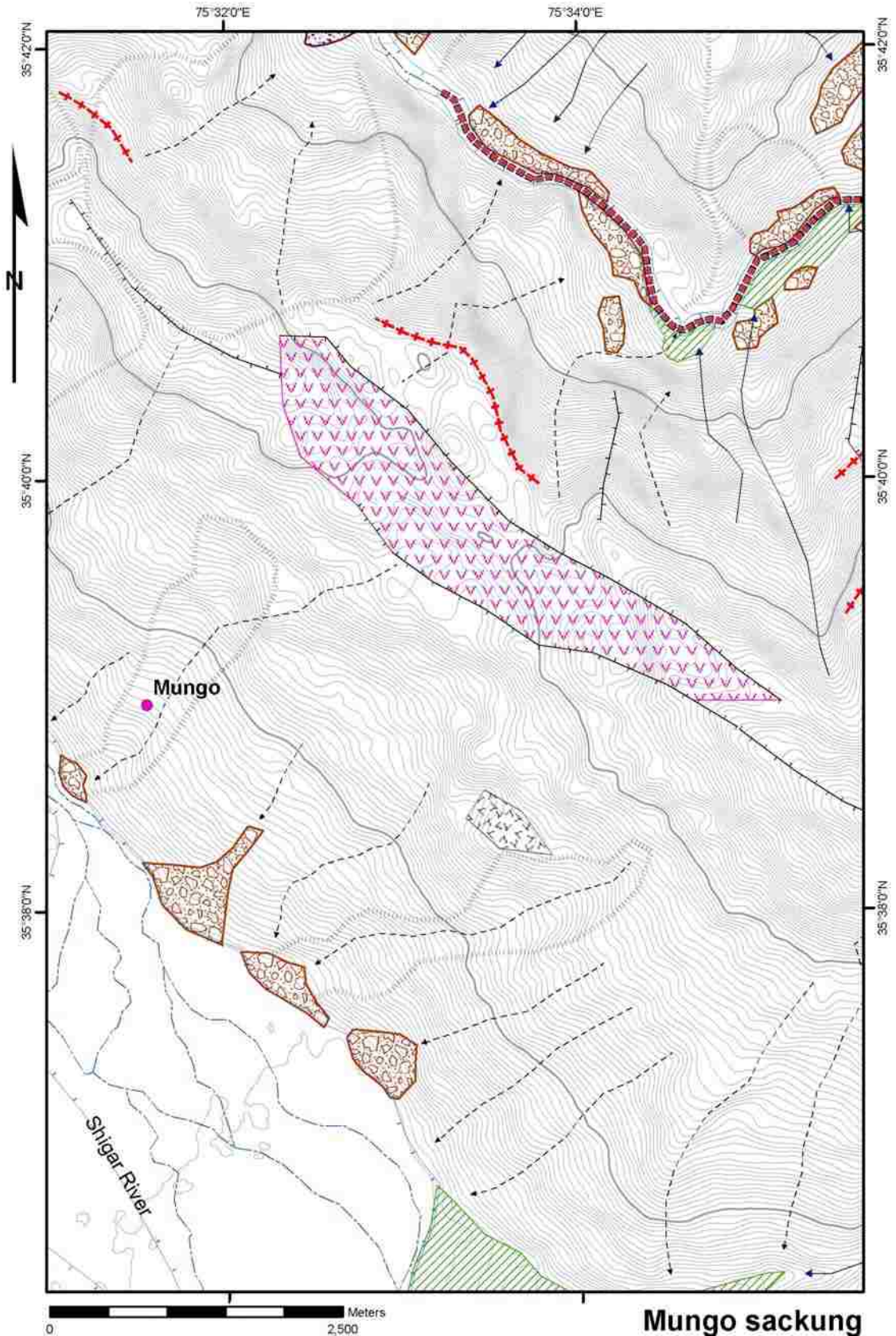
Map 46. Tsago rock avalanche: slope map.

D. Belden 2008



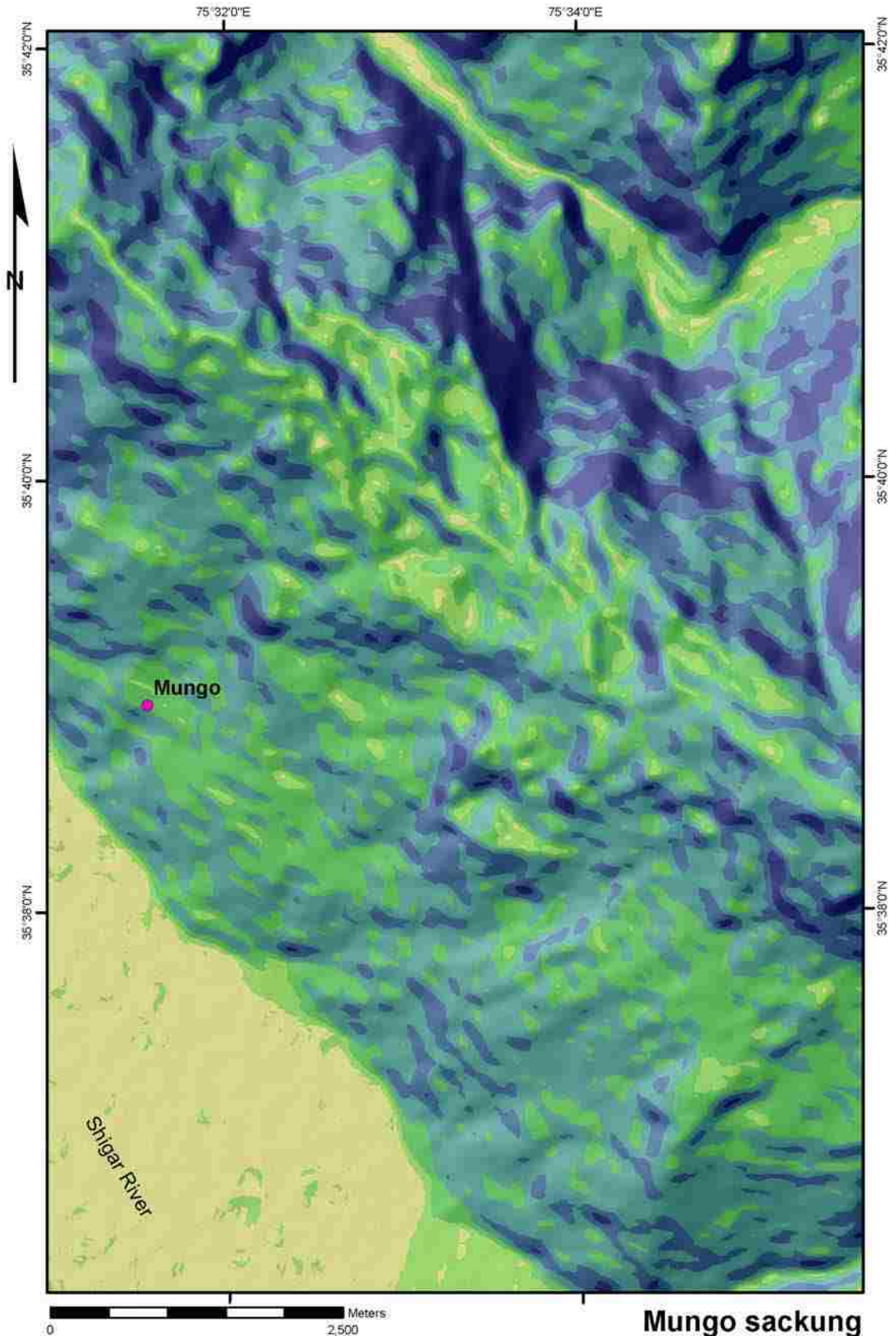
Map 47. Mungo sacking: ASTER imagery.

Mungo sacking
D. Belden 2008



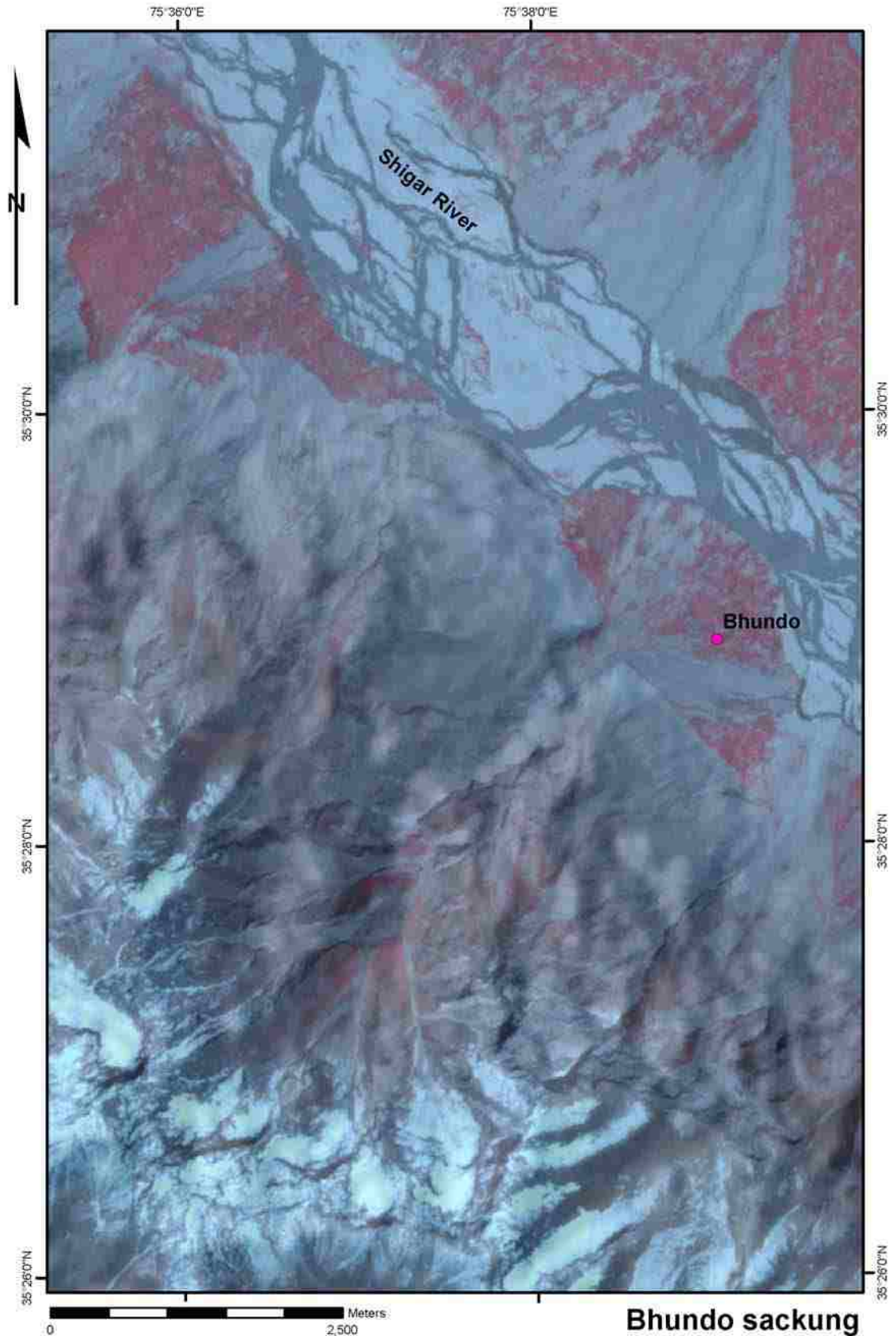
Map 48. Mungo sacking: geomorphological map.

D. Belden 2008



Map 49. Mungo sacking: slope map.

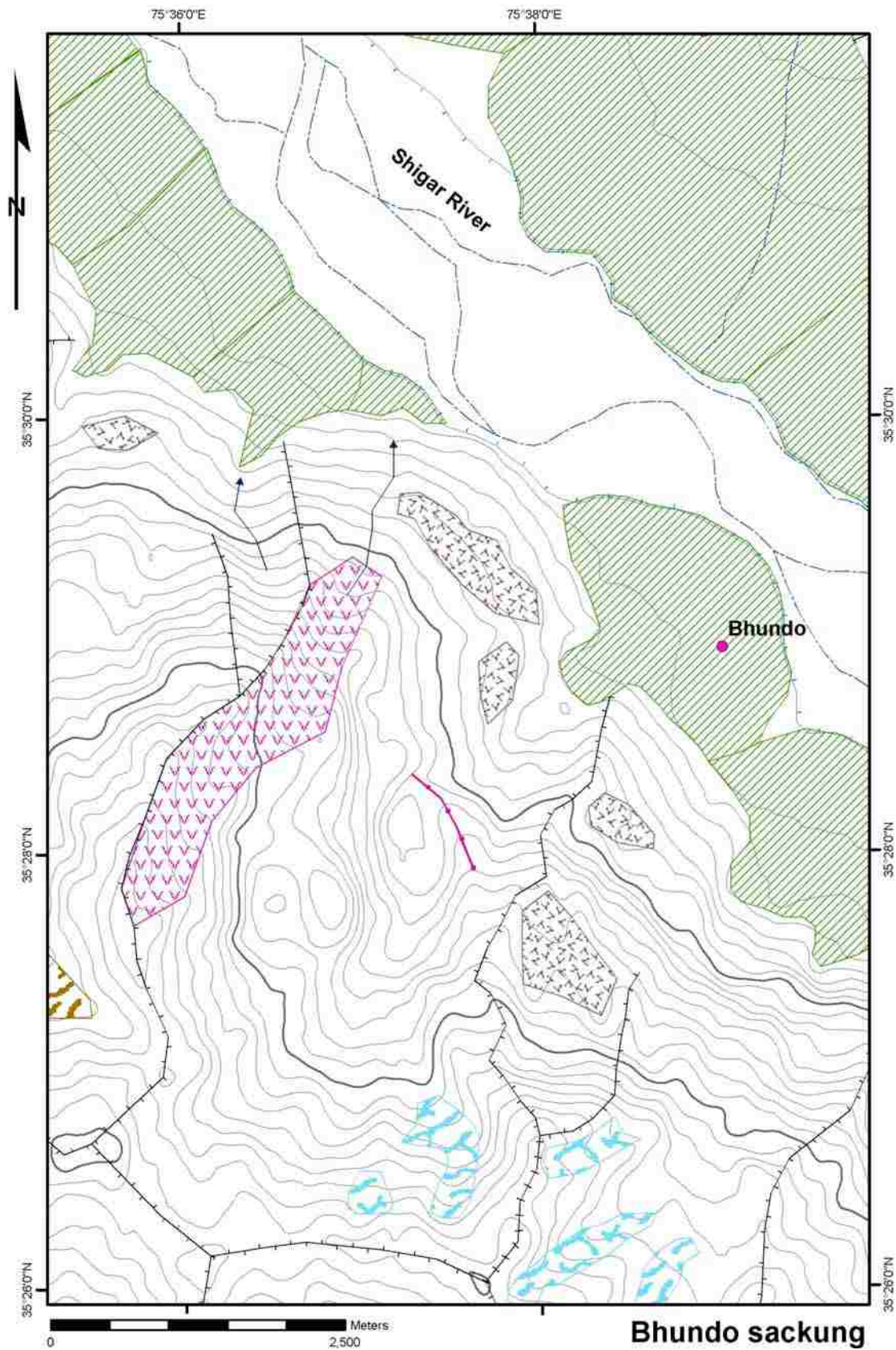
Mungo sacking
D. Belden 2008



Bhundo sackung

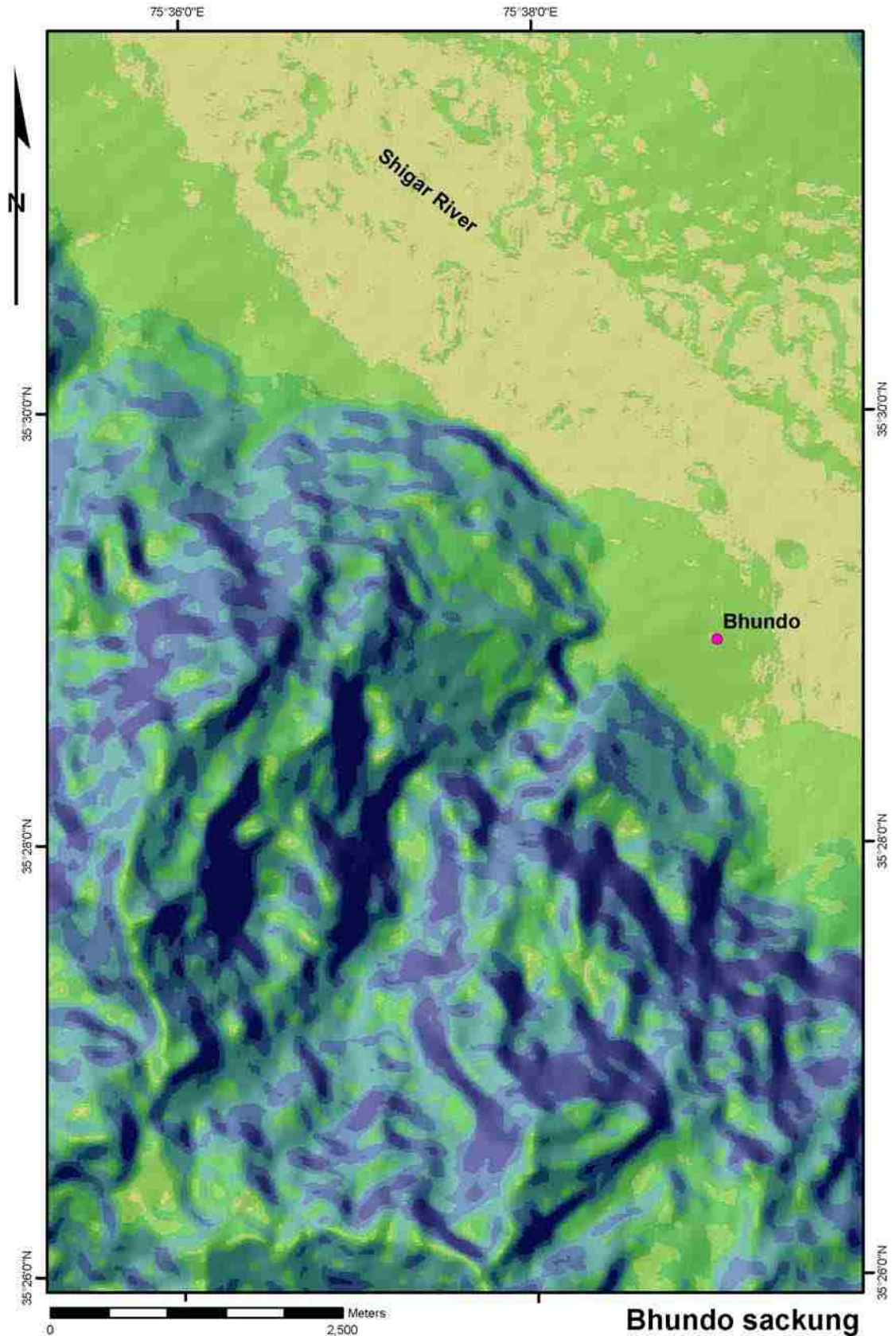
Map 50. Bhundo sackung: ASTER imagery.

D. Belden 2008



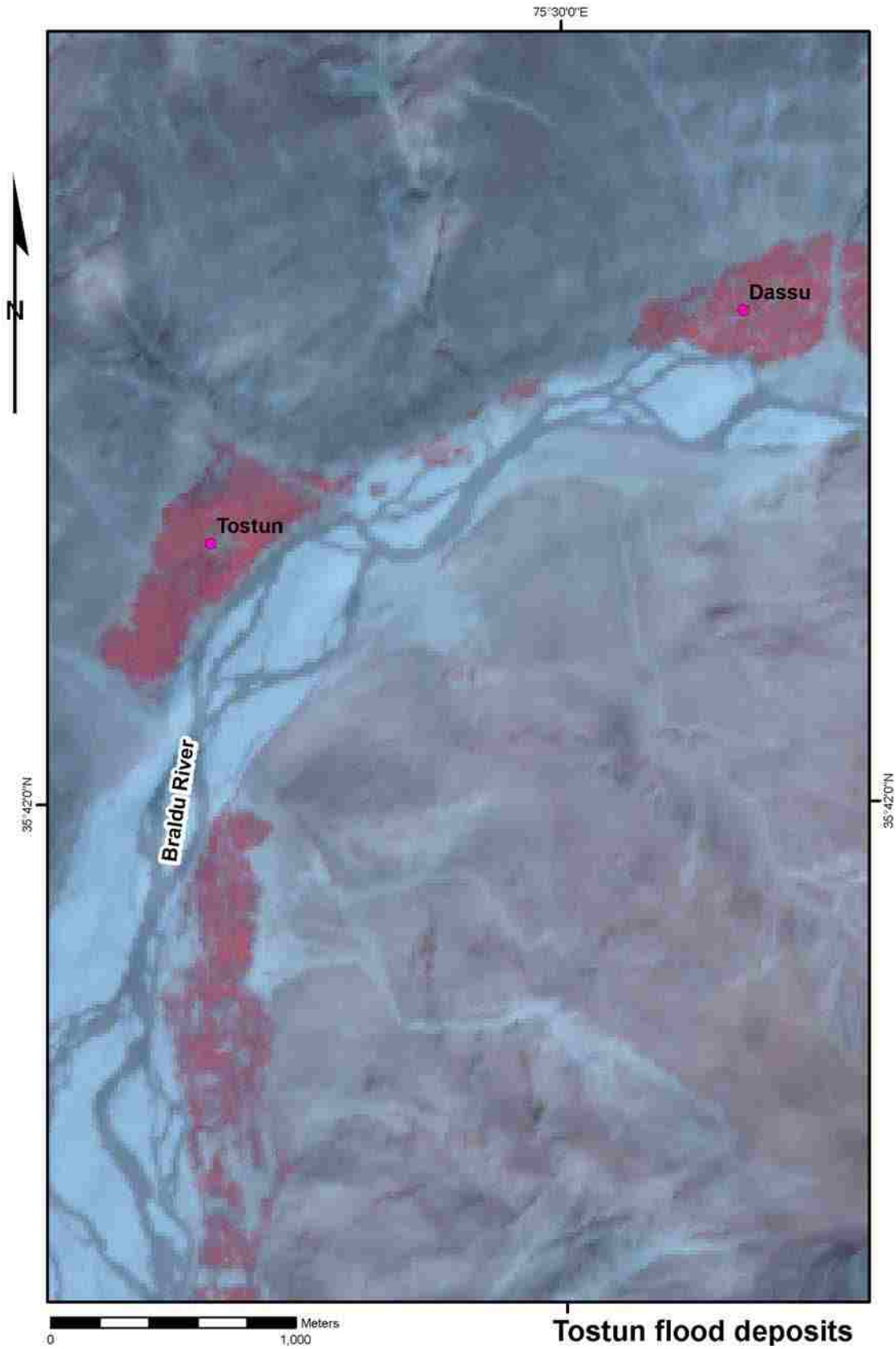
Map 51. Bhundo sacking: geomorphological map.

D. Belden 2008



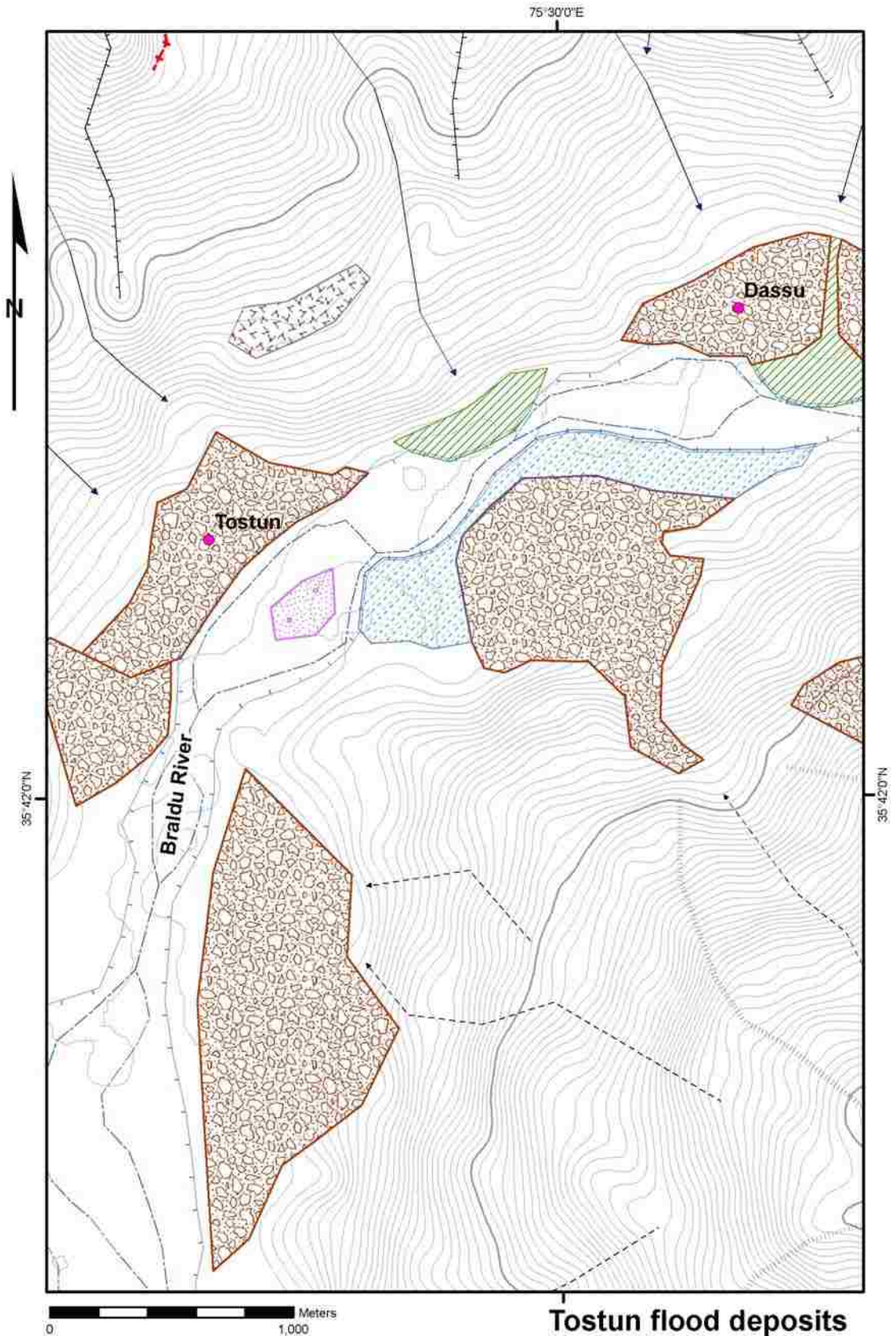
Map 52. Bhundo sacking: slope map.

D. Belden 2008



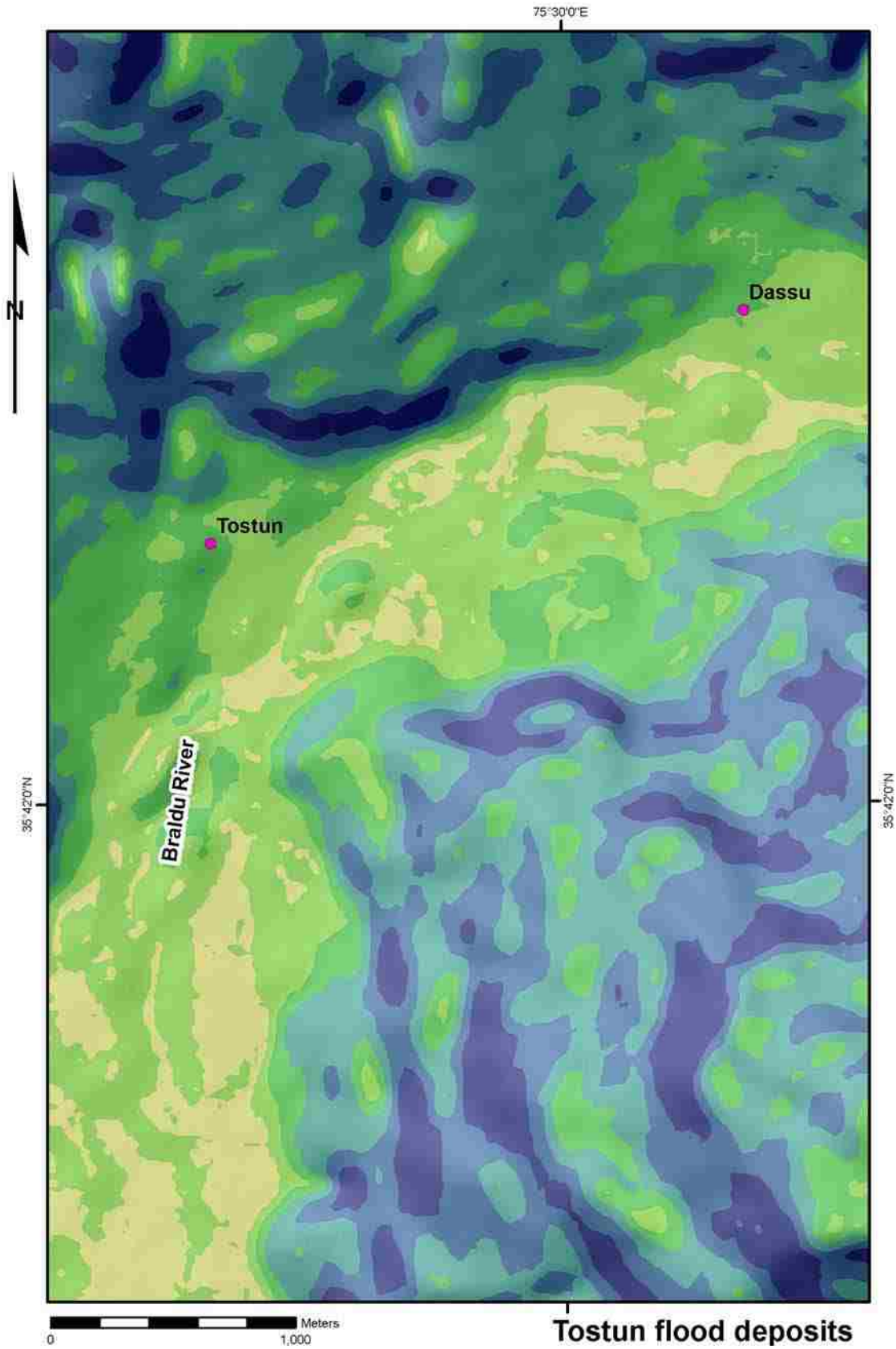
Map 53. Tostun flood deposits: ASTER imagery.

D. Belden 2008



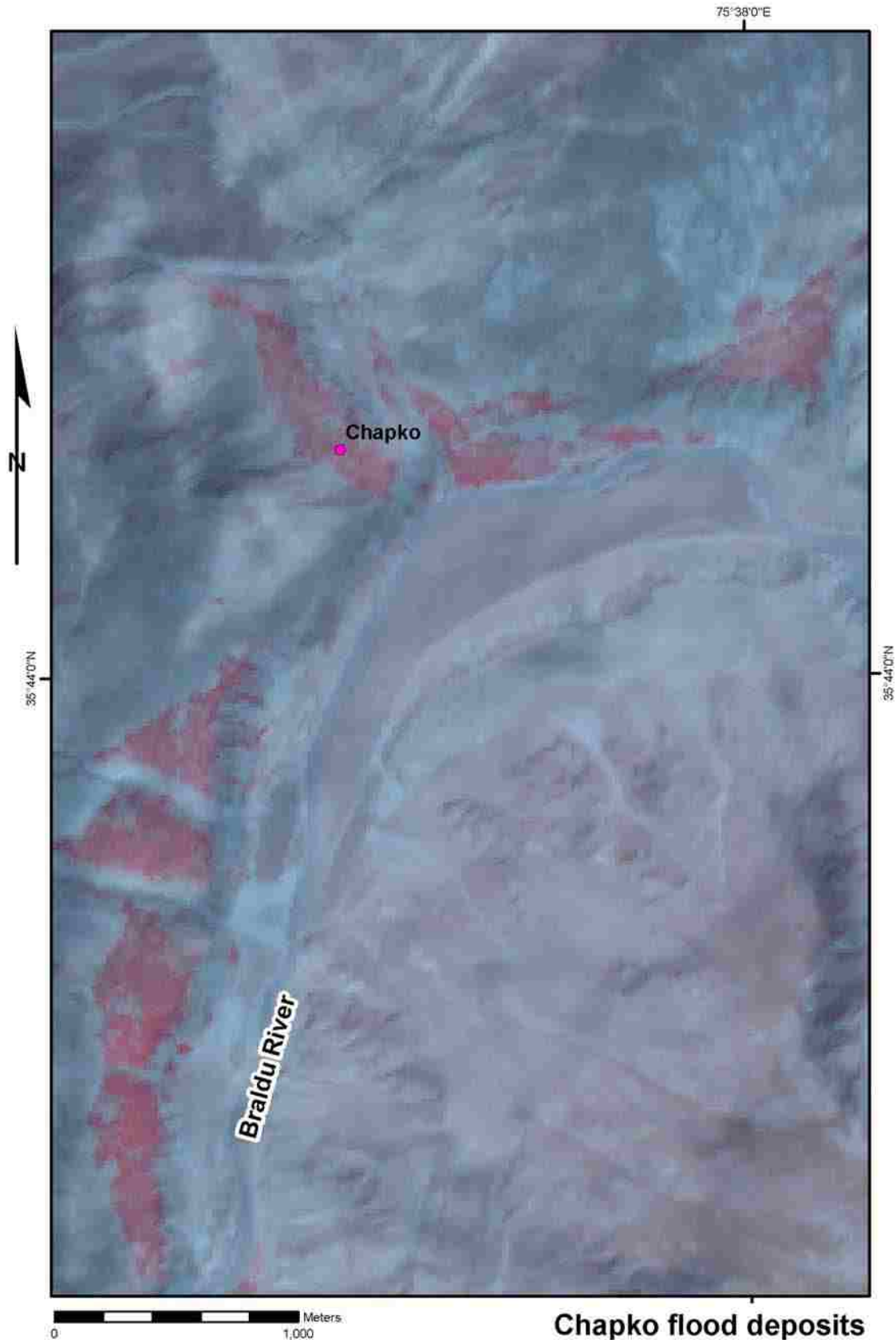
Map 54. Tostun flood deposits: geomorphological map.

D. Belden 2008



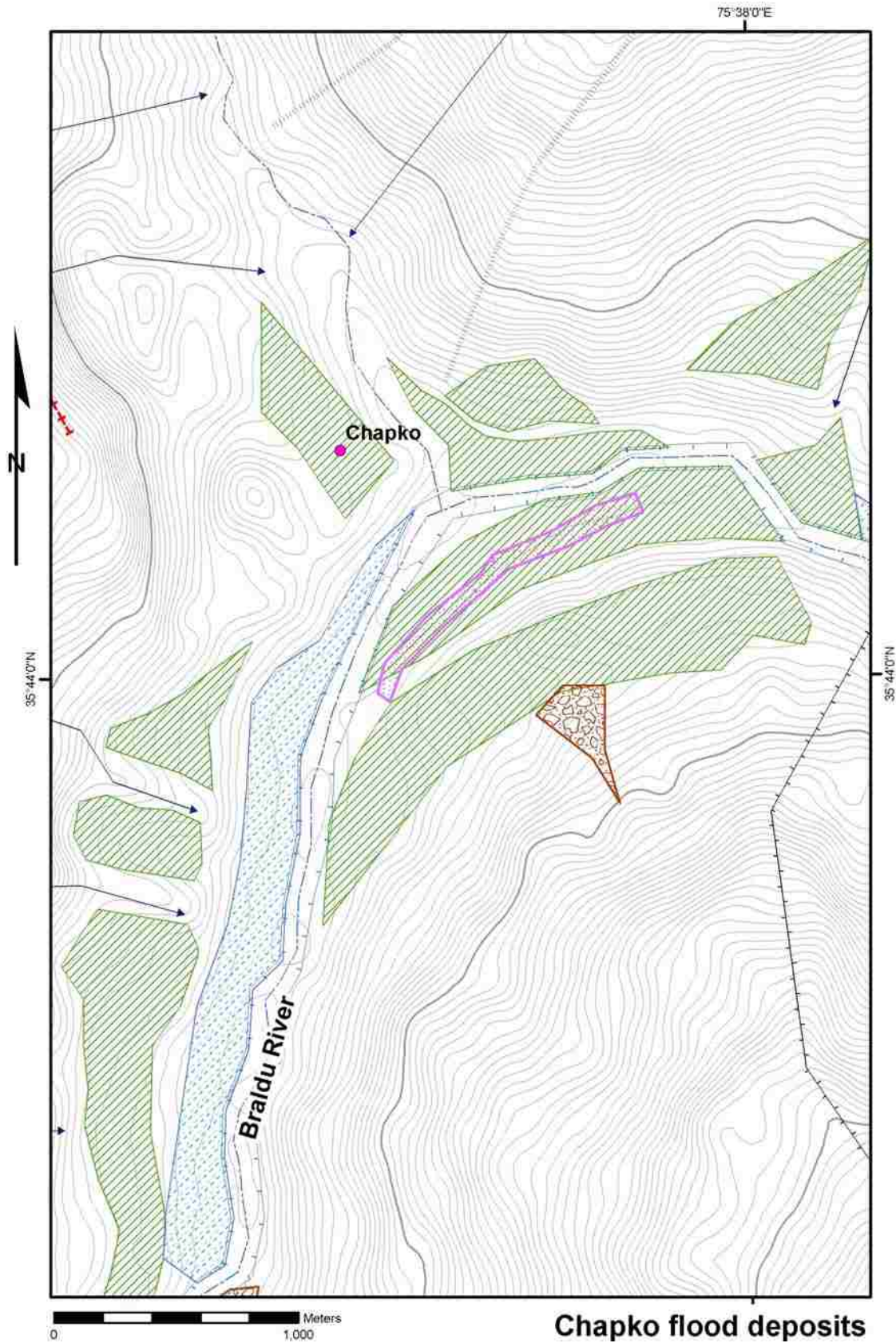
Map 55. Tostun flood deposits: slope map.

D. Belden 2008



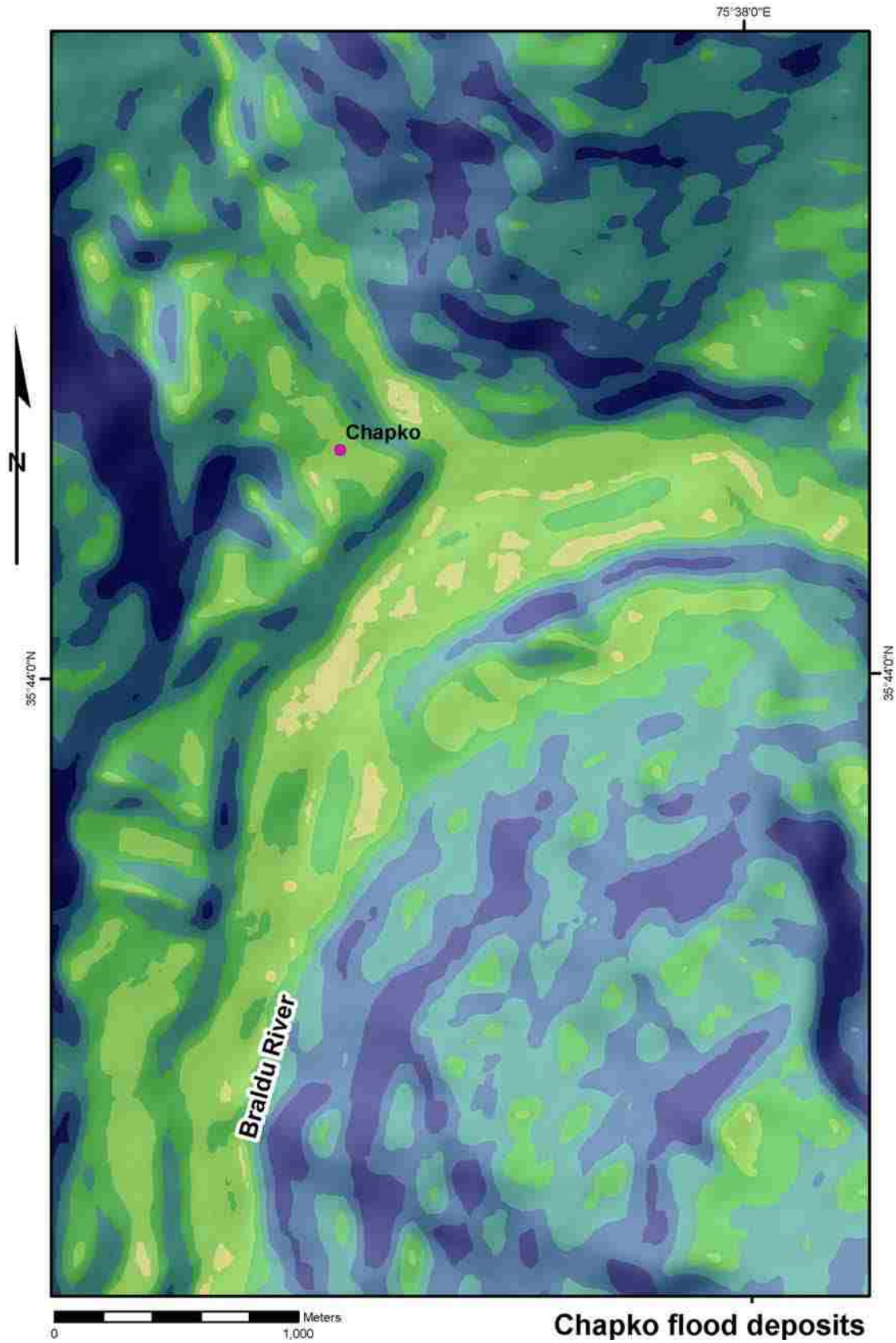
Map 56. Chakpo flood deposits: ASTER imagery.

D. Belden 2008



Map 57. Chakpo flood deposits: geomorphological map.

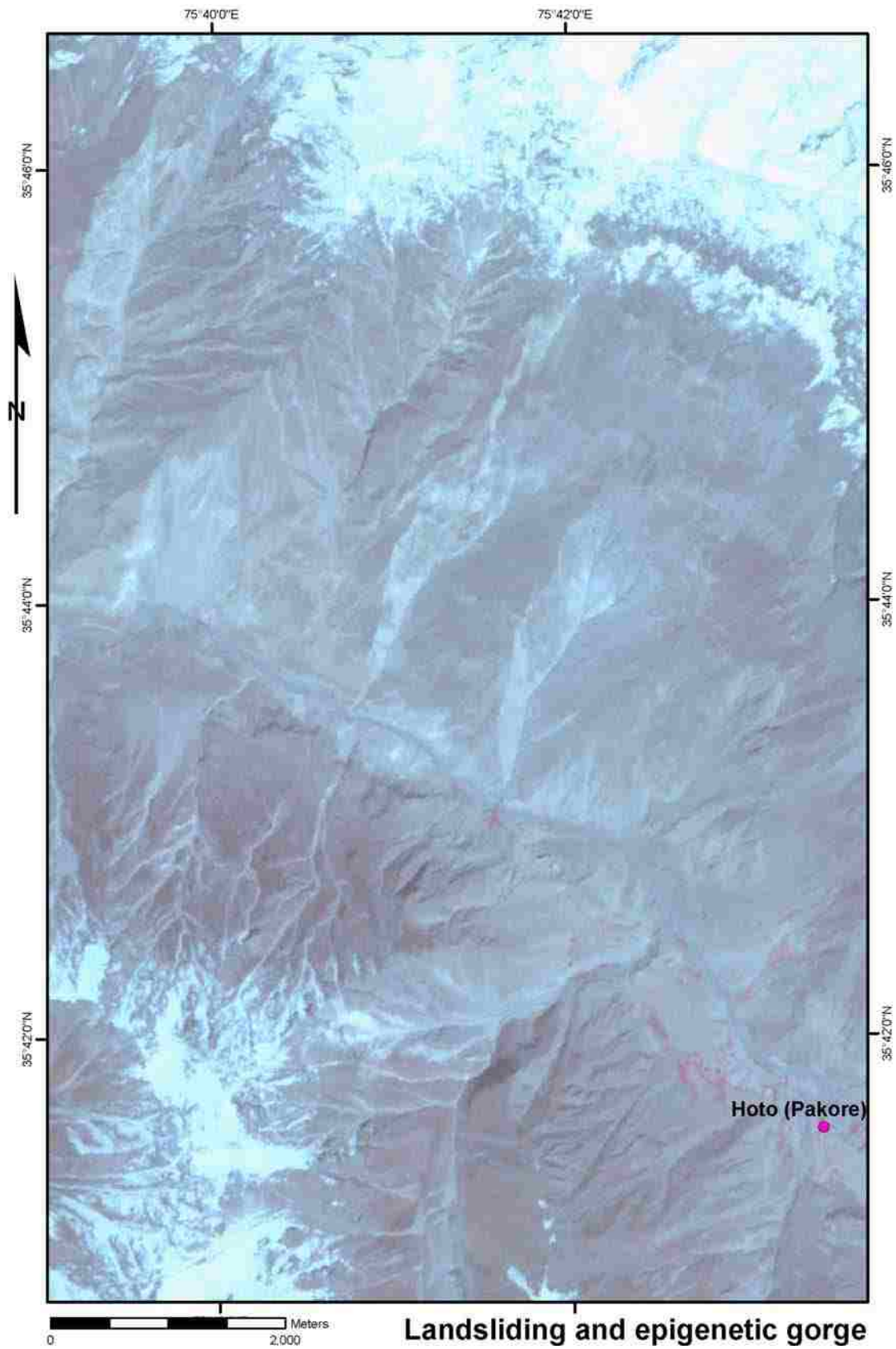
D. Belden 2008



Map 58. Chakpo flood deposits: slope map.

Chapko flood deposits

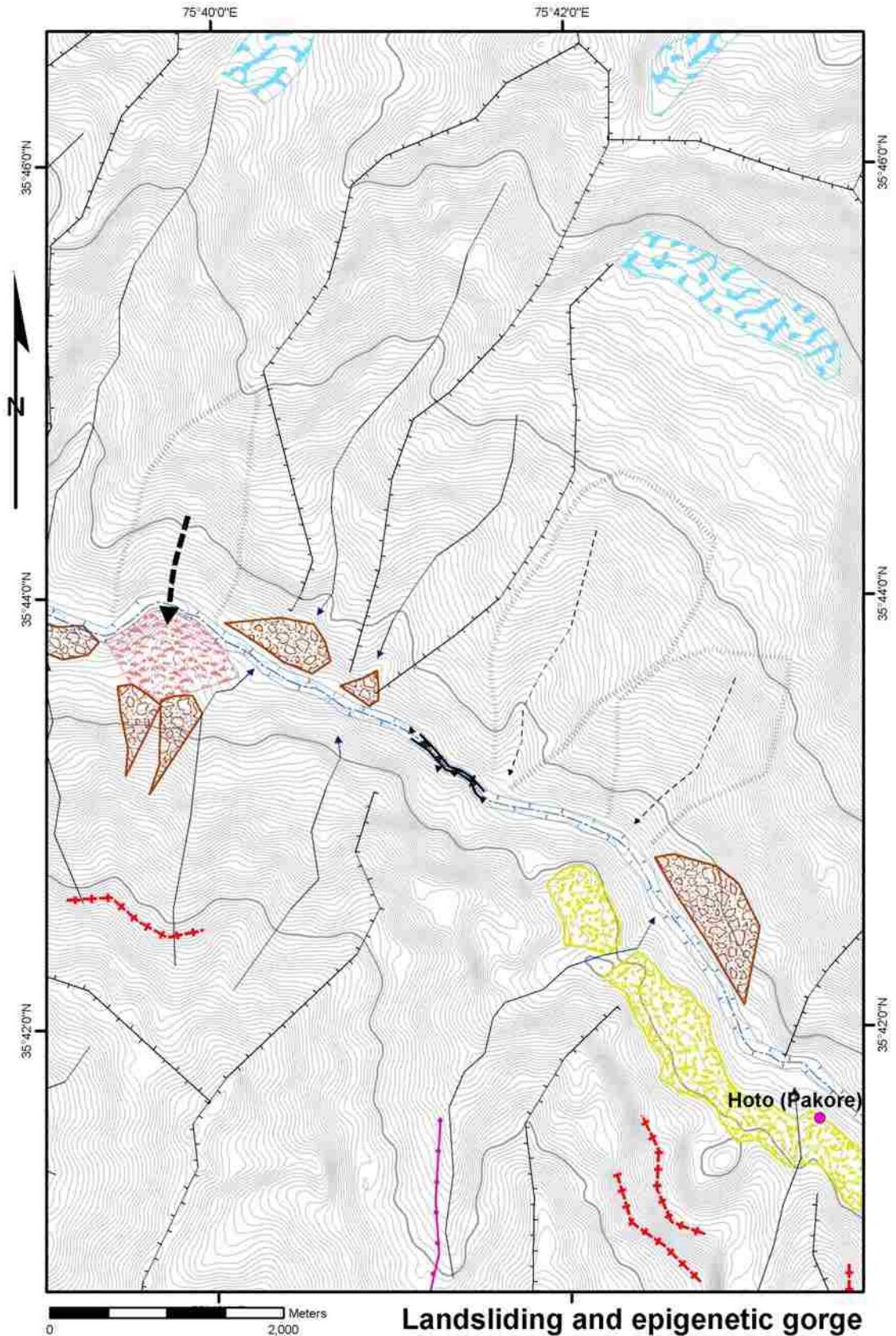
D. Belden 2008



Landsliding and epigenetic gorge

Map 59. Landsliding and epigenetic gorge: ASTER imagery.

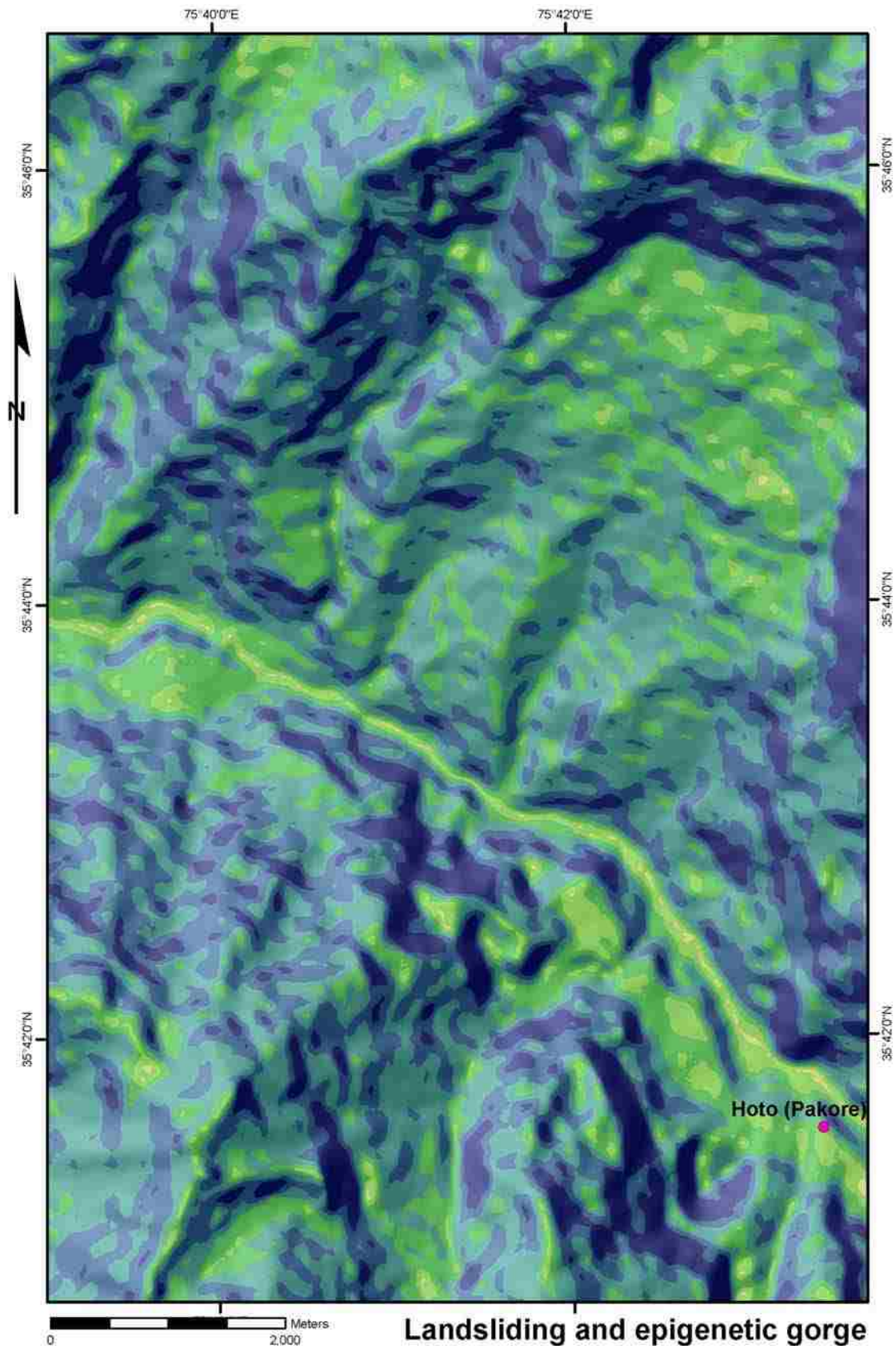
D. Belden 2008



Landsliding and epigenetic gorge

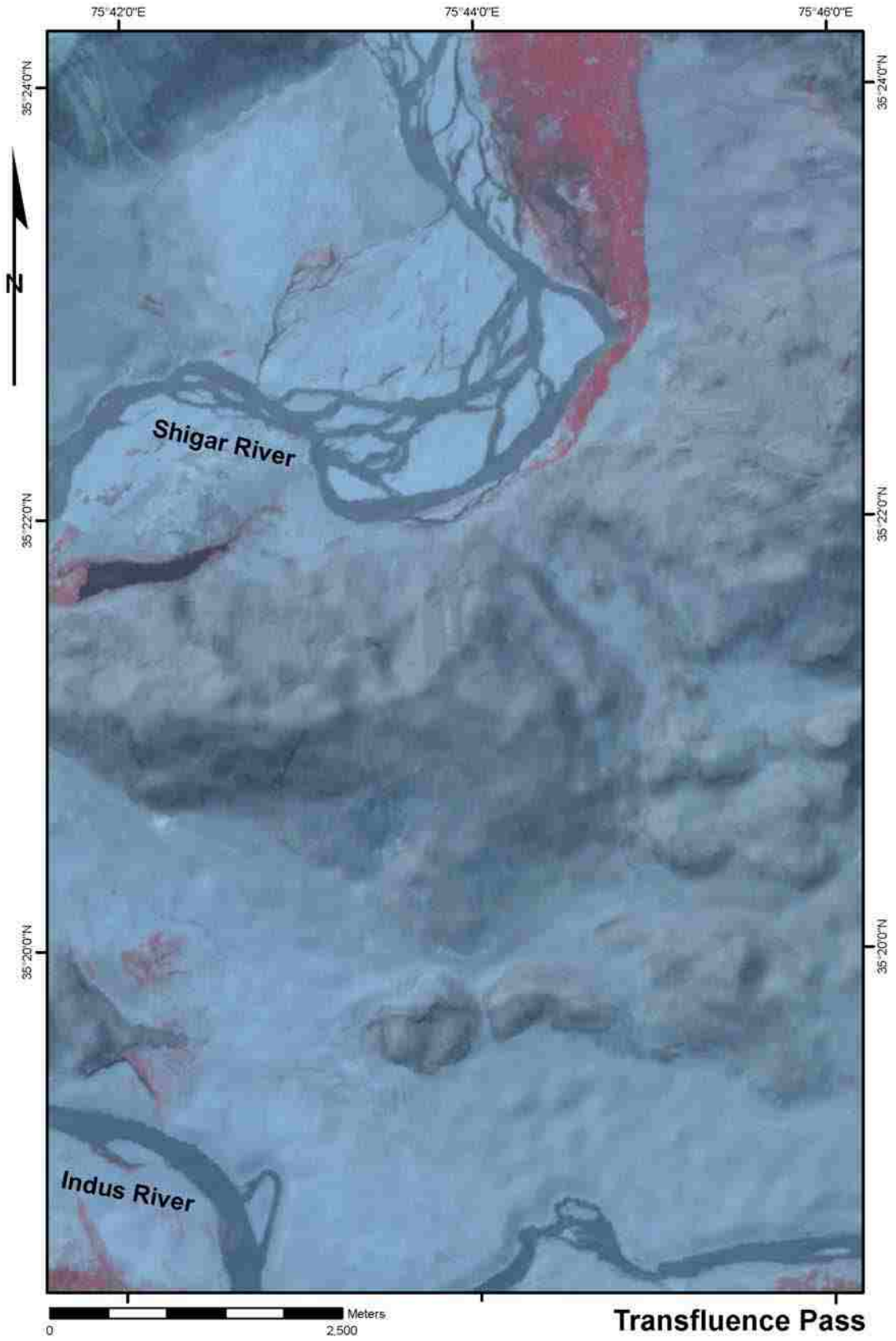
Map 60. Landsliding and epigenetic gorge: geomorphological map.

D. Belden 2008



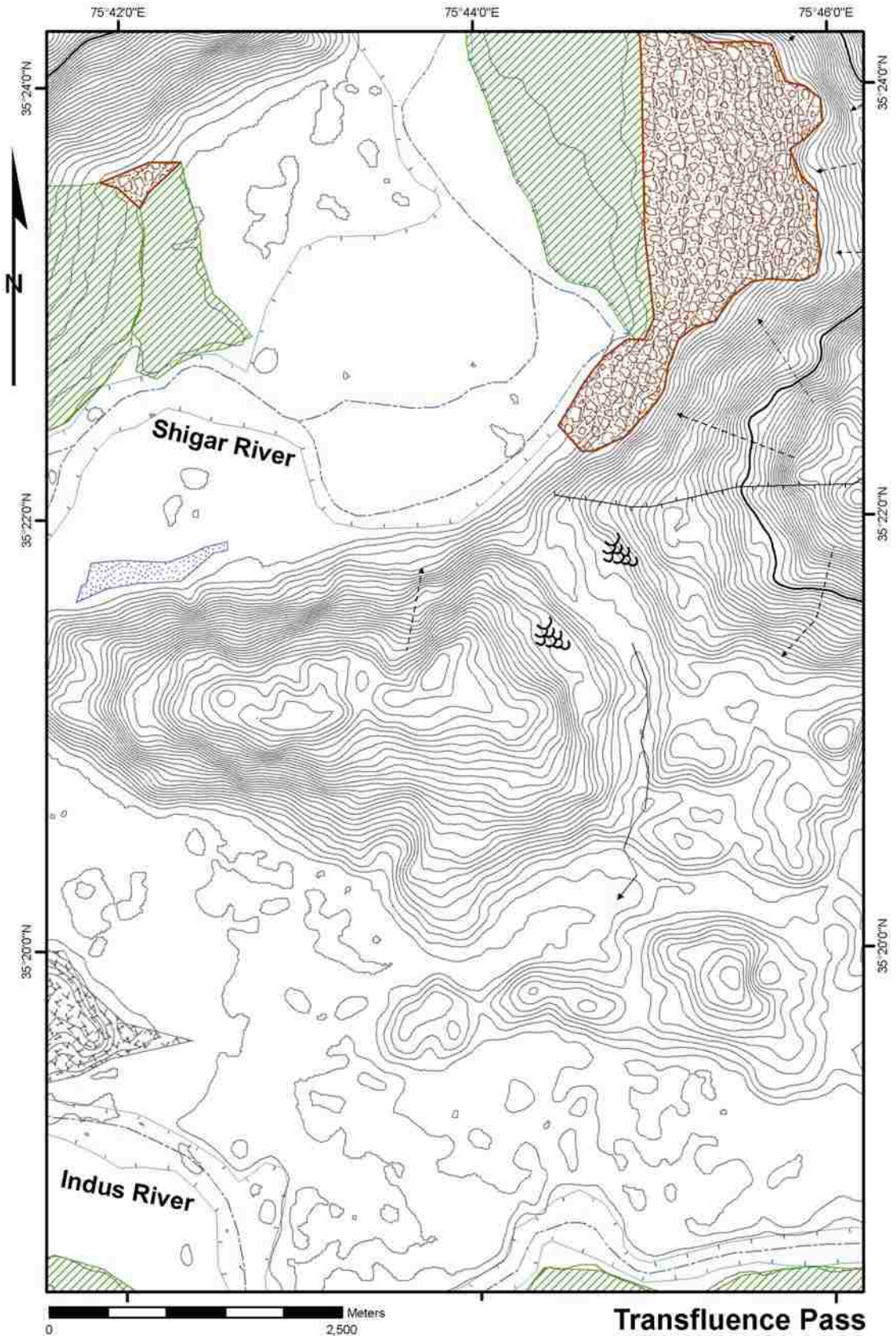
Map 61. Landsliding and epigenetic gorge: slope map.

D. Belden 2008



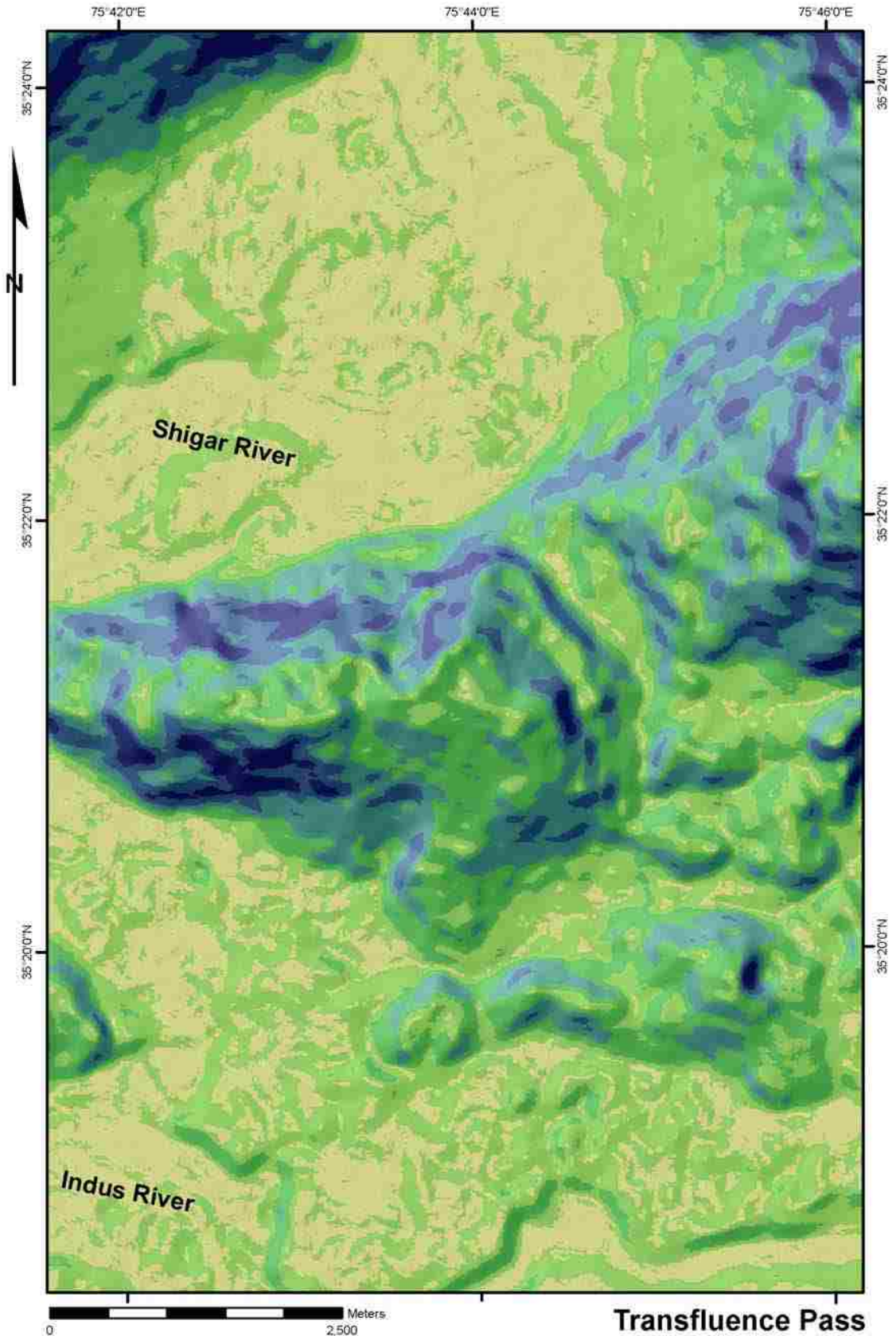
Map 62. Transfluence pass: ASTER imagery.

D. Belden 2008



Map 63. Transfluence pass: geomorphological map.

D. Belden 2008



Map 64. Transfluence pass: slope map.

D. Belden 2008